Investigation of Ca^{2+}-dependent transport and sorting processes of soluble secreted proteins in the Golgi apparatus

Dissertation an der Fakultät für Biologie
der Ludwig-Maximilians-Universität München

Tobias Karl-Heinz Hecht

aus
Marktredwitz, Deutschland

2020

Diese kumulative Dissertation wurde im Sinne der vierten Satzung der Promotionsordnung vom 29. September 2016 der Ludwig-Maximilians-Universität München für die Fakultät für Biologie von Frau Prof. Dr. Barbara Conradt betreut.

Teile dieser Arbeit wurden in folgenden Publikationen veröffentlicht:

Natalia Pacheco-Fernandez, Mehrshad Pakdel, Birgit Blank, Ismael Sanchez-Gonzalez, Kathrin Weber, Mai Ly Tran, **Tobias Karl-Heinz Hecht**, Renate Gautsch, Gisela Beck, Franck Perez, Angelika Hausser, Stefan Linder, Julia von Blume; Nucleobindin-1 regulates ECM degradation by promoting intra-Golgi trafficking of MMPs. *J Cell Biol* 3 August 2020; 219 (8): e201907058. doi: https://doi.org/10.1083/jcb.201907058

Tobias Karl-Heinz Hecht *, Birgit Blank *, Martin Steger, Victor Lopez, Gisela Beck, Bulat Ramazanov, Matthias Mann, Vincent Tagliabracci, Julia von Blume; Fam20C regulates protein secretion by Cab45 phosphorylation. J Cell Biol 1 June 2020; 219 (6): e201910089. doi: https://doi.org/10.1083/jcb.201910089. * These authors contributed equally to this work

Die labortechnische Arbeit dazu, wurde in der Forschungsgruppe von Dr. Julia von Blume am Max-Planck-Institut für Biochemie (Martinsried, Deutschland), sowie an der Yale Universität (New Haven, USA) absolviert.

1. Gutachter: Prof. Dr. Barbara Conradt

2. Gutachter: Prof. Dr. Jürgen Soll

Tag der Abgabe: 08. Oktober 2020

Tag der mündliche Prüfung: 16. Dezember 2020

Eidesstattliche Versicherung

Ich versichere hiermit an Eides statt, dass die vorgelegte Dissertation von mir selbständig und ohne unerlaubte Hilfe angefertigt ist.

München, den 28. September 2020

....
Tobias Karl-Heinz Hecht

Erklärung

Hiermit erkläre ich, dass die Dissertation nicht ganz oder in wesentlichen Teilen einer anderen Prüfungskommission vorgelegt worden ist.
Zudem, habe ich mich nicht anderweitig einer Doktorprüfung ohne Erfolg unterzogen.

München, den 28. September 2020

....
Tobias Karl-Heinz Hecht

Table of contents

List of abbreviations

ADF	Actin depolymerizing factor
ADP	Adenosine diphosphate
AFK	Actin-fragmine kinase
AIF	Apoptosis inducing factor
AP	Adapter protein complexes
ARH	Autosomal recessive hypercholesterolemia
ATF6	Activating transcription factor 6
ATP	Adenosine triphosphate
ATP7B	ATPase copper transporting beta
Bcl-2	B-cell lymphoma 2
BiP	Binding immunoglobulin protein
BSP	Bone sialoprotein
Ca^{2+}	Calcium
Cab45	Ca^{2+}-binding protein, 45 kDa
Cab45-5pXA	Phosphorylation-deficient mutant of Cab45
Cab45-5pXE	Phosphorylation-mimicking mutant of Cab45
Cab45-6EQ	Ca^{2+}-binding-deficient mutant of Cab45
cADPR	Cyclic adenosine diphosphate ribose
CALM	Clathrin assembly lymphoid myeloid leukemia protein
CaM	Calmodulin
CaMKII	Calmodulin kinase II
CAML	Ca^{2+}-modulating cyclophilin ligand
CARTS	Carriers of the TGN to the cell surface
CatD	Cathepsin D
CCV	Clathrin-coated vesicle
CD-MPR	Cation-dependent mannose-6 phosphate receptor
CERT	Ceramide transfer protein
CgA, B	Chromogranin A, B
CI-MPR	Cation-independent mannose-6 phosphate receptor
CICR	Ca^{2+}-induced Ca^{2+}-release
CLASP	Cytoplasmic linker proteins-associated proteins
CLEM	Correlative light-electron microscopy
CNX	Calnexin
COMP	Cartilage oligomeric matrix protein
COPI,II	Coatamer protein complex I/II
CPLA2α	Cytosolic phospholipase A2 alpha
CRT	Calreticulin
CSQ	Calsequestrin
CtkA	Cell translocating kinase A
CTx	Cholera toxin
Cytc	Cytochrome c
DAG	Diacylglycerol
DHPR	Dihydropyridine receptor
DMP	Dentin matrix protein
DNA	Deoxyribonucleic acid
DRM	Detergent-resistant glycolipid-enriched membranes
DSPP	Dentin sialophosphoprotein
ECM	Extracellular matrix
EDEM	ER degradation-enhancing alpha-mannosidase-like protein
Eg5	Microtubule-associated kinesin-5 motor protein
EGF	Epidermal growth factor
EGFR	Epidermal growth factor receptor
EM	Electron microscopy
Ent 3, 5	Equilibrative nucleoside transporter 3, 5
ER	Endoplasmic Reticulum
ERAD	ER-associated degradation

ERES	ER exit sites
ERGIC	ER-Golgi intermediate compartment
ERManI	ER mannosidase I
Ero1α	ER oxidoreductin 1α
Fam20A, B, C	Family with sequence similarity of 20, member; A, B, C
Fjx	Four jointed box 1
FKBP	FK506-binding protein
GEF	Guanosine exchange factor
GFP	Green fluorescence protein
GGA	Gamma-ear-containing Arf-binding proteins
GGT	Glycolipid glycosyltransferases
GI, II	Glucosidase I, II
Glc	Glucose
GlcNAc	N-Acetylglucosamine
GMAP-210	Golgi microtubule-associated protein 210 kDa
GPCR	G-protein coupled receptor
GPI	Glycosylphosphatidylinositol
GPLs	Glycerophospholipids
GRASP	Golgi reassembly stacking proteins
GSL	Glycosphingolipids
GTP	Guanosine triphosphate
GUV	Giant unilamellar vesicles
HaxI	HS-1 associated protein X-1
Hip	Hsc70-interacting protein 1
HipA	High persistence factor A
HRD	3-hydroxy-3-methylglutaryl (HMG) CoA reductase
Hrs	Hepatocyte growth factor regulated tyrosine kinase
Hsc70	Heat shock cognate protein, 70 kDa
HSP	Heat shock protein
IP3	Inositol 1,4,5-trisphosphate
IP3R	IP_3 receptor
IRE1	Inositol-requiring enzyme 1
KO	Knockout
LacCer	Lactosylceramide
LAMP1	Lysosome-associated membrane glycoprotein
LDL-R	Low densitiy lipoprotein receptor
LIMP2	Lysosomal integral membrane protein-2
LPA	Lysophosphatidic acid
LPC	Lysophosphatidylcholine
LTPs	Lipid transfer proteins
LyzC	Lysozyme C
M2	M2 muscarinic acetylcholine
M6P	Mannose-6 phosphate
M6PRBP1	Mannose-6 phosphate-binding protein, 47 kDa
MAM	Mitochondria-associated membranes
Man	Mannose
MCS	Membrane contact sites
MEPE	Matrix extracellular phosphoglycoprotein
MGP	Matrix glia protein
MMP	Matrix metalloproteinase
MPR	Mannose-6 phosphate receptor
MT1-MMP	Membrane type 1-matrix metalloproteinase
MTOC	Microtubule-organizing center
NAADP	Nicotinic acid adenine dinucleotide phosphate
NUCB1,2	Nucleobindin-1, -2
OPN	Osteopontin
Orai1	Calcium release-activated calcium channel protein 1
P56	Phosphoglycerate kinase 56
PA	Phosphatidic acid

PAGE	Polyacrylamidgelelectrophoresis
PC	Phosphatidylcholine
Pc-9	Procaspase-9
PCSK9	Protein convertase subtilisin/kexin type 9
PDI	Protein disulfide isomerase
PE	Phosphatidylethanolamin
PERK	Protein kinase R-like ER kinase
PI	Phosphatidylinositol
PIgR	Polymetric immunoglobulin receptors
PIP_2	Phosphatidylinositol 4,5-bisphosphate
PKA	Protein kinase A
PKD	Protein kinase D
PLC	Phospholipase C
PLN	Cardiac phospholamban
PM	Plasma membrane
PMCA	Plasma membrane Ca^{2+}-ATPase
PS	Phosphatidylserine
RNA	Ribonucleic acid
rTK	Receptor tyrosine kinases
RyR	Ryanodine receptor
SDF4	Stromal cell derived factor 4
SERCA	Sarco/Endoplasmic Reticulum Ca^{2+}-ATPase
SG	Secretory granules
SgII	Secretogranin
SIBLING	Small integrin-binding ligand, N-linked glycoprotein
SLN	Sarcolipin
SM	Sphingomyelin
SMS	Sphingomyelin synthase
SNARE	Soluble N-ethylmaleimide-sensitive factor attachment protein receptor
SorLA	Sortilin-related receptor with A-type repeats
SP	Signal peptide
SPCA1	Secretory Pathway Ca^{2+}-ATPase
SR	Sarcoplasmic Reticulum
SRP	Signal recognition particle
ss-HRP	Horseradish peroxidase with signal sequence
SSH	Slingshot
STARD	StAR-related lipid transfer protein
StART	Steroidogenic acute regulatory transfer
Stam	Signal transducing adapter molecule
STIM	Stromal interaction molecule
STx	Shiga toxin
SV40	Simian virus 40
TA	Tail-anchored
TfR	Transferrin receptors
TGN	*trans*-Golgi network
TIMP	Tissue inhibitors of metalloproteinase
TRAPP	Transport protein particles
TRC40	Transmembrane domain recognition complex, 40 kDa
UB	Ubiquitin
UBA	Ubiquitin-associated
UBC	Ubiquitin-conjugating enzyme
UGGT	UDP-glucose:glycoprotein glucosyltransferase
UIM	Ubiquitin interaction motif
UPR	Unfolded protein response
VLK	Vertebrate lonesome kinase
VPS10	Vacuolar protein sorting/targeting protein 10
VSVG	Vesicular stomatitis virus glycoprotein G
WRB	Tryptophan-rich basic protein
Wt	Wildtype

List of figures

Declaration of content

LONDON'S GLOBAL UNIVERSITY

Professor Barbara Conradt
Head of Research Department
Department of Cell & Developmental Biology
Division of Biosciences, University College London
G21, Anatomy Building
Gower Street, London WC1E 6BT
P: (+44) 020-3108-6268
E: b.conradt@ucl.ac.uk **W:** www.ucl.ac.uk/biosciences

An das
Dekanat der Fakultät für Biologie
Biozentrum
Großhaderner Str. 2
82152 Planegg-Martinsried

06. Oktober 2020

Bestätigung des Eigenanteils von Tobias Karl-Heinz Hecht für seine Dissertation an der Fakultät für Biologie der Ludwig-Maximilians-Universität München

Hiermit bestätige ich die erbrachten Leistungen an den folgend aufgeführten Publikationen, die zur Erstellung der kumulativen Dissertation verwendet wurden.

Publikation: Fam20C regulates protein secretion by Cab45 phosphorylation

Abbildung 1 A-E	Abbildung S1 A-C
Abbildung 2 A, C-E	Abbildung S2 C-E
Abbildung 4 A-E	Abbildung S3 A, B
Abbildung 5 A-G	Abbildung S4 A-C
Abbildung 6 A-G	Abbildung S5 A-C
Abbildung 7 A-D	
Abbildung 8	

Publikation: Nucleobindin-1 regulates ECM degradation by promoting intra-Golgi trafficking of MMP2.

Abbildung 5 C, D

Zudem, Etablierung und Hilfestellung bei der Aufreinigung von rekombinanten MMP2 und NUCB1, verwendet in Abbildung 1 G, H und Abbildung S3.

Mit freundlichen Grüßen,

Barbara Conradt, PhD

University College London, Gower Street, London WC1E 6BT
Tel: +44 (0)20 7679 2000
email@ucl.ac.uk
www.ucl.ac.uk

X

Erklärung über die erbrachte Leistung und substanziellen Beiträge bei gemeinsamer Erstautorenschaft

Hiermit erklären wir unsere Anteile und Beiträge zur gemeinsamen Publikation „Fam20C regulates protein secretion by Cab45 phosphorylation".

Von beiden gemeinsam erarbeitet: Konzeptualisierung, Methodik, Investigation, Verfassung & Verbesserung des Manuskripts.

Die experimentelle Untersuchung zu den einzelnen Abbildungen ergab sich wie folgt:

Tobias Karl-Heinz Hecht

Abbildung 1 A-E	Abbildung S1 A-C
Abbildung 2 A, C-E	Abbildung S2 C-E
Abbildung 4 A-E	Abbildung S3 A, B
Abbildung 5 A-G	Abbildung S4 A-C
Abbildung 6 A-G	Abbildung S5 A-C
Abbildung 7 A-D	
Abbildung 8	

Dr. Birgit Renate Karin Blank

Abbildung 2 B	Abbildung S1 D-E
Abbildung 3 C, D	Abbildung S2 A, B
Abbildung 8	Abbildung S4 D, E

_____
Tobias Karl-Heinz Hecht

_____
Dr. Birgit Renate Karin Blank

Summary

The Golgi apparatus is the main transport and sorting hub of the Secretory Pathway. Here, newly synthesized proteins that have arrived from the Endoplasmic Reticulum travel through the Golgi stack and are sequentially modified before they reach the *trans*-Golgi network (TGN). At the TGN proteins are sorted into specific vesicles and transported to other compartments or out of the cell. In general, these processes have been well described for e.g. transmembrane proteins or lysosmal hydrolases; however, how soluble secretory molecules are transported through the Golgi apparatus and packed into secretory vesicles is still elusive. Recently, our lab has identified a Ca^{2+}-based sorting mechanism for soluble secretory proteins via the TGN-luminal EF-hand Ca^{2+}-binding protein Cab45. Thereby, Ca^{2+} that has been locally pumped into the TGN by the Ca^{2+}-ATPase SPCA1 leads to the oligomerization of Cab45 and the concentration of bound cargo proteins like lysozyme C. In a so far unknown manner, these Cab45-client-complexes are sorted into specific sphingomyelin(SM)-rich vesicles and secreted from the cell. Within the scope of my thesis, I further elucidated this sorting process. I showed that Cab45 is phosphorylated on five specific residues by the Golgi kinase Fam20C, which is important for cargo sorting at the TGN. Moreover, I proved that mimicking of phosphorylation disassembles Cab45 oligomers and translocates Cab45 into TGN-derived SM-rich vesicles. Altogether, my results demonstrate that phosphorylation of Cab45 by Fam20C regulates its TGN-retention, the entry into secretory vesicles and as a consequence actively drives the export and secretion of its clients.

Notwithstanding the above, we were additionally interested if Ca^{2+} might be also involved in the transport of soluble secretory proteins through the Golgi apparatus. Analogous to Cab45, we revealed that another Ca^{2+}-binding protein nucleobindin-1 (NUCB1) exhibits a similar Ca^{2+}-based mechanism for the transport of these molecules. NUCB1, that localizes at the *cis*-Golgi binds Ca^{2+} with its EF-hand domain, thereby changes its secondary structure and so directly interacts with cargo proteins e.g. matrix metalloproteinases (MMPs). As a consequence, NUCB1 expression significantly drives intra-Golgi transport of MMP2 and was further necessary for proper cell migration and matrix invasion of MDA-MB-231 cells and human macrophages.

Overall, our results reveal the relevance of Ca^{2+} in the transport and sorting of soluble secretory molecules at the Golgi apparatus. Furthermore they give new insights into how these proteins are properly transported and secreted, despite missing cargo sorting receptors and

recognition motifs.

Zusammenfassung

Der Golgi-Apparat ist der Hauptknotenpunkt im biosynthetischen Proteintransport. Vom Endoplasmatischem Retikulum kommende, neusynthetisierte Proteine, die durch den Golgi-Komplex transportiert werden, werden hier schrittweise modifiziert und erreichen schließlich das trans-Golgi-Netzwerk (TGN). Im TGN werden Proteine in spezifische Vesikel gepackt und zu anderen Organellen oder aus der Zelle transportiert. Während diese Prozesse für z.B. Transmembranproteine oder lysosomale Hydrolasen gut erforscht sind, ist nicht bekannt wie lösliche sekretorische Proteine durch den Golgi-Apparat transportiert und in Sekretionsvesikel verpackt werden. In den letzten Jahren erforschte unser Labor einen Ca^{2+}-basierten Sortierungsmechanismus für lösliche sekretorische Proteine über ein TGN-luminales, Ca^{2+}-bindendes Protein, Cab45. Dabei, oligomerisiert Cab45 mittels Ca^{2+}, das über die Ca^{2+}-ATPase SPCA1 in das TGN gepumpt wurde und konzentriert so zu transportierende Proteine wie beispielsweise Lysozym C. In einem bisher unbekannten Mechanismus, wird dieser Cab45-Fracht-Komplex in spezifische Sphingomyelin(SM)-reiche Vesikel sortiert und aus der Zelle sekretiert. Im Rahmen meiner Doktorarbeit entschlüsselte ich diesen Sortierungsprozess weiter. Diesbezüglich konnte ich zeigen, dass Cab45 durch die im Golgi lokalisierte Proteinkinase Fam20C an fünf spezifischen Aminosäuren phosphoryliert wird und dabei signifikant zur Sortierung im TGN beiträgt. Zudem konnte ich verdeutlichen, dass die Nachahmung dieser Phosphorylierungen zu einer Auflösung der Cab45-Oligomere und weiter zur Um-lokalisierung von Cab45 in vom TGN-stammende, SM-reiche Vesikel führt. Zusammenfassend zeigen meine Ergebnisse, dass die Phosphorylierung von Cab45 durch Fam20C dessen Retention im TGN, sowie die Verpackung in Sekretionsvesikel reguliert und somit aktiv den Export und die Sekretion von Proteinen steuert.

Unabhängig davon waren wir interessiert daran, ob Ca^{2+} ebenfalls Einfluss auf den Transport von löslichen sekretorischen Proteinen durch den Golgi-Apparat hat. Dabei enthüllten wir einen vergleichbaren Ca^{2+}-basierenden Mechanismus für den Transport solcher Proteine. Analog zu Cab45 konnten wir nachweisen, dass Nucleobindin-1 (NUCB1), ebenfalls ein Ca^{2+}-bindendes Protein im *cis*-Golgi, Ca^{2+} mittels seiner EF-Hand-Domäne bindet, die Sekundärstruktur ändert und so direkt mit Proteinen wie z.B. Matrixmetalloproteinasen

2

(MMPs) interagiert. Insgesamt zeigte sich, dass die Expression von NUCB1 essentiell für den intra-Golgi Transport von MMP2 und zudem für die Migration und Matrix-Invasion von MDA-MB-231 Zellen und humanen Makrophagen notwendig ist.

Alles in Allem legen unsere Ergebnisse die Notwendigkeit von Ca^{2+} für den Transport und die Sortierung von löslichen sekretorischen Proteinen dar. Sie beschreiben weiterhin eine neue Möglichkeit wie diese Proteine trotz fehlender Sortierungrezeptoren sowie Erkennungssequenzen gezielt transportiert und sekretiert werden.

1. Introduction

1.1 Compartmentalization - the requirement for protein distribution

The cell is considered as the smallest viable unit of life (Campbell 2008). Originated from a simple cellular ancestor, evolution including mutations and endosymbiosis led to the formation of the three domains and the development of complex eukaryotic cells (Archibald 2015; Brown and Doolittle 1997; Delaye and Becerra 2012). Over hundred of millions of years, eukaryotic cells have developed membrane-bound organelles that allow them to physically separate and improve the efficiency of their biochemical reactions, but also to elaborate defined cross-talk signaling networks (Diekmann and Pereira-Leal 2013; Koonin 2010). However, intracellular compartmentalization is also challenging, as organelles require a crucial set of biological macromolecules, ions as well as the correct pH to maintain a proper functional environment (Alonso et al. 2017b; Bohnsack and Schleiff 2010; Garcia-Moreno 2009; Van Meer et al. 2008; Xu, Martinoia, and Szabo 2016). Therefore, e.g. newly synthesized proteins have to be transported within the cell and translocate into the destined organelles, where they can fulfill their biological functions (Gabaldón and Pittis 2015). Eukaryotic cells have overcome this problem by an endomembrane system called the Secretory Pathway (Dacks, Peden, and Field 2009; Field and Dacks 2009). The Secretory Pathway - composed of the Endoplasmic Reticulum (ER), the ER-Golgi intermediate compartment (ERGIC), the Golgi apparatus, the *trans*-Golgi network (TGN) and post-Golgi vesicles - is responsible for the distribution of proteins and lipids to various destinations within and out of the cell (see Figure 1) (Farhan and Rabouille 2011; Lippincott-Schwartz, Roberts, and Hirschberg 2000). Along the Secretory Pathway, lipids and proteins are stepwise moved and further modified, a process that requests the recognition, segregation, congregation and transport of those molecules (Barlowe and Miller 2013; Kienzle and von Blume 2014; Matlin and Caplan 2017; Pakdel and von Blume 2018).

The following introduction will especially highlight how proteins are transported and modified within the Secretory Pathway. Particularly, it will focus on the transport and the sorting-dependent recognition of proteins in the Golgi complex.

By addressing the anterograde transport, the ER is the first component of the Secretory Pathway.
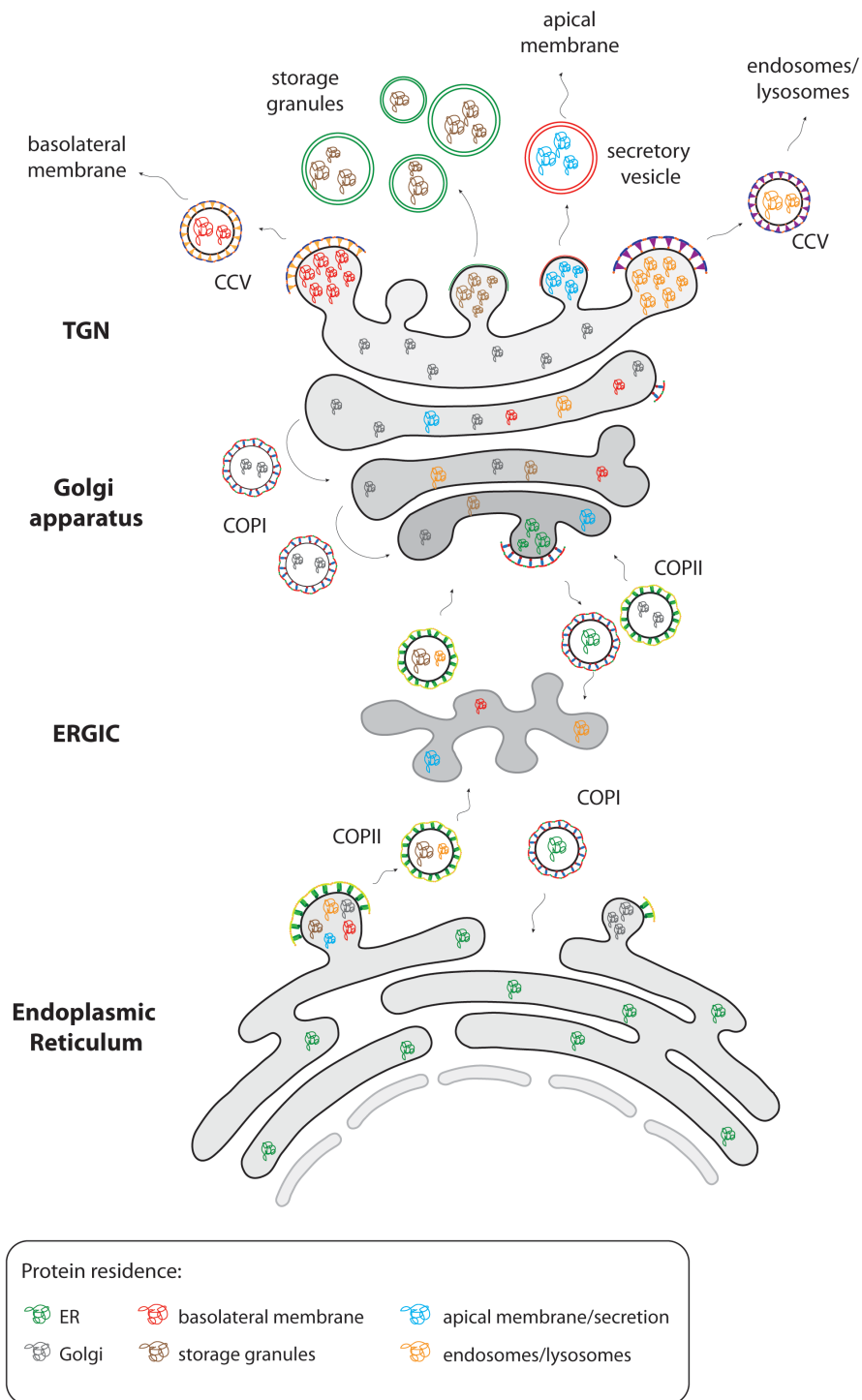
Figure 1: Scheme of the Secretory Pathway - the distribution trail of the cell. After translocation into the ER, correctly folded proteins, together with lipids, are packed into COPII vesicles and are transported across the ER-Golgi intermediate compartment (ERGIC) to the *cis*-face of the Golgi apparatus. By migrating through the different Golgi cisternae, proteins and lipids are further modified before they reach the *trans*-Golgi network (TGN). At the TGN, cargos are sorted into transport carriers, e.g. CCVs and transported to their final destination: to the basolateral or apical membrane, to endosomes and lysosomes or are stored in specific granules. Besides this anterograde transport, the retrograde trafficking of e.g. specific Golgi enzymes or ER-resident proteins is mediated by COPI vesicles. Abbreviations: ER (Endoplasmic Reticulum); COPI + II (coatomer protein complex I + II); CCV (clathrin-coated vesicles). Figure created according to Pakdel and von Blume 2018.

1.2   The Endoplasmic Reticulum

1.2.1   Protein translocation into the ER

As part of the Secretory Pathway, the Endoplasmic Reticulum (ER) has a multitude of functions, including protein and lipid synthesis, protein folding, modification or quality control (Alberts et al. 2002; Schwarz and Blower 2016).

Whereas lipids are *de novo* synthesized in the lumen of the ER, protein translation takes place in the cytoplasm of the cell. Therefore, around one third of all cellular proteins that are predestined for the Secretory Pathway initially have to translocate across the ER membrane (Alberts et al. 2002; Nyathi, Wilkinson, and Pool 2013; Reid and Nicchitta 2015). In this regard, most of the Secretory Pathway proteins carry a N-terminal signal peptide (SP) and are co-translationally translocated into the ER by interaction with the signal recognition particle (SRP) (Janda et al. 2010). Binding of SRP arrests protein translation and guides the translation machinery to the ER membrane, where it enters the compartment by proceeding translation (see Figure 2A) (Gilmore, Walter, and Blobel 1982; Halic and Beckmann 2005; Linxweiler, Schick, and Zimmermann 2017).

Alternatively, some proteins whose SPs are either to short or not sufficiently hydrophobic to be recognized by the SRP enter the ER post-translationally, after termination of protein translation (see Figure 2B). Accordingly, these fully synthesized polypeptides are protected by HSPs[1] that prevent aggregation and self-folding within the cytosol and furthermore transport them to the ER membrane (Craig 2018; Jan, Williams, and Weissman 2014; Johnson, Powis, and High 2013). In both processes, proteins enter the lumen of the ER through the translocon, a pore-forming Sec61/62/63 protein channel (Aviram and Schuldiner 2017; Linxweiler et al. 2017).

The insertion of transmembrane proteins into the ER is much more complex and can take place via both mechanisms: co-translationally via SRP that also recognizes transmembrane domains or post-translationally as shown for tail-anchored (TA) proteins. In this case, TA proteins are bound by TRC40[2], which transports the polypeptide to the ER membrane, where it interacts with receptors WRB[3] and CAML[4]. Subsequently, transmembrane proteins are

---

[1] HSP = Heat shock protein
[2] TRC40 = Transmembrane domain recognition complex 40 kDa
[3] WRB = Tryptophan-rich basic protein
[4] CAML = Ca^{2+}-modulating cyclophilin ligand

inserted into the membrane bilayer in a multi-step process (Daniels et al. 2003; Shao and Hegde 2011; Stefanovic and Hegde 2007; Yamamoto and Sakisaka 2012).
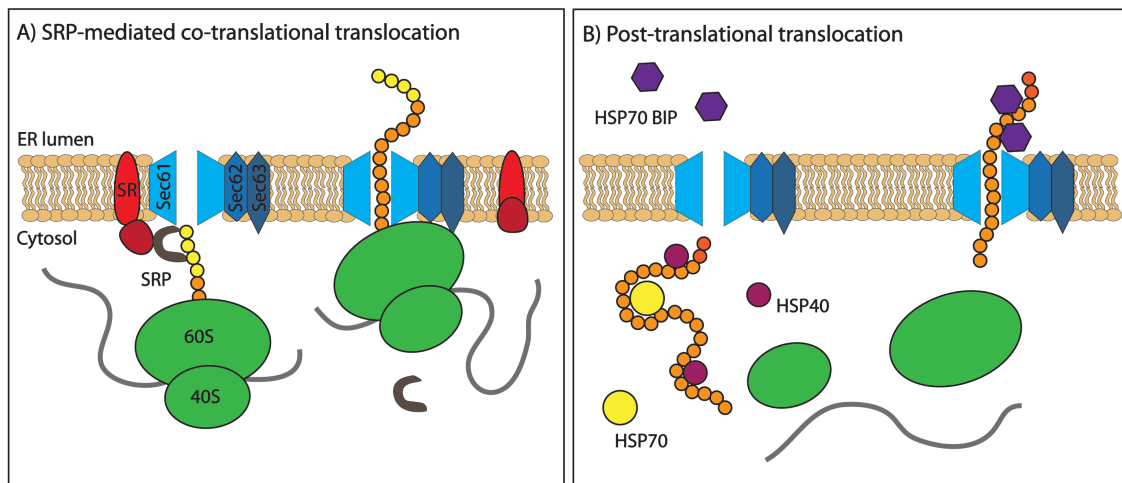
Figure 2: Protein translocation into the ER. (A) Proteins that enter the Secretory Pathway in a co-translational process are recognized by the signal recognition particle (SRP) in their emerging N-terminal signal peptide (SP, yellow). This interaction pauses the translation and brings the RNA-ribosome-polypeptide complex to the ER membrane. GTP-dependent interaction between SRP and the SRP receptor (SR) guides the translation machinery to the Sec61/62/63 pore-forming translocon complex. Upon GTP-hydrolysis, SRP and SR dissociate, translation proceeds and the protein is "pushed" into the lumen of the ER. (B) Post-translational translocation occurs after protein translation. Therefore, the protein is bound by heat shock proteins (HSPs), which prevent protein aggregation and folding in the cytosol. Similarly, these polypeptides are guided to the Sec61/62/63 translocon complex and enter the ER. Thereby luminal HSPs, e.g. HSP70 BIP are "pulling" the polypeptide through the channel into the lumen. Figure created according to Johnson et al. 2013 and Linxweiler et al. 2017.

1.2.2 Protein processing, modification and folding

To be functional, unfolded proteins that have entered the lumen of the ER have to be further processed, modified and folded. In this regard, the ER provides an optimal milieu with an incredible number of different enzymes and chaperones (Araki and Nagata 2012). Among them are the signal-peptidase complex, which cleaves the N-terminal SP from the protein or the membrane-bound OST[5] that transfers $Glc_3Man_9GlcNAc_2$ to asparagine residues in a specific Asn-x-Ser/Thr motif (with x as any amino acid, except of prolin) in around 90 % of all glycoproteins (Barlowe and Miller 2013; Bieberich 2014; Helenius and Aebi 2004). Furthermore, several (co)chaperones (e.g HSP70 BiP[6], HSP90, HSP40), oxidoreductases (e.g. PDI[7]) or peptidyl prolyl *cis*/*trans* isomerases (e.g. FKBPs[8]) act together in a very complex way, responsible for the modification, remodeling and folding of the protein (see Figure 3) (Blair et

---

[5] OST = Oligosaccharide transferase
[6] BiP = Binding immunoglobulin protein
[7] PDI = Protein disulfide isomerases
[8] FKBPs = FK506-binding proteins

al. 2015; Braakman and Bulleid 2011; Ellgaard et al. 2016; Ghartey-Kwansah et al. 2018; Gonzalez, Pal, and Narayan 2010; Simmen et al. 2010).
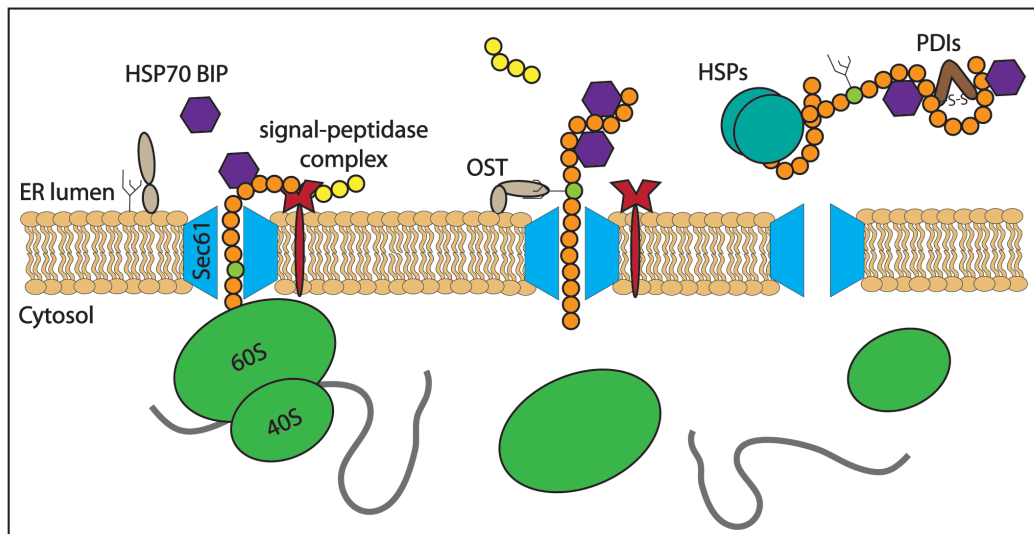
Figure 3: Processing, modification and folding of translocated proteins. Immediately after passing the Sec61 translocon, a multitude of ER enzymes are acting on the entering protein. In this regard the polypeptide is bound by heatshock proteins (HSPs), e.g. HSP70 BIP to prevent aggregation of hydrophobic regions and the signal peptide (SP, yellow) is cleaved by a specific signal-peptidase. Moreover, N-linked oligosaccharides are covalently attached on asparagine residues (light green) in a specific N-x-S/T motif, mediated in a single enzymatic step by the membrane-bound oligosaccharide transferase (OST). Overall, several other enzymes e.g. chaperons like HSPs that fold the protein or protein disulfide isomerases (PDIs) that form disulfide bonds ensure the correct native state of the protein. Figure created according to Barlowe and Miller 2013.

1.2.3   Protein quality control and degradation

For proper folding, proteins need a correct set of post-translational modifications, e.g. glycosylation or the formation of disulfide-bonds (Helenius 1994; Kosuri et al. 2012). However, besides its structural functions, glycosylation is also used to activate and control the folding process of the proteins in several rounds by the interplay of glucosidases, folding chaperons and glucosyltransferases (Helenius and Aebi 2004; Xu and Ng 2015). Hereof, the removal of terminal glucose residues from $Glc_3Man_9GlcNAc_2$ by GI and II[9] recruits the lectin-like ER chaperons CNX[10] and CRT[11] for protein folding (Araki and Nagata 2012). Subsequently, the glucosyltransferase UGGT[12] that controls the folding status of the polypeptide, re-glucosylates the N-glycans if necessary and passes the protein through another CNX/CRT folding cycle (Caramelo and Parodi 2008). Finally, correctly folded proteins are

---

[9] GI and II = Glucosidase I and II
[10] CNX = Calnexin
[11] CRT = Calreticulin
[12] UGGT = UDP-glucose:glycoprotein glucosyltransferase

processed by ERManI[13] that cleaves a mannose residue from the N-glycan (see Figure 4) (Xu and Ng 2015).
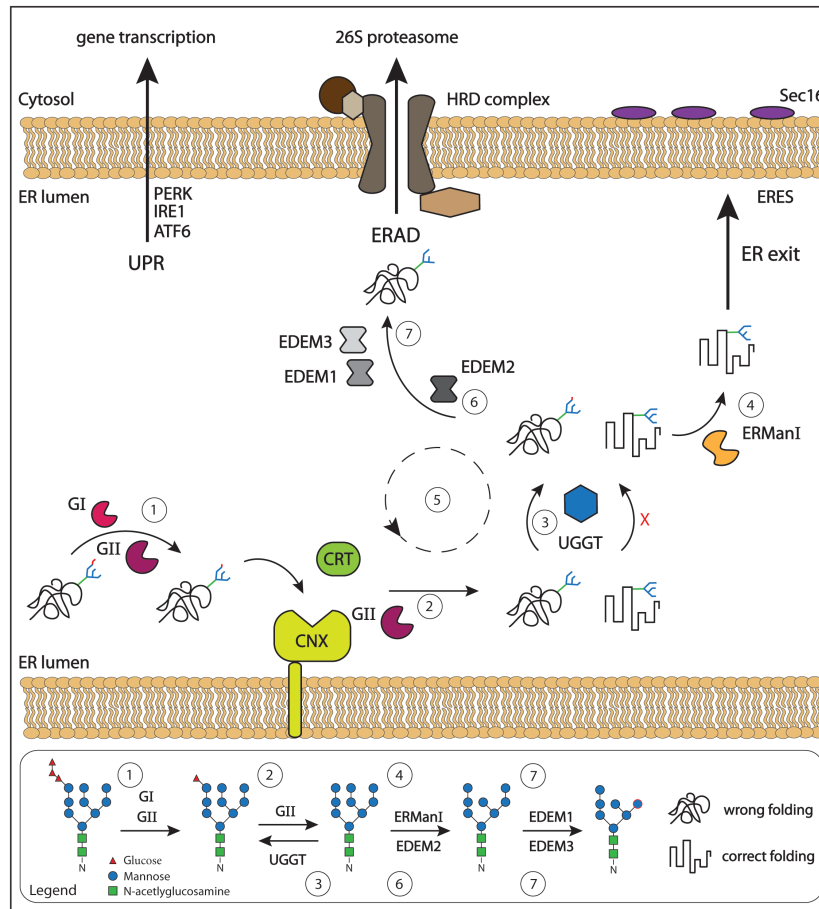
Figure 4: Protein quality control in the Endoplasmic Reticulum (ER). Protein folding can be controlled in a glycan-dependent way. (1) N-glycans of unfolded proteins are cleaved by glucosidase I and II (GI; GII), which recruits the lectin-like folding chaperons calnexin (CNX) and calreticulin (CRT) for folding, and GII for further processing (2). Subsequently, the glycosyltransferase UGGT controls the protein structure (3). In case of correct protein folding, N-glycans of those proteins are further trimmed by ER mannosidase I (ERManI) (4), which marks the proteins for ER exit and transport to the Golgi apparatus from special ER exit sites (ERES), positive for Sec16. In contrast, incorrectly folded proteins are re-glycosylated by UGGT and passing through another CNX/CRT- folding cycle (5). This cycle can be repeated several times (5). Finally, proteins that do not gain their native structure are degraded via ER-associated degradation (ERAD). Therefore, proteins are "marked" by clipping their mannose residues via EDEM2, EMED1 and 3 (6, 7). This is leading to a single α-1,6-linked mannose residue (highlighted red in legend), which is recognized by proteins of the HRD complex for degradation via the 26S proteasome. Additionally, ER stress due to overload of the ER folding capacity, actives the unfolded protein response (UPR), mediated via the ER-membrane proteins PERK, IRE1 and ATF6 that induce expression of proteins involved in folding and degradation. Abbreviations: UGGT (UDP-glucose:glycoprotein glucosyltransferase); EDEM (ER degradation-enhancing α-mannosidase-like protein); HRD (HMG CoA reductase); PERK (protein kinase R-like ER kinase); IRE1 (inositol-requiring enzyme 1); ATF6 (activating transcription factor 6). Figure created according to Xu and Ng 2015.

In contrast, the accumulation of unfolded or aggregated polypeptides is leading to ER stress, a condition where the folding capacity of the ER is saturated (Lin, Walter, and Yen 2008). This

---

[13] ERManI = Endoplasmic Reticulum mannosidase I

is crucial, as misfolding and structural defects are associated with many diseases e.g. Parkinson's and Alzheimer's disease (Valastyan and Lindquist 2014; Wang and Kaufman 2016). To overcome this problem, cells activate the unfolded protein response (UPR) - a series of mechanisms and signaling crosstalks that are involved in the activation of three major ER-membrane proteins; PERK[14], IRE1[15] and ATF6 [16]. Their aim is to downregulate the global protein synthesis, to increase the expression of relevant UPR proteins e.g. chaperons or glycosylation enzymes and to mediate the ER-associated degradation (ERAD) of misfolded or aggregated proteins (see Figure 4) (Hetz 2012; Liu and Kaufman 2003).

During ERAD, N-linked glycans of misfolded proteins are clipped by EDEM1[17] and EDEM3. As a consequence, these "marked" proteins are translocated back into the cytosol by passing through a membrane channel formed by the multi-spanning HRD[18] complex (Clerc et al. 2009; Xu and Ng 2015). In a multistep mechanism, proteins are polyubiquitinated and further degraded by the 26S proteasome (see Figure 4) (Wu, Rapoport, and Avenue 2018).

1.2.4   ER exit of proteins and lipids via COPII vesicles

However, as most of the proteins have achieved their correct modification and folding, non-resident ER proteins can be further transported along the Secretory Pathway via coatamer protein II (COPII) vesicles (see Figure 5) (Gillon, Latham, and Miller 2012).

In general, vesicular transport requires the recruitment of cargo molecules and coat components to the donor membrane, the formation and scission of the vesicle, followed by the transport and fusion of the carrier with an acceptor membrane (Bonifacino and Glick 2004; Guo, Sirkis, and Schekman 2014).

COPII vesicles that mediate cargo transport to the Golgi apparatus are forming at specific ER exit sites (ERES), positive for Sec16 (Kurokawa and Nakano 2019; Venditti, Wilson, and Matteis 2014). Here, the GTPase Sar1 that has been recruited to the ERES is activated by the guanine nucleotide exchange factor (GEF) Sec12, which in turn brings the inner coat components Sec23/Sec24 to the vesicle budding site (Hong 2005; Watson et al. 2006). Interaction of this heterodimer with membrane components and cargo proteins stabilizes the

---

[14] PERK = Protein kinase R-like Endoplasmic Reticulum kinase
[15] IRE1 = Inositol-requiring enzyme 1
[16] ATF6 = Activating transcription factor 6
[17] EDEM = ER degradation-enhancing alpha-mannosidase-like protein
[18] HRD = 3-hydroxy-3-methylglutaryl (HMG) CoA reductase

forming pre-budding complex and furthermore accumulates cargo molecules inside the forming vesicle (Miller et al. 2003; Sato and Nakano 2007).

As a next step, coat proteins induce membrane curvature to accomplish vesicle formation. In this regard, the outer coat components Sec13/Sec31 assemble, which results in the polymerization of the inner and outer coat to a cage-like structure that bends the lipid bilayer (Gillon et al. 2012; Jensen and Schekman 2011). After fission and transport along microtubules, COPII vesicles reach the ERGIC (in mammalian cells), where they are captured by tethering complexes e.g. TRAPPs[19] at the acceptor membrane (Lupashin and Sztul 2005; Sacher et al. 2001; Yu et al. 2006). Finally, vesicles fuse with the acceptor membrane upon SNARE[20] pairing between one SNARE complex that is located on the vesicle (v-SNARE) and three SNAREs on the target membrane (t-SNAREs). As a consequence, soluble cargo molecules are released into the ERGIC/*cis*-Golgi (Cai, Reinisch, and Ferro-novick 2007; Hong 2005).
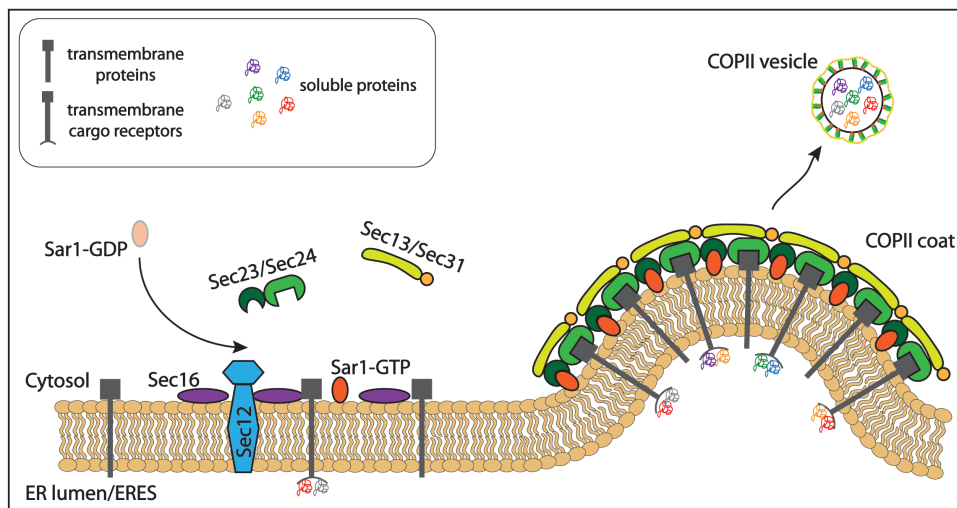
Figure 5: COPII vesicle formation at ER exit sites (ERES). Cargo molecules, destined for further transport to the Golgi apparatus are congregated at Sec16 positive ERES. After recruitment of the guanine exchange factor (GEF) Sec12 and the GTPase Sar1, Sar1 is activated upon exchange of GDP to GTP. This brings the inter coat proteins Sec23/Sec24 to the vesicle budding site, where they are interacting with cargo molecules and membrane components to further stabilize the pre-budding complex. As a next step, the outer coat proteins Sec13/Sec31 assemble, which leads to the oligomerization of the inner and outer coat proteins and the formation of the COPII vesicle. Finally, COPII vesicles bud off and are transported via microtubules to the ER-Golgi intermediate compartment or the *cis*-Golgi, where they fuse with the acceptor membrane after tethering and SNARE pairing (not shown). Abbreviations: COPII (coatomer protein complex II). Figure created according to Jensen and Schekman 2011.

---

[19] TRAPPs = Transport protein particles
[20] SNARE = Soluble N-ethylmaleimide-sensitive factor attachment protein receptor

1.2.5 Lipid synthesis and transport

In line with the results of this thesis, this introduction is predominately focusing on the transport, processing and sorting of proteins along the Secretory Pathway. Nevertheless, the ER is the main organelle for lipid synthesis, and lipids are essential for these processes (Fagone and Jackowski 2009; Jacquemyn, Cascalho, and Goodchild 2017). Besides their different functions, i.a. as signaling molecules or energy sources, lipids are also the main component of cellular membranes (Casares, Escrib, and Rossello 2019). Membrane lipids mainly grouped to sterols, sphingolipids and glycerophospholipids (GPLs), play an important structural role and are involved in the sorting of molecules and the formation of transport carriers by interacting with proteins (Coskun and Simons 2011; Harayama and Riezman 2018). Lipids within each group differ from each other as they vary in their fatty acid chain length or the amount and position of double bonds. The hydrophilic head groups of amphiphilic lipids can further be modified as seen for the five major mammalian GPLs - phosphatidylcholine (PC), phosphatidylethanolamin (PE), phosphatidylserine (PS), phosphatidylinositol (PI) and phosphatidic acid (PA) (van Meer and de Kroon 2011; Van Meer et al. 2008). As most organelles have a defined lipid composition that is necessary to maintain their cellular functions, not only proteins, but also lipids have to be distributed within the cell (Balla, Sengupta, and Kim 2019; Jackson et al. 2016).

In this regard, lipids can be transported to target membranes via vesicular and non-vesicular transport mechanisms (Funato, Riezman, and Muñiz 2019). Vesicular transport occurs as described above via COPII vesicles, whereas the non-vesicular lipid transfer is mediated by lipid transfer proteins (LTPs) mainly at membrane contact sites (MCS), which are formed between the ER and several organelles or the plasma membrane (PM) (Funato et al. 2019; Lev 2010, 2012). One of the most investigated LTPs are the members of the StART[21] family, which are involved in the lipid exchange between different organelles and different substrates, e.g. the ER to Golgi transport of ceramide, mediated by STARD11[22] (also named CERT[23]) (Alpy and Tomasetto 2005; Peretti et al. 2020).

---

[21] StART = Steroidogenic acute regulatory transfer
[22] STARDs = StAR-related lipid transfer protein 11
[23] CERT = Ceramide transfer protein

1.3 The ER-Golgi intermediate compartment

As mentioned by the name, the ERGIC was identified as a vesicular-tubular membrane complex that localizes between the ER and the *cis*-Golgi in mammalian cells (Appenzeller-Herzog and Hauri 2006). So far, the ERGIC is considered as an anterograde and retrograde sorting station, positive for the transmembrane cargo receptor ERGIC-53 that mediates sorting of soluble proteins into COPII vesicles at the ER (Barlowe and Helenius 2016; Saraste and Marie 2016). Together with other cargo receptors, ER-proteins or COPII v-SNARES, ERGIC-53 is recycled back to the ER via COPI vesicles, which form in a COPII vesicle-similar way but have different components e.g. coat protein subunits (α/β/β'/ε/γ/δ/ζ) or GTPase (Arf1) (Arakel et al. 2018). Therefore, these cargo proteins share specific motifs in their cytoplasmic tail or have a KDEL sequence for the interaction with KDEL receptors to be packed into COPI vesicles (Gao et al. 2014; Jackson 2014; Kirchhausen 2000b). In plant as well as yeast cells that do not have an ERGIC, the retrograde COPI vesicles bud off at the *cis*-Golgi (Linders et al. 2019; Neumann, Brandizzi, and Hawes 2003).

By contrast, non-ER cargo molecules that arrive at the ERGIC are further transported to the *cis*-Golgi. However, how these proteins reach the Golgi apparatus is controversial discussed and might occur via vesicle transport or membrane fusion events (Appenzeller-Herzog and Hauri 2006; Brandizzi and Barlowe 2013).

1.4 The Golgi apparatus

1.4.1 The composition of the Golgi apparatus

The Golgi apparatus embodies a highly dynamic and interconnected cellular organelle (Dröscher 1998; Golgi 1989; Presley et al. 1998). Besides its function in membrane transport - the main aspect in this thesis - the Golgi apparatus also plays an important role in cell growth, apoptosis or cell signaling (Zappa, Failli, and Matteis 2018). Therefore, it is noteworthy, that the Golgi apparatus structurally can highly differ between eukaryotic cells (Munro 2011b).

Originally and generally described, the Golgi apparatus consists of multiple piled disk-like compartments, the so-called cisternae that together form the Golgi stack. In mammalian cells, several of these stacks additionally can be interconnected with each other to a Golgi ribbon that localizes in the perinuclear region in close proximity to the microtubule-organizing

center (MTOC) (Klumperman 2011). In this regard, the cytoskeleton-network not only plays an important role in vesicle transport but also in positioning and structural support of the Golgi apparatus, e.g. by CLASP[24]-dependent microtubules that form around the Golgi membranes (Corthesy-Theulaz and Pfeffer 1992; Kulkarni-Gosavi, Makhoul, and Gleeson 2019; Miller et al. 2009; Sandoval et al. 1984). Furthermore, the Golgi complex is linked to the cytoskeleton-network e.g. via microtubule-associated proteins like GMAP-210[25] (Kulkarni-Gosavi et al. 2019; Munro 2011b).

To maintain its structural organization, the Golgi apparatus is additionally stabilized by a Golgi matrix, which includes i.a. Golgi-resident proteins of the GRASP[26] and golgin family (see Figure 6) (Barinaga-Rementeria Ramirez and Lowe 2009; Xiang and Wang 2011). GRASP55 and GRASP65, the first identified GRASPs, belong to a family of Golgi stacking factors, as they tether two facing Golgi membranes upon *trans*-dimerization, and so stabilize Golgi stacks and Golgi ribbons. Both are peripheral membrane proteins that attach to the Golgi membrane by myrostoylation of a glycine residue and interaction with golgins (Rabouille and Linstedt 2016). Golgins are large coiled-coil proteins that associate to the Golgi membrane via its C-terminus. This interaction can either be direct via intrinsic transmembrane domains or indirect via Rabs, ARL or ARF proteins that are recruited to the Golgi membrane (Short, Haas, and Barr 2005). Beside their functions in vesicle tethering, these proteins were also shown to have a structural role, e.g. Bicaudal-D that interacts with microtubule motor protein dynactin (Chia and Gleeson 2014; Hoogenraad et al. 2003; Munro 2011a). Overall, knockdown or depletion of golgins (e.g. golgin-97, golgin-160), Rabs (e.g. Rab2, Rab6), GRASPs (e.g. GRASP55, GRASP65) or motor proteins (e.g. dynein, dynactin) is leading to Golgi fragmentation with disperse stacks (Rabouille and Linstedt 2016; Yadav and Linstedt 2011).

Locally and functionally, the Golgi stack is divided into a *cis*-, medial-, and *trans*-Golgi, whereas every section has a distinct protein composition as well as a different pH and ion concentration, e.g. Ca^{2+} concentration (Kellokumpu 2019; Klumperman 2011; Li et al. 2013).

---

[24] CLASP = Cytoplasmic linker proteins-associated proteins
[25] GMAP-210 = Golgi microtubule-associated protein 210 kDa
[26] GRASPs = Golgi reassembly stacking proteins
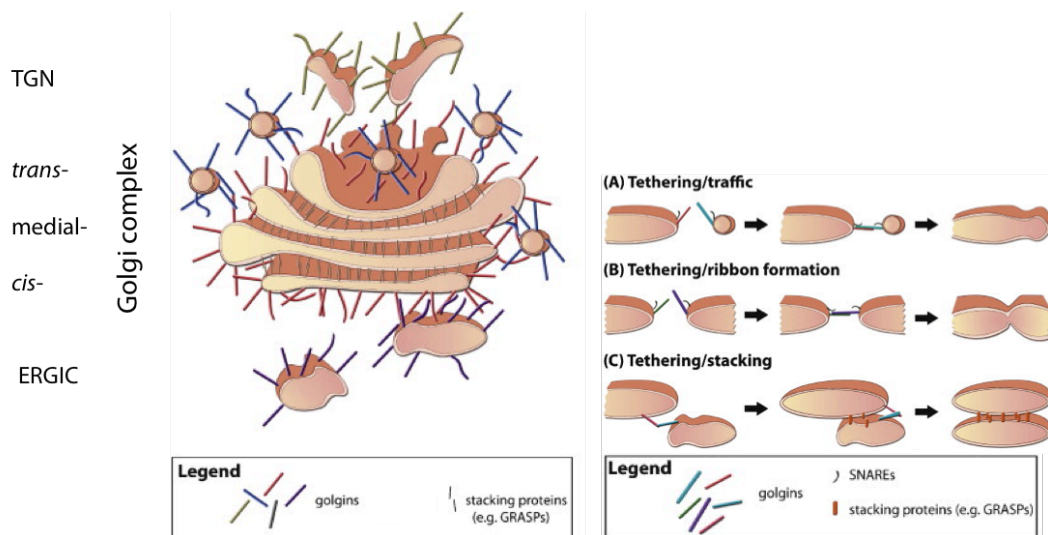
Figure 6: Structural composition of the Golgi apparatus. The Golgi complex, composed of a *cis*-/medial- and *trans*-part as well as the *trans*-Golgi network (TGN), is formed by several cisternae that are stacked together. To maintain its structural organization, the different cisternae are hold together by stacking proteins of e.g. the GRASP family. In addition, golgin tethering factors, which are C-terminally anchored in the Golgi membrane are essential for the highly dynamic character of the Golgi apparatus. By tethering of vesicles or other Golgi cisternae, golgins are involved in vesicle fusion, ribbon formation as well as Golgi stacking. Abbreviations: GRASPs (golgi reassembly and stacking proteins); ERGIC (ER-Golgi intermediate compartment). Figure adapted from Barinaga-Rementeria Ramirez and Lowe 2009.

Considering its function in membrane trafficking, cargo molecules that entering at the *cis*-part of the Golgi are transported through the medial-stack to reach the *trans*-Golgi and its *trans*-most cisterna, called the *trans*-Golgi network (TGN) (Day, Staehelin, and Glick 2013). This transport through the Golgi apparatus is highly regulated, as unique enzymes that differ from cisterna to cisterna further modify cargo molecules in a sequential manner (Jackson 2009). But how is this intra-Golgi transport facilitated?

1.4.2   Intra-Golgi transport - a mystery

Although, its known for a long time that the Golgi apparatus plays a key role in the modification, distribution and sorting of cargo molecules, the way how molecules are transported within the Golgi is highly debated in the field and to some extend still a mystery (Emr et al. 2009; Jamieson and Palade 1968; Marsh and Howell 2002; Pelham and Rothman 2000). Findings over the past decades led to different trafficking models, whereas all of them have strengths but also weaknesses (Emr et al. 2009). In the following, the three most prominent models are discussed.

Starting with the initially formulated one, the vesicle transport model postulates that the Golgi cisternae are stable compartments with a defined set of proteins and other factors that are required to modify cargo molecules (see Figure 7A). In this regard, the cargo itself moves from the *cis*-part of the Golgi to the TGN via anterograde vesicles that bud from a younger cisterna and fuse with the next one (Glick and Luini 2011). Therefore, due to its stable sub-compartments, this model explains the polarized character of Golgi stack with the distinct Golgi-resident proteins in each cisterna as well as the ion and pH gradient (Saraste and Prydz 2019). Moreover, secretory proteins have been identified in COPI vesicles and studies could also show that there are two different types of COPI vesicles in cells (Malsam et al. 2005; Orci et al. 1997; Ostermann et al. 1993). Hence, the vesicle transport model suggests, that COPI has a bidirectional role in vesicle trafficking and regulates retrograde transport, as well as the anterograde transport of secretory proteins between the Golgi cisternae. The observed different kinetics of cargo molecules can thereby be explained by different sorting and budding rates of COPI vesicles (Glick and Luini 2011). Interestingly, golgins like giantin or golgin-84 have been identified to tether intra-Golgi COPI vesicles (Gillingham and Munro 2016).

However, the contribution of COPI vesicles in anterograde transport has not been confirmed yet and hereof, it is also not clear how large cargo molecules, e.g. procollagen I (> 300 nm) can be sorted into COPI vesicles with a diameter of around 60-80 nm (Glick and Luini 2011; Stephens and Pepperkok 2002). Consistently, EM studies focusing on the intra-Golgi transport of procollagenI revealed that the extracellular matrix protein reaches the TGN without leaving the "*cis*-Golgi" (Bonfanti et al. 1998).

Thus and also because of lacking evidences, another model was suggested that could explain the intra-Golgi transport of large cargo proteins. The cisternal maturation model hypothesizes the gradual maturation of the *cis*-cisterna in a TGN compartment. In contrast to the vesicle transport model, not the cargo itself traverses the Golgi stack, rather the modifying enzymes and factors are exchanged via retrograde transport by COPI vesicles. These vesicles fuse with the younger cisterna and ensure successive cargo modification. Simultaneously, arriving COPII vesicles or ERGIC compartments homotypically fuse and generate the "new" *cis*-cisterna (Glick and Luini 2011). In line with the model, Golgi-resident as well as specific enzymes have been identified in COPI vesicles and Golgi-maturation was visualized in *S. cerevisiae*, using fluorescence proteins (Casler et al. 2019; Martínez-Menárguez et al. 2001). Contradictory, this model cannot explain the different kinetics of secretory proteins in intra-

Golgi transport as well as their different rates in Golgi export that have been demonstrated. Moreover, it is questionable if COPI vesicles are able to transport a significant amount of glycosylation enzymes between the cisternae (Glick and Luini 2011; Kweon et al. 2004; Orci et al. 2000).

As a result, scientist came up with an extended version of the cisternal maturation model, where Golgi cisternae are additionally linked by heterotypic tubules (see Figure 7B). These tubules enable the fast anterograde transport of cargo proteins across the Golgi apparatus as well as the exchange of Golgi-resident proteins and glycosylation enzymes, in addition to COPI vesicles (Emr et al. 2009; Glick and Luini 2011). So far, this model accommodates most of the recent findings and critical questions.
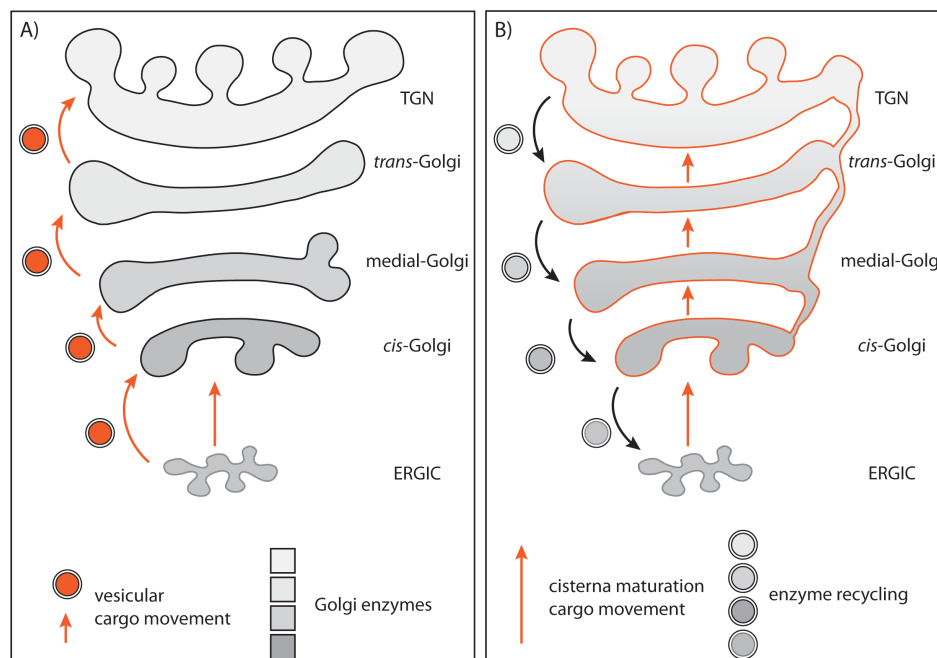
Figure 7: The intra-Golgi transport - two potential models. To reach the TGN, cargo molecules have to traverse through the Golgi apparatus. A) The anterograde vesicular transport model postulates that the Golgi cisternae are stable compartments with a defined set of enzymes and co-factors (grey scale). Therefore, cargo molecules are transported from one cisternae to another via a specific class of COPI vesicles, responsible for the anterograde transport (orange vesicles). B) In contrast, the cisternal maturation model with heterotypic tubules suggests that cargo molecules stay within a cisterna that matures from a "*cis-*" to a "*trans-*" cisterna (orange). In this case, enzymes and co-factors are exchanged by retrograde COPI vesicles (grey vesicles). Additionally, heterotypic tubules between cisternae allow the fast transport of cargo molecules as well as of Golgi enzymes. Abbreviations: ERGIC (ER-Golgi intermediate compartment); TGN (*trans-*Golgi network). Figure created according to Glick and Luini 2011.

However, as the Golgi apparatus structurally differs between yeast, plant but even within mammalian cells, the overall existence and function of these heterotypic tubules is also debated and is again leading to variations and modifications of this model, which will not be

further discussed (Glick and Luini 2011; Martínez-Menárguez et al. 2001; Munro 2011b). In summary, the critical evaluation of all this models highlighted that besides secretory cargo molecules that have to reach the TGN to be further distributed, models of the intra-Golgi transport also have to explain how these cargo molecules gain their proper post-translational modification.

1.4.3   Post-translational modification and lipid synthesis in the Golgi complex

The Golgi apparatus contains a multitude of different enzymes that are involved in lipid synthesis as well as protein modification, including: acetylation, methylation, palmitylation, proteolytic cleavaging, sulfation, glycosylation and phosphorylation. Since protein maturation and lipid biogenesis are essential for cellular functions, defects in these processes are associated with several human diseases (Hannun and Obeid 2018; Potelle, Klein, and Foulquier 2015; Wang, Peterson, and Loring 2014). In scope of this thesis, it will further be focused on sphingolipid synthesis, substrate glycosylation and protein phosphorylation.

1.4.3.1   (Glyco)Sphingolipid biogenesis

The ER is responsible for the *de novo* synthesizes of lipids, such as cholesterol or glycerol phospholipids, however, some of these molecules are additionally transported to the Golgi apparatus, where they are further modified (van Meer and de Kroon 2011; Van Meer et al. 2008). Therefore, the Golgi apparatus turned out to be the main organelle for the synthesis of sphingomyelin (SM) and highly complex glycosphingolipids, both derived from ceramide as a common precursor (Fang, Rivas, and Bankaitis 1998). Ceramide, which is generated in the ER, reaches the Golgi complex either non-vesicular via LTPs (see 1.2.5) or to a smaller amount via vesicular transport (Funato et al. 2019). In a single enzymatic step, ceramide is metabolized to SM and diacylglycerol (DAG) by the Golgi-localizing SM synthase (SMS) that transfers a phosphocholine head group from PC to ceramide. Aside from that, SM is "re-converted" to ceramide by the activity of the sphingomyelinase (SMase) (Hannun and Obeid 2008).

According to the different sphingoid base lengths and types, double bonds, the hydroxylation status, the N-Acyl chain type or the head group, lipids gain a huge chemical and structural diversity. Furthermore, this is even more complex, as the Golgi apparatus is responsible for

the glycosylation of sphingolipids to highly branched glycolipids (see below) (Harayama and Riezman 2018).

1.4.3.2 Glycosylation in the Golgi apparatus

Although glycosylation initially occurs in the ER (see 1.2.2) and assures e.g. correct folding of the protein, the Golgi apparatus is considered as the main organelle for protein and lipid glycosylation (Reily et al. 2019).

As a general mechanism, high nucleotide sugars that have been synthesized in the cytoplasm are transported into the lumen of the Golgi cisternae by sugar transporters. Here, more than 200 different type-II membrane-bound glycosyltransferases (GTs) add these sugars specifically to substrates. Moreover, several glycosidases can remove sugars from existing sugar chains. Based on the huge variety of GTs and glycosidases that act in different Golgi cisterna, the successive addition and removal of glycans can result in complex structures with more than 200 linked sugars (Reynders et al. 2011; Stanley 2011).

Besides N-linked glycosylation, three other forms of protein glycosylation in the Golgi apparatus have been described, namely O-glycosylation of hydroxyl groups of serine, threonine, hydroxylysine and tyrosine; C-mannosylation of the C2 atom of tryptophane and Glypiation that covalently links the GPI[27]-anchor to a protein (Coussen et al. 2001; Reily et al. 2019; Zhang and Wang 2016). Similarly, not only proteins but also lipids are glycosylated by glycolipid glycosyltransferases (GGTs) to lactosylceramide (LacCer) and other complex glycolipids (Fang et al. 1998; Kopitz 2017; Maccioni 2007).

Overall, the glycosylation of proteins and lipids is a highly regulated process and allows the fine-tuning of substrates. This is essential for a variety of cellular functions, as it mediates i.a. substrate stability, cell signaling, protein-protein/protein-lipid interactions and recognition (Varki et al. 2009, 2015).

1.4.3.3 Golgi-mediated protein phosphorylation by Fam20C

Phosphorylation is one of the most abundant post-translational protein modification and involved in several cellular mechanisms, including signaling pathways, growth, differentiation, membrane trafficking and much more (Ubersax and Ferrell 2007). Since it is fast, sensitive and also reversible due to the activity of phosphatases, phosphorylation allows the activation or deactivation of proteins, according to an extra- and intracellular stimulus

---

[27] GPI = Glycosylphosphatidylinositol

(Ardito et al. 2017; Nishi, Shaytan, and Panchenko 2014). Hence, it is not surprising that approximately 30 % of all human proteins contain at least one phosphorylation site and that the human "kinome" comprises more than 500 different kinases, encoded by around 2 % of the human genome (Jiménez et al. 2007; Ubersax and Ferrell 2007).

Although the secreted milk protein casein was the first detected phosphoprotein, it is astonishing that it took more then 100 years to identify Fam20C[28], the kinase that is responsible and able to enter the Secretory Pathway. To date, only a very few Secretory Pathway kinases are known, e.g. VLK[29] or Fam198 A and B[30] and most of them have not been characterized so far (Sreelatha, Kinch, and Tagliabracci 2015; Tagliabracci et al. 2015). In the scope of this thesis I will further focus on the Golgi-kinase Fam20C.

Fam20C is ubiquitously expressed and encoded by the *DMP4*[31] gene. The kinase was identified by a genomic screen, searching for proteins with a sequence similarity to Fjx1[32], the human orthologous of a known *D. melanogaster* Secretory Pathway kinase Fjx. This resulted i.a. in three members of a Family of proteins with the sequence similarity of 20 residues; Fam20A, Fam20B, Fam20C (see Figure 8A). Whereas Fam20A was mentioned as a pseudo-kinase and does not show any kinase activity, Fam20B is a sugar kinase that phosphorylates xylose within the tetrasaccharide linker region of proteoglycans (Cui et al. 2015; Koike et al. 2009).

Contrary, Fam20C was confirmed as a serine/threonine kinase that localizes in the Golgi apparatus, but is also secreted from cells. In this regard, Fam20C carries an N-terminal SP to enter the secretory pathway as well as Golgi-typical N-linked glycosylation on three sites (N101, N335, N470, see Figure 8C). Glycosylation might be important for folding, since mutation of asparagine residues inhibits protein secretion and kinase activity. Furthermore, five disulfide bonds as well as its autophosphorylation have been predicted, albeit without any functional verification (Sreelatha et al. 2015; Tagliabracci et al. 2012, 2015; Tagliabracci, Pinna, and Dixon 2013).

---

[28] Fam20C = Family with sequence similarity 20, member C
[29] VLK = Vertebrate lonesome kinase
[30] Fam198 A and B = Family with sequence similarity 198, member A and B
[31] DMP4 = Dentin matrix protein 4
[32] Fjx1 = Four jointed box 1
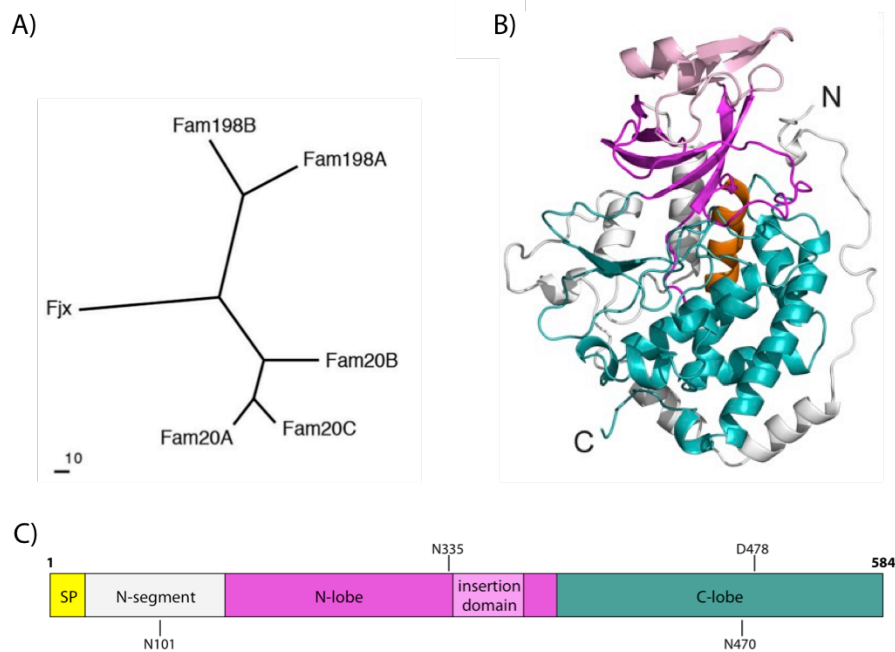
Figure 8: Fam20C an atypical protein kinase in the Secretory Pathway. A genomic screen of Fjx identified Fam20C. A) The phylogenetic tree shows the relationship of Fam20C to other kinase members. The tree was build with MOLPHY using distances (-J option) calculated from alignments of human sequences. B) The ribbon diagram shows the Fam20 protein structure of *C. elegans* (ceFam20). The atypical protein kinase shows a two-lobe structure consisting of a N-lobe (magenta) and a C-lobe (teal). The insertion domain (pink) caps the N-lobe, whereas the N-segment wraps around the C-lobe. The α6 helix (orange), important for kinase activity, is untypically locates in the C-lobe. C) Schematic representation of the human Fam20C kinase using the same color code as in B). Fam20C carries a N-terminal signal peptide (SP, yellow), which is cleaved in the ER. Fam20C is N-glycosylated on three asparagine residues (N101, N335 and N470) and has a "DFG" metal binding site (aspartic acid) at position D478 (human). Abbreviations: Fjx (four-jointed box). Figure adapted from Tagliabracci et al. 2015 and Xiao et al. 2013.

Structural analysis of the *C. elegans* orthologous ceFam20 revealed that ceFam20 shows an atypical protein kinase-like fold, similar to some prokaryotic kinases e.g. HipA[33], CtkA[34] and AFK[35]. Indeed, ceFam20 forms a protein kinase typical two-lobe structure, consisting of an N-lobe and a C-lobe, however especially the C-lobe differs from genuine protein kinases, as it has no scaffolding αF helix and no GHI subdomain - normally involved in protein-protein interactions and allosteric regulation (see Figure 8B). The catalytic domain (ce = D366, human = D478) as well as a variant of the DFG motif, important for metal-ion binding, are localized in the C-lobe. The N-lobe of ceFam20 is more similar to eukaryotic kinases, however, it is lacking the αC helix (here α6) - a hallmark of protein kinases as it regulates activity. In ceFam20 the αC helix is predominately located in the C-lobe and might have a different function. Additionally, ceFam20 shows some unique domains as a Fam20-specific

---

[33] HipA = High persistence factor A
[34] CtkA = Cell translocating kinase A
[35] AFK = Actin-fragmin kinase

loop that mediates substrate specificity and a shell-like structure consisting of an N-terminal segment and an insertion domain that are surrounding the two lobes. Hereby, the N-terminal segment is wrapping around the C-lobe and forms a base, whereas the insertion domain caps the N-lobe. The ATP-binding pocket of ceFam20 is located in the cleft between N- and C-lobe and is protected by the $\beta 1$-$\beta 2$ loop together with insertion domain (Sreelatha et al. 2015; Tagliabracci et al. 2015; Xiao et al. 2013).

Fam20C specifically phosphorylates serine and threonine within an **S/T**-x-E or less frequent within a **S**-X-Q-X-X-D-E-E motif (with x as any amino acid). In addition to casein, Fam20C phosphorylates more than 100 secreted phosphoproteins, among them soluble secreted Ca^{2+}-binding proteins of the SIBLING[36] family; OPN[37], DMP1[38], BSP[39], DSPP[40] and MEPE[41] (Tagliabracci et al. 2012, 2015). Phosphorylation of SIBLING proteins regulates precipitation of calcium phosphate in form of e.g. hydroxylapatite. Therefore, members of this family play important roles in formation and mineralization of dentin, bone and cementum (Chen et al. 2008; George and Veis 2008; Gericke et al. 2005; Xie et al. 2014). Along with this, biallelic mutations in Fam20C cause a rare osteosclerotic bone dysplasia, called Raine syndrom. In most cases, carrier of this autosomal recessive disease die as newborns, whereas patients with a "mild" and non-lethal phenotype develop severe clinical phenotypes as exophthalmos, osteosclerosis, cerebral calcification, enamel deformation, stenosis or hearing loss (Elalaoui et al. 2016; Sheth et al. 2018; Vishwanath, Srinivasa, and Shankar 2014). Furthermore, bone lesions as well as dental abnormalities have also been reported in Fam20C-KO mouse models (Liu et al. 2017; Wang et al. 2012). However, phosphorylation is not limited to Ca^{2+}-binding proteins. Overall, more than 75 % of all secreted phosphoproteins carry a typical Fam20C phosphorylation motif, herein factors involved in wound healing, cell migration or membrane-bounded vesicle formation (Tagliabracci et al. 2012, 2015).

Interestingly, Fam20C prefers Mn^{2+} over Mg^{2+} as a cofactor and was shown to form a heterotetramer with Fam20A, which stabilizes the kinase and might influence its activation and secretion (Cui et al. 2015; J. Cui et al. 2017; Nalbant et al. 2005; Ohyama et al. 2016; Sreelatha et al. 2015; H. Zhang et al. 2018). In addition to that, several sphingolipids have been illustrated that drive Fam20C activity (Cozza et al. 2015, 2017). Nevertheless, this has to be further investigated.

---

[36] SIBLING = Small integrin-binding ligand, N-linked glycoprotein
[37] OPN = Osteopontin
[38] DMP1 = Dentin matrix protein 1
[39] BSP = Bone sialoprotein
[40] DSPP = Dentin sialophosphoprotein
[41] MEPE = Matrix extracellular phosphoglycoprotein

Besides secreted proteins, recently published paper could also confirm that Fam20C phosphorylation affects proteins within the Secretory Pathway and so has intracellular regulatory function. An example is the phosphorylation of Ero1α[42], which is involved in oxidative folding in the ER. According to hypoxia and reductive stress, Ero1α is transported to the Golgi, phosphorylated by Fam20C, which increases its redox activity and again retrograde-transported to the ER. As a result, Fam20C tunes ER redox homeostasis and protein folding (J. Zhang et al. 2018). Interestingly, Ero1α might additionally regulate Ca^{2+} homeostasis by regulating Ca^{2+}-influx and -efflux (Anelli et al. 2012; Li et al. 2009; Marino et al. 2015). Since many Fam20C substrates play a role in Ca^{2+} homeostasis, and Ca^{2+}-regulated cargo transport is the scope of this thesis, the next chapter will focus on Ca^{2+} homeostasis in the Secretory Pathway, especially in the Golgi apparatus.

1.4.4 Ca^{2+} in the Golgi complex

Ca^{2+} is one of the most important signaling molecules and essential for many cellular processes, including cell proliferation, development, motility or secretion (Kahl and Means 2003). According to the multiple responses Ca^{2+} elicits, the cell has to tightly regulate its availableness (Berridge, Lipp, and Bootman 2000). Therefore, especially the ER but also other organelles as the Golgi apparatus function as Ca^{2+}-storage compartments with luminal Ca^{2+} concentrations of up to 2 mM, thereby reaching four orders of magnitude above cytosolic Ca^{2+} levels (Alonso et al. 2017a; Prins and Michalak 2011). Upon external and internal stimuli, Ca^{2+} can be released into the cytoplasm via Ca^{2+}-channels or exchanged with other organelles via MCS (Burgoyne, Patel, and Eden 2015; Prinz 2014; Shah, Chagot, and Chazin 2006). Nevertheless, the Ca^{2+}-storage of the Golgi apparatus might have other functions and be independent from the ER, or Sarcoplasmic Reticulum (SR) in muscle cells, as depletion of Ca^{2+} in one organelle did not affect Ca^{2+}-release of the other (Canato et al. 2010; Yang et al. 2015). In this regard, Golgi Ca^{2+}-depletion was shown to change morphology of Golgi cisternae and is leading to a more vesicular and fragmented structure (Lissandron et al. 2010). Additionally, several studies could confirm that Ca^{2+} homeostasis in the Golgi apparatus is crucial for intra-Golgi cargo transport as well as the cargo export at the TGN (Blank and von Blume 2017; Chen, Ahluwalia, and Stamnes 2002; Kienzle et al. 2014; Micaroni et al. 2010; Mikhaylova et al. 2009; Porat and Elazar 2000). Interestingly, the Secretory Pathway forms out

---

[42] Ero1α = ER oxidoreductin 1α

a Ca^{2+}-gradient, from high Ca^{2+} concentrations in the ER to low Ca^{2+} concentrations in the TGN and secretory vesicles, which even differs between neighboring cisternae (see Figure 9) (Pizzo, Lissandron, and Pozzan 2010). As a consequence, the Golgi apparatus is meticulously regulating its luminal Ca^{2+} levels by Ca^{2+}-pumps, Ca^{2+}-release channels and Ca^{2+}-binding proteins (Li et al. 2013; Pizzo et al. 2011).
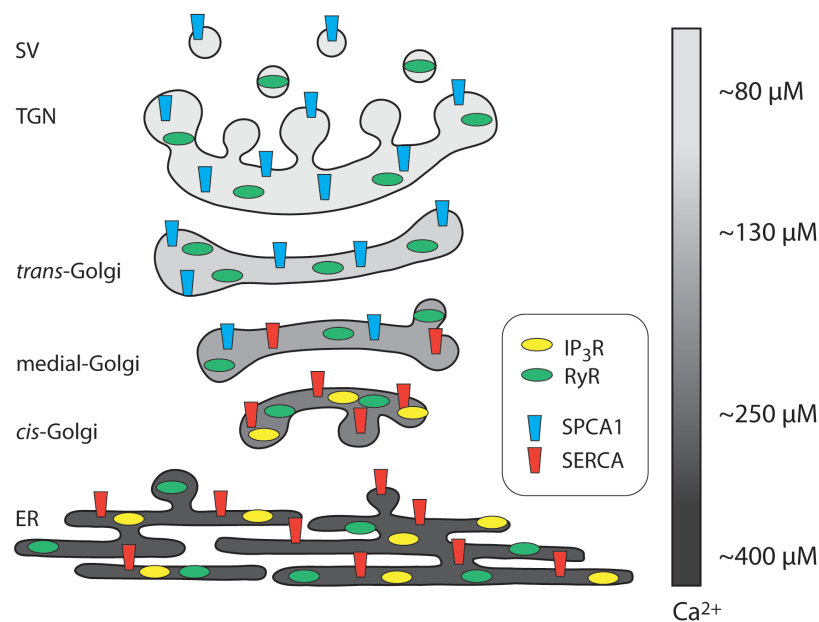
Figure 9: The Ca^{2+}-gradient across the Secretory Pathway. The Ca^{2+} level differs between compartments, from high Ca^{2+} concentrations in the Endoplasmic Reticulum (ER - 400 µM) to low Ca^{2+} concentrations in the *trans*-Golgi network (TGN) and secretory vesicles (SV - 80 µM). To maintain and control Ca^{2+} homeostasis, Ca^{2+}-pumps (SPCA1 and SERCA) and Ca^{2+}-release channels (IP3R and RYR) localize at each compartment/cisternae. Abbreviations: SPCA1 (Secretory Pathway Ca^{2+}-ATPase 1); SERCA (Sarco/Endoplasmic Reticulum Ca^{2+}-ATPase); IP3R (inositol 1,4,5-trisphosphate receptor); RyR (ryanodine receptor). Figure created according to Pizzo et al. 2011.

1.4.4.1   Golgi Ca^{2+}-pumps

Ca^{2+}-influx into the lumen of the Golgi cisternae is mediated by specific P-type Ca^{2+}-ATPases. These Ca^{2+}-pumps transport Ca^{2+} against an electrochemical gradient across the Golgi membrane in an ATP-consuming manner. In mammalian cells, three of these P-type Ca^{2+}-ATPases have been described. SERCA[43] and SPCA[44] are both localizing in the Secretory Pathway and have some overlapping compartments in the Golgi apparatus. However, SERCA is mainly localizing to the ER/SR and *cis*-part of the Golgi complex, whereas SPCA was found more in the medial- and *trans*-Golgi (see Figure 9). The third one, PMCA[45], pumps Ca^{2+} into

---

[43] SERCA = Sarco/Endoplasmic Reticulum Ca^{2+}-ATPase
[44] SPCA = Secretory Pathway Ca^{2+}-ATPase
[45] PMCA = Plasma membrane Ca^{2+}-ATPase

the extracellular space. All three Ca^{2+}-ATPases have similar membrane topology with N- and C-terminus facing the cytoplasm, ten transmembrane domains and four cytosolic loops - containing a nucleotide domain (N-domain), a phosphorylation domain (P-domain) and an actuator domain (A-domain). Furthermore the pumps share the principle reaction mechanism, a process that involves two conformational states E1 and E2 (Brini and Carafoli 2009; Gong et al. 2018; Pizzo et al. 2011).

In the E1 state, Ca^{2+} binds to polar and negatively charged residues in the transmembrane domain, followed by ATP that is binding to the cytosolic N-domain of the ATPase. Upon conformational change, which traps Ca^{2+}, the P-domain is auto-phosphorylated (referring to P-type) by transferring the γ-phosphate from the ATP to a highly conserved aspartate residue, using Mg^{2+} as a cofactor. As a result, ADP dissociates, which switches the ion-pump in a low energy, low affinity E2 state and releases the Ca^{2+} into the lumen of the Golgi. Hereby, binding of counter-ions at the luminal site is possible for some ATPases. Finally, the TGE-loop in the A-domain catalyzes the dephosphorylation of the aspartyl-phophosphoanhydride in the P-domain by coordinating the nucleophilic attack of H_2O. Release of the P_i group brings the ATPase back to the E1 state for a new cycle (see Figure 10) (Apell 2004; Bublitz, Morth, and Nissen 2012; Jensen et al. 2006; Kühlbrandt 2004).
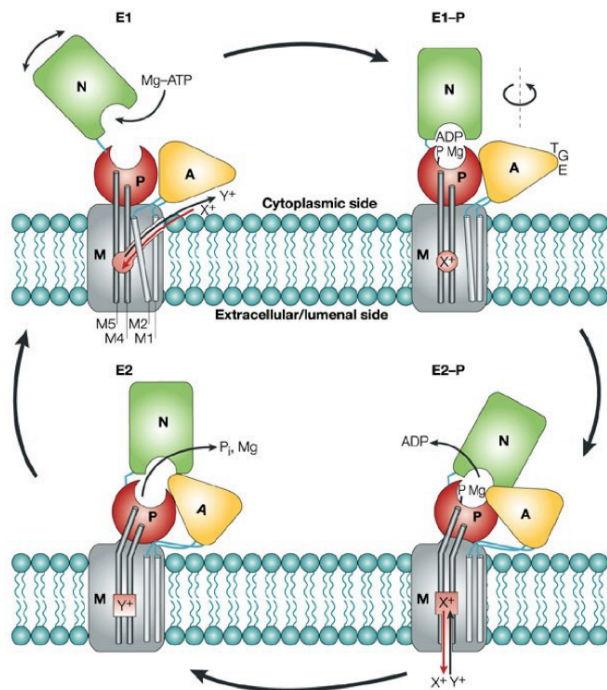
Figure 10: Scheme of the reaction cycle of P- type ATPases. In the E1 state the ATPase binds cytosolic Ca^{2+} (X^+) with high affinity in its transmembrane domain (M). After binding of ATP in the N-domain (N), auto-phosphorylation of the P-domain (P) is leading to a conformational change (E1-P). ADP dissociates and Ca^{2+} is released into the lumen (E2-P). At this stage, some ATPases are able to bind luminal counter-ions (Y^+). Upon A-domain-mediated dephosphorylation of the P-domain (via the TGE motif), Pi as well as Mn^{2+} is released and the ATPase goes back into the E1 state, ready for another ion-translocation-cycle. Abbreviations: N (nucleotide domain), P (phosphorylation domain), A (actuator domain); Pi (inorganic phosphate). Figure adapted from Kühlbrandt 2004.

By comparing the two Secretory Pathway Ca^{2+}-pumps, SERCA has two Ca^{2+}-binding sites and transfers two Ca^{2+}-ions at a time, while SPCA according to a mutation in one binding site only pumps one Ca^{2+}-ion. In comparison to SERCA, SPCA has not shown transport of counter-

ions from the lumen of the Golgi into the cytosol but shows a roughly 10-fold higher Ca^{2+}-affinity (Brini and Carafoli 2009; Clarke et al. 1989; Dode et al. 2005, 2006; Toyoshima et al. 2000). SERCA is expressed in three different isoforms; SERCA 1, SERCA 2 and SERCA 3, but can have several different splicing variants, thereby showing tissue-specific expression.

SPCA in addition to Ca^{2+} also pumps Mn^{2+}, which is cofactor of many glycosylation enzymes. Since cytosolic Mn^{2+} is toxic, SPCA is involved in detoxification (Leitch et al. 2011; Lissandron et al. 2010). There are two different isoforms of SPCA and several splicing variants. SPCA1 is ubiquitously expressed, whereas SPCA2 expression is restricted to mucus-secreting cells (Vandecaetsbeek et al. 2011). Overall, Ca^{2+}-regulation of SPCA1 was revealed to play a role in Ca^{2+}-dependent cargo sorting in the TGN, which will be further discussed in chapter 1.5.4 (Blank and von Blume 2017; Kienzle and von Blume 2014; Pakdel and von Blume 2018).

1.4.4.2 Golgi Ca^{2+}-release channels

Ca^{2+}-signaling involves the rapid increase of the cytosolic Ca^{2+} levels. According to an external or internal stimulus, cells are able to uptake Ca^{2+} from the extracellular space or release it from intracellular storage compartments as the ER or Golgi complex. Therefore, electrical, hormonal or mechanical stimulation is transmitted into the generation of secondary messengers e.g. IP_3[46], cADPR[47] or NAADP[48] that bind and open Ca^{2+}-channels. One of the best-described examples is the IP_3 signaling pathway: In a cascade of events, activation of membrane receptors like heterotrimeric GPCRs[49] or rTKs[50], activates PLC[51], which cleaves PIP_2[52] into DAG[53] and IP_3, which in turn is able to bind and activate the tetrameric IP_3R[54] - a Ca^{2+}-channel (Bootman 2012; Lissandron et al. 2010; Thatcher 2010). However, binding of IP_3 is not enough to release luminal Ca^{2+}. In a process called Ca^{2+}-induced Ca^{2+}-release (CICR), luminal or cytosolic Ca^{2+} is able to bind to IP_3R and regulate the sensitivity of IP_3R towards IP_3. This allows the cell to meticulously control Ca^{2+}-release and uptake (Bootman 2012; Taylor and Tovey 2010). IP_3R predominately localizes to the ER, *cis-* and medial-part of the Golgi (see Figure 9), similar to the localization of SERCA (Pizzo et al. 2011).

---

[46] IP_3 = Inositol 1,4,5-trisphosphate
[47] cADPR = Cyclic adenosine diphosphate ribose
[48] NAADP = Nicotinic acid adenine dinucleotide phosphate
[49] GPCRs = G-protein coupled receptors
[50] rTKs = Receptor tyrosin kinases
[51] PLC = Phospholipase C
[52] PIP_2 = Phosphatidylinositol 4,5-bisphosphate
[53] DAG = Diacylgcerol
[54] IP_3R = Inositol 1,4,5-trisphosphate receptor

For quite a long time, IP$_3$P was the only Ca^{2+}-release channel that has been identified in the Golgi apparatus. However, recent work could reveal that in some cells another ER-known Ca^{2+}-release channel, RyR, locates at the Golgi complex (Gallegos-Gomez et al. 2018; Pizzo et al. 2011). Regulation of RyR[55] is highly complex and involves ions, receptors and luminal proteins like: Mg^{2+}, DHPR[56], PKA[57] or FKBP (Lanner et al. 2010). Studies could also show that activation of RyR underlies secondary messenger Ca^{2+} (CICR) and cADPR (Gerasimenko et al. 2005; Ogunbayo et al. 2011; Partida-Sanchez et al. 2001). Overall, further studies are necessary to elucidate the roles and exact mechanisms of Ca^{2+}-release channels in the Golgi apparatus.

1.4.4.3   EF-hand Ca^{2+}-binding proteins in the Golgi apparatus

Besides the described Ca^{2+}-ATPases and Ca^{2+}-release channels that regulate Golgi Ca^{2+}-influx and -efflux, luminal proteins as well play an important role in organelle Ca^{2+} homeostasis. In the lumen, most of the luminal Ca^{2+} is not free, but buffered by Ca^{2+}-binding proteins (Brini and Carafoli 2009; Pizzo et al. 2010). So far, four different luminal Ca^{2+}-binding proteins have been detected in the Golgi apparatus; calumenin, NUCB1 (also named calnuc), NUCB2 (also named p54/NEFA[58]) and Cab45[59] (Dolman and Tepikin 2006; Pizzo et al. 2011). All of them carry EF-hand domains, a helix-loop-helix structure that mediates Ca^{2+}-binding in its loop structure with a pentagonal bipyramidal binding pocket (see Figure 11A) (Bhattacharya, Bunick, and Chazin 2004). EF-hand proteins were shown to be the most common Ca^{2+}-binding proteins. Hereby, the number of EF-hand motifs, the affinity to bind Ca^{2+} (from 10^{-6} M to 10^{-3} M) as well as the binding capacity differs from protein to protein. Accordingly, these proteins have different functions, e.g. as high capacity Ca^{2+}-buffer proteins or sensitive Ca^{2+}-sensors (Bagur and Hajnoczky 2017; Strynadka and James 1989; Zhou, Xue, and Yang 2013). Calumenin carries seven EF-hand motifs and was shown not only to localize to the Golgi apparatus, but rather is distributed throughout the whole Secretory Pathway, wherefrom it is also secreted (Narayanasamy and Aradhyam 2018). Calumenin belongs to the CREC family, the abbreviation of members of EF-hand Ca^{2+}-binding proteins (Cab45, reticulocalbin, ERC-55[60] and calumenin) with low Ca^{2+}-binding affinity. Reticulocalbin and ERC-55 are Ca^{2+}-binding proteins in the ER but share structural similarities with the other members including

---

[55] RyR = Ryanodine receptor
[56] DHPR = Dihydropyridine receptor
[57] PKA = Protein kinase A
[58] p54/NEFA = DNA-binding/EF-hand/acidic amino acid-rich region.
[59] Cab45 = Ca^{2+}-binding protein, 45 kDa
[60] ERC-55 = Endoplasmic Reticulum Ca^{2+}-binding protein, 55 kDa

a SP, a molecular weight between 37 and 45 kDa or an acidic pI between 4.1 to 4.7 (Honore 2009; Honore and Vorum 2000). Because of the different localizations, calumenin might have several cellular functions. Many binding partners of calumenin were shown to play a role in muscle contraction and coagulation. In this regard, calumenin is able to bind RyR and SERCA and so directly regulates Ca^{2+} homeostasis (Honore 2009; Vandecaetsbeek et al. 2011).

The both nucleobindin proteins are widely expressed from two separated, unlinked gene loci but share a sequence similarity of 62 % and structural domains, i.a. two EF-hand motifs (see Figure 11B). In addition to the Golgi-localizing protein, both proteins have also a SP-lacking cytosolic variant, which probably explains features like the putative nuclear localization signal, a DNA-binding domain or a leucin zipper region (Kapoor et al. 2010; Valencia et al. 2008). Within the secretory pathway, NUCB1 localizes in the *cis*-Golgi and was shown to peripheral associate with the luminal membrane, where it acts as the major regulator of Golgi Ca^{2+} homeostasis (Lin et al. 1998). Thereby, the Ca^{2+}-binding capacity of NUCB1 is rather low with (1.1 µmol Ca^{2+}/µmol NUCB1), but compensates this effect due to its high abundance (3.8 µg/mg Golgi protein). In this regard, overexpression of NUCB1 further increases the Ca^{2+}-storage capacity of the Golgi apparatus up to 3.0 fold, compared to wildtype cells (Lin et al. 1999). NUCB1 was also partially detected in the extracellular space, however the reason for its transport and secretion is rather unknown (Lavoie et al. 2002). Besides the Ca^{2+}-buffering effect of NUCB1, multiple other roles and binding partners have been mentioned. The cytosolic variant might be involved in gene transcription as well as Ca^{2+}-signaling by binding to G-protein α-subunits, whereas the Golgi-localizing form might also function as a chaperon-like binding protein and prevent protein aggregation (Bonito-Oliva et al. 2017; Kapoor et al. 2010; Lavoie et al. 2002; Valencia et al. 2008) .

In contrast to NUCB1, NUCB2 localizes in the medial-Golgi, e.g. with Golgi marker mannosidsase II and in Golgi-associated vesicles. Similarly, NUCB2 was shown to associate with the membrane, but its role is also elusive (Morel-Huaux et al. 2002).

Structural studies could furthermore reveal that both NUCBs are rather unstructured but getting more α-helical, after binding of Ca^{2+} with its EF-hand domain (see Figure 11B) (De Alba and Tjandra 2004; Kroll et al. 1999; Miura, Kurosawa, and Kanai 1994).
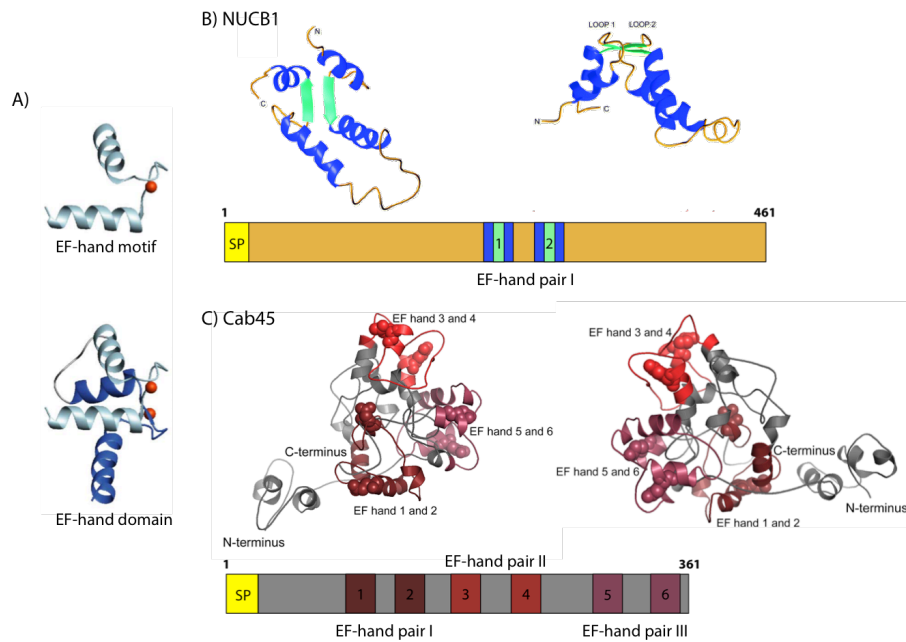
Figure 11: NUCB1 and Cab45 - EF-hand Ca²⁺-binding proteins in the Golgi apparatus. A) Typical helix-loop-helix structure of an EF-hand motif. Ca²⁺ (red spherical) is bound in the loop structure (upper image). In many EF-hand proteins, EF-hand motifs are binding Ca²⁺ in a pairwise manner, by forming an EF-hand pair/domain (lower image). B) Ribbon diagrams of NUCB1 EF-hand motifs forming an EF-hand domain to bind Ca²⁺; left - top view; right - front view; below - general structure of NUCB1 with the signal peptide (SP, yellow) and two EF-hand motifs. Color code shows helix (blue) and loop (green) structure. C) Ribbon diagrams of Golgi-localized Cab45. The six EF-hand motifs (red colors) bind Ca²⁺ (spherical) in a pairwise manner, leading to three EF-hand pairs I, II and III; left - front view; right - rear view; below - general structure of Cab45 with SP (yellow) and six EF-hand motifs. Color code shows pairwise EF-hand formation. Figure created according to Bhattacharya et al. 2004; de Alba and Tjandra 2004; Blank and von Blume 2017.

The last Ca²⁺-binding proteins, Cab45, localizes in TGN and to some extend is also secreted into the extracellular space of the cell (Deng et al. 2018). Literature also has described a cytosolic version of Cab45, which is lacking the SP to enter the secretory pathway as well as the EF-hand motif 1 to 3. Cytosolic Cab45 might act in exocytose of zymogens; however, its physiological function is not really known (Lam et al. 2007). Hence, in the following it will be focused on the Golgi-isoform. Encoded by the *SDF4* gene, Cab45 is ubiquitously expressed and highly conserved between different mammalian species. A N-linked glycosylation on N39 is thus far the only confirmed post-translational modification (Blank and von Blume 2017). Circular Dichroism studies unveiled that Cab45 binds Ca²⁺ with its six EF-hand motifs in a pairwise manner (EF-hand pair I, II, III - see Figure 11C), which induces conformational change and is leading to a more α-helical secondary structure - similar to NUCBs (Deng et al. 2018). Since Cab45 is a major player in this thesis, its function will be discussed later in more detail (see chapter 1.5.4).

In summary, the Golgi apparatus is a very divers and highly regulated organelle. Each cisterna with its specific environment e.g. Ca^{2+} concentration and subset of enzymes, designed to modify incoming cargo. After passing through the Golgi stack, cargo molecules reach the most distal cisternae of the Golgi apparatus, the *trans*-Golgi network (TGN). Here, proteins and lipids are sorted and further distributed to their final destination. In this regard, the last chapter will highlight how cargo is sorted at the TGN.

1.5 The *trans*-Golgi network - a cellular sorting station

1.5.1 Transport routes from the TGN

The TGN functions as the main sorting hub of the Secretory Pathway. Modern imaging techniques like cryosectioning and immunoelectron microscopy revealed that the TGN is a highly dynamic compartment, forming a tubular, branching but also vesicular network (Anitei and Hoflack 2011; Klumperman 2011; Mogelsvang et al. 2004). Interestingly, the morphology of the TGN varies strongly between different cell types but is also dependent on other factors as protein synthesis or the cell cycle (Clermont, Rambourg, and Hermo 1995; Griffiths et al. 1989; Li, Ahat, and Wang 2019). Since this thesis approaches the sorting and export of molecules from the Golgi apparatus, the successive chapters are predominately focusing on processes describing the anterograde transport of molecules that exit the TGN.

At the TGN proteins are recognized, segregated from each other, packed into transport carriers and are transported to various destinations. As described in Figure 1, this includes the transport to the apical or basolateral PM or the transport to recycling, early and late endosomes (Guo et al. 2014). Recent publications have also shown, that in addition to these direct routes, some newly synthesized proteins reach the apical or basolateral PM via a transendosomal transport (De Matteis and Luini 2008). In this regard, e.g. VSVG[61], TfR[62] or pIgR[63] were detected in endosomal compartments before they have reached the PM of the cell (Ang et al. 2004; Futter et al. 1995; Orzech et al. 2000). However, the reason for this stopover remains still obscure (Gonzalez and Rodriguez-Boulan 2009). In specialized cells like

---

[61] VSVG = Vesicular stomatitis virus glycoprotein G
[62] TfR = Transferrin receptors
[63] pIgR = Polymetric immunoglobulin receptors

secretory cells, proteins can be furthermore transported to other compartments as secretory storage granules (De Matteis and Luini 2008).

Since all these transport events require vesicle formation out of phospholipid bilayers, not only proteins, but also lipids are transported from the TGN to various destinations, as e.g. shown for SM, GSLs and PC. These molecules for instance are transported to the extracellular leaflet of the PM (Blom, Somerharju, and Ikonen 2011).

1.5.2 Vesicle formation at the TGN

To reach their final destination, proteins are packed at the TGN and transported in specific membrane-enclosed transport carriers. As mentioned earlier (see chapter 1.2.4), vesicle formation is a multistep process that includes the recruitment of coat components to the site of action, where they either directly or indirectly interact with congregated cargo molecules (Bonifacino 2014; Bonifacino and Glick 2004; Guo et al. 2014). Moreover, publications revealed that a correct lipid composition as well as protein-lipid interactions are essential for many of these budding events (Deng et al. 2018; Huttner and Schmidt 2000; Wakana et al. 2015). Whereas the bidirectional cargo transport between ER and Golgi is mediated by only two classes of vesicle (COPII and COPI), transport carriers that derive from the TGN serve multiple destinations.

1.5.2.1 Clathrin-coated vesicles

Clathrin-coated vesicles (CCVs) are the best-characterized vesicles that bud from the TGN. The clathrin coat consists of three heavy and three light clathrin chains forming a triskelion. Stringing together, these triskelia build the major structural cage of the vesicle (Conner and Schmid 2003; Faini et al. 2013). Formation of CCVs occurs in a similar fashion to the one of COPII and COPI, but in contrast, the clathrin coat is not directly interacting with cargo molecules. Here, clathrin adapters that link the cargo with the clathrin components are necessary. Besides the four classical APs[64] in mammalian cells; AP-1, -2, -3, -4 and each consisting of different subunits, also "alternative" mono- or dimeric adapters like GGAs[65] exist. Even more complicated, several accessory proteins e.g. epsins or β-arrestins that interact with those adapters are itself able to bind clathrin and cargo molecules (Boehm and

---

[64] AP = Adapter protein complexes
[65] GGA = Gamma-ear-containing Arf-binding proteins

Bonifacino 2001; McMahon and Mills 2004; Popova, N. V. Deyev, I. E. Petrenko 2015). Therefore, more than 20 different adapter proteins have been identified, which are binding different cargo molecules and are involved in specific transport routes; e.g. between TGN and endosomes or in endocytosis (Nakatsu, Hase, and Ohno 2014; Owen, Collins, and Evans 2004; Sanger et al. 2019). These adapter complexes are recruited from the cytosol by two mechanisms. They can either bind to activated membrane-associated small G proteins or to phospholipids, particularly PIPs (for details see Figure 12) (Bonifacino and Glick 2004; Ford et al. 2002; Gaidarov et al. 1999; Kirchhausen 2000a; Rohde, Wenzel, and Haucke 2002).

Adapter Protein	Membrane recruitment	Transport	Accessory Proteins
AP-1	Arf/Arl/ Sar/Rabs	endosome to TGN TGN to endosomes to basolateral PM?	epsinR, GGAs
AP-2	PIPs	endocytosis	CALM, epsins, β-arrestin, ARH, amphiphysin, HIP1, Dab2
AP-3	Arf/Arl/ Sar/Rabs	TGN to lysosome endosome - lysosome	Vps41?
AP-4	Arf/Arl/ Sar/Rabs	TGN to endosomes to basolateral PM?	tepsin
GGA1 GGA2 GGA3	Arf/Arl/ Sar/Rabs	TGN to endosomes to basolateral PM?	γ-synergin, p56, radaptin-5, enthoprotin, ent3, ent5

Figure 12: The variety of clathrin-coated vesicles (CCVs). The clathrin coat consists of three heavy (CHC) and three light (CLC) clathrin chains that assemble together to a triskelia. To interact with cargo molecules, the clathrin coat is linked via special adapter proteins, the APs and GGAs. Four types of APs are known in human cells that are formed out of different large (γ, α, δ, ε, β), medium (μ) and small (σ) subunits, leading to high complexity. Thereby the subunits have multifunctional roles, like cargo binding, membrane recruitment, binding to clathrin or binding to accessory proteins. In contrast, GGAs are monoadapters with a VHS domain for cargo binding, a GAT domain for membrane recruitment via Arf-GTP binding, the Hinge region for interaction with clathrin chains and the GAE domain for binding to accessory proteins. The table summarizes how adapters are recruited to the membrane, their transport routes and accessory binding proteins of the two adapter protein families. Some information is still elusive. In this regard, AP-4 might mediate CCV-independent transport. Abbreviations: Vps (vacuolar protein sorting-associated protein); CALM (clathrin assembly lymphoid myeloid leukemia protein), ARH (autosomal recessive hypercholesterolemia); HIP (Hsc70-interacting protein1); Hsc70 (heat shock cognate protein, 71 kDa); Dab2 (disabled homolog 2); p56 (phosphoglycerate kinase 56); ent 3+5 (equilibrative nucleoside transporter 3 + 5). GGA (golgi-localized γ-ear-containing ARF-binding); GAE (γ-adaptin ear); GAT (GGA and Tom); VHS (tree folded domains of Vps27); Hrs (hepatocyte growth factor-regulated tyrosine kinase) and Stam (signal transducing adapter molecule). Figure adapted from and created according to Nakatsu et al. 2014; Conner and Schmid 2003; Bonifacino 2004; Owen et al. 2004; Sanger et al. 2019 and Popova et al. 2013.

At the TGN membrane, adapter proteins recognize cargo molecules via specific canonical amino sequences in the cytoplasmic region of the cargo or via post-translational modifications like ubiquitination. Despite the high level of complexity, almost all adapter proteins share the same domain arrangement and are binding to the N-terminal 7-bladed propeller that is formed out of the clathrin heavy chains (Owen et al. 2004; Traub 2005). Subsequently, polymerization of the recruited clathrin components is leading to cargo concentration, membrane curvature and vesicle formation (see chapter 1.2.4) (Ford et al. 2002; McMahon and Mills 2004).

In clathrin-coated endocytosis it was shown that dynamin, a large multidomain GTPase, assembles around the neck of the forming CCV, polymerizes and facilitates membrane fission upon GTP hydrolysis (Chappie and Dyda 2013; Cocucci, Gaudin, and Kirchhausen 2014; Morlot and Roux 2013). However, the role of dynamin in vesicle scission at the TGN is controversially discussed and not confirmed (Henley, Cao, and Mcniven 1999; Hinshaw 2000; Kasai et al. 1999). Also how CCVs are transported to the acceptor compartment is debated, since different cytoskeletal networks might be used (Almeida et al. 2011; Huckaba et al. 2004; Lakadamyali, Rust, and Zhuang 2006). For a long time it was also not known, how v-SNARS are incorporated into the forming CCVs. New evidence indicates that adapter proteins as well are responsible (Miller et al. 2007).

In summary, CCVs represent highly complex transport carriers that according to the huge variety of adapter proteins regulate cargo transport in a very divers but also very specific manner. Whereas protein transport in CCVs from the PM and mediated by endocytosis was well described in the past, the contribution of CCVs in the direct transport of cargo from the TGN to the PM is still an open question (see Figure 12). In this concern, just a few studies could confirm the role of AP-4, GGA or specific subunits of AP-1 in PM trafficking of transmembrane proteins in polarized cells (Fölsch et al. 1999; Gravotta et al. 2012; Ma et al. 2018; Simmen et al. 2002).

1.5.2.2 CARTS

Recently, a new class of vesicles was identified by purifying TGN46-containing carriers that were transported from the TGN to the cell surface - leading to the name CARriers of the TGN to the cell Surface (CARTS). So far, no coat-forming components were identified for these vesicles. Further characterization of CARTS revealed that their biogenesis is lipid dependent, since blocking the ceramide transfer at ER-TGN membrane contact sites resulted in a

decreased conversion of ceramide to SM and DAG in the Golgi and therefore reduced their organization in microdomains at the TGN. DAG in turn, recruits the cytosolic PKD[66], which is important for the fission of CARTS (Liljedahl et al. 2001; Wakana et al. 2012, 2015; Yeaman et al. 2004). Studies in HeLa cells moreover suppose that the transport of CARTS to the cell surface occurs on microtubules and is maintained by Eg5[67], as inhibition of Eg5 does not interfere with vesicle biogenesis but with the accumulation of CARTS around the Golgi apparatus (Wakana et al. 2013). CARTS contain Rab6a and Rab8a GTPs, both involved in the fusion of secretory carriers; as well as synaptotagmin II, a Ca^{2+}-binding protein in synaptic vesicles that also regulates fusion by interacting with SNARES and phospholipids at the PM (Ang et al. 2003; Grigoriev et al. 2007, 2011; Tucker and Chapman 2002; Wakana et al. 2012). With a diameter of 100 to 250 nm, CARTS are slightly bigger than CCVs (diameter: 80-120 nm) and carry specific proteins that are transported to the PM like LyzC[68], desmoglein-1 or desmoplakin (Jensen and Schekman 2011; Wakana et al. 2012). Albeit CARTS represent a new kind of carriers transporting cargo to the PM, there are many open questions that have to be addressed. How is cargo recognized and sorted into CARTS? What and are there coat-forming components?

Up to now, other transport carriers that bud from the TGN and convey secretory proteins directly to the cell surface remain unknown. This is astonishing, since a multitude of known proteins have to be transported to the PM or be secreted into the extracellular space to fulfill their functions. In this regard, genes encoding for the exomer - a coat complex facilitating the transport of transmembrane proteins from the TGN to the PM in yeast - is absent in metazoans (Paczkowski et al. 2012; Wang et al. 2006).

1.5.2.3 Membrane lipids in vesicle formation

For quite a long time, proteins and lipids were mainly considered separately from each other. Therefore, the Golgi apparatus especially the TGN was seen as a distribution compartment for proteins, whereas lipid metabolism and sorting were hardly mentioned. However, over the last years, more and more evidences were provided how lipids and proteins interplay to ensure Golgi dynamics and membrane trafficking (Fang et al. 1998). In this regard, several studies were able to show how failures in phospholipid biosynthesis also affect protein transport and vice versa (von Blume and Hausser 2019; van Echten and Sandhoff 1989).

---

[66] PKD = Protein kinase D
[67] Eg5 = Microtubule-associated kinesin-5 motor protein
[68] LyzC = Lysozyme C

Hereof, phospholipids form interaction platforms to recruit soluble factors to the membrane (e.g. Arfs, Rabs, APs; see 1.5.2.1) or to segregate cargo molecules by lipid-protein interaction and lipid re-organization (discussed later on) (Bankaitis, Garcia-Mata, and Mously 2012).

Membrane lipids are determined by their head groups and acyl chain composition, resulting in three possible different molecular shapes (see Figure 13): Cylindrical lipids (e.g. PC, PS, SM), conical lipids (e.g. PE, PA, DAG) and inverted conical lipids (e.g. LPC[69], PI4P[70], PI(4,5)P2[71], PI(3,4,5)P3[72]). According to their localization in the inner or outer leaflet, lipids can actively promote and initiate membrane curvature (McMahon and Boucrot 2015; Zhang et al. 2019).
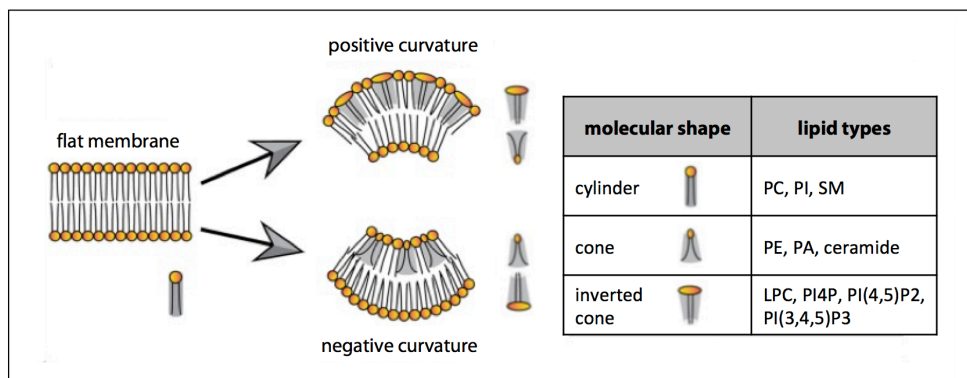
Figure 13: Molecular shapes of membrane lipids. According to their head group and chain composition, membrane lipids can have a cylindrical, conical or inverted conical molecular shape. As shown, inverted conical lipids in the outer leaflet and/or conical lipids in the inner leaflet induce positive membrane curvature, whereas conical lipids in the outer leaflet and/or inverted conical lipids in the inner leaflet induce negative membrane curvature. The table shows different lipids with their molecular shapes. Abbreviations: PC (phosphatidylcholine); PI (phosphatidylinositol); SM (sphingomyelin); PE (phosphatidylethanolamin), PA (phosphatidic acid); LPC (lysophosphatidylcholine); PI4P (phosphatidylinositol-4-phosphate); PI(4,5)P2 (phosphatidylinositol (4,5)-bisphosphate); PI (3,4,5)P3 (phosphatidylinositol (3,4,5)-trisphosphate). Note: in the original figure PA was annotated as cylindrical lipid. As several publications e.g. McMahon and Boucrot 2015 define PA as a conical lipid, it was modified. Figure adapted and modified from Zhang et al. 2019.

Changes in the lipid composition, due to lipid exchange or lipid modification - e.g. the phosphorylation of the inositol ring of PI to PIxPx derivatives by cytoplasmic lipid kinases - furthermore allow structural deformation of the membrane and can affect vesicle budding (Dickson and Hille 2019; McMahon and Gallop 2005; J. Zhang et al. 2018). Interestingly, some budding mechanisms have been proposed lacking the involvement of cage-forming proteins. Referring to this, multiple interactions of the Cholera toxin or the VP1[73] capsid

---

[69] LPC = Lysophosphatidylcholine
[70] PI4P = Phosphatidylinositol-4-phosphate
[71] PI(4,5)P2 = Phosphatidylinositol (4,5)-bisphosphate
[72] PI(3,4,5)P3 = Phosphatidylinositol (3,4,5)-trisphosphate
[73] VP1 = Viral protein 1

protein of the simian virus with membrane lipids were shown to create membrane asymmetry, leading to membrane curvature and favoring endocytosis without a cytosolic machinery (Ewers et al. 2010; Johannes and Römer 2010; Römer et al. 2007; Stachowiak et al. 2012).

Indeed, no mechanism for the budding of uncoated vesicles from the TGN has been described, however, there is also no other machinery known that drives the formation of post-Golgi vesicles to the PM (Stalder and Gershlick 2020).

1.5.3   Cargo recognition and sorting at the TGN

For packaging cargo into distinct transport carriers, highly sophisticated sorting machineries and mechanisms are essential. This last section will highlight how different cargo molecules are recognized and sorted at the TGN. Some of these sorting events have been well described in the past, whereas for others, especially for soluble secretory molecules, the sorting and the involvement of other components are rather unknown.

1.5.3.1   Sorting of transmembrane proteins

The sorting of transmembrane proteins was highly investigated in the last decades. By spanning the TGN membrane, these molecules can directly be recognized by adapter proteins via specific motifs in the cytosolic domains of the transmembrane proteins and so achieve the packaging into TGN-derived vesicles (Mellman and Nelson 2008; Traub and Kornfeld 1997). Two main sorting motifs have been described according to the most critical residues they contain; these are tyrosines or leucines.

The tyrosine-based sorting signals are NPXY and YXX∅, with X as a variable residue and ∅ as an amino acid with a bulky hydrophobic side chain. NPXY is located in many type I integral transmembrane proteins at the cell surface, like the LDL-R[74] or β-integrin (Chen, Goldstein, and Brown 1990; Bonifacino and Traub 2003; Lazarovits and Roth 1988). Therefore, interaction of the motif with the μ2 subunit of AP-2 is regulating the internalization of the cargo molecules (Boll et al. 2002; Kibbey et al. 1998; Mishra et al. 2002). YXX∅ in comparison, was found in all types of membrane-spanning transmembrane proteins: at cell surface proteins (e.g. transferrin receptors) as well as lysosomal membrane

---

[74] LDL-R = Low densitiy lipoprotein receptor

proteins (e.g. LAMP1[75]) (Bonifacino and Traub 2003; Braulke and Bonifacino 2009; Nesterov et al. 1999; Rous et al. 2002). Different μ subunits of four APs can interact with YXX∅ and so facilitate the sorting into transport carriers (Boll et al. 1996; Hirst et al. 1999; Ohno et al. 1995, 1996). Interestingly, in lysosomal transmembran proteins the variable residues (X) often are acidic and the recognition motif itself is located close to the transmembrane domain or at the very terminus. In contrast, PM localizing transmembrane proteins do not have the motif at the very terminal end (see Figure 14) (Bonifacino and Traub 2003; Rohrer et al. 1996; Rous et al. 2002).

The dileucine-based sorting motifs function as another class of recognition motif, consisting of the two main sequences [DE]XXXL[LI] and DXXLL. Similar as for the YXX∅ motif, acidic residues as well as position of the motif close to the transmembrane domain or at the terminal end are important for sorting to late endosomes and lysosomes (Geisler et al. 1998). Depending on the exact amino acid sequence (acidic residues, leucin or isoleucin etc.), [DE]XXXL[LI] is recognized by AP-1, -2 or -3. In contrast, the second dileucine-based sorting motif DXXLL shows a similar amino acid sequence, however is recognized by GGAs but not by APs (see Figure 14) (Bonifacino 2004; Braulke and Bonifacino 2009; Von Einem et al. 2015; Puertollano et al. 2001; Zhu et al. 2001).

Another mechanism for the sorting of transmembrane proteins that was described is upon ubiquitination of cytosolic domains (Bonifacino and Traub 2003). In a multi-step process, ubiquitin (Ub), a 76-amino acid peptide, is attached to the lysine side chain of a target protein. Clathrin adapter proteins like epsins (accessory protein) or GGAs are able to recognize ubiquitinated receptors via a ubiquitin interaction motif (UIM) or the GAT domain and mediate vesicle formation (Owen et al. 2004; Shiba et al. 2004; Shih et al. 2002). Similar domains called ubiquitin-associated (UBA) or ubiquitin-conjugating enzyme like (UBC) were also found in other proteins. Despite all this new evidence, the role of ubiquitination is still not fully understood, especially since some ubiquitinated cargos e.g. EGFR can also be sorted in an ubiquitin-independent manner (Haglund, Di Fiore, and Dikic 2003).

---

[75] LAMP = Lysosome-associated membrane glycoproteins
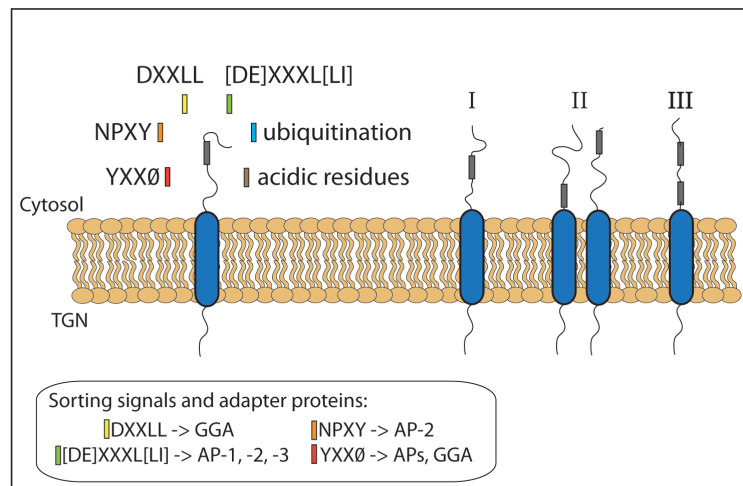
Figure 14: Transmembrane proteins carry a variety of sorting motifs in their cytoplasmic domain. Known sorting motifs are the tyrosine motifs YXXØ (red) and NPXY (orange) and the dileucine motifs DXXLL (yellow) and [DE]XXXL[LI] (green). Furthermore, acidic residues (brown) or post-translation modifications like ubiquitination (blue) are also used as sorting sequences. With these motifs, transmembrane proteins are interacting with adapter proteins of clathrin-coated vesicles (CCVs). Thereby, not only the sorting motif itself (grey can be any sorting motif), but also the position can play a role for the destination. Sorting domains of PM proteins are often found somewhere in the middle of the cytoplasmic tail (I), whereas sorting motifs of lysosomal transmembrane proteins were detected close to the transmembrane domain or the terminal end (II). Additionally, proteins often carry more than one sorting motif, e.g. one for the internalization from the PM and one that facilitates the TGN to endosome transport (III). Abbreviations: X (any amino acid); Ø (amino acid with a bulky hydrophobic side chain); AP (adapter protein complex); GGA (γ-ear-containing Arf-binding protein). Figure created according to Bonifacino and Traub 2003.

In line with the uncertainty how adapter proteins faciliate CCV-dependent transport to the cell surface (see Figure 12), there is also no canonical sorting signal in the cytosolic domain of transmembrane proteins or sorting receptors that mediates transport to the PM (Hunziker et al. 1991; Matter, Yamamoto, and Mellman 1994; Mellman and Nelson 2008; Mostov, Su, and ter Beest 2003). Some of these PM proteins e.g. TGN38 or E-cadherin contain tyrosine- or dileucine-based motifs, whereas recognition sequences of others e.g. of the transferrin receptor are independent of those critical residues (Miranda et al. 2001; Rajasekaran et al. 1994; Odorizzi and Trowbridge 1997). AP-1 and -4 were shown to mediate transport of basolateral proteins in a CCV-dependent manner. Nevertheless, protein transport for some proteins e.g. a Na^+/K^+-ATPase was not affected upon knockdown of clathrin, speaking for the existence of additional CCV-independent trafficking routes (Mellman and Nelson 2008; Simmen et al. 2002).

In contrast to basolateral transmembrane proteins, just a few individual sorting motifs have been identified in cytoplasmic domains of apical transmembrane proteins, like in Rhodopsin,

M2 receptor[76] or ATP7B[77] (Braiterman et al. 2009; Chmelar and Nathanson 2006; Chuang and Sung 1998). Many of the noticed apical proteins carry basolateral sorting motifs, therefore are first transported to the basolateral surface, before they are reaching the apical PM upon sorting in apical recycling endosomes; a process called transcytosis (Brown et al. 2000; Chmelar and Nathanson 2006; Mostov 1994; Orzech et al. 2000). The cytosolic domains of apical transmembrane proteins in general, seem to be less important for sorting and trafficking (Mellman and Nelson 2008). Sorting of those proteins might occur via recognition sites or post-translational modifications like N- or O-linked glycosylation, located in their transmembrane or luminal domains (Cao et al. 2012; Mellman and Nelson 2008; Nelson and Yeaman 2001). How these sorting events might occur will be described in another sections.

1.5.3.2 Sorting via cargo receptors

In contrast to transmembrane proteins, soluble luminal proteins cannot directly interact with cytosolic components. Therefore many of these proteins are sorted indirectly with the help of cargo receptors that are spanning the TGN membrane and instead are recognized by cytosolic components (Guo et al. 2014). Among those molecules, the sorting of lysosomal hydrolases via MPR[78] is probably the best characterized sorting process at the TGN and is involved in the sorting of approximately 60 different lysosomal proteins, mainly cathepsins (Dahms, Olson, and Kim 2008; Griffiths et al. 1988). According to their specific mannose-6 phosphate (M6P) modifications, these soluble proteins are captured by MPRs and sorted into CCVs (Ghosh, Dahms, and Kornfeld 2003). To generate the M6P recognition motif, lysosomal hydrolases that have been initially glycosylated on asparagine residues at the ER are further modified in the Golgi (Braulke and Bonifacino 2009).

Two different classes of MPRs have been identified for the sorting of M6P-modified lysosomal hydrolases (see Figure 15). The 46-kDa CD-MPR[79] is mainly found as homodimer complex and contains a ~150 amino acid luminal domain that binds M6P. In contrast, CI-MPRs[80] exist as monomers (300 kDa) and contain 15 repeats of this homologous luminal domain, whereas domain 3 and 9 bearing M6P-binding sites (Le Borgne and Hoflack 1998; Braulke and Bonifacino 2009; Hille-Rehfeld 1995; Kornfeld 1992). Both type-1 integral membrane receptors carry the DXXLL motif for the GGA-dependent formation of CCVs as well as

---

[76] M2 receptor = M2 muscarinic acetylcholine receptor
[77] ATPB7 = Adenosine triphosphate-ase copper transporting beta
[78] MPR = Mannose-6 phosphate receptor
[79] CD-MPR = Cation-dependent mannose-6 phosphate receptor
[80] CI-MPR = Cation-independent mannose-6 phosphate receptor

several binding motifs for AP-1 (YXX∅ and [DE]XXXL[LI]) in their cytosolic domains. As a result, lysosomal hydrolases are transported to endosomal/lysosomal compartments in a clathrin-dependent manner (Dahms et al. 2008; Ghosh and Kornfeld 2003, 2004; Höning et al. 1997; Puertollano et al. 2001). At the endosomes, the soluble proteins are released according to the acidic pH and MPRs can be recycled back to the TGN, mediated by Rab9, M6PRBP1[81] and the retromer complex (Guo et al. 2014).

Sortilin is another identified type-I membrane receptor that sorts lysosomal cargos at the TGN, but in an M6P-independent way (Coutinho, Prata, and Alves 2012). Sortilin is a member of the VPS10[82] family that binds cargo in the inside of its tunnel-forming luminal β-propeller domain (see Figure 15) (Quistgaard et al. 2009). Known cargos are the acid sphingomyelinase, cathepsin D and H, but also non-lysosomal proteins like the PCSK9[83] (Braulke and Bonifacino 2009; Canuel et al. 2008; Gustafsen et al. 2014). Similar to MPRs, sortilin carries GGAs and APs interaction sites in its cytoplasmic tail for vesicle formation and is recycled back to the TGN in a retromer-dependent manner (Guo et al. 2014; Pfeffer 2011).
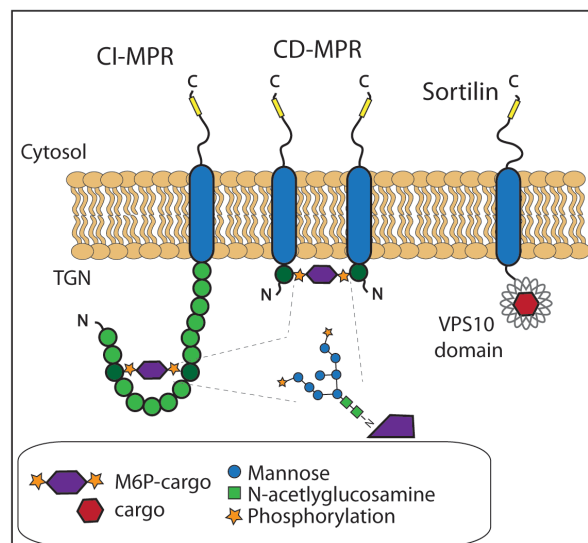
Figure 15: Sorting of soluble lysosomal proteins via transmembrane sorting receptors. As these proteins cannot directly interact with coat components, soluble proteins bind to cargo receptors that carry a sorting motif (yellow) in their cytoplasmic tail and interact with adapter proteins of clathrin-coated vesicles (CCVs). Lysosomal proteins gain a M6P-modification in the Golgi apparatus and are sorted via the homodimeric CD-MPR or via the monomeric CI-MPR that binds cargo proteins in its luminal domains 3 and 9. In contrast, sortilin sorts cargo molecules in a M6P-independent manner by binding them in its VPS10-domain. All receptors interact with several adapter proteins but predominately sort via GGA. Abbreviations: M6P (mannose-6 phosphate); CI-MPR (cation-independent mannose-6 phosphate receptor); CD-MPR (cation-dependent mannose-6 phosphate receptor); VPS10 (vacuolar protein sorting/targeting protein 10); GGA (γ-ear-containing Arf-binding protein). Figure created according to Guo et al. 2014.

---

[81] M6PRBP1 = Mannose-6 phosphate-binding protein, 47 kDa
[82] VPS10 = Vacuolar protein sorting/targeting protein 10
[83] PCSK9 = Protein convertase subtilisin/kexin type 9

Moreover, other M6P-independent cargo receptors like SorLA[84], LIMP-2[85] and Wntless have been identified that might be responsible for cargo sorting into CCVs in a similar way. However as their exact sorting mechanism is still unknown they will not be further discussed.

1.5.3.3 Sorting via lipid domains

Studies also revealed that some proteins are sorted by the interaction with lipids, in form of lipid rafts (Simons and Ikonen 1997; Simons and Van Meer 1988). According to the lipid raft hypothesis, saturated lipids like glycosphingolipids (GSL) and sterols, together with proteins, assemble with each other to functional signaling and protein sorting platforms. These domains are highly dynamic and can vary in size, lifetime and stability (Hanzal-Bayer and Hancock 2007; Lingwood and Simons 2010; Simons and Gerl 2010). Since apical membrane proteins were identified to associate with those isolated detergent-resistant glycolipid-enriched membranes (DRMs), lipid rafts might especially bear an important sorting function for apically targeted proteins (Keller and Simons 1997; Mayor and Riezman 2004).

In line with this, evidences become more frequent as specific lipid domains, rich in cholesterol and sphingolipids, are involved in the sorting of GPI-anchored proteins at the TGN (Brown and Rose 1992; Muñiz and Zurzolo 2014; Zurzolo and Simons 2016). This class of proteins is anchored in the membrane via a GPI-modification that is attached via an amide linkage to the ω-site at the C-terminus of the protein (Kinoshita 2014). Coupling of the GPI-core-anchor occurs in the ER, whereas the core structure can further be modified by acylation, the addition of various sugars or the exchange of fatty acids and so enhancing its functionality (Mayor and Riezman 2004; Paulick and Bertozzi 2008).

Interestingly, raft-associated GPI-anchored proteins were shown to oligomerize to high molecular weight complexes; and that oligomerization is important for apical sorting (Paladino et al. 2004, 2007). It was furthermore reported that lipids like cholesterol can support or even drive the oligomerization of GPI-anchored proteins and so creating distinct sorting platforms (Paladino et al. 2008; Zurzolo and Simons 2016). In fact, GPI-anchored proteins were detected in TGN-derived secretory vesicles, rich in SM and sterols (see Figure 16) (Deng et al. 2016; Klemm et al. 2009).

---

[84] SorLA = Sortilin-related receptor with A-type repeats
[85] LIMP-2 = Lysosomal integral membrane protein-2

Additionally, N- and O-linked glycosylation was supposed to be crucial for self-aggregation of GPI-anchored proteins and depletion of N- or O-linked glycosylation was shown to missort apically targeted proteins in polarized cells; however glycosylation itself was not important for all investigated apical sorting events (Alfalah et al. 1999; Benting, Rietveld, and Simons 1999; Fiedler and Simons 1995; Gut et al. 1998; Imjeti et al. 2011; Scheiffele, Peränen, and Simons 1995; Yeaman et al. 1997). Moreover, not all glycosylated apical proteins have self-association features to direct lipid raft formation, which leads to the idea that some unidentified cargo receptors might function as clustering agents (Potter et al. 2004; Rodriguez-Boulan, Kreitzer, and Müsch 2005).

Notably, members of the lectin family (Galelectin-3, -4 and -9) are highly discussed to play a part in the lipid-based apical sorting of proteins. These carbohydrate-binding proteins have potential to guide lipid raft formation and were shown to self-associate and regulate transport of N-glycosylated cargos (Brewer, Miceli, and Baum 2002; Hara-Kuge et al. 2002; Hauri et al. 2000; Yamashita, Hara-Kuge, and Ohkura 1999). Despite the described effects and functions of galectins, their role in apical cargo sorting has to be further investigated (Furtak, Hatcher, and Ochieng 2001; Stechly et al. 2009; Straube et al. 2013; Zurzolo and Simons 2016).
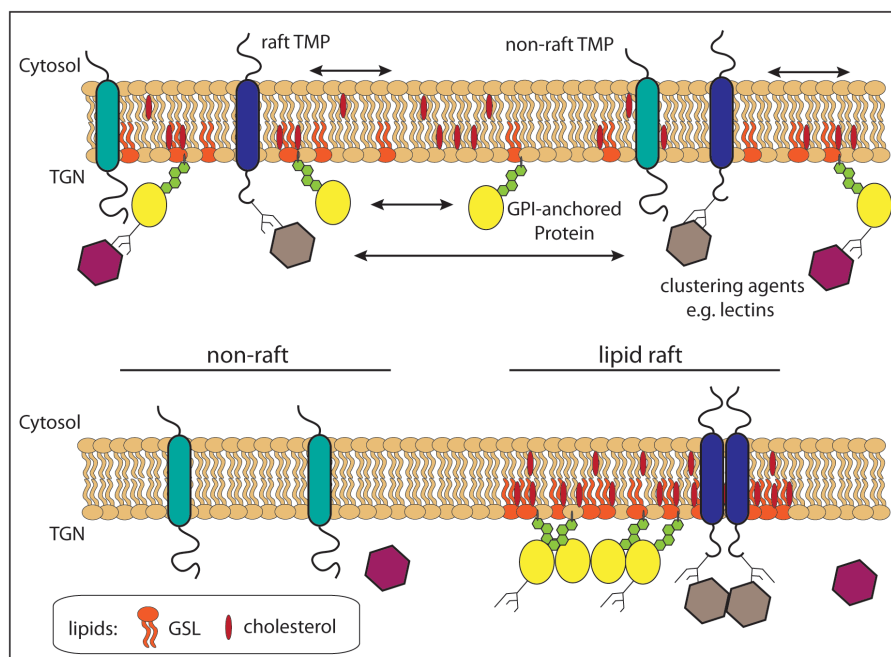
Figure 16: Sorting of apical proteins via lipid raft formation. Proteins are distributed throughout the TGN membrane (top). For sorting, apical proteins are organized in lipid rafts (bottom). Therefore, GPI-anchored proteins and apical raft transmembrane proteins (TMPs) are clustering due to self-oligomerization or via clustering agents as lectins that recognize N- or O-linked glycosylation. Furthermore, also lipids like cholesterol drive the formation of lipid rafts. As a consequence, non-raft TMPs are excluded from lipid rafts. Abbreviations: GSL (glycosphingolipids), GPI (glycosylphosphatidylinositol). Figure created according to Lingwood and Simons 2010 and Simons and Gerl 2010.

Altogether, studies could show that the sorting of many apical proteins is dependent on the membrane lipid composition, the glycosylation status, the GPI-anchor or the interaction with clustering agents. As a result, the depletion, modification or knock down of those features was leading to missorting effects (Hansen et al. 2000; Lipardi, Nitsch, and Zurzolo 2000; Nelson and Yeaman 2001; Surma, Klose, and Simons 2012; Zurzolo and Simons 2016). Nevertheless, how these congregated proteins are finally packaged and which vesicles are used for transport, remains to be analyzed.

1.5.3.4 Aggregation-based sorting of secretory storage granule proteins

Specialized cells like exocrine, endocrine, neuroendocrine or neuronal cells contain secretory granules (SGs); specific dense core post-Golgi organelles that function as a storage compartment for (pro)hormones or glycoproteins before they are secreted upon external stimuli (Arvan and Castle 1998; Elias et al. 2010; Tooze 1998). SGs are formed as immature SGs that undergo a maturation, a process which is still obscure (Morvan and Tooze 2008; Tooze and Tooze 1986; Urbé, Page, and Tooze 1998).

Two different models have been described for the sorting of proteins into SGs in the past. The "sorting by retention" model suggests, that immature SGs are formed out of the TGN, containing a variety of proteins. Subsequently, non-granule proteins are specifically sorted away from the SG via CCVs to e.g. endosomes and lysosomes, whereas SG proteins are retained in the SG, probably due to aggregation (Borgonovo, Ouwendijk, and Solimena 2006; Dannies 1999; Tooze 1998). In this regard, studies were able to detect lysosomal proteins like procathepsin L or procathepsin B in immature SGs that have been removed during the SG maturation process (Kuliawat et al. 1997; Kuliawat and Arvan 1994). Moreover, adapter proteins as GGA and AP-1A - necessary for the formation of CCVs, as well as MPRs - important for the transport of lysosomal cargo, localized at SGs. As a result, CCV cargos were retained in the SGs, when adapter proteins like GGA were blocked (Dittié, Hajibagheri, and Tooze 1996; Dittié, Klumperman, and Tooze 1999; Kakhlon et al. 2006; Klumperman et al. 1998; Orci et al. 1985).

In contrast, the "sorting for entry" model postulates that sorting of SG molecules actively occurs at the TGN. There, secretory proteins interact with the TGN membrane most likely by selective aggregation and therefore are sorted into immature SGs (Borgonovo et al. 2006; Dannies 1999; Tooze 1998). Evidence for this is shown by the proteins of the granin family,

which are highly expressed in SG containing cells. Members of this family like SgII[86], CgA[87] or CgB[88] are proned to aggregate at mildly acidic pH and high Ca^{2+} concentrations, which enables segregation and sorting of cargos (Chanat and Huttner 1991; Colomer, Kicska, and Rindler 1996; Cowley et al. 2000; Gerdes et al. 1989). Furthermore it is assumed that aggregating proteins function as "helper proteins" for (pro)hormones that do not aggregate and sort them into immature SGs (Dannies 2001; Elias et al. 2010). Regarding this, CgA knockout mice showed an decreased amount of secretory storage granules and physiological defects due to defects in (pro)hormone as well as neurotransmitter storage and secretion (Gayen et al. 2010; Gayen, Gu, et al. 2009; Gayen, Saberi, et al. 2009). Other SG proteins like SgIII, PC-1/3 and PC-2 are known to interact with lipid rafts and so potentially regulate sorting (Blazquez et al. 2000; Dikeakos et al. 2009; Hosaka et al. 2004).

In summary, the findings for the different models are not necessarily contradictory. Not much is known about the processing of SGs and which proteins and factors are needed for proper SG maturation. Whereas SG proteins might be actively sorted into immature SGs, these organelles might still function as another sorting station for the recycling of non-secretory molecules. Aggregation might be important for both described scenarios, as it can drive the active sorting of SG components, as well as it mediates the retention of proteins that should stay in the SGs and not be sorted into budding vesicles (Dannies 1999). Both models also comply with the *bona fide* sorting of transmembrane proteins or lysosomal hydrolases as described above and so preventing their secretion (Borgonovo et al. 2006; Tooze 1998).

1.5.4 Ca^{2+}-dependent sorting of soluble secreted proteins via the Cab45-machinery

The sorting of soluble secreted proteins still poses a challenge in the field, as neither common recognition motifs, nor cargo receptors have been identified for those molecules. Actively transported out of the cell, these molecules are involved in many physiological events like cell-cell communication, development or tissue integrity (Blank and von Blume 2017; Cavalli and Cenci 2020; Farhan and Rabouille 2011; Kelly 1985; Kienzle and von Blume 2014).

Three of those proteins are part of the present thesis and therefore mentioned briefly. Among them is LyzC, a hydrolytic enzyme involved in the hydrolysis of β-(1,4)-glycosidic bonds and

---

[86] SgII = Secretogranin
[87] CgA = Chromogranin A
[88] CgB = Chromogranin B

important for the degradation of peptidoglycan in bacterial cell walls (Callewaert and Michiels 2010; Ragland and Criss 2017). As a result, defects in LyzC secretion are e.g. associated with decreased immune defense or inflammation of the gastrointestinal tract (Deckers et al. 2008; Ragland and Criss 2017; Rubio 2015).

COMP[89] another secreted cargo, interacts with many ECM proteins like fibronectins, collagens or aggrecan as well as with cell surface receptors like integrin subunits (Di Cesare et al. 2002; Chen et al. 2005, 2007; Thur et al. 2001). Therefore, COMP is a major factor in ECM remodeling (Acharya et al. 2014). Depletion of COMP is linked to skeletal disorders in humans as short-limb dwarfism or early-onset osteoarthritis, due to matrix degenerations (Di Cesare et al. 1996; Svensson et al. 2002).

Other secreted proteins that play an important role in ECM turnover are the members of the MMP[90] family. MMPs are Zn^{2+}-dependent proteases that are mainly synthesized in an inactive form and activated by cleavage of their propeptide that is blocking the catalytic pocket (Tallant, Marrero, and Gomis-Rüth 2010). Activation is mediated by TIMPs[91] and might be supported in the presence of other MMPs (Fernandez-Catalan et al. 1998; Han et al. 2015). According to their substrate specificity, MMPs are grouped to e.g. collagenases, gelatinases, stromelysins, elastases or aggrecanases, however many of them are able to degrade more than one substrate, i.e. MMP2 (N. Cui, Hu, and Khalil 2017). Mainly considered as a gelatinase, MMP2 is also able to degrade collagens or fibronectins (Hardy, Hardy-Sosa, and Fernandez-Patron 2018). Furthermore, MMP2 is activated at the cell surface by TIMP2 in a complex together with the membrane-bound MT1-MMP[92] (also known as MMP14) (Egawa et al. 2006; Fernandez-Catalan et al. 1998; Han et al. 2015; Remacle, Murphy, and Roghi 2003). In general, the meticulous secretion and activation of MMPs is crucial, as defects are linked to many diseases i.a. skeletal disorders, arthritis or metastatic cancer (Malemud 2006).

As there is no known mechanism for the sorting of these molecules, the laboratory of Dr. Julia von Blume investigates how soluble secreted proteins are sorted at the TGN. In the recent years, von Blume and coworkers identified a receptor-independent sorting machinery that is based on Ca^{2+} and the interplay of cofilin/ADF[93], the Secretory Pathway Ca^{2+}-ATPase 1 (SPCA1), sphingomyelin (SM) and the Ca^{2+}-binding protein 45 kDa (Cab45) (Blank and von

---

[89] COMP = Cartilage oligomeric matrix protein
[90] MMP = Matrix metalloproteinase
[91] TIMP = Tissue inhibitors of metalloproteinase
[92] MT1-MMP = Membrane type 1-matrix metalloproteinase
[93] ADF = Actin depolymerizing factor

Blume 2017; von Blume et al. 2009, 2011, 2012; Crevenna et al. 2016; Curwin, von Blume, and Malhotra 2012; Deng et al. 2018; Kienzle et al. 2014; Pakdel and von Blume 2018). By exploring those components in greater detail, important questions have been solved, regarding: How do these components facilitate cargo sorting? What is the role of Ca^{2+} in the TGN? How is Ca^{2+} imported? Which cargo molecules are concentrated and sorted? And how are sorted cargo molecules shuttled to the PM?

1.5.4.1 Cofilin regulates SPCA1-mediated Ca^{2+}-influx into the TGN

To identify novel genes that are involved in the sorting and trafficking of soluble secreted molecules, a secretion-based, genome-wide RNA-interference screen in *Drosophila* S2 cells was performed. Measuring the secretion of the artificial cargo ss-HRP[94] revealed that besides other factors, twinstar was required (Bard et al. 2006). Further studies could also show that knockdown of the twinstar orthologous in yeast (cof1) and mammals (cofilin1/cofilin2/ADF) led to secretion defects of secretory proteins (von Blume et al. 2009; Curwin et al. 2012). Cofilin/ADF are actin-binding proteins that bind filamentous as well as globular actin via an α-helix structure, and are able to (dis)assemble actin polymers (Bamburg and Bernstein 2010; Kanellos and Frame 2016; Moriyama 1999). Phosphorylation by LIM-kinase keeps cofilin/ADF in an inactive state, whereas dephosphorylation by slingshot phosphatases activates their actin remodeling function (Agnew, Minamide, and Bamburg 1995; Arber et al. 1998; Bamburg 1999; Niwa et al. 2002). In addition to the role in apoptosis or contractility, the *Drosophila* homolog twinstar was also shown to regulate planar cell polarity (Blair et al. 2006; Kanellos and Frame 2016). But what is the consequence of actin remodeling for protein sorting?

Using a mass spectrometry approach of cofilin1 immunoprecipitations identified actin and SPCA1 as potential interaction partners (von Blume et al. 2011). As introduced in chapter 1.4.4.1, SPCA1 is a Ca^{2+}-ATPase in the TGN membrane and faces the cytosol with its N- and C-terminus and 4 cytosolic loops (Blank and von Blume 2017; Missiaen et al. 2007). Immunofluorescence and interaction studies demonstrated that activated cofilin1 localizes at the TGN and interacts with the P-domain of SPCA1, present in the second cytosolic loop (see Figure 17). Interestingly, this interaction recruits F-actin to the TGN, which is necessary for Ca^{2+}-influx into the lumen of the sorting compartment (von Blume et al. 2009, 2011; Kienzle et al. 2014). Which other upstream components and signaling pathways are necessary to

---

[94] ss-HRP = Horseradish peroxidase with signal sequence

activate SPCA1 are unknown, however crosslinking experiments further could show that the Ca^{2+}-pump localizes in locally enriched SM domains (Deng et al. 2018).

As an overall finding, each of these components is able to regulate pumping activity of SPCA1. Either the depletion of SM, the knockdown of cofilin1 or the knockdown of SPCA1 itself significantly decreased free TGN Ca^{2+} levels and was linked to sorting defects (Bard et al. 2006; von Blume et al. 2009, 2011; Deng et al. 2018; Kienzle et al. 2014; Kienzle and von Blume 2014).

1.5.4.2 Cab45 oligomerizes and binds specific cargo molecules

SPCA1 mediates Ca^{2+}-uptake into the TGN, but what is the role of Ca^{2+} in secretory cargo sorting? Whereas the knockdown of cofilin-1 showed that secretion of many proteins was decreased, some proteins were also hyper-secreted. Interestingly, among them was Cab45 - a Ca^{2+}-binding protein (von Blume et al. 2009). As mentioned before (see chapter 1.4.4.3), Cab45 is a TGN-localized protein that binds Ca^{2+} with its EF-hand motifs in a pairwise-manner (Blank and von Blume 2017; Scherer et al. 1996). *In vitro* oligomerization and interaction studies further unveiled that Cab45 oligomerizes in the presence of Ca^{2+} to high weight complexes that bind specific client molecules like LyzC or COMP (see Figure 17).

In contrast, the Cab45 Ca^{2+}-binding-deficient mutant Cab45-6EQ (replacement of glutamic acid to glutamin in all 6 EF-hand motifs) failed oligomerization and cargo binding (Blank and von Blume 2017; von Blume et al. 2012; Crevenna et al. 2016). Later on it was shown that especially EF-hand pair I and pair III were essential for Ca^{2+}-binding and oligomerization (Deng et al. 2018). 3D structural illumination microscopy experiments further could confirm that SPCA1, Cab45 and the client LyzC are clustering in the TGN, and that all the components are in close proximity with each other (Crevenna et al. 2016).

1.5.4.3 Sorting of the Cab45-cargo-complex into SM-rich vesicles

As discussed before, there is no general described mechanism for the sorting of soluble secreted molecules at the TGN. Strikingly, similar to the behavior of Cab45, also SG proteins and GPI-anchored proteins are claimed to be sorted upon oligomerization (Colomer et al. 1996; Dannies 2001; Simons and Gerl 2010; Zurzolo and Simons 2016). Moreover, the latter are sorted into SM- and cholesterol-rich vesicles, and SM is enriched at SPCA1 localization sites (von Blume and Hausser 2019; Deng et al. 2016, 2018; Klemm et al. 2009; Simons and Ikonen 1997).

In line with this, analysis of cytosolic SM-rich vesicles via mass spectrometry was able to detect Cab45 as well as LyzC in those transport carriers (Deng et al. 2018). This was surprising, since Cab45 was annotated as a Golgi-resident protein (Scherer et al. 1996). However, further studies by live cell imaging confirmed that Cab45 together with LyzC is specifically sorted into SM-rich vesicles that bud from TGN (see Figure 17). Additionally, the oligomerization-potential of Cab45 seems to be important for the sorting process, as Cab45-6EQ buds in different, uncharacterized vesicles (Deng et al. 2018). Overall, several secretion assays could demonstrate that a knockout or knockdown of cofilin1, SPCA1, Cab45 or SM synthases 1&2 resulted in a decreased secretion of LyzC or COMP (Bard et al. 2006; von Blume et al. 2009, 2011, 2012; Crevenna et al. 2016; Deng et al. 2018; Kienzle et al. 2014).
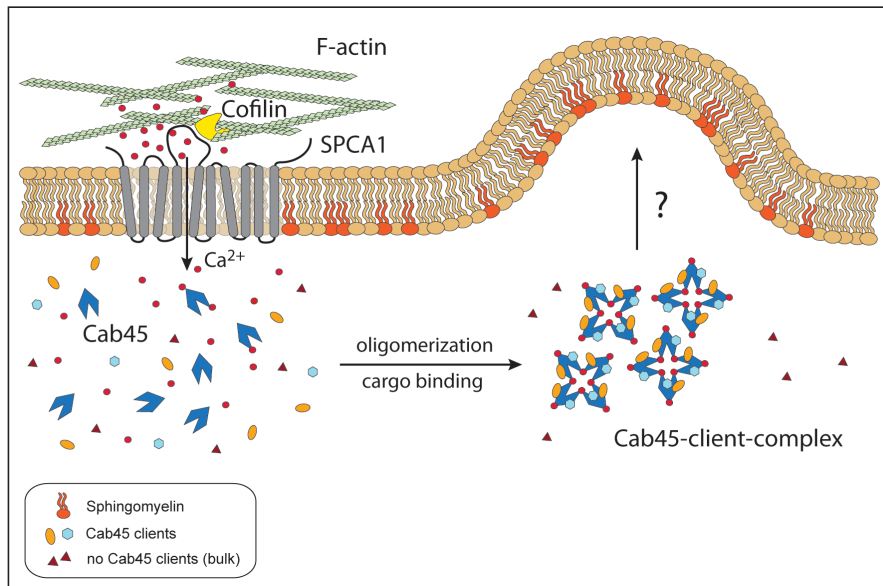
Figure 17: The sorting of soluble secreted cargo molecules via the Cab45/SPCA1-machinery. Some secretory molecules are sorted in a Ca^{2+}-dependent, receptor-independent sorting mechanism. Upon activation, cofilin1 interacts with the P-domain of the Secretory Pathway Ca^{2+}-ATPase 1 (SPCA1) in its second cytosolic loop and recruits F-actin to the *trans*-Golgi network (TGN). As a result, Ca^{2+} is pumped into the lumen of the TGN and locally increases the Ca^{2+} concentration. The Ca^{2+}-binding protein Cab45 oligomerizes in a Ca^{2+}-dependent way and binds specific cargo molecules like LyzC or COMP. In an unknown manner, Cab45 together with its clients is sorted into sphingomyelin(SM)-rich vesicles and transported to the PM, where they are released into the extracellular space. Abbreviations: LyzC (lysozyme C); COMP (cartilage oligomeric matrix protein); PM (plasma membrane). Figure created according to Deng et al. 2018.

2. Aims of the thesis

As part of the Secretory Pathway, the Golgi apparatus plays a major role in protein trafficking and sorting in eukaryotic cells. Although many of those mechanisms have been identified during the last decades, especially how soluble secreted molecules are transported within the Golgi apparatus and secreted into the extracellular space, still poses a challenge. For this very reason, protein trafficking and secretion became an important research topic, as defects were associated with severe diseases like diabetes, neurological disorders or cancer (Dong and Kwon 2009; Meas and Guillausseau 2011; Villarreal et al. 2013).

Due to the lack of recognition motifs and cargo receptors for those molecules, our lab is focusing on Ca^{2+}-mediated sorting processes at the Golgi apparatus that involve the luminal Ca^{2+}-binding protein Cab45 in an interplay with lipids and the Ca^{2+}-ATPase SPCA1. To further strengthen our proposed mechanism and to deepen our knowledge of how Ca^{2+} is additionally contributing in the transport and sorting of soluble secreted proteins, the main aims of this thesis were:

1) Identification of similar Ca^{2+}-dependent transport and sorting processes in the Golgi complex

2) Identification of missing factors that are involved in Cab45-dependent cargo sorting

3) Analysis of Cab45 post-translational modifications and their contribution to its oligomerization and sorting behavior

3.   Results

3.1   NUCB1 regulates ECM degradation by promoting intra-Golgi trafficking of MMPs

The eukaryotic cell is defined by the presence of membrane-bound organelles, each with its own unique array of proteins and defined lipid compositions that enable them to perform important specialized biochemical functions. Therefore, the correct modification and distribution of proteins and lipids is crucial to maintain cellular homeostasis. As part of the Secretory Pathway, the Golgi apparatus plays an essential role in both of these processes. Here, proteins and lipids are modified in a step-wise manner, migrating through the Golgi cisternae before finally being transported to their downstream destinations. As Ca^{2+} homeostasis has been shown to be essential for cargo transport, the Golgi apparatus meticulously regulates its Ca^{2+} levels via Ca^{2+}-pumps, ion channels and Ca^{2+}-binding proteins. Nevertheless, how exactly cargo molecules are transported within the Golgi complex remains a subject of intense debate in the field. In this study the trafficking of MMPs along the Secretory Pathway, particularly the secreted gelatinase MMP2, was investigated.

By performing pull-down experiments, followed by mass spectrometry analysis of isolated Golgi fractions of cells transfected with MMP2-GFP[95] or GFP only as a control, we initially identified the *cis*-Golgi Ca^{2+}-binding protein NUCB1 as potential interaction partner of MMP2 (Pacheco-Fernandez et al. 2020 - Figure 1). Using co-immunoprecipitation and analytical ultracentrifugation, we furthermore could confirm a direct interaction between the two proteins (Pacheco-Fernandez et al. 2020 - Figures 1 and S3). Consequently, we generated NUCB1-KO cells to elucidate its role in intra-Golgi transport of MMP2 (Pacheco-Fernandez et al. 2020 - S1). By monitoring the synchronous transport of MMP2 along the Secretory Pathway, we demonstrated that depletion of NUCB1 leads to delayed cargo transport exclusively through the Golgi complex (Pacheco-Fernandez et al. 2020 - Figures 2, 3 and 4). Subsequently, MMP2 mediated cell migration and matrix invasion was impaired as a result of the delayed transport of MMP2 along the Golgi (Pacheco-Fernandez et al. 2020 - Figures 7 and 8). Similarly, MT1-MMP, another MMP and activator of MMP2, exhibits a delayed transport to the cell surface of NUCB1-KO cells, whereas other Golgi traversing proteins like

---

[95] GFP = Green fluorescence protein

LyzC and CatD[96] were not affected (Pacheco-Fernandez et al. 2020 - Figures S4 and S5). Finally, we investigated the influence of Ca^{2+} in these trafficking processes. Initially, we mutated the two Ca^{2+}-binding EF-hand motifs in NUCB1 and revealing their importance in MMP2 binding and transport (Pacheco-Fernandez et al. 2020 - Figure 5). Moreover, by utilizing various Golgi Ca^{2+}-sensors we determined that NUCB1 is essential for the Ca^{2+} homeostasis of the *cis*-Golgi (Pacheco-Fernandez et al. 2020 - Figure 6).

---

[96] CatD = Cathepsin D

ARTICLE

Nucleobindin-1 regulates ECM degradation by promoting intra-Golgi trafficking of MMPs

Natalia Pacheco-Fernandez[1], Mehrshad Pakdel[1], Birgit Blank[2], Ismael Sanchez-Gonzalez[3], Kathrin Weber[4], Mai Ly Tran[1,2], Tobias Karl-Heinz Hecht[1,2], Renate Gautsch[1], Gisela Beck[1], Franck Perez[5], Angelika Hausser[3], Stefan Linder[4], and Julia von Blume[1,2]

Matrix metalloproteinases (MMPs) degrade several ECM components and are crucial modulators of cell invasion and tissue organization. Although much has been reported about their function in remodeling ECM in health and disease, their trafficking across the Golgi apparatus remains poorly understood. Here we report that the cis-Golgi protein nucleobindin-1 (NUCB1) is critical for MMP2 and MT1-MMP trafficking along the Golgi apparatus. This process is Ca²⁺-dependent and is required for invasive MDA-MB-231 cell migration as well as for gelatin degradation in primary human macrophages. Our findings emphasize the importance of NUCB1 as an essential component of MMP transport and its overall impact on ECM remodeling.

Introduction

Organogenesis, growth, and physiological tissue turnover require constant rearrangement and degradation of ECM proteins (Apte and Parks, 2015; Theocharis et al., 2019). For these purposes, human cells secrete a wide variety of different proteases, among which matrix metalloproteinases (MMPs) have been identified as a major group promoting ECM turnover (Kessenbrock et al., 2010; Jobin et al., 2017).

MMPs are Zn^{2+}-dependent proteases that degrade various ECM components, such as collagen, gelatin, and fibronectin (Endo et al., 2003; Khokha et al., 2013; Cui et al., 2017). To date, 23 MMPs have been described in humans, which can be grouped into different families based on their substrate specificity (Cui et al., 2017). For instance, MMP2, a well-studied member of the family of gelatinases, is involved in endothelial transmigration, angiogenesis, inflammatory responses, and cancer metastasis (Reichel et al., 2008; Vandooren et al., 2013; Könnecke and Bechmann, 2013; Bonnans et al., 2014; Hannocks et al., 2019).

To ensure proper functioning of these critical processes, the activity of all MMPs is meticulously controlled. All MMPs except MMP23 share a basic structure, with three domains designated as propeptide, catalytic, and hemopexin (Fig. 1 A; Cui et al., 2017). The propeptide is crucial for MMP activation because it contains a "cysteine switch" motif in which cysteine binds to the Zn^{2+} ion of the catalytic pocket. Once this linkage is cleaved, the catalytic pocket is accessible and the MMP becomes active (Tallant et al., 2010; Cui et al., 2017; Alaseem et al., 2019). For MMP2, this activation step occurs mainly at the plasma membrane and is mediated by membrane type 1 (MT1)-MMP, a

membrane-bound protein of the same family that, in conjunction with tissue inhibitor of metalloproteinase 2 (TIMP2), cleaves the propeptide domain (Fernandez-Catalan et al., 1998; Brew and Nagase, 2010; Han et al., 2015). This interplay between MT1-MMP and MMP2 is the main step in invasive cell migration and ECM proteolysis, as shown by previous studies that have demonstrated their accumulation at characteristic proteolytic adhesion spots, such as podosomes in myeloid cells and invadopodia in cancer cells (Van Goethem et al., 2010; Jacob et al., 2013; Shaverdashvili et al., 2014; Han et al., 2015; Linder and Wiesner, 2015).

Soluble and membrane-associated MMPs are synthesized as inactive precursors (zymogens) in the ER and then transported to the Golgi apparatus, as described for other cargoes of the secretory pathway (Barlowe and Miller, 2013; McCaughey and Stephens, 2018). Upon reaching the Golgi, they are sorted and transported to specific membrane domains at the cell surface (Deryugina et al., 2004; Kean et al., 2009; Frittoli et al., 2014; Kajiho et al., 2016). Thus far, several cytosolic factors such as microtubules and motor proteins as well as Rab GTPases are considered necessary for MMP transport (Sbai et al., 2010; Wiesner et al., 2010, 2013; Gueye et al., 2011; Frittoli et al., 2014; Linder and Scita, 2015; Jacob et al., 2016).

The divalent ion calcium (Ca^{2+}) is a key component of the reaction by which secretory cargoes are sorted and packed for transport out of the Golgi apparatus (Porat and Elazar, 2000; Ton and Rao, 2004; Pizzo et al., 2010; Lissandron et al., 2010; Rayl et al., 2016; Margulis et al., 2016). Recent studies have

[1]Max Planck Institute of Biochemistry, Martinsried, Germany; [2]Department of Cell Biology, Yale University School of Medicine, New Haven, CT; [3]Institute of Cell Biology and Immunology, University of Stuttgart, Stuttgart, Germany; [4]Institut für Medizinische Mikrobiologie, Virologie und Hygiene, Universitätsklinikum Hamburg, Hamburg, Germany; [5]Institute Curie, PSL Research University, Centre National de la Recherche Scientifique, UMR 144, Paris, France.

Correspondence to Julia von Blume: julia.vonblume@yale.edu.
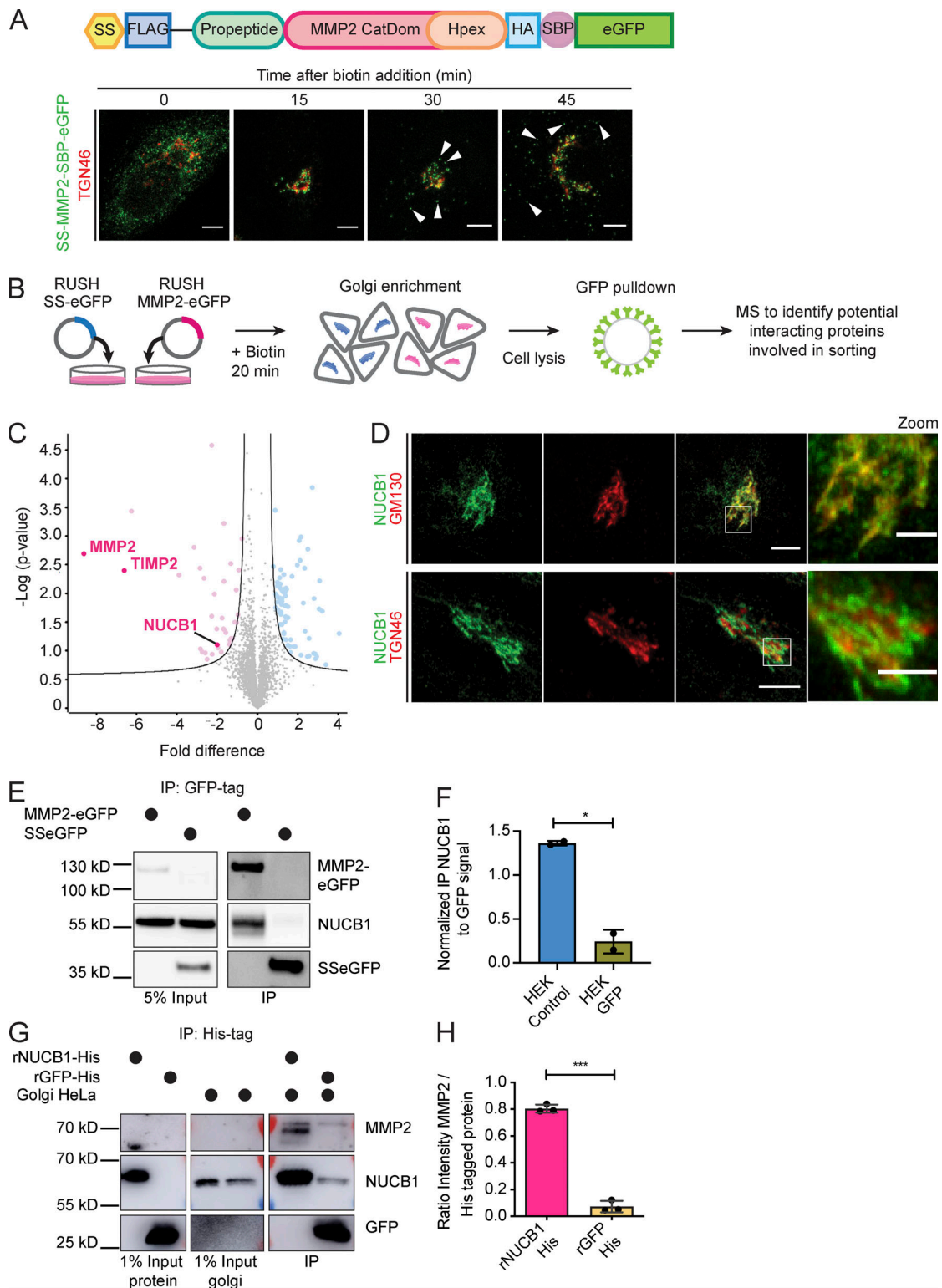
Figure 1.   **Identification of candidates involved in the trafficking of MMP2. (A)** Scheme of the MMP2 RUSH construct. SS-Flag-MMP2-HA-SBP-eGFP was used as a reporter. Fluorescence images show HeLa cells expressing MMP2-SBP-eGFP counterstained against TGN46 (red). Without biotin, MMP2 is retained in the ER (0 min). It reaches the Golgi 15 min after biotin addition and is sorted into vesicles (arrowheads) at 30 and 45 min, respectively. Scale bars, 5 µm. **(B)** MS strategy to identify MMP2 interacting partners in the Golgi. HeLa cells expressing MMP2-SBP-eGFP or SS-SBP-eGFP were incubated for 20 min with biotin to enrich reporter proteins at the Golgi. After GFP IP, samples were analyzed using MS (*n* = 3). **(C)** Volcano plot highlights significantly enriched MMP2 interactors in pink. 42 sorting-related candidates were found, among them TIMP2, a known inhibitor of MMP2, and NUCB1. Two-sample *t* test, false discovery rate = 0.3, minimum fold change = 0.5. **(D)** Fluorescence images of HeLa cells labeled with endogenous NUCB1 (green) and GM130 or TGN46 (red). Scale bars, 5 µm;

zoom, 2 µm. **(E)** HEK 293T cells expressing SS-MMP2-SBP-eGFP or SS-SBP-eGFP were processed for GFP IP and WB analysis. **(F)** Semiquantitative analysis of the normalized NUCB1 to GFP signal from two independent experiments. Significance: one-sample t test. **(G)** His-tag coIP of recombinant rNUCB1-His. Endogenous MMP2 from HeLa Golgi membranes coimmunoprecipitated with rNUCB1-His but not rGFP-His. **(H)** Semiquantitative analysis of the MMP2 signal from three independent experiments. Bars, mean ± SD. Paired t test: *, $P < 0.05$; ***, $P < 0.001$.

revealed the molecular mechanisms by which Ca^{2+}-based cargo sorting and export occur at the Golgi (Micaroni et al., 2010; Deng et al., 2018). In this regard, Cab45, a soluble Ca^{2+}-binding protein, acts on local, transient Ca^{2+} influx at the trans-Golgi network (TGN). After mediated influx by Ca^{2+} ATPase SPCA1, Cab45 assembles into oligomers and sorts secretory cargoes into sphingomyelin-rich transport carriers (von Blume et al., 2011, 2012; Crevenna et al., 2016; Deng et al., 2018).

Human cells express another luminal Golgi Ca^{2+}-binding protein called nucleobindin-1 (NUCB1), which, in contrast to Cab45, localizes to the cis-Golgi compartment (Lin et al., 1998, 1999; Lavoie et al., 2002; Tulke et al., 2016). Earlier studies have postulated NUCB1 to be a regulator of endosomal recycling of lysosomal receptors (Brodeur et al., 2009; Larkin et al., 2016); however, whether NUCB1 has a role in the anterograde intra-Golgi (IG) transport of proteins is unknown.

Here we identify NUCB1 as an MMP2 binding partner and show that NUCB1 is required for its trafficking through the Golgi apparatus. The functional association of MMP2 and NUCB1 occurs in the lumen of the cis-Golgi compartment in a Ca^{2+}-dependent manner and is required for MMP2 and MT1-MMP trafficking through the Golgi. We provide further evidence that NUCB1 silencing perturbs ECM degradation in human primary macrophages, as well as MMP-dependent ECM degradation and invasive cell migration in MDA-MB-231 cells, highlighting the physiological relevance of NUCB1 in MMP2 and MT1-MMP trafficking. Our study provides insight into the molecular mechanisms underlying MMP IG transport and identifies NUCB1 as a central regulator of protein trafficking at the cis-Golgi.

Results

Visualization of MMP2 trafficking in living cells

The "retention using selective hooks" (RUSH) system was used to investigate MMP2 trafficking (Boncompain et al., 2012). This system allows quantitative analysis of the secretory pathway by synchronous release of cargo, which is achieved at a physiological temperature using biotin (Boncompain et al., 2012). We generated an MMP2 construct C-terminally tagged with streptavidin binding peptide (SBP) followed by an enhanced green fluorescent protein (eGFP) to obtain the fusion protein signal sequence (SS)-MMP2-SBP-eGFP as a reporter, whereas streptavidin tagged KDEL was used as an ER retention hook (Fig. 1 A). Confocal microscopy images show that in the absence of biotin, MMP2 localized to the ER. Upon 15 min of biotin incubation, MMP2 reached the Golgi and localized to secretory vesicles after 30 and 45 min (Fig. 1 A). We also confirmed that MMP2-eGFP is actually secreted from cells by staining the released protein with an anti-GFP antibody (Fig. S1 A). Furthermore, we costained MMP2-GFP vesicles with Rab5, Rab6, Rab7, Rab8, Rab11, mCherry lysosomes, and Lysozyme C (LyzC)-mCherry (Fig. S2).

MMP2 containing TGN-derived vesicles did not overlap with any of these endosomal, lysosomal, or Rab GTPase markers. Nevertheless, MMP2 TGN-derived vesicles partially colocalized with LyzC, a protein sorted into sphingomyelin-rich vesicles. Hence, the RUSH assay robustly monitors MMP2 trafficking through the secretory pathway.

Identification of novel interaction partners controlling MMP2 trafficking

To gain insight into the molecular mechanism of MMP2 trafficking, we implemented a novel proteomics approach to identify endogenous interacting proteins involved in protein transport (Fig. 1 B). HeLa cells expressing either SS-MMP2-SBP-eGFP or SS-SBP-eGFP were incubated for 20 min with biotin to enrich the reporter proteins at the Golgi, subjected to GFP immunoprecipitation (IP), and analyzed by mass spectrometry (MS, Fig. 1 B). We identified 42 interacting proteins significantly enriched in SS-MMP2-SBP-eGFP IPs (Table S1 and Fig. 1 C). MMP2 and a widely described interacting protein (TIMP2) were significantly enriched, validating our results (Fig. 1 C). Furthermore, NUCB1, an EF-hand domain (EFh) Ca^{2+}-binding protein that localizes to the cis-Golgi and is considered to be its major luminal Ca^{2+} regulator, was identified. NUCB1 and Cab45 share several similarities, as both are luminal Ca^{2+} resident proteins in the Golgi and belong to the same EFh protein family. Given that Cab45 has been described as crucial in Ca^{2+}-dependent sorting of soluble secretory proteins (von Blume et al., 2012; Crevenna et al., 2016; Deng et al., 2018), we focused on elucidating the role of NUCB1 in MMP2 trafficking.

NUCB1 interacts with MMP2 at the Golgi

We first corroborated the reported localization of NUCB1 in HeLa cells by costaining endogenous NUCB1 with the cis- and trans-Golgi markers GM130 and TGN46, respectively (Fig. 1 D). Colocalization with GM130 but not with TGN46 indicates a cis-Golgi localization, in agreement with previous reports (Lin et al., 1998). Based on the MS results, we performed IP experiments to verify the interaction of MMP2 with NUCB1 (Fig. 1 E). To this end, HEK293T cells expressing SS-MMP2-SBP-eGFP or SS-SBP-eGFP were incubated with biotin for 15 min to accumulate MMP2-eGFP or SS-eGFP in the Golgi, and IPs were performed. Western blotting (WB) with GFP and NUCB1 antibodies (Fig. 1 E) evidenced an interaction between endogenous NUCB1 and MMP2-eGFP but not with SS-SBP-GFP (Fig. 1, E and F). To further validate such interaction in the Golgi, we incubated recombinant His-tagged NUCB1 (rNUCB1-His; Fig. S3 A) or GFP (rGFP-His) with detergent-solubilized Golgi membranes purified from HeLa cells (von Blume et al., 2012). Ni-NTA pull-downs showed endogenous MMP2 coIP with rNUCB1-His, but not with rGFP-His (Fig. 1, G and H).

To better characterize the interaction between NUCB1 and MMP2, we generated purified recombinant His-SUMO-MMP2

Pacheco-Fernandez et al.
Nucleobindin-1 regulates MMP secretion

Journal of Cell Biology 3 of 23
https://doi.org/10.1083/jcb.201907058

(rHS-MMP2; Fig. S3, B and C) and performed analytical ultracentrifugation (AUC), a technique that shows sedimentation of macromolecules in solution. For this experiment, rHS-MMP2 was bioconjugated with Cy3 via maleimide labeling and analyzed by AUC. As expected, the sedimentation peak of rHS-MMP2-Cy3 occurred at 4.705 S (measured Stokes radius at 20°C: 4.41 nm), and the calculated molecular weight was ∼87.1 kD (Fig. S3 D). Then, we evaluated the AUC profiles of rHS-MMP2-Cy3 and rNUCB1-His in solution (Fig. S3 E), finding a peak at 3.189 S that indicates a shift in the sedimentation velocity and is associated with a direct interaction between NUCB1 and MMP2 (Stokes radius at 20°C: 8.41 nm). The calculated molecular weight was 112 kD, close to the theoretical molecular weight of the complex (Fig. S3 E). Altogether, these data confirmed that NUCB1 interacts with MMP2 in the Golgi.

MMP2 trafficking is delayed in NUCB1 knockout (KO) cells

Next, we generated NUCB1-KO HeLa cells using CRISPR/Cas9 and confirmed the KO by WB and immunofluorescence (Fig. S1, B–D). We then analyzed the impact of NUCB1 on MMP2 trafficking by monitoring the transport kinetics of MMP2 at a single-cell level using the RUSH system in control and NUCB1-KO cells (Fig. 2 A). Quantification of SS-MMP2-SBP-eGFP–containing vesicles showed that the median number of vesicles in control cells after 30 min of biotin addition was 29 (interquartile range [IQR], 17–52.75), whereas it was significantly reduced to 8 (IQR, 3–26) in NUCB1-KO cells (Fig. 2 B). Reexpression of NUCB1-WT fully restored the amount of SS-MMP2-SBP-eGFP–positive vesicles to control levels in NUCB1-KO cells (median, 36.5; IQR, 17–51.75; Fig. 2 B).

Previous studies have documented the expression of NUCB1 in the lumen of the Golgi as well as in the cytosol (Brodeur et al., 2009; Kapoor et al., 2010). To confirm that Golgi-localized NUCB1 is exclusively required to rescue the described MMP2 trafficking delay, NUCB1-KO cells were transfected with cytosolic NUCB1 (NUCB1-cyto). Importantly, NUCB1-cyto could not rescue the delay observed in NUCB1-KO cells, further confirming that Golgi-localized NUCB1 is necessary for MMP2 trafficking (Fig. S4, A and B).

To assess the specificity of this defect, we performed RUSH experiments using the Cab45 cargo lysozyme C (LyzC)-eGFP (LyzC-SBP-eGFP; Deng et al., 2018). Cells were imaged at 20, 40, and 60 min after biotin incubation to quantify cytosolic vesicles (Fig. 2 C), showing that NUCB1 depletion does not alter LyzC trafficking (Fig. 2 D). Simultaneously, we monitored Flag-tagged SS-MMP2-SBP-eGFP and SS-LyzC-SBP-eGFP secretion in a pool of control and NUCB1-KO HeLa cells. WB analysis of cell culture supernatants showed reduced secretion of SS-MMP2-SBP-eGFP in NUCB1-KO cells after 45 min of biotin incubation (Fig. 2, E and F); however, no effect was observed for SS-LyzC-SBP-eGFP. To further validate the specificity of NUCB1 and MMP2 binding, we evaluated whether there was an interaction between LyzC-eGFP with NUCB1. Whereas NUCB1 specifically interacted with MMP2, it did not bind to LyzC in HeLa control, NUCB1-KO, or NUCB1-WT reconstituted cells (Fig. 2, G and H).

Moreover, to evaluate whether NUCB1 is required for the trafficking of other members of the MMP family, we analyzed

the trafficking of MT1-MMP (Fig. S4 C). Control and NUCB1-KO cells with or without reexpression of NUCB1-WT were transiently transfected with the RUSH construct SS-MT1-MMP-SBP-mCherry and analyzed at 30, 60, and 90 min after biotin addition (Fig. S4 D). Quantification of SS-MT1-MMP-SBP-mCherry–positive vesicles at 60 min after biotin addition showed a significant reduction in number of vesicles in NUCB1-KO cells (median, 2.5; IQR, 0.25–7) compared with the HeLa control (median, 10; IQR, 4–36; Fig. S4 E). Importantly, reexpression of NUCB1-WT restored the numbers of positive MT1-MMP vesicles to control levels (median, 13; IQR, 7.5–21; Fig. S4 E).

To determine if the trafficking of endogenous MT1-MMP to the cell surface was affected by NUCB1, we performed a cell surface biotinylation assay. Briefly, after HeLa or NUCB1-KO cells were incubated with sulfo-NHS-SS-biotin for 90 min, biotinylated proteins were pulled down using NeutrAvidin beads. WB analysis revealed less endogenous MT1-MMP on the cell surface of NUCB1-KO cells than on HeLa control cells (Fig. S4 F), confirming a defect in the transport of endogenous MT1-MMP to the cell surface (Fig. S4 G).

Taken together, these results indicate that NUCB1 is a specific component for the trafficking of MMP2 and MT1-MMP. Given that MT1-MMP can activate MMP2 at the plasma membrane, we investigated whether reduced secretion of MMP2 could be related to a defect in the surface availability of MT1-MMP. For this purpose, we performed gel zymography of cell culture supernatants from HeLa and NUCB1-KO cells expressing SS-MMP2-SBP-eGFP after 45 min of biotin incubation. We observed no differences in MMP2 activity between NUCB1-KO and HeLa control cells (Fig. S5, A and B), indicating that the differences observed in the secretion phenotype are not caused by an activation defect.

To further investigate the role of NUCB1 in secretory protein trafficking, we analyzed the secretion of SS-HRP in control and NUCB1-KO cells. Similar to LyzC, SS-HRP secretion was not affected by NUCB1-KO (Fig. S5, C and D). We also tested if NUCB1 impacted protein transport to lysosomes by monitoring the trafficking of cathepsin D (cathD). After 20, 40, and 60 min of biotin incubation, confocal microscopy images of control and NUCB1-KO cells expressing SS-SBP-eGFP-cathD revealed no differences in the number of cathD vesicles between these cells, indicating that protein transport to lysosomes was not affected by NUCB1 (Fig. S5, E and F). Overall, our data show that NUCB1 is not a universal regulator of protein trafficking in the secretory pathway, but rather it plays a specific role in MMP2 trafficking.

NUCB1 facilitates MMP2 IG transport

To better dissect the role of NUCB1 in the trafficking of MMP2, we performed RUSH experiments in control and NUCB1-KO cells costained with ER–Golgi intermediate compartment (ERGIC) and Golgi markers. Early trafficking of MMP2 from the ER to ERGIC was monitored by colocalization of MMP2 and ERGIC-resident 53-kD membrane protein (ERGIC53). After 2.5, 5, and 7.5 min of biotin incubation (Fig. 3 A), Pearson's correlation coefficients (PCs) of MMP2 and ERGIC53 showed no significant differences between control and NUCB1-KO cells, suggesting no traceable MMP2 trafficking defect from ER to Golgi (Fig. 3 B). In

Pacheco-Fernandez et al.
Nucleobindin-1 regulates MMP secretion

Journal of Cell Biology 4 of 23
https://doi.org/10.1083/jcb.201907058
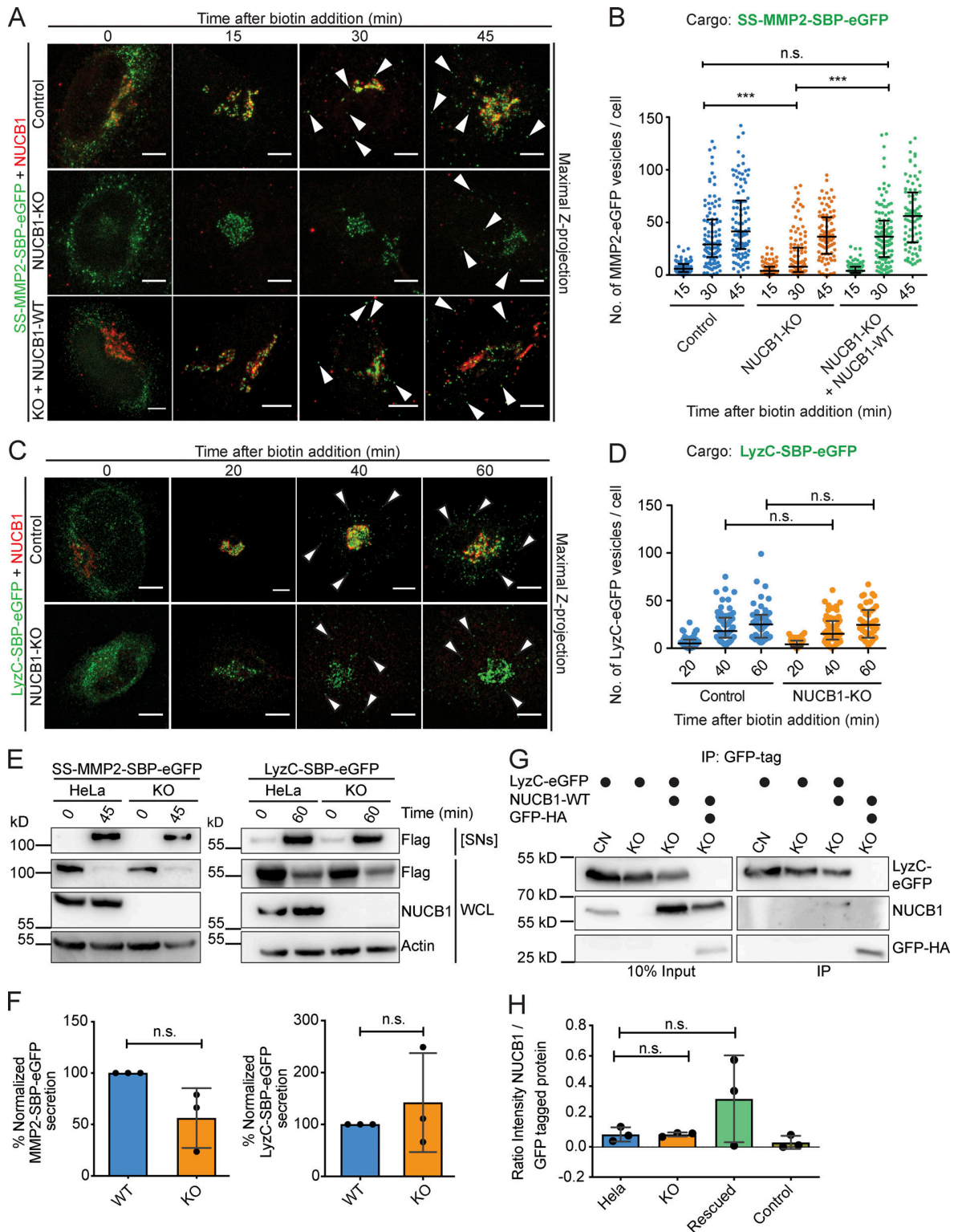
Figure 2. **NUCB1-KO impairs the trafficking of MMP2. (A)** Fluorescent images of HeLa or NUCB1-KO cells expressing SS-MMP2-SBP-eGFP with or without NUCB1-WT, counterstained against NUCB1 (red) and captured after 0, 15, 30, and 45 min of biotin incubation. Arrowheads, cytoplasmic vesicles. Scale bars, 5 μm. **(B)** Cytoplasmic vesicle counts as described in A are plotted as number of vesicles per cell ($n \geq 90$ cells, median ± IQR of two independent experiments; ***, $P < 0.001$; n.s., not significant). **(C)** Confocal microscopy images of HeLa or NUCB1-KO cells expressing LyzC-SBP-eGFP and counterstained against NUCB1 (red) after 0, 20, 40, and 60 min of biotin incubation. Arrowheads, cytoplasmic vesicles. Scale bars, 5 μm. **(D)** Cytoplasmic vesicle counts from C of two independent experiments ($n \geq 42$ cells, median ± IQR). **(E)** Secretion assay of HeLa or NUCB1-KO cells expressing SS-MMP2-SBP-eGFP or LyzC-SBP-EGFP and incubated with biotin for 45 or 60 min, respectively. WCL, whole-cell lysates. [SNs], 10×-concentrated supernatants. **(F)** Semiquantitative analysis from three

Pacheco-Fernández et al.
Nucleobindin-1 regulates MMP secretion

Journal of Cell Biology 5 of 23
https://doi.org/10.1083/jcb.201907058

independent experiments, one-sample *t* test. Bars, mean ± SD. **(G)** GFP-coIP of HeLa or NUCB1-KO cells expressing LyzC-eGFP, with or without NUCB1-WT. GFP-HA, negative control; CN, HeLa control; KO, NUCB1-KO. **(H)** Semiquantitative analysis of NUCB1 to GFP signal from three independent experiments. Bars, mean ± SD; paired *t* test.

---

contrast, PC quantification of MMP2 with the cis-Golgi marker GM130 (Fig. 3 C) revealed reduced colocalization in NUCB1-KO cells at 10, 15, and 20 min after biotin addition (Fig. 3 D). After 25 and 30 min, MMP2–GM130 colocalization recovered to similar control cell levels, indicating that MMP2 transport is delayed in the absence of NUCB1 at the early stages of the cis-Golgi (Fig. 3 D).

Finally, we analyzed the colocalization of MMP2 with the trans-Golgi marker TGN46 (Fig. 3 E). PC of MMP2 with TGN46 showed significant differences in NUCB1-KO cells only at 20 and 25 min of biotin incubation but not at later time points (Fig. 3 F). Therefore, MMP2 IG trafficking appears to be affected from cis- to trans-Golgi in the absence of
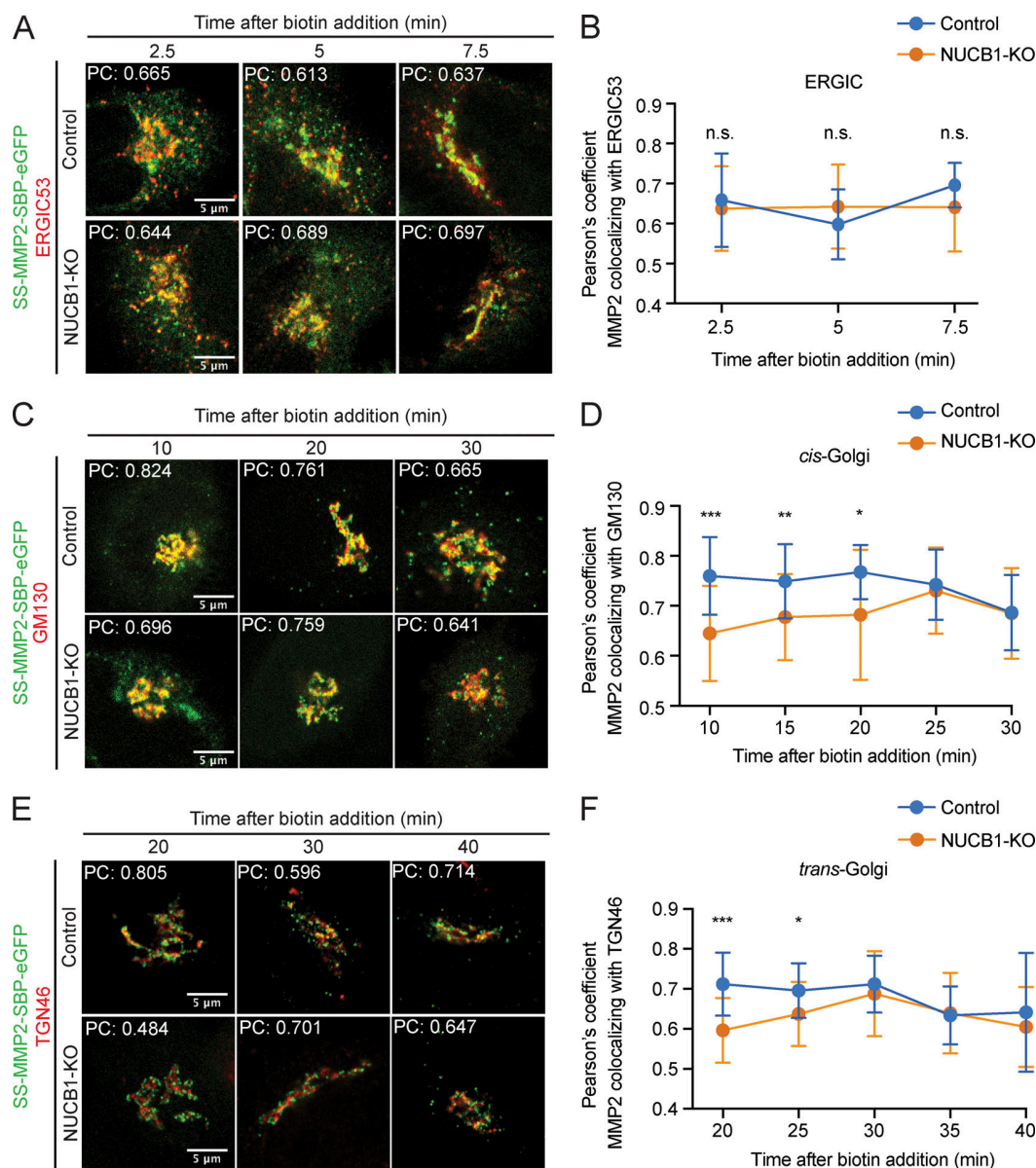
Figure 3.   **MMP2 trafficking delay occurs at the cis-Golgi. (A)** Fluorescence images of HeLa or NUCB1-KO cells transiently expressing SS-MMP2-SBP-eGFP, fixed at 2.5, 5, and 7.5 min after biotin addition, and counterstained against ERGIC53 (red). Scale bars, 5 μm. **(B)** Average PC per time point. **(C)** Colocalization of HeLa or NUCB1-KO cells expressing SS-MMP2-SBP-eGFP with GM130 (red) after 10, 15, 20, and 25 min of biotin incubation. Scale bars, 5 μm. **(D)** Average PC illustrates decreased colocalization at 10, 15, and 20 min after biotin addition. **(E)** Colocalization of SS-MMP2-SBP-eGFP with TGN46 (red) expressed in HeLa or NUCB1-KO cells at 20, 25, 30, 35, and 40 min after biotin addition. Scale bars, 5 μm. **(F)** Average PC shows that MMP2 is equally colocalizing with TGN46 in HeLa and NUCB1-KO cells upon arrival at the TGN. Error bars represent SD; *, P < 0.05; **, P < 0.01; ***, P < 0.001; n.s., not significant.

NUCB1, but not protein sorting into vesicles upon arrival at the TGN.

To further substantiate the trafficking defect observed in NUCB1-KO cells, we performed live-cell wide-field microscopy experiments in cells expressing SS-MMP2-SBP-eGFP after biotin addition (Fig. 4 A). To obtain a better temporal resolution of MMP2 trafficking and sorting into vesicles, we quantified MMP2 vesicles at 1-min time intervals (Fig. 4 B). Within the first 32 min of MMP2 transport after cargo release from the ER, no significant differences were observed in the number of MMP2-containing vesicles between HeLa and NUCB1-KO cells. Interestingly, between 33 and 43 min, MMP2 vesicle numbers were significantly lower in NUCB1-KO cells (Fig. 4 B), supporting our previous findings (Fig. 2, A and B) and indicating that NUCB1 is indeed required for proper MMP2 IG trafficking.

Furthermore, to confirm that the observed delay in NUCB1-KO cells is not due to a defect in ER-to-Golgi transport, we evaluated the arrival of MMP2 to the Golgi over time. Using live-cell time-lapse videos, we evaluated Golgi compaction as a measure of MMP2 kinetics by calculating the Golgi area in each 1-min time frame normalized to the ER area at time 0, i.e., without biotin addition (Fig. 4 C). Within the first 18 min of MMP2 transport, no significant differences between control and NUCB1-KO cells were observed (Fig. 4 D). Between 19 and 26 min, NUCB1-KO cells showed a significant delay in MMP2 trafficking that peaked at 21 min. After this period, MMP2 transport in NUCB1-KO cells was similar to control (Fig. 4 D). These data corroborate our previous results (Fig. 3, A–F) and show that MMP2-eGFP requires more time traveling through the Golgi, suggesting that NUCB1 is specifically required for MMP2 trafficking from the cis-Golgi compartment.

To rule out the "premature" export of SS-MMP2-SBP-eGFP from the ER, we analyzed its localization before biotin addition in control and NUCB1-KO cells in relation to the ER exit site marker Sec16. Confocal microscopy images showed only partial colocalization between MMP2 and Sec16, and quantification of the colocalization of these proteins showed no significant difference between HeLa control and NUCB1-KO cells, indicating that MMP2 export is similar in both cell lines at ER exit sites (Fig. 4, E and F).

Ca²⁺ binding by NUCB1 is essential for IG trafficking of MMP2

Proteins in the EFh family of Ca^{2+}-binding proteins differ in the number of their EFh motifs. For example, Calumenin and Cab45 have 6 EFhs, CaM has 4, and NUCB1 has a single pair (Fig. 5 A; Leung et al., 2019; Honoré and Vorum, 2000; Honoré, 2009). The NUCB1 EFhs show high similarity to EFh 3 of Calumenin, EFhs 3 and 4 of Cab45, and EFhs 1 and 2 of CaM (Lin et al., 1999). As a characteristic feature, a highly conserved glutamic acid residue (E) flanks both EFhs (Miura et al., 1994; Gonzalez et al., 2012). Together with aspartic acid (D), these residues are part of what Lin et al. (1999) described as an ideal EF-hand motif, in which the interaction between the oxide groups of D or E, plus carbonyl groups of the peptide chain and water, constitute the Ca^{2+}-binding site. Besides that, previous reports have shown that the EFhs of a recombinant cytosolic version of NUCB1 are essential for its interaction with the α-subunit of G-protein–coupled receptors (Kapoor et al., 2010).

To investigate the significance of these EFhs for MMP2 binding, we generated a Ca^{2+}-binding deficient mutant of NUCB1 (NUCB1-mEFh1+2) by substituting E264 in EFh1 and E316 in EFh2 (Fig. 5 B, dark blue) with a glutamine (Q; Fig. 5 B, pink). Then, we evaluated the relevance of Ca^{2+} in the interaction of NUCB1 to MMP2 using GFP IPs of NUCB1-KO cells expressing SS-Flag-MMP2-HA-eGFP (MMP2-eGFP) and reconstituted with NUCB1-WT or NUCB1-mEFh1+2. WB analysis revealed a significant reduction in the interaction between NUCB1 and MMP2 when both EFhs were mutated, indicating that Ca^{2+}-binding is crucial for the interaction of NUCB1 with MMP2 (Fig. 5, C and D).

Next, SS-MMP2-SBP-eGFP was expressed in control, NUCB1-KO, and NUCB1-KO cells reconstituted with either NUCB1-WT or NUCB1-mEFh1+2 (Fig. 5 E), to evaluate if Ca^{2+} binding impacts MMP2 trafficking. The number of MMP2-eGFP–positive vesicles in NUCB1-KO and NUCB1-EFh1+2–expressing cells was significantly reduced compared with control cells and NUCB1-WT–reexpressing cells (Fig. 5 F), confirming the essential role of Ca^{2+} binding in the trafficking of MMP2.

To assess the role of NUCB1 in Golgi Ca^{2+} homeostasis, Ca^{2+} influx into the Golgi was monitored using a previously established workflow (Lissandron et al., 2010; von Blume et al., 2011; Kienzle et al., 2014; Deng et al., 2018). To this end, we generated a novel low-affinity Förster resonance energy transfer (FRET)-based Ca^{2+} sensor called GPP130-Twitch5, which localized to the cis-Golgi membrane and allowed the measurement of local Ca^{2+} uptake.

Ca^{2+} uptake was measured by depleting luminal Ca^{2+} in control or NUCB1-KO cells expressing GPP130-Twitch5 with ionomycin. Next, Ca^{2+} was added, and FRET signals were captured (Fig. 6 A). Cis-Golgi $[Ca^{2+}]$ fluorescence signals were normalized to $\Delta R/R_0$ (see Materials and methods; Deng et al., 2018). After adding 2.2 mM $CaCl_2$ to the culture medium, fluorescent microscopy images showed a stronger increase in cis-Golgi Ca^{2+} levels in control compared with NUCB1-KO cells (Fig. 6 A). Quantification of Ca^{2+} influx showed a 30.0 ± 8.8% increase in FRET signal in control cells compared with 16.3 ± 10.3% in NUCB1-KO cells (Fig. 6 B). Reexpression of NUCB1-WT restored FRET increase to control levels after Ca^{2+} addition, whereas expression of NUCB1-EF1+2 did not (Fig. 6 B). Importantly, defects in Ca^{2+} homeostasis were exclusively observed at the cis-Golgi, as the analysis of cells expressing the TGN-localized FRET Ca^{2+} sensor Go-D1-cpv (Lissandron et al., 2010) showed no significant differences in Ca^{2+} influx into the TGN in NUCB1-KO cells (Fig. 6, C and D). These results demonstrate that NUCB1 depletion or NUCB1 EFh point mutations disrupt Ca^{2+} homeostasis specifically in the cis-Golgi but not the TGN.

NUCB1 modulates invasive cell migration and ECM degradation

Given the relevance of MMP2 in ECM remodeling, we hypothesized that silencing of NUCB1 would have a direct effect on ECM degradation and MMP-dependent invasive migration. To further investigate the role of NUCB1, we transfected invasive human breast adenocarcinoma MDA-MB-231 cells stably expressing MT1-MMP (Sakurai-Yageta et al., 2008) with two different siRNAs for NUCB1 (Fig. 7, A and B) or MMP2 (Fig. 7 C). The secretion of endogenous MMP2 was evaluated in control or

Pacheco-Fernandez et al.
Nucleobindin-1 regulates MMP secretion

Journal of Cell Biology
https://doi.org/10.1083/jcb.201907058

7 of 23
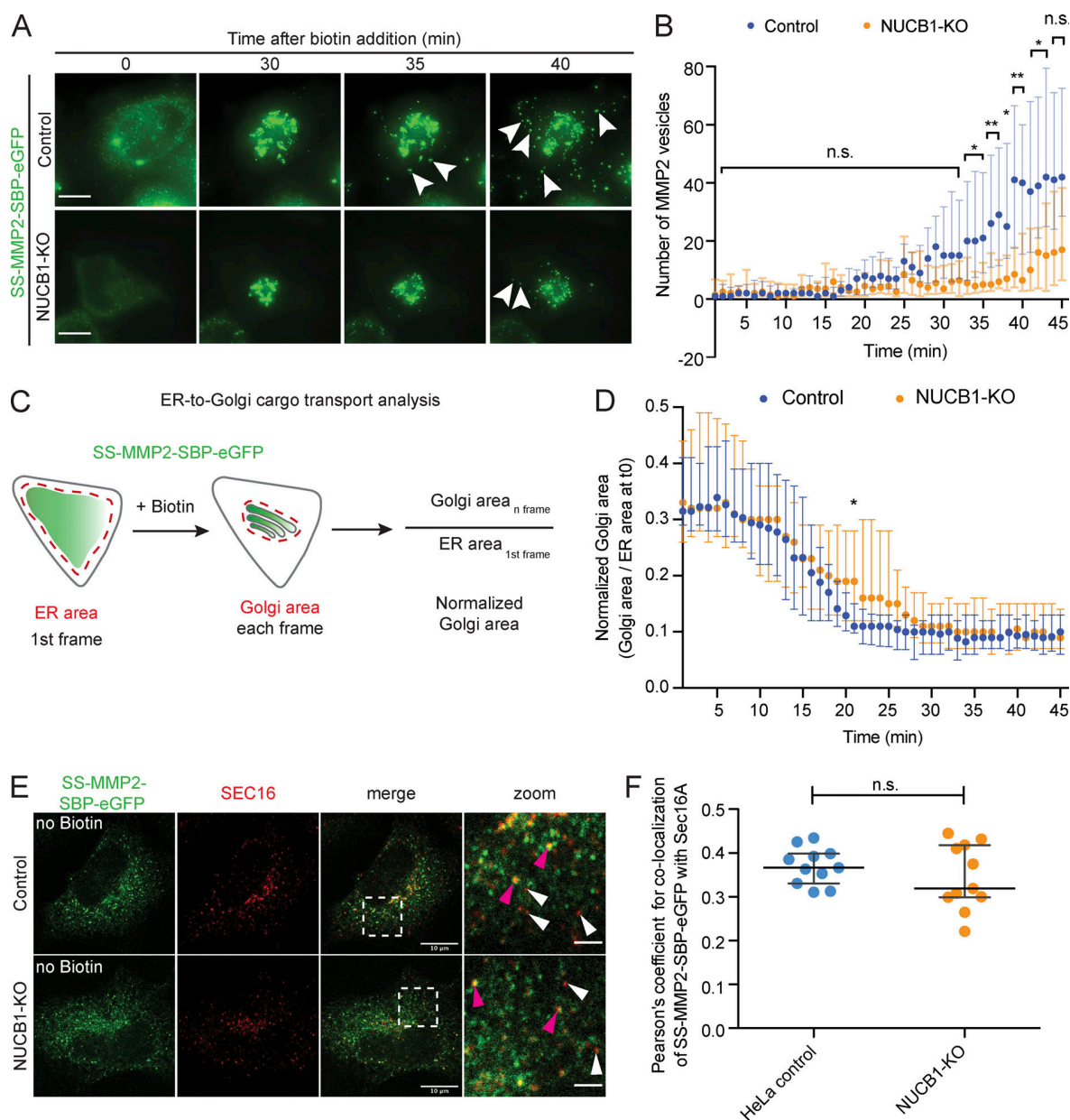
Figure 4. **MMP2 trafficking is exclusively delayed at the Golgi in living cells. (A)** HeLa or NUCB1-KO cells expressing SS-SBP-MMP2-eGFP were analyzed by live-cell wide-field microscopy. Representative images of MMP2 trafficking after 0, 30, 35, and 40 min of biotin incubation. Images were acquired in 1-min frames for each analyzed cell. Arrowheads, cytoplasmic MMP2 vesicles. Scale bars, 10 μm. **(B)** Quantification of cytoplasmic MMP2 vesicles per frame from cells shown in A. n.s., nonsignificant. *, $P < 0.05$; **, $P < 0.01$. **(C)** Schematic representation of ER–Golgi cargo transport analysis, measured as normalized Golgi area over time in cells shown in A. **(D)** Normalized Golgi area for each time point (median ± IQR). A reduced Golgi compaction was observed in the time range 15–23 min in NUCB1-KO cells compared with HeLa control. *, $P < 0.05$. **(E and F)** HeLa or NUCB1-KO cells ($n = 11$) expressing SS-SBP-MMP2-eGFP fixed without biotin addition and immunostained for ER exit site marker Sec16 (red). Scale bar, 10 μm; zoom, 2 μm. Retained MMP2 in the ER partially colocalized with Sec16 in both control and NUCB1-KO cells to the same extent (F). Magenta arrowheads, MMP2 structures that colocalized with ER exit sites; white arrowheads, ER exit sites. t test: $P < 0.05$.

NUCB1 MDA-MB-231–silenced cells. Upon collection of cell culture media and whole-cell lysate, WB analysis revealed reduced MMP2 secretion in NUCB1-silenced cells compared with control (Fig. 7, D and E), validating our findings with overexpressed MMP2-eGFP in HeLa cells (Fig. 2, E and F).

To assess the invasive phenotype of NUCB1 silencing in these cells, we performed Transwell invasion and gelatin degradation assays. Compared with control cells, gelatin degradation in both NUCB1- and MMP2-silenced cells was significantly reduced; however, only NUCB1 depletion also had a significant impact on cell invasion (Fig. 7, F–I). These results illustrate the critical role played by NUCB1 in the trafficking of MMPs.

We next investigated whether the silencing of NUCB1 in human blood–derived primary macrophages (Fig. 8 A) would

Pacheco-Fernandez et al.
Nucleobindin-1 regulates MMP secretion

Journal of Cell Biology   8 of 23
https://doi.org/10.1083/jcb.201907058

Figure 5. **NUCB1 EFhs are essential for Golgi trafficking of MMP2. (A)** Protein alignment of human NUCB1 (Q02818, aa 241–400), CaM (P0DP23), Calumenin (O43852), and Cab45 (Q9BRK5). Pink boxes, NUCB1 EFhs. **(B)** NUCB1 adapted PDB protein model (accession no. 1SNL); NUCB1 EFhs, cyan; NUCB1-WT, EFhs with first and last amino acid of the domain in dark blue; NUCB1-mEFh1+2, amino acid substitutions E264Q and E316Q in pink. **(C)** CoIP of MMP2-eGFP transiently expressed in NUCB1-KO cells transfected with NUCB1-WT or NUCB1-mEFh1+2. $n = 4$ biological replicates. **(D)** Semiquantitative analysis of NUCB1 signal per sample normalized to the one of NUCB1-KO cells reexpressing NUCB1-WT. Bars, mean ± SD; one-sample t test. **(E)** Confocal fluorescence images of HeLa or NUCB1-KO cells expressing SS-MMP2-SBP-eGFP and cotransfected with or without NUCB1-WT or NUCB1-mEFh1+2. After 15, 30, and 45 min of biotin incubation, cells were fixed and costained with NUCB1 antibody (red). Scale bars, 5 µm. Arrowheads, cytoplasmic vesicles. **(F)** Quantification of cytoplasmic vesicles as in E from two independent experiments (median ± IQR), $n ≥ 19$ cells. *, $P < 0.05$; **, $P < 0.01$; ***, $P < 0.001$; ****, $P < 0.0001$.
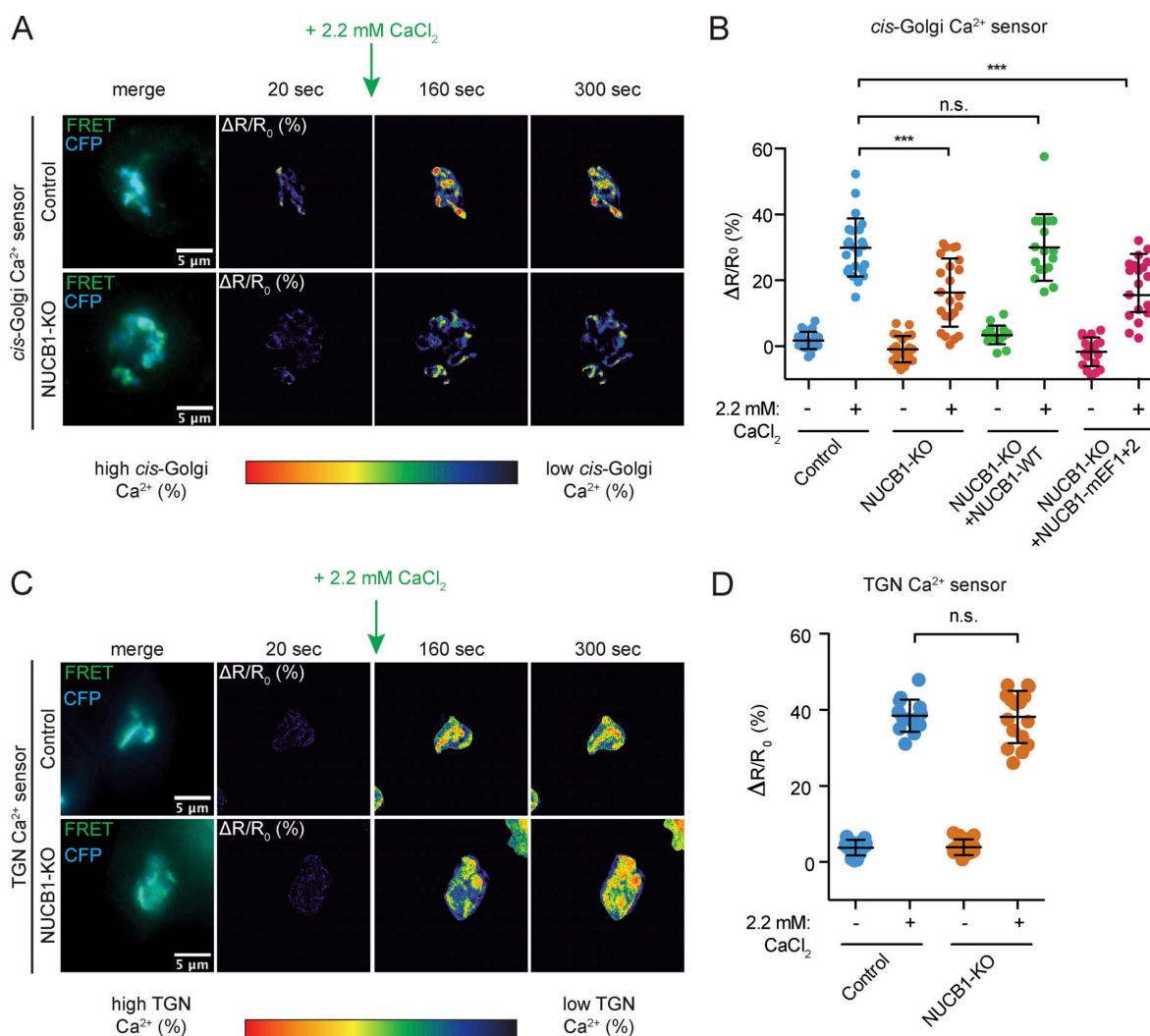
Figure 6. **NUCB1 EFhs are essential for Ca²⁺ homeostasis at the cis-Golgi. (A)** Fluorescent images of HeLa or NUCB1-KO cells expressing the GPP130-Twitch5 cis-Golgi Ca²⁺ sensor. Cells were treated with ionomycin for 20 s to deplete endogenous Ca²⁺ in the Golgi lumen; 2.2 mM Ca²⁺ were added, and cells were monitored using life-cell ratiometric FRET microscopy. **(B)** Quantification of the cis-Golgi $\Delta R/R_0$ FRET ratio from A. **(C)** Pictures illustrate the same experiment described in A but using the Go-D1-cpv trans-Golgi Ca²⁺ sensor. **(D)** Quantification of the trans-Golgi $\Delta R/R_0$ FRET ratio from C. Quantification of ≥20 cells (median ± IQR) from at least two independent experiments. n.s., not significant; ***, $P < 0.001$.

also display a similar phenotype. To this end, human primary macrophages were seeded onto Rhodamine-labeled gelatin, incubated for 6 h, and evaluated by confocal microscopy. The degree of gelatin degradation was estimated as the Rhodamine intensity under each cell normalized by the intensity of the surrounding area and compared with the silenced control cells (siControl -LUC-). Interestingly, we observed a significant reduction in the number of degraded spots of both NUCB1- and MMP2-silenced cells compared with the control (Fig. 8, B and C), but no significant difference was observed between MMP2 and NUCB1 knockdowns.

Taken together, these results illustrate the striking effect of NUCB1 in MMP2 trafficking of human invasive cell models, both in human primary macrophages and under pathological conditions (as observed with MDA-MB-231 cells), and highlight the

importance of NUCB1 in the IG trafficking of MMPs and its impact on ECM remodeling.

Discussion

MMPs are the central drivers for ECM turnover and invasive cell migration (Cauwe and Opdenakker, 2010; Shimoda and Khokha, 2017; Cui et al., 2017; Hannocks et al., 2019; Jobin et al., 2017). To date, known regulators of intracellular MMP transport include cytosolic factors such as microtubules that, in collaboration with motor proteins such as kinesins, steer TGN-derived vesicles toward the cell surface (Poincloux et al., 2009; Sbai et al., 2010; Wiesner et al., 2010; Cornfine et al., 2011; Gueye et al., 2011; Jacob et al., 2013). In addition, cytosolic Rab GTPases play an essential role in MMP trafficking and recycling (Bravo-Cordero et al., 2007; Jacob et al., 2013; Wiesner et al., 2013). Our colocalization
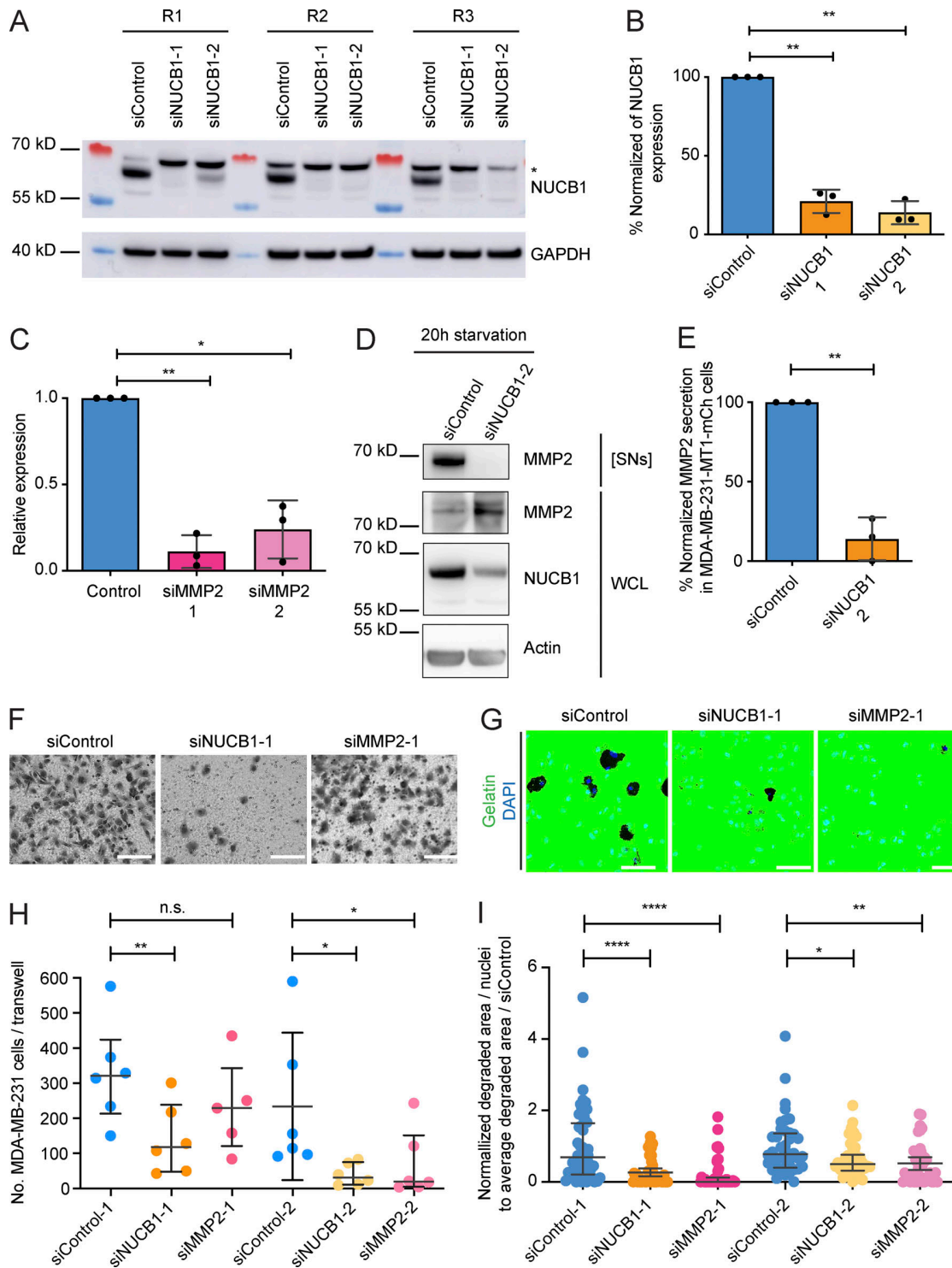
Figure 7. **NUCB1 depletion impairs ECM invasion and degradation in MDA-MB-231 cells. (A)** Expression levels of NUCB1 after siRNA-mediated silencing (n = 3 independent experiments: R1, R2, and R3). *, unspecific band. **(B)** Semiquantitative analysis of normalized NUCB1 signal from A in silenced cells compared with control. Bars, mean ± SD. **(C)** Quantitative PCR analysis of relative MMP2 expression in siRNA-treated MDA-MB-231 cells (n = 3 independent experiments, one-sample t test). **(D)** Secretion assay of endogenous MMP2 in MDA-MB-231 cells. [SN], 20×-concentrated supernatant; WCL, whole cell lysates. **(E)** Semiquantitative analysis of three independent experiments. Bars, mean ± SD. Significance, one-sample t test. **(F and G)** Representative pictures of Matrigel-coated Transwell invasion (F) or gelatin degradation (G) experiments. Scale bars, 150 μm. **(H and I)** Quantification of the number of migrating cells (H) and degraded gelatin area (I). Both invasion and degradation were reduced in siNUCB1 cells. Data: median ± IQR; n = 3 independent experiments. Paired t test: *, P < 0.05; **, P < 0.01; n.s., not significant.

Pacheco-Fernandez et al.
Nucleobindin-1 regulates MMP secretion

Journal of Cell Biology   11 of 23
https://doi.org/10.1083/jcb.201907058
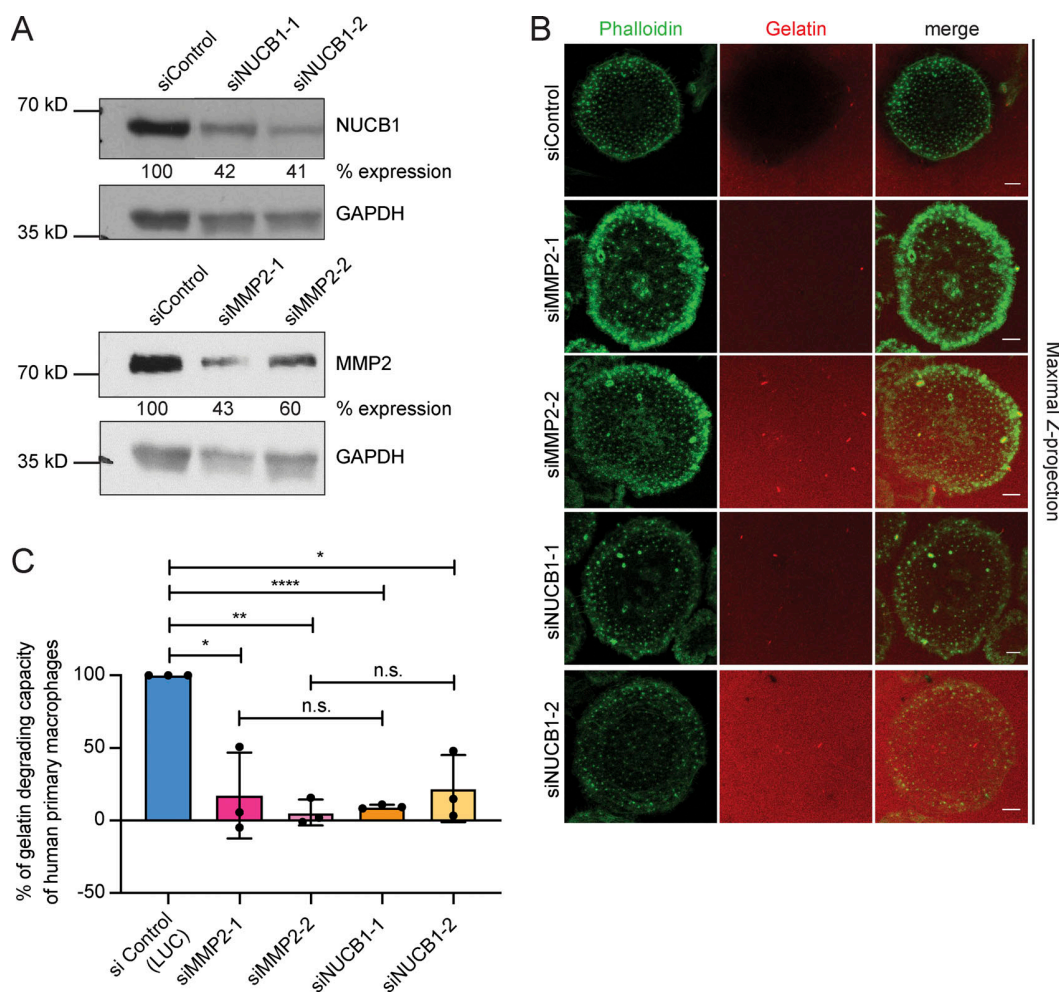
Figure 8. **Matrix degradation is reduced in NUCB1-silenced human primary macrophages. (A)** Validation of NUCB1 silencing. WB is representative of at least three independent experiments. %, relative expression compared with siControl. **(B)** Representative images of human-derived primary macrophages seeded on Rhodamine-conjugated gelatin and incubated for 6 h. Scale bars, 5 µm. n = 3 donors. **(C)** Quantification of gelatin degrading capacity of human primary macrophages. Bars, % of degraded gelatin compared with siControl. At least eight fields of view per condition were analyzed. Data: median ± IQR. One-sample t test: *, $P < 0.05$; **, $P < 0.01$; ***, $P < 0.001$; ****, $P < 0.0001$; n.s., not significant.

experiments using different Rab proteins and MMP2-eGFP (Fig. S2) showed no colocalization with classic markers for TGN-derived vesicles such as Rab8 and Rab6. Also, we did not observe colocalization between MMP2-eGFP vesicles and early endosomes (Rab5), late endosomes (Rab7), recycling endosomes (Rab11), or lysosomes (mCherry-lysosomes), although a partial overlap was observed with LyzC in TGN-derived vesicles, suggesting a possible shared carrier for MMP2 and LyzC transport from the TGN to the plasma membrane.

Molecular mechanisms of anterograde cargo transport through the Golgi remain a major question in the field of membrane trafficking (Malhotra et al., 1989; Glick and Malhotra, 1998; Glick and Luini, 2011; Beznoussenko et al., 2014; Mironov and Beznoussenko, 2019). In this context, there is still a big debate in the field about how anterograde cargo, such as MMPs that arrive in the cis-Golgi, are segregated from retrograde cargo trafficking to the ER (Glick and Nakano, 2009; Mironov and Beznoussenko, 2019; Kurokawa et al., 2019).
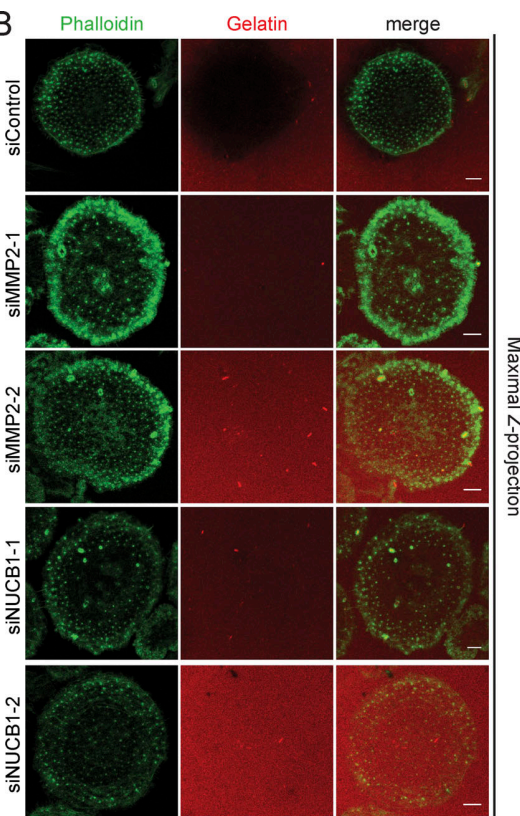
To gain insight into this process, we combined a RUSH trafficking assay with MS to identify IG MMP2 interactors. This approach revealed NUCB1 as an interactor of MMP2, and this interaction seems to be direct, as we can detect the complex in solution by AUC (Fig. S3, D and E). Furthermore, the number of MMP2 and MT1-MMP secretory vesicles was significantly reduced in NUCB1-KO cells after 30 and 60 min of release, respectively, demonstrating that NUCB1 modulates their transport in living cells.

At which step of the secretory pathway, then, is MMP2 trafficking impaired? Colocalization experiments using ER-GIC53, GM130, and TGN46, as well as live-cell microscopy experiments, showed a delay in the cis-Golgi, where NUCB1 localizes. In contrast, ER export and TGN-to-cell surface targeting of MMP2 seem to be intact.

It remains unclear, though, why a delay rather than a complete block of trafficking occurs at the cis-Golgi. We speculate that there are compensatory mechanisms present in the Golgi:

Pacheco-Fernandez et al.
Nucleobindin-1 regulates MMP secretion

Journal of Cell Biology 12 of 23
https://doi.org/10.1083/jcb.201907058

for instance, several EFh Ca^{2+}-binding proteins in the Golgi may have similar functions (Honoré, 2009). For example, calumenin is broadly distributed throughout the secretory pathway, but its function is not well understood (Vorum et al., 1999). Nevertheless, it has been demonstrated that it interacts with ECM proteins in the Golgi, such as thrombospondins (Hansen et al., 2009), and could play a role in their transport through the secretory pathway. Moreover, EFh proteins, such as calumenin and Cab45, travel through the cis-Golgi compartment and might partially compensate for the loss of NUCB1. In this scenario, a full compensation would not be possible because these proteins are not concentrated in the cis-Golgi.

Luminal Ca^{2+} in the Golgi evolves as an overall regulator of protein transport

Previous work has shown that Ca^{2+} channels and Ca^{2+} pumps, as well as Ca^{2+}-binding proteins, generate and maintain a concentration gradient inside the Golgi stack, with cis-Golgi containing the highest Ca^{2+} concentration (Missiaen et al., 2004; Vanoevelen et al., 2004, 2005; Lissandron et al., 2010; Pizzo et al., 2010; Aulestia et al., 2015). NUCB1 localizes to the cis-Golgi and has been proposed to regulate Ca^{2+} homeostasis in the lumen of this compartment (Lin et al., 1998, 1999; de Alba and Tjandra, 2004; Kanuru et al., 2009). Interestingly, we observed that NUCB1 absence affects Ca^{2+} homeostasis of the cis- but not trans-Golgi compartment, suggesting that these compartments are separate entities with individual regulation of their luminal Ca^{2+} content. Because NUCB1-KO induces a loss in luminal cis-Golgi Ca^{2+}, it might be also a regulator of SERCA pumps, as suggested by Lin et al. (1999).

What, then, is the role of luminal Ca^{2+} in the regulation of NUCB1 function? We evaluated the effect of Ca^{2+} in NUCB1 secondary structure via circular dichroism (CD) measurements. Using rNUCB1-His (Fig. S3 A) or recombinant NUCB1 with mutated EFhs (rNUCB1-mEFh1+2; Fig. S3, F and G), we observed a decreased molar ellipticity for rNUCB1-mEF1+2 compared with rNUCB1-His (Fig. S3 H). These findings confirm that the NUCB1 EFh motifs have an open conformation under physiological conditions and fold upon Ca^{2+} addition, as described by de Alba and Tjandra (2004).

Interestingly, NUCB1 and Cab45 share similar features, such as the luminal exposure of their Ca^{2+} binding EFhs (Scherer et al., 1996; von Blume et al., 2012). Moreover, CD measurements of EFh pair domain mutants of His-SUMO-Cab45 showed a similar spectrum to the one observed in rNUCB1-mEFh1+2 (Crevenna et al., 2016; Deng et al., 2016). Furthermore, previous studies have shown that a local increase in Ca^{2+} provided by SPCA1 at specific TGN subdomains induces Cab45 oligomerization and sorting of soluble cargo molecules before their packing into sphingolipid-rich transport vesicles (Deng et al., 2018; Crevenna et al., 2016; von Blume et al., 2012). Finally, coIP experiments using NUCB1-mEFh1+2 clearly show that the interaction with MMP2 requires Ca^{2+} to promote its anterograde transport through the Golgi and final delivery at the cell surface. Taken together, these data propose that Ca^{2+} impacts several steps in IG transport and suggest that Ca^{2+} controls trafficking at sequential steps of cargo transport across a Golgi stack: NUCB1 at cis-Golgi and Cab45 at the TGN.

Physiological role of NUCB1–MMP interaction

It is well known that both podosomes and invadopodia are cytoskeleton structures with a high proteolytic activity, which is needed for the proper invasion of interstitial tissue (Murphy and Courtneidge, 2011; Linder and Wiesner, 2016). In this regard, several studies have reported that MT1-MMP is a potential regulator of tumor invasion directly at the invadopodia mediating MMP secretion, activation, cell adhesion, and angiogenesis (Frittoli et al., 2011; Monteiro et al., 2013; Kajiho et al., 2016). In addition, MT1-MMP is the main source of MMP2 activation at the plasma membrane (Shaverdashvili et al., 2014; Han et al., 2015), both in steady state (Itoh, 2015; Sbai et al., 2008) and under pathological conditions (Jacob et al., 2013, 2016), implying that an impairment or delay in its delivery can strongly inhibit cell invasion and ECM degradation.

In line with these data, we were able to show that NUCB1 is required for efficient trafficking of MT1-MMP through the Golgi, strongly supporting the role of NUCB1 as a critical component of MMP trafficking in the secretory pathway. Although the phenotype observed in matrix degradation of MMP2 in MDA-MB-231 siRNA-treated cells was expected, as gelatin is the principal substrate for MMP2 proteolysis, the impact on invasion in NUCB1-silenced cells is noticeable and hints toward a global modulation of MMP trafficking by NUCB1, which does not seem to be limited to the regulation of MMP2.

Based on the obtained data, we hypothesize that cis-Golgi–localized NUCB1 binds and concentrates incoming MMP2, and probably other MMPs such as MT1-MMP, at specific cis-Golgi "exit sites" at the rim of cisternae, where the vesicle transport machinery is known to accumulate (Farquhar, 1985; Orci et al., 1986; Lavieu et al., 2013; Dancourt et al., 2016; Dunlop et al., 2017; Ernst et al., 2018). EM studies have shown that cargo accumulates at these rims compared with the flatter center of the cisternae (Orci et al., 1986; Lavieu et al., 2013). Moreover, a recent paper by Ernst et al. (2018) uncovered a cargo sorting mechanism regulated by S-palmitoylation in the cis-Golgi that supports these findings. In this model, palmitoylation acts as a biophysical switch to sort cargoes to the cisternal rim of the Golgi, promoting their further transport (Ernst et al., 2018).

Furthermore, Lin et al. (1998) showed that, in contrast to Cab45, NUCB1 is bound to the luminal surface of Golgi membranes by an unknown mechanism. Based on these findings, we speculate that NUCB1 might interact with an unknown transmembrane protein anchored in the cis-Golgi membrane via palmitoylation. In this context, it is interesting to note that MT1-MMP is palmitoylated at Cys574 in its cytosolic domain (Anilkumar et al., 2005). Altogether, this evidence suggests that NUCB1 could be enriched at palmitoylated cis-Golgi rims, which allow MMP molecules to concentrate in a Ca^{2+}-dependent manner to facilitate vesicle or tubule budding from the cisternal rim by local membrane bending.

Another possibility is that NUCB1 associates to the membrane in a Ca^{2+}-dependent manner or via conformational changes after cargo binding. In this regard, our CD measurements showed that NUCB1 acquires a compact conformation upon Ca^{2+} addition, and this change may expose residues that have a higher affinity for negative charges, stimulating NUCB1 association with

Pacheco-Fernandez et al.
Nucleobindin-1 regulates MMP secretion

Journal of Cell Biology   13 of 23
https://doi.org/10.1083/jcb.201907058

cis-Golgi membranes. We speculate that this association could stochastically accumulate MMP cargo and facilitate MMP trafficking to the next compartment in a protein maturation–dependent manner. This hypothesis would be in line with previously published in vitro data that postulate NUCB1 as a chaperone-like protein (Bonito-Oliva et al., 2017; Kanuru and Aradhyam, 2017).

Whether NUCB1 acts as a "switch protein" or exerts a chaperone-like activity on MMP2 at the cis-Golgi remains to be elucidated in future studies. The role of NUCB1 on the proper maturation of MMPs should be addressed to elucidate a more comprehensive mechanism of MMP trafficking. Further investigation is required to determine which other components might influence MMP sorting, as well as how impaired Ca^{2+} homeostasis by NUCB1 depletion delays cargo trafficking.

In conclusion, we report for the first time the involvement of NUCB1 and Ca^{2+} in MMP2 IG trafficking. This process promotes MMP2 anterograde transport along the secretory pathway and is essential for efficient ECM remodeling in both breast cancer cell lines and primary human macrophages. Our findings encourage the exploration of regulators of MMP trafficking as alternative targets to therapeutically modulate cell invasion.

Materials and methods
Cell culture
HeLa cells were obtained from Cell Line Service, and HEK293T cells from the American Type Culture Collection (ATCC; CRL-3216). Regular evaluation for mycoplasma contamination was performed to guarantee mycoplasma-free cell culture (LookOUT, MP0035; Sigma-Aldrich). These cell lines were cultured in DMEM supplemented with 10% FCS and 1% penicillin/streptomycin at 37°C and 5% CO_2. To generate the CRISPR/Cas9 KO cell lines, viral infection was performed using a method described by Crevenna et al. (2016).

For recombinant protein production, stable cell lines were generated using the piggyback system in HEK293T cells. rHS-MMP2, rNUCB1-His, and rNUCB1-mEFh1+2 pB-T-PAF constructs were transfected together with pBase and pB-RN constructs using linear polyethyleneimine (PEI; Alfa Aesar Chemicals) and 1.5 µg of DNA. After overnight incubation, the medium was replaced, and cells were allowed to recover for 24 h. The cells were selected with puromycin (1 µg/ml) and G418 (0.5 µg/ml) for at least 24 h. The medium was replaced, and cells were allowed to recover and expand. Confirmation of the stable cell line was performed via WB analysis.

MDA-MB-231 cells stably expressing mCherry–MT1-MMP (kindly provided by Philippe Chavrier, Institute Curie, Paris, France) were cultured in Leibovitz L-15 medium (Thermo Fisher Scientific) supplemented with 15% FCS and 50 ng/ml G418 (Calbiochem) in a humidified atmosphere with 1% CO_2 at 37°C. All cell lines tested negative for mycoplasma (LT07-318, Mycoplasma Detection Kit; Lonza) and were maintained in culture for ≤3 mo.

Isolation and culture of primary human macrophages
Human peripheral blood monocytes were isolated from buffy coats as described previously (Wiesner et al., 2013). The analysis

of anonymized blood donations was approved by the Ethical Committee of the Ärztekammer Hamburg (Hamburg, Germany). Cells were cultured in RPMI 1640 (containing 100 units/ml penicillin, 100 µg/ml streptomycin, 2 mM glutamine, and 20% autologous serum) at 37°C, 5% CO_2, and 90% humidity. Monocytes were differentiated in culture for ≥7 d with the addition of 20% human autologous serum.

Antibodies
MMP-2 and Rab11 antibodies were purchased from Abcam (rabbit ab92536 and rabbit ab3612, respectively). NUCB1, β-actin, and monoclonal anti-FLAG M2 peroxidase antibodies were obtained from Sigma-Aldrich (rabbit HPA008176 and mouse A5441 and A8592, respectively); ERGIC53 was acquired from ENZO Life Sciences (mouse ENZ-ABS300); GM130 antibody and β-integrin were purchased from BD Bioscience (mouse 610822 and mouse 610467, respectively); Rab5, Rab7, and streptavidin-HRP antibodies were from Cell Signaling (rabbit C8B1, D95F2, and 3999S, respectively); and TGN46 antibody was obtained from AbD Serotec (sheep AHP500G). MMP-14 antibody was purchased from Millipore (mouse MAB3328), and GFP antibody (rabbit sc8334) and HRP-coupled secondary antibodies (anti-rabbit IgG, anti-mouse IgG, and anti-sheep IgG) were purchased from Santa Cruz Biotechnology. Sec16A antibody (KIAA0310 polyclonal rabbit) was purchased from Biomol (now Thermo Fisher Scientific, A300-648A-M). Anti-rabbit HRP antibody used with primary macrophages was purchased from Cell Signaling (7074). The Alexa Fluor secondary antibodies used for immunofluorescence (488, 594, 633, and phalloidin-Alexa Fluor 488, different species) were purchased from Thermo Fisher Scientific.

Other reagents
All cell culture reagents (DMEM medium + glucose, FCS, and penicillin/streptomycin) were obtained from Gibco-Thermo Fisher Scientific. The SDS gels used for MS were purchased from Invitrogen (NP0321BOX, NuPAGE 4–12% Bis-Tris Protein Gels, 1.0 mm, 10-well). All restriction enzymes were purchased from New England Biolabs. cOmplete Tablets, Mini EDTA-free, EASYpack protease inhibitor tablets (from here on, cOmplete tablets) were purchased from Roche Diagnostics.

Plasmids
The human *MMP2* gene was amplified from a pCMV3-SP-Flag-MMP2 vector (Sino Biological) using 5′-CCCAAGCTTATGCCACTGCTGCTCTTGCT-3′ as a forward (Fw) primer and 5′-TTTTCCTTTTGCGGCCGCTCAAGCGTAATCTGGAACATCGTATGGGTAGCAGCCTAGCCAGTCGGATTT-3′ as a reverse (Rv) primer. For the RUSH experiments, the gene was engineered by substitution of ST in a Str-KDEL-ST-SBP-EGFP vector (Addgene_65264), using the following pairs of primers: (a) Fw: 5′-TTGGCGCGCCATGGCTACAGGCTCCCGGAC-3′, Rv: 5′-CTTATCGTCGTCATCCTTGTAATCGGATAAGGGAATGGTTGGGAAGGC-3′; and (b) Fw: 5′-GCCTTCCCAACCATTCCCTTATCCGATTACAAGGATGACGACGATAAG-3′, Rv: 5′-CCGGAATTCCCCAGCGTAATCTGGAACATCGTATG-3′. The fragment was inserted after the sequence of the signal peptide of human growth hormone, and all plasmids containing this as signal sequence are named SS-(construct).

Pacheco-Fernandez et al.
Nucleobindin-1 regulates MMP secretion

Journal of Cell Biology   14 of 23
https://doi.org/10.1083/jcb.201907058

For the CRISPR-KO of NUCB1, we used a pSpCas9(BB)-T2A-Puro (PX459) backbone vector (Addgene_48139) containing the following guide RNA: 5′-CACCGGCTCCTGCTTCGCGCCGTGC-3′, which was designed using the Optimized CRISPR design tool from Zhang Lab (https://zlab.bio/guide-design-resources, accessed on August 7, 2017).

The SS-Flag-MMP2-HA-eGFP construct was cloned using Gibson assembly with two fragment insertion and the following primers: Fw1: 5′-GGGCCCATAAAGCTTATACGAATTCCATGGCT ACAGGCTCCCGGAC-3′, Rv1: 5′-TCCTCGCCTTTGCTCACCATA GCGTAATCTGGAACATCGTATGGGTA-3′; and Fw2: 5′-TACCCA TACGATGTTCCAGATTACGCTATGGTGAGCAAAGGCGAGGA-3′, Rv2: 5′-GCGGCCGCTTGTCGACACTCGAGTTAAGGCCGGCCCTT GTACAG-3′. For this cloning, the restriction enzymes EcoRI and XhoI were used. The SS-LyzC-SBP-eGFP construct was previously reported by Deng et al. (2018).

For the rescue experiments, we performed Gibson assembly to insert the NUCB1 gene myc tagged from a pCMV3 vector from OriGene (RG201786) in a pLPCX vector using HindIII-HF and BamHI. The Fw primer was 5′-GATCTGGGCCCATAAAGCTTC CATGCCTCCCTCTGGGC-3′, and the Rv primer was 5′-CGACAC TCGAGTATGGATCCTCACAAGTCTTCTTCAGAGATGAGTTTC TGCTCCAGATGCTGGGGCACCTCAAC-3′. To generate the EFh-binding mutants of NUCB1, we substituted E264Q and E316Q via Gibson assembly using two complementary fragments amplified with the primers Fw1: 5′-CGGACTCAGATCTGGGCCCATAAA GCTTCCATGCCTCCCTCTGG-3′; Fw2: 5′-GGATGAGCAGCAGCT GGAGGCAC-3′; Rv1: 5′-GTGCCTCCAGCTGCTGCTCATCC-3′; and Rv2: 5′-CCCCTTTTTCTGGAGACTAAATAAAATCTTTTATTTTA TCGATGTATATGCTCACAAGTCTTCTTCAGAGATGAGTTTCTG CTCC-3′. The nontagged version of NUCB1-WT was inserted in the pLPCX backbone by restriction cloning of the pCMV3 vector from OriGene (see above) using EcoRI and NotI. The GFP–HA plasmid used as a control contained the acGFP sequence C-terminally tagged with HA in a pLPCX vector.

For the expression of a HIS-SUMO-tagged version of MMP2 in HEK293T cells, cDNA was amplified from the pLPCX-SS-Flag-MMP2-HA-eGFP plasmid using the primer pair 5′-GGCGGCCAT CACAAGTTTGTACAGCTAGCATGGCTACAGGCTCCCGGAC-3′ (Fw) and 5′-GGCGGCCATCACAAGTTTGTACAGCTAGCATGG CTACAGGCTCCCGGAC-3′ (Rv). A GST tag also was amplified using the primer pair 5′-CAAATCCGACTGGCTAGGCTGCATGTC CCTATACTAGGTTATTG-3′ and 5′-CCAGCACACTGGATCAGT TATCTATGCGGCCGCTTAGATCCGATTTTGGAGGATGGTC-3′. Together, the fragments were inserted into a pB-T-PAF Vector (Core Facility, Max Planck Institute of Biochemistry) using Gibson assembly to generate a plasmid coding for MMP2-GST fusion protein, which was then used as a template to amplify the MMP2 sequence with the plasmids 5′-GAACAGATTGGAGGT GAATGCGATTACAAGGATGACGACGATAAG-3′ (Fw) and 5′-GATCAGTTATCTATGCGGCCGCTCAGCAGCCTAGCCAGTCGG ATTTG-3′. The His-SUMO sequence was amplified from a vector published by Crevenna et al. (2016), and both fragments replaced the Cab45 cassette in the mentioned plasmid using Gibson assembly.

For the expression of the His-tagged version of NUCB1-WT (rNUCB1-His), cDNA sequence was amplified from the pLPCX-

NUCB1-myc construct using the primer pair 5′-GGCGGCCAT CACAAGTTTGTACAGCTAGCCATGCCTCCCTCTGGGC-3′ (Fw) and 5′-GCGGCCGCTTGTCAGTGATGATGATGGTGATGACCGCCT CCACCCAGATGCTGGGGCACCTCAAC-3′ (Rv) and inserted in the pB-T-PAF backbone using NheI and NotI restriction enzymes. For the expression of the His-tagged version of NUCB1-EFh1+2 (rNUCB1-mEFh1+2), cDNA sequence was amplified from the pLPCX-NUCB1-EFh1+2 construct using the primer pair 5′-GGCGGCCATCACAAGTTTGTACAGCTAGCCATGCCTCCCTCT GGG-3′ (Fw) and 5′-GCGGCCGCTTGTCAGTGATGATGATGGTGA TGACCGCCTCCACCCAGATGCTGGGGCACCTCAAC-3′ (Rv). All primers were purchased from Metabion International.

The Twitch 5 Ca²⁺ sensor was kindly provided by Oliver Griesbeck (Max Planck Institute of Neurobiology, Martinsried, Germany; Thestrup et al., 2014). The plasmid carrying rat-GPP130 cis-Golgi targeting sequence pME-zeo-GPP130-pHluorin was kindly provided by Yusuke Maeda (Research Institute for Microbial Diseases, Osaka, Japan; Maeda and Kinoshita, 2010). The Twitch 5 ORF was amplified using primers Twitch5-MluI forward, 5′-CACACGCGTGTGAGCAAGGGCGAGGAG-3′, and reverse, 5′-CACGCGGCCGCTCAATCCTCAATGTTGTGACGG-3′, and inserted into pME-zeo-GPP130-pHluorin using MluI and NotI restriction enzymes and replacing the pHluorin fragment.

The luminal part of human MT1-MMP (MMP14, NP_004986.1) was amplified via PCR using the primer pair 5′-AAG TGGCGCGCCATGTCTCCCGCCCCAAGA-3′ and 5′-GCGCGAATT CGCTCCGCCCTCCTCGTCCA-3′ from a plasmid containing MT1-MMP-mCherry (kind gift of P. Chavrier, Institut Curie, Paris, France). This fragment was then inserted into the RUSH plasmid Str-KDEL_SS-SBP-EGFP (Boncompain et al., 2012) using AscI and EcoRI restriction enzymes. The fragment coding for the transmembrane and cytoplasmic domains of MT1-MMP was amplified by PCR using the primer pair 5′-AGATGGCCGGCCATT AGGCGGGGCGGTGAGCG-3′ and 5′-AATCGGCCCTCGAGGCCT CAGACCTTGTCCAGCAGGG-3′. The PCR fragment was then inserted into the previously described plasmid using FseI and SfiI restriction enzymes. This cloning strategy generated a plasmid coding for Str-KDEL_MT1-MMP-SBP-EGFP with SBP-EGFP cassette located between the luminal and transmembrane domains of MT1-MMP. The EGFP cassette was then replaced by an mCherry coding sequence obtained from the RUSH plasmid Str-KDEL_SBP-mCherry-GPI using BsrGI and SbfI restriction enzymes. The mCherry-Lysosome construct was a gift from Florian Basserman (Technische Universität, München, Germany). Rab6-GFP and Rab8-GFP constructs were a gift from Vivek Malhotra (Centre for Genomic Regulation, Barcelona, Spain).

Oligonucleotides

siRNAs were purchased from Life Technologies, with the following epitopes: 5′-UCAUGCAGUAUGAAGAAGGUCUUGG-3′ (siNUCB1-1), 5′-GAGCUGGAGAAAGUGUACGACCCAA-3′ (siNUB1-2), 5′-AGUAGAUCCAGUAUUCAUUCCCUGC-3′ (siMMP2-1), and 5′-CCAGAUGUGGCCAACUACAACUUCU-3′ (siMMP2-2).

siRNA treatment

MDA-MB-231 cells were transfected with a negative siRNA control (4390843; Life Technologies) and with NUCB1 or MMP2

Pacheco-Fernandez et al.
Nucleobindin-1 regulates MMP secretion

Journal of Cell Biology   15 of 23
https://doi.org/10.1083/jcb.201907058

siRNA at a final concentration of 5 nM using RNAiMax (Life Technologies) according to the manufacturer's instructions. siRNA targeting firefly luciferase mRNA (D-001210-02-20; Dharmacon) was used as a negative control in primary human macrophages, which were transfected with NUCB1 or MMP2 siRNA at a final concentration of 100 nM. Knockdowns were achieved 72 h after transfection using the Viromer Blue Kit according to the manufacturer's instructions. Reduction of targeted proteins was validated by WB of respective cell lysates.

Quantitative RT-PCR experiments
Total RNA was isolated from cells using the NucleoSpin RNA kit (Macherey-Nagel) according to the manufacturer's instructions. 100 ng of RNA was used for the real-time PCR reaction using the QuantiTect SYBR Green RT-PCR Kit (Qiagen). Quantitative RT-PCR was performed with a Cfx96 device (Bio-Rad) using a Power SYBR Green RNA-to-Ct 1-Step kit (Applied Biosystems). QuantiTect Primer assays (Qiagen) were used to amplify MMP2 (Hs_MMP2_1_SG) and peptidylprolyl isomerase (Hs_PPIA_4_SG), and changes in the relative expression levels were determined using the 2–ΔΔCt method (Bio-Rad CFX Manager software 3.1).

IP
HEK293T or HeLa cells (3×10^5 cells/ml) were seeded in 15-cm plastic dishes (two per sample). After overnight incubation, each plate was transfected with 15 µg DNA using 1.25 mg/ml PEI as a transfection reagent (DNA/PEI, 1:7.5) and incubated for 20 h. Cells were then washed twice with PBS, scraped, and centrifuged for 3 min at 3,400 rpm. Supernatants were discarded, and pellets were washed two more times. Then, 300 µl lysis IP buffer (50 mM Tris, 150 mM NaCl, and 0.1% Triton X-100 + cOmplete tablets) were added, and samples were incubated for 30 min on ice. Samples were then filtered through a 27G needle and centrifuged at >13,000 rpm, 4°C, for 5 min. Supernatants were placed in a new Eppendorf tube and centrifuged once more for ≥20 min, >13,000 rpm, 4°C. Next, total protein was estimated using Bradford assay and normalized to the lowest protein concentration. A volume of 27 µl per sample was taken, mixed with 9 µl of 4× Laemmli buffer and labeled as input sample (10% input). Then, 35 µl of GFP beads, previously equilibrated with the lysis buffer, were added to the samples and incubated in an end-to-end rotator at 4°C for 1 h. Cells were centrifuged at 3,400 rpm, 4°C, for 3 min, supernatants were discarded, and samples were washed with 1 ml lysis buffer (1× PBS + 1% Triton X-100). This step was repeated twice, and after the last removal of supernatant, 35 µl Laemmli buffer 4× was added to the samples, and the mixtures were incubated at 95°C for 10 min. Finally, the samples were centrifuged at maximal speed (room temperature), and supernatants were collected and labeled as IP sample for loading in 10% SDS gel.

For the IP experiments using rNUCB1-His, ~100 µl of the recombinant protein was dialyzed overnight using the Pur-A-Lyzer mini dialysis Kit (Sigma-Aldrich) in 500 ml of 50 mM Tris + 100 mM NaCl. After dialysis, protein concentration was determined via absorbance measurement at 280 nm using a Nanodrop ND-1000 Spectrophotometer (PEQLAB Biotechnologie). Proteins were normalized and incubated with

previously washed Protino Ni-NTA agarose beads (Macherey-Nagel) for 2 h on a rotator at 4°C. At the same time, Golgi preps (prepared using a method described by von Blume et al. [2012]) were lysed using 50 µl of the described lysis IP buffer for 15 min on ice and centrifuged at 13,200 rpm for 10 min to remove membranes. After incubation, beads were washed 5× with lysis IP buffer and centrifuged at 3,400 rpm, 4°C, for 3 min each time. The lysed Golgi preps were added to the beads and incubated for 2 h with rotation at 4°C. After incubation, beads + Golgi preps were centrifuged at 3,400 rpm, 4°C, for 3 min. The beads were transferred to a new tube in the last step, 35 µl of Laemmli buffer 4× was added to the samples, and the mixtures were incubated at 95°C for 10 min. Finally, samples were centrifuged at maximal speed (room temperature), and supernatants were collected and labeled as IP sample for loading in a NuPAGE 4–12% Bis-Tris protein gel. The IP blot depicted (Fig. 1 G) is a mirrored image. Semiquantitative analyses of band intensities were performed using Fiji (ImageJ). Statistical evaluations are described in each figure legend.

SDS-PAGE and WB
SDS-PAGE was performed using 10% homemade acrylamide gels or NuPAGE 4–12% gradient gels. For WB, samples were transferred to nitrocellulose membranes for 75 min and blocked in 5% BSA in Tris-buffered saline (TBS) for at least 1 h at room temperature. The membranes were incubated overnight with primary antibody in a shaker at 4°C, washed for 1 h with TBS + 0.1% Tween-20 (TBS-T), and incubated with secondary antibody for 2 h at 4°C. Then, membranes were washed for half an hour with TBS-T and documented in a ChemiDoc Imaging System (Bio-Rad), an ImageQuant LAS 4000 series (GE Healthcare Life Sciences), or an Amersham Imager 600 (GE Healthcare Life Sciences).

MS analysis
MS samples were processed at the core facility of the Max Planck Institute of Biochemistry. Samples from gel lanes were digested with trypsin using in-gel digestion protocol, and peptides were extracted and purified via C18 StageTips. Peptides were analyzed in a Q Exactive HF machine with a data-dependent acquisition scheme using higher-energy collisional dissociation fragmentation. Raw data were processed using the MaxQuant computational platform, and the peak lists were searched against a human reference proteome database from Uniprot. All identifications were filtered at 1% false discovery rate and label-free quantitation. Proteomic data were analyzed with the Perseus 1.5.5.3 software (Tyanova et al., 2016), and results from a t test using Perseus were plotted as logarithmic ratios against logarithmic P values. The final selection of positive hits was done by filtering out potential contaminants, reverse sequences, and hits identified only by site.

Immunofluorescence and confocal microscopy
HeLa cells (3×10^4 cells/ml) were seeded into six-well plates with two glass slides per well. After incubation for 24 h, the cells were transfected with PEI (2 µg DNA, 15 µl PEI, and 200 µl OptiMEM) and incubated for no more than 24 h. Afterward, the

Pacheco-Fernandez et al.
Nucleobindin-1 regulates MMP secretion

Journal of Cell Biology   16 of 23
https://doi.org/10.1083/jcb.201907058

cells were washed three times with 1× PBS, fixed with 4% PFA for 10 min, and permeabilized with either 0.2% Triton X-100 and 0.5% SDS in PBS for 5 min or 0.05% saponin in 5% BSA in PBS for 1 h at room temperature (if no costaining was involved, cells were directly mounted after fixation). Subsequently, cells were incubated with 5% BSA in PBS overnight at 4°C. Primary antibody was added, and the mixture was incubated either overnight at 4°C or for 1 h at room temperature. After washing, secondary antibody was added and incubated for 1 h at room temperature. Finally, cells were mounted in glass slides using ProLong Gold antifade reagent (Invitrogen) and evaluated using confocal microscopy.

Images were acquired at 22°C on a Zeiss laser scanning LSM780 confocal microscope (Carl Zeiss) equipped with a 100× (NA 1.46, oil) objective. To detect Alexa Fluor, the 488-nm laser line was used. Pictures were acquired using Leica software (Zen 2010) and processed, merged, and gamma adjusted in ImageJ (v1.37).

Cellular vesicle number analysis was conducted using a custom-made ImageJ macro previously described (Deng et al., 2018). The macro uses ImageJ's rolling ball background subtraction algorithm, the "enhance contrast" function, and maximum z-projection of the RUSH reporter channel to cover all vesicles of the cell volume in a 2D image. After using a median filter, suitable cells were selected via polygon selection. A binary image was generated using the "threshold" function. The threshold algorithm "Yen" was used as default, whereas the threshold required manual correction for low-intensity images. The vesicle objects in the binary images were compared with the original image and controlled via visual inspection. In the binary image, vesicle objects with sizes 4–20 pixels were quantified using the Analyze Particles function. All macros used for image analysis are available at https://github.com/MehrshadPakdel.

RUSH cargo sorting assay
The RUSH cargo sorting assay was performed as previously described (Deng et al., 2018). HeLa or NUCB1-KO cells were cultured on sterile glass slides in 6-well dishes. Cells were transfected using pIRESneo3-SS-Str-KDEL-Flag-MMP2-SBP-HA-eGFP, pIRESneo3-SS-Str-KDEL-acGFP-HA, pIRESneo3-Str-KDEL-LyzC-SBP-eGFP, pIRESneo3-SS-Str-KDEL-cathD-SBP-eGFP, or pIRESneo3-Str-KDEL-MT1MMP-SBP-mCherry alone or together with NUCB1-WT, NUCB1-WT-myc, or its EFh mutants for 16 h. Cells were incubated with 40 µM D-biotin (Supelco, 47868) in DMEM supplemented with 10% FCS and 1% penicillin/streptomycin for the indicated times. At time point 0, cells were incubated with complete medium without D-biotin to confirm reporter retention. The cells were then washed twice in 1× PBS, fixed in 4% PFA in PBS for 10 min, and further processed for immunofluorescence microscopy as described above. Samples were quantified using confocal microscopy. Only cells that showed proper reporter transport to the Golgi after biotin addition were processed, whereas those showing ER signal after biotin addition were discarded. To cover the whole volume of the cells, typically 8–16 z-stacks with a step size of 0.39 µm were acquired for each field of view.

RUSH live-cell trafficking assay
We seeded 30,000 HeLa or NUCB1-KO cells into live-cell dishes (µ-Dish 35 mm, High Glass Bottom from Ibidi) and transfected them the next day with the SS-SBP-MMP2-eGFP RUSH construct for 24 h. Cells were washed in PBS and incubated in DMEM, high glucose, Hepes, no phenol red (Gibco by Life Technologies). Image acquisition was performed at the Imaging Facility of the Max Planck Institute of Biochemistry on a GE DeltaVision Elite system based on an Olympus IX-71 inverted microscope, an Olympus 60×/1.42 PLAPON oil objective, and a PCO sCMOS 5.5 camera at intervals of 1 min per frame. At $t = 0$ min of the video, DMEM + biotin was added to the cells to reach a final concentration of 40 µM biotin. Images were acquired using softWoRx 5.5 software (GE Healthcare).

Live-cell vesicle image analysis
Quantification of cytoplasmic vesicles per frame was conducted using a custom-made ImageJ macro based on RUSH vesicle analysis, as described previously (Deng et al., 2018). The macro uses ImageJ's rolling ball background subtraction algorithm followed by a mean filter to smooth edges of the objects. A binary image was generated by the Auto Threshold function using the "minimum" algorithm for frames 1–25 and the "moments" algorithm for frames 26–45 to optimize image thresholding for ER-like objects and then for Golgi and vesicular structures. The vesicle objects in the binary images were compared with the original images and controlled via visual inspection. Finally, vesicle objects with sizes ranging between 4 and 40 pixels were quantified using the "analyze particles" function. Data from 17 HeLa and 22 NUCB1-KO cells from two independent experiments were plotted as the median ± IQR. Significant differences with $P < 0.05$ were analyzed using the nonparametric Kruskal–Wallis test with Dunn's multiple comparison test.

Live-cell ER–Golgi cargo transport analysis
Quantification of normalized Golgi area over time was conducted using the custom-made ImageJ macros. The first part of the macro used a median filter to smooth the edges of objects. A binary image was generated for the first frame of the video to extract the ER signal of RUSH reporter using the threshold function of ImageJ and to manually extract the ER object. The ER area was then measured using the "analyze particles" function with pixel sizes 50–infinity. The second part of the macro was optimized for extracting Golgi objects for each frame and for quantifying their area. The macro used ImageJ's rolling ball background subtraction algorithm followed by a median filter. A binary image was generated for each frame with the "auto threshold" function using the "moments" algorithm. Areas of binary Golgi objects were then quantified for each frame with the "analyze particles" function using pixel sizes 15–infinity. The normalized Golgi area was calculated as the ratio of Golgi compacted area at each frame and the ER area at the first frame. Normalized Golgi area for 15 control and NUCB1-KO cells were plotted for each time point as the median ± IQR. Significant differences at $t = 22$ min with $P < 0.05$ were analyzed using the nonparametric Mann–Whitney U test.

Secretion assays
For the RUSH secretion assay, we followed the protocol described by Deng et al. (2018). HeLa and NUCB1-KO cells (10^3)

Pacheco-Fernandez et al.
Nucleobindin-1 regulates MMP secretion

Journal of Cell Biology 17 of 23
https://doi.org/10.1083/jcb.201907058

were seeded into six-well plates, incubated overnight, and then transfected with SS-Flag-MMP2-SBP or LyzC-Flag-SBP-eGFP for 24 h using PEI. Thereafter, the cells were incubated in DMEM serum-free medium for 45 or 60 min, and supernatants were collected and concentrated 20× using Centrifugal Filters (Amicon Ultra). The cells were then lysed using 1× PBS + 0.05% Triton A-100, and the total protein was quantified. All samples were normalized to the corresponding lysate protein concentrations. Laemmli buffer was added to a final concentration of 1×, and the samples were evaluated via SDS-PAGE and WB.

The HRP transport and secretion assay was performed as previously described (von Blume et al., 2011, 2012; Kienzle and von Blume, 2014). We seeded 125,000 HeLa or NUCB1-KO cells stably expressing SS-HRP-FLAG as technical triplicates into 12-well plates for 24 h. Before the start of HRP secretion, HeLa Brefeldin A (BFA) samples were preincubated with 10 μg/μL BFA in medium for 1 h. Cells were then washed 5× with PBS and incubated in medium with or without BFA for 4 h. Cell culture supernatants were harvested and filtered, and the cells were lysed in 0.5% Triton X-100 in PBS. Finally, 50 μl of medium and whole-cell lysis were mixed with 50 μl Liquid Substrate System solution (2,2′-azino-bis (3-ethylbenzothiazoline-6-sulfonic acid; Sigma-Aldrich, A3219). HRP activity was measured on a Magellan plate reader (Tecan Group) at 405 nm. The ratio of secreted HRP and cellular HRP was then normalized to HeLa control samples set to 100%. Normalized data from three independent experiments were plotted as mean ± SD. Significant differences with P < 0.05 were analyzed using the nonparametric Kruskal–Wallis test with Dunn's multiple comparison test.

For the endogenous MMP2 secretion assay, MDA-MB-231 cells expressing MT1-MMP-mCherry were seeded into six-well plates and incubated overnight. Cells were silenced using the described siNUCB1-1 and incubated until 80% confluence was reached. At that point, cells were incubated in 2 ml L15 serum-free medium for 16–20 h, and the supernatants were collected and concentrated 20× using Centrifugal Filters (Amicon Ultra). Cells were then lysed using 1× PBS + 0.05% Triton X-100, and total protein was quantified and normalized by the corresponding cell lysate protein concentration. Samples were analyzed via SDS-PAGE and WB.

Semiquantitative analysis of band intensities was performed using Fiji, following the protocol described by (Deng et al., 2018). Normalized data from three independent experiments were plotted as the mean ± SD. Significant differences with P < 0.05 were analyzed using the nonparametric Kruskal–Wallis test with Dunn's multiple comparison test.

Enrichment of cell surface biotinylated proteins
MT1-MMP transport to the cell surface in HeLa and NUCB1-KO cells was evaluated by pulldown of biotinylated cell surface proteins using NeutrAvidin agarose beads (Pierce). Cells were cultivated as described above and seeded in 10-cm culture dishes (75 × 10³ cells per dish) until 60% confluence. Cells were labeled with sulfo-NHS-SS-biotin (250 μg/ml) for 90 min or covered in ice-cold DPBS for control (– biotin, time 0) condition at 4°C on a platform rocker. Excess biotin was removed by washing once with ice-cold glycine in PBS (150 mM) before quenching the

biotinylation reaction by incubating in the same glycine solution for 25 min (5 ml in dish platform rocker). Cells were washed with ice-cold DPBS, collected using cell scrapers, and lysed in 1 ml lysis buffer (100 mM Tris-HCl, 150 mM NaCl, 0.1% SDS, 1% Triton, 1% deoxylcholic acid, pH 7.4, + cOmplete tablets) for 30 min on ice. Cell lysates were separated from membrane and cell debris by centrifugation for 15 min at 14,000 rpm (4°C). NeutrAvidin beads were prepared for incubation by washing 2× with 0.5 ml DPBS and 0.5 ml lysis buffer (3,400 rpm, 4°C, 3 min). After determining the total protein amount per cell lysate by Bradford (absorption λ = 595 nm), the equalized cell lysates were incubated with 150 μl NeutrAvidin bead slurry overnight at 4°C (rotating wheel). To reduce nonspecific protein binding, the beads were washed with lysis buffer (1 ml, 5×) on ice by centrifugation (3,400 rpm, 4 and 3 min). Subsequently, biotinylated proteins were eluted in 80 μl Laemmli sample buffer containing 50 mM DTT (10 min, 95°C) and analyzed by SDS-PAGE. Detection was performed via WB. Semiquantitative analysis of band intensities was performed using Fiji. Endogenous MT1-MMP band intensities were normalized to the intensity of β-integrin and then to the HeLa control sample at 90 min (100%). Normalized data from three independent experiments were plotted as the mean ± SD. Significant differences with P < 0.05 were analyzed using a one-sample t test.

Zymography
Gel zymography was performed as described by Toth et al. (2012). HeLa or NUCB1-KO cells (1.5 × 10⁵ cells/ml) were seeded in 10-cm Petri dishes. After overnight incubation, cells were transfected with either SS-Flag-MMP2-SBP-eGFP or LyzC-Flag-SBP-eGFP using PEI. After 24 h, cells were starved for 45 min by incubating in serum-free medium containing 40 μM biotin. The supernatants were collected and concentrated 20× using Centrifugal Filters (Amicon Ultra, Ultracel 10K). Cell lysates were prepared via incubation with 300 μl zymography lysis buffer (25 mM Tris, 100 mM NaCl, and 0.1% NP-40) on ice for 15 min and centrifugation of lysates at maximal speed for 20 min. The samples were prepared by adding 1× sample buffer (zymography running buffer, 35% glycerol, 8% SDS, and 1 mg/ml Bromophenol Blue) and run on a Novex 10% Zymogram Plus (Gelatin) gel at 150 V for 80 min. Gels were briefly washed with distilled water and incubated with 100 ml 1× renaturing solution for at least 3 h. The gels were washed 3× with distilled water, incubating each time with ≥100 ml distilled water for 10 min. The water was replaced with 100 ml developing solution and incubated for 30 min at room temperature. Buffer was replaced with new 1× renaturing solution and incubated for ≥20 h at 37°C on a shaker. Finally, the gels were briefly washed with water and stained with Coomassie solution until completely dark blue. Bands appeared as sharp clear areas. If necessary, gels were briefly (<5 min) destained in a 5% methanol + 10% acetic acid solution. Semiquantitative analysis was performed with Fiji by quantifying the degraded area on the gel and setting the degraded intensity of HeLa control cells to 100% in each experiment. The degraded area of NUCB1-KO cells is expressed as percentage relative to HeLa control. Significant differences were evaluated using a one-sample t test.

Pacheco-Fernandez et al.
Nucleobindin-1 regulates MMP secretion

Journal of Cell Biology 18 of 23
https://doi.org/10.1083/jcb.201907058

Structural visualization of NUCB1 E264Q and E316Q substitutions

The molecular graphics of the nuclear magnetic resonance structure of NUCB1 (1SNL, Research Collaboratory for Structural Bioinformatics Protein Data Bank [RCSB PDB]) were visualized and performed with UCSF Chimera (developed by the Resource for Biocomputing, Visualization, and Informatics at the University of California, San Francisco, with support from NIH P41-GM103311). The depicted rotamer was selected according to the highest probable candidate from the Dunbrack backbone-dependent rotamer library (Shapovalov and Dunbrack, 2011), and the pictures were adapted from the available model 1SNL (de Alba and Tjandra, 2004) in RCSB PDB using the UCSF Chimera software (Pettersen et al., 2004).

Protein purification of His-tagged proteins

The expression of rHS-MMP2, rNUCB1-His, and rNUCB1-mEF1+2-His in HEK293T cells was induced by incubating the cells with DMEM serum-free medium supplemented with doxycycline and aprotinin (1 µg/ml each) for ≥20 h. For His-SUMO-MMP2 and rNUCB1-His, proteins were purified using a column packed with cOmplete His-tag purification resin from Roche, as described by Crevenna et al. (2016). For rNUCB1-mEFh1+2-His purification, the supernatant was collected, concentrated 100× using Centrifugal Filters (Amicon Ultra, Ultracel 10K), and incubated with previously NaP pH 8.0 equilibrated Protino Ni-NTA agarose beads for 2 h at 4°C with rotation. The proteins were then washed and incubated with 250 mM imidazole for protein elution.

CD spectroscopy

CD measurements were performed as described previously (Crevenna et al., 2016) with the following modifications. Measurements were performed at 4°C using 20 mM Tris + 500 mM NaCl buffer. The mean of four independent spectra (from 198 to 250 nm with 0.1-nm spacing) was recorded. CONTIN analysis was performed using CDPro. CONTIN decomposes the CD signal into six secondary structural elements: regular α-helical, distorted α-helical, regular β sheet, distorted β sheet, turn, and unordered. Reported values in the main text for the α-helical and β sheet content were the sum of regular and distorted fractions for each secondary element.

Maleimide protein labeling

Recombinant His-SUMO-MMP2 was labeled with Cy3-NHS-Ester according to the manufacturer's instructions. After labeling, the protein was dialyzed in 20 mM Tris and 100 mM NaCl, pH 7.0, to remove excess free dye.

AUC

Sedimentation velocity experiments were performed on an Optima XL-I analytical ultracentrifuge (Beckman) using an An 60 Ti rotor and double-sector epon center pieces. The proteins were added to a 20 mM Tris + 100 mM NaCl buffer at 0.6 and 1.6 mg/ml for rHS-MMP2 and rNUCB1-His, respectively. Buffer density and viscosity were measured using a DMA 5000 densitometer and a AMVn viscosimeter, respectively (both Anton Paar). Fluorescently labeled protein concentration distribution was monitored at 544 nm at 50,000 rpm and 20°C. Time-derivative analysis was computed using the SEDFIT software package, v12.1b (Schuck, 2000), resulting in a $c(s)$ distribution and an estimate of the molecular weight Mf (from the sedimentation coefficient and the diffusion coefficient, as inferred from the broadening of the sedimentation boundary, assuming all observed species share the same frictional coefficient f/f_0).

Ca²⁺ influx assay

Ca^{2+} entry into the TGN or cis-Golgi was measured as described previously (Deng et al., 2018; Lissandron et al., 2010). Ca^{2+} measurements in the TGN or cis-Golgi were performed using a fluorescent Ca^{2+} sensor Go-D1-cpv (which targets the TGN) or GPP130-Twitch5 (which targets the cis-Golgi). Changes in Ca^{2+} concentration in the TGN by the Go-D1-cpv sensor were observed as changes in FRET efficiency between CFP and YFP fluorescent proteins linked by a modified CaM and CaM-binding domain. On the other hand, changes in Ca^{2+} concentration in the cis-Golgi were observed as FRET efficiency between enhanced CFP and Citrine fluorescent proteins linked by a modified C-terminal domain of *Opsanus tau* troponin C (Thestrup et al., 2014). HeLa or NUCB1-KO cells were transfected with either Go-D1-cpv or GPP130-Twitch5 alone or with NUCB1-WT or NUCB1-EFh1+2 mutant for 24 h. Ca^{2+} entry into the TGN or cis-Golgi were measured in Ca^{2+}-depleted cells after incubating for 1 h at 4°C in HBSS (20 mM Hepes, Ca^{2+}/Mg^{2+}-free HBSS [Gibco by Life Technologies], 2 g/liter glucose, 490 µM $MgCl_2$, and 450 µM $MgSO_4$, 300 mOsmol/liter, pH 7.4) with 1 µM ionomycin (Abcam) and 0.5 mM EGTA; von Blume et al., 2011; Deng et al., 2018). The cells were then washed twice in HBSS + 0.5 mM EGTA followed by washing three times in HBSS only. Image acquisition was performed on a DeltaVision Elite (GE Healthcare Life Sciences) as described by Deng et al. (2018). The excitation filter (430/24), dual-band Sedat CFP/YFP beam splitter (Chroma Technology Corp.), and the emission filters (535/25 for FRET and 470/24 for CFP) were rapidly changed using an external filter wheel controlled by a motorized unit to generate the images. Fluorescent signals reflecting TGN or cis-Golgi $[Ca^{2+}]$ were presented as $\Delta R/R_0$, where R_0 is the value obtained before the addition of 2.2 mM $CaCl_2$ to the cell's bathing solution. Images were acquired using softWoRx 5.5 software (GE Healthcare Life Sciences). Image analysis was conducted using a custom-made ImageJ macro based on ratiometric FRET analysis described previously (Kardash et al., 2011; Kienzle et al., 2014; Deng et al., 2018). The macro uses ImageJ's rolling ball background subtraction algorithm followed by a mean filter to smooth out the edges of the objects. A binary image was generated by the "auto threshold" function using the "moments" algorithm. FRET and CFP channel images were multiplied by the ImageCalculator plugin with their respective binary images, resulting in images that show 0 intensities outside of the threshold Golgi region while retaining intensities within the Golgi. Next, a ratio image of FRET/CFP was generated using the Ratio Plus plugin. The Golgi objects were detected using the "find maxima" function and added to the region of interest manager. The mean intensities of each region of interest were then measured in the ratio

Pacheco-Fernandez et al.
Nucleobindin-1 regulates MMP secretion

Journal of Cell Biology   19 of 23
https://doi.org/10.1083/jcb.201907058

image for each frame. The ratio values of each frame were subtracted with those in the first frame. These values were normalized to the first frame and presented as percentage $\Delta R/R_0$ to obtain the normalized ratio values before the addition of $CaCl_2$.

Invasion assay
Transwells (pore size 8 µm; Costar; Corning) were coated on the upper side with 50 µl growth factor–reduced Matrigel (BD Biosciences) diluted 1:20 in L-15 medium containing 0.5% FCS and allowed to polymerize for 1 h at 37°C. Transfected cells (5×10^4 cells/ml) were seeded in Transwells in 100 µl of L-15 medium containing 0.5% FCS, whereas the bottom chamber of the Transwell contained L-15 medium supplemented with 10% FCS. After 24 h of invasion, cells on the bottom of the membrane were fixed and stained with crystal violet, and six independent fields at 10× magnification were quantified using ImageJ (v1.49s). Significant differences between the number of migrating cells in each experiment were evaluated with a paired t test comparing each sample to the corresponding experiment control (siControl-1 or siControl-2). $P < 0.05$ was considered significant.

Matrix degradation of MDA-MB-231 cells
Coverslips were coated with Oregon488-conjugated gelatin (1 mg/ml; Invitrogen) followed by cross-linking with 0.5% glutaraldehyde (Carl Roth). Transfected cells (5×10^4 cells/ml) were seeded on coverslips, and after 5 h of incubation at 37°C, cells were fixed and nuclei were counterstained with DAPI. Imaging was performed on a confocal laser scanning microscope LSM 710 (Carl Zeiss) equipped with a Plan-Apochromat 20×/0.8. 40 confocal images per condition were acquired using identical settings for 488 and DAPI channels. Quantitative image analysis of gelatin degradation was performed using CellProfiler software v3.0.0. Relative degraded area was defined as the measured area normalized by the average area of the siControl in each experiment. Significant differences were evaluated with a paired t test comparing each sample to the corresponding experiment control (siControl-1 or siControl-2). $P < 0.05$ was considered significant.

2D gelatin degradation assay of human primary macrophages
Gelatin (from swine; Carl Roth) was fluorescently labeled with NHS Rhodamine (Thermo Fisher Scientific) according to the method described by Chen and Ko (1994). Coverslips were coated with labeled Rhodamine–gelatin, fixed in 0.5% glutaraldehyde (Carl Roth), and washed in RPMI 1640 and culture medium. 72 h after siRNA transfection, cells were reseeded on coated coverslips at a density of 5×10^4 cells; fixed and permeabilized 4, 6, and 8 h after seeding; and stained with Alexa Fluor 488–phalloidin. After the cells were labeled, the coverslips were mounted on Mowiol (Calbiochem) containing 1,4-diazabicyclo[2.2.2]octane (25 mg/ml; Sigma-Aldrich) as antifading reagent. Matrix degradation values were determined as 1 minus the ratio of fluorescent intensity under:around each cell using ImageJ. These values were normalized to the control (siLUC) per donor (three in total), represented as 100%, and reported in percentage relative to control. For comparison, laser intensity

was not changed between measurements. Two donors of independent experiments were analyzed, with at least eight fields of view (400–1,000 cells) per condition.

Images were acquired using confocal laser scanning microscopes (Leica DMi8 confocal point scanner equipped with a 20× HC PL APO IMM/CORR CS2 and oil-immersion 63× HC PL APO Oil CS2 objective and 3× HyD, 2× PMT, 1× Trans-PMT detector). Acquisition and processing were performed using Leica LAS X SP8 confocal software (Leica Camera), Volocity 6.1.1 software (PerkinElmer), and ImageJ. Statistical differences between siN-UCB1 and siMMP2 samples compared with siControl were evaluated with a one-sample t test. Differences among si-NUCB1 and si-MMP2 degraded areas were compared with a paired t test for each pair of siRNAs analyzed in parallel.

Statistical analysis
Microscopy quantification data were first evaluated for normality fit. If the data did not follow a normal distribution, we performed a nonparametric Kruskal–Wallis test with Dunn's comparison for most statistical significance evaluations. For the evaluation of statistical differences in Ca^{2+} influx assays, we used the Mann–Whitney U test. For semiquantitative evaluation of blots, band intensities were evaluated with ImageJ, and ratios between each band and its correspondent pulled protein band or a positive control were determined (see figure legends for more details). Statistical analyses (one-sample t test or paired t test) were performed using Prism software (GraphPad), unless otherwise stated.

Online supplemental material
Fig. S1 shows data on MMP2-eGFP secretion and generation of CRISPR NUCB1-KO cells. Fig. S2 shows colocalization experiments with Rab GTPases, lysosomes, and LyzC. Fig. S3 details experiments with recombinant proteins. Fig. S4 depicts RUSH experiments using NUCB1-cyto and MT1-MMP-mCherry, as well as an MT1-MMP cell surface biotinylation assay. Fig. S5 shows zymography and secretion assays with different cargoes than MMPs. Table S1 lists the hits found in our MS analysis.

Acknowledgments

Pacheco-Fernandez et al.
Nucleobindin-1 regulates MMP secretion

Journal of Cell Biology   20 of 23
https://doi.org/10.1083/jcb.201907058

References

Alaseem, A., K. Alhazzani, P. Dondapati, S. Alobid, A. Bishayee, and A. Rathinavelu. 2019. Matrix Metalloproteinases: A challenging paradigm of cancer management. *Semin. Cancer Biol.* 56:100–115. https://doi.org/10.1016/j.semcancer.2017.11.008

Anilkumar, N., T. Uekita, J.R. Couchman, H. Nagase, M. Seiki, and Y. Itoh. 2005. Palmitoylation at Cys574 is essential for MT1-MMP to promote cell migration. *FASEB J.* 19:1326–1328. https://doi.org/10.1096/fj.04-3651fje

Apte, S.S., and W.C. Parks. 2015. Metalloproteinases: A parade of functions in matrix biology and an outlook for the future. *Matrix Biol.* 44–46:1–6. https://doi.org/10.1016/j.matbio.2015.04.005

Aulestia, F.J., M.T. Alonso, and J. García-Sancho. 2015. Differential calcium handling by the cis and trans regions of the Golgi apparatus. *Biochem. J.* 466:455–465. https://doi.org/10.1042/BJ20141358

Barlowe, C.K., and E.A. Miller. 2013. Secretory protein biogenesis and traffic in the early secretory pathway. *Genetics.* 193:383–410. https://doi.org/10.1534/genetics.112.142810

Beznoussenko, G.V., S. Parashuraman, R. Rizzo, R. Polishchuk, O. Martella, D. Di Giandomenico, A. Fusella, A. Spaar, M. Sallese, M.G. Capestrano, et al. 2014. Transport of soluble proteins through the Golgi occurs by diffusion via continuities across cisternae. *eLife.* 3. e02009. https://doi.org/10.7554/eLife.02009

Boncompain, G., S. Divoux, N. Gareil, H. de Forges, A. Lescure, L. Latreche, V. Mercanti, F. Jollivet, G. Raposo, and F. Perez. 2012. Synchronization of secretory protein traffic in populations of cells. *Nat. Methods.* 9:493–498. https://doi.org/10.1038/nmeth.1928

Bonito-Oliva, A., S. Barbash, T.P. Sakmar, and W.V. Graham. 2017. Nucleobindin 1 binds to multiple types of pre-fibrillar amyloid and inhibits fibrillization. *Sci. Rep.* 7:42880. https://doi.org/10.1038/srep42880

Bonnans, C., J. Chou, and Z. Werb. 2014. Remodelling the extracellular matrix in development and disease. *Nat. Rev. Mol. Cell Biol.* 15:786–801. https://doi.org/10.1038/nrm3904

Bravo-Cordero, J.J., R. Marrero-Diaz, D. Megías, L. Genís, A. García-Grande, M.A. García, A.G. Arroyo, and M.C. Montoya. 2007. MT1-MMP proinvasive activity is regulated by a novel Rab8-dependent exocytic pathway. *EMBO J.* 26:1499–1510. https://doi.org/10.1038/sj.emboj.7601606

Brew, K., and H. Nagase. 2010. The tissue inhibitors of metalloproteinases (TIMPs): an ancient family with structural and functional diversity. *Biochim. Biophys. Acta.* 1803:55–71. https://doi.org/10.1016/j.bbamcr.2010.01.003

Brodeur, J., H. Larkin, R. Boucher, C. Thériault, S.C. St-Louis, H. Gagnon, and C. Lavoie. 2009. Calnuc binds to LRP9 and affects its endosomal sorting. *Traffic.* 10:1098–1114. https://doi.org/10.1111/j.1600-0854.2009.00933.x

Cauwe, B., and G. Opdenakker. 2010. Intracellular substrate cleavage: a novel dimension in the biochemistry, biology and pathology of matrix metalloproteinases. *Crit. Rev. Biochem. Mol. Biol.* 45:351–423. https://doi.org/10.3109/10409238.2010.501783

Chen, L., and C.P. Ko. 1994. Extension of synaptic extracellular matrix during nerve terminal sprouting in living frog neuromuscular junctions. *J. Neurosci.* 14:796–808. https://doi.org/10.1523/JNEUROSCI.14-02-00796.1994

Cornfine, S., M. Himmel, P. Kopp, K. El Azzouzi, C. Wiesner, M. Krüger, T. Rudel, and S. Linder. 2011. The kinesin KIF9 and reggie/flotillin proteins regulate matrix degradation by macrophage podosomes. *Mol. Biol. Cell.* 22:202–215. https://doi.org/10.1091/mbc.e10-05-0394

Crevenna, A.H., B. Blank, A. Maiser, D. Emin, J. Prescher, G. Beck, C. Kienzle, K. Bartnik, B. Habermann, M. Pakdel, et al. 2016. Secretory cargo sorting by Ca2+-dependent Cab45 oligomerization at the trans-Golgi network. *J. Cell Biol.* 213:305–314. https://doi.org/10.1083/jcb.201601089

Cui, N., M. Hu, and R.A. Khalil. 2017. Biochemical and Biological Attributes of Matrix Metalloproteinases. *Prog. Mol. Biol. Transl. Sci.* 147:1–73. https://doi.org/10.1016/bs.pmbts.2017.02.005

Dancourt, J., H. Zheng, F. Bottanelli, E.S. Allgeyer, J. Bewersdorf, M. Graham, X. Liu, J.E. Rothman, and G. Lavieu. 2016. Small cargoes pass through synthetically glued Golgi stacks. *FEBS Lett.* 590:1675–1686. https://doi.org/10.1002/1873-3468.12210

de Alba, E., and N. Tjandra. 2004. Structural studies on the Ca2+-binding domain of human nucleobindin (calnuc). *Biochemistry.* 43:10039–10049. https://doi.org/10.1021/bi049310a

Deng, Y., M. Pakdel, B. Blank, E.L. Sundberg, C.G. Burd, and J. von Blume. 2018. Activity of the SPCA1 Calcium Pump Couples Sphingomyelin Synthesis to Sorting of Secretory Proteins in the Trans-Golgi Network. *Dev. Cell.* 47:464–478.e8. https://doi.org/10.1016/j.devcel.2018.10.012

Deng, Y., F.E. Rivera-Molina, D.K. Toomre, and C.G. Burd. 2016. Sphingomyelin is sorted at the *trans* Golgi network into a distinct class of secretory vesicle. *Proc. Natl. Acad. Sci. USA.* 113:6677–6682. https://doi.org/10.1073/pnas.1602875113

Deryugina, E.I., B.I. Ratnikov, Q. Yu, P.C. Baciu, D.V. Rozanov, and A.Y. Strongin. 2004. Prointegrin maturation follows rapid trafficking and processing of MT1-MMP in Furin-Negative Colon Carcinoma LoVo Cells. *Traffic.* 5:627–641. https://doi.org/10.1111/j.1600-0854.2004.00206.x

Dunlop, M.H., A.M. Ernst, L.K. Schroeder, D.K. Toomre, G. Lavieu, and J.E. Rothman. 2017. Land-locked mammalian Golgi reveals cargo transport between stable cisternae. *Nat. Commun.* 8:432. https://doi.org/10.1038/s41467-017-00570-z

Endo, K., T. Takino, H. Miyamori, H. Kinsen, T. Yoshizaki, M. Furukawa, and H. Sato. 2003. Cleavage of syndecan-1 by membrane type matrix metalloproteinase-1 stimulates cell migration. *J. Biol. Chem.* 278:40764–40770. https://doi.org/10.1074/jbc.M306736200

Ernst, A.M., S.A. Syed, O. Zaki, F. Bottanelli, H. Zheng, M. Hacke, Z. Xi, F. Rivera-Molina, M. Graham, A.A. Rebane, et al. 2018. S-Palmitoylation Sorts Membrane Cargo for Anterograde Transport in the Golgi. *Dev. Cell.* 47:479–493.e7. https://doi.org/10.1016/j.devcel.2018.10.024

Farquhar, M.G.. 1985. Progress in unraveling pathways of Golgi traffic. *Annu. Rev. Cell Biol.* 1:447–488. https://doi.org/10.1146/annurev.cb.01.110185.002311

Fernandez-Catalan, C., W. Bode, R. Huber, D. Turk, J.J. Calvete, A. Lichte, H. Tschesche, and K. Maskos. 1998. Crystal structure of the complex formed by the membrane type 1-matrix metalloproteinase with the tissue inhibitor of metalloproteinases-2, the soluble progelatinase A receptor. *EMBO J.* 17:5238–5248. https://doi.org/10.1093/emboj/17.17.5238

Frittoli, E., A. Palamidessi, A. Disanza, and G. Scita. 2011. Secretory and endo/exocytic trafficking in invadopodia formation: the MT1-MMP paradigm. *Eur. J. Cell Biol.* 90:108–114. https://doi.org/10.1016/j.ejcb.2010.04.007

Frittoli, E., A. Palamidessi, P. Marighetti, S. Confalonieri, F. Bianchi, C. Malinverno, G. Mazzarol, G. Viale, I. Martin-Padura, M. Garré, et al. 2014. A RAB5/RAB4 recycling circuitry induces a proteolytic invasive program and promotes tumor dissemination. *J. Cell Biol.* 206:307–328. https://doi.org/10.1083/jcb.201403127

Glick, B.S., and A. Luini. 2011. Models for Golgi traffic: a critical assessment. *Cold Spring Harb. Perspect. Biol.* 3. a005215. https://doi.org/10.1101/cshperspect.a005215

Glick, B.S., and V. Malhotra. 1998. The curious status of the Golgi apparatus. *Cell.* 95:883–889. https://doi.org/10.1016/S0092-8674(00)81713-4

Glick, B.S., and A. Nakano. 2009. Membrane traffic within the Golgi apparatus. *Annu. Rev. Cell Dev. Biol.* 25:113–132. https://doi.org/10.1146/annurev.cellbio.24.110707.175421

Pacheco-Fernandez et al.
Nucleobindin-1 regulates MMP secretion

Journal of Cell Biology 21 of 23
https://doi.org/10.1083/jcb.201907058

Gonzalez, R., H. Mohan, and S. Unniappan. 2012. Nucleobindins: bioactive precursor proteins encoding putative endocrine factors? *Gen. Comp. Endocrinol*. 176:341–346. https://doi.org/10.1016/j.ygcen.2011.11.021

Gueye, Y., L. Ferhat, O. Sbai, J. Bianco, A. Ould-Yahoui, A. Bernard, E. Charrat, J.-P. Chauvin, J.-J. Risso, F. Féron, et al. 2011. Trafficking and secretion of matrix metalloproteinase-2 in olfactory enshesthing glial cells: A role in cell migration? *Glia*. 59:750–770. https://doi.org/10.1002/glia.21146

Han, K.-Y., J. Dugas-Ford, M. Seiki, J.-H. Chang, and D.T. Azar. 2015. Evidence for the Involvement of MMP14 in MMP2 Processing and Recruitment in Exosomes of Corneal Fibroblasts. *Invest. Ophthalmol. Vis. Sci*. 56:5323–5329. https://doi.org/10.1167/iovs.14-14417

Hannocks, M.-J., X. Zhang, H. Gerwien, A. Chashchina, M. Burmeister, E. Korpos, J. Song, and L. Sorokin. 2019. The gelatinases, MMP-2 and MMP-9, as fine tuners of neuroinflammatory processes. *Matrix Biol*. 75–76:102–113. https://doi.org/10.1016/j.matbio.2017.11.007

Hansen, G.A.W., H. Vorum, C. Jacobsen, and B. Honoré. 2009. Calumenin but not reticulocalbin forms a Ca2+-dependent complex with thrombospondin-1. A potential role in haemostasis and thrombosis. *Mol. Cell. Biochem*. 320:25–33. https://doi.org/10.1007/s11010-008-9895-1

Honoré, B.. 2009. The rapidly expanding CREC protein family: members, localization, function, and role in disease. *BioEssays*. 31:262–277. https://doi.org/10.1002/bies.200800186

Honoré, B., and H. Vorum. 2000. The CREC family, a novel family of multiple EF-hand, low-affinity Ca(2+)-binding proteins localised to the secretory pathway of mammalian cells. *FEBS Lett*. 466:11–18. https://doi.org/10.1016/S0014-5793(99)01780-9

Itoh, Y.. 2015. Membrane-type matrix metalloproteinases: Their functions and regulations. *Matrix Biol*. 44–46:207–223. https://doi.org/10.1016/j.matbio.2015.03.004

Jacob, A., J. Jing, J. Lee, P. Schedin, S.M. Gilbert, A.A. Peden, J.R. Junutula, and R. Prekeris. 2013. Rab40b regulates trafficking of MMP2 and MMP9 during invadopodia formation and invasion of breast cancer cells. *J. Cell Sci*. 126:4647–4658. https://doi.org/10.1242/jcs.126573

Jacob, A., E. Linklater, B.A. Bayless, T. Lyons, and R. Prekeris. 2016. The role and regulation of Rab40b-Tks5 complex during invadopodia formation and cancer cell invasion. *J. Cell Sci*. 129:4341–4353. https://doi.org/10.1242/jcs.193904

Jobin, P.G., G.S. Butler, and C.M. Overall. 2017. New intracellular activities of matrix metalloproteinases shine in the moonlight. *Biochim. Biophys. Acta Mol. Cell Res*. 1864(11 Pt A):2043–2055. https://doi.org/10.1016/j.bbamcr.2017.05.013

Kajiho, H., Y. Kajiho, E. Frittoli, S. Confalonieri, G. Bertalot, G. Viale, P.P. Di Fiore, A. Oldani, M. Garre, G.V. Beznoussenko, et al. 2016. RAB2A controls MT1-MMP endocytic and E-cadherin polarized Golgi trafficking to promote invasive breast cancer programs. *EMBO Rep*. 17:1061–1080. https://doi.org/10.15252/embr.201642032

Kanuru, M., and G.K. Aradhyam. 2017. Chaperone-like Activity of Calnuc Prevents Amyloid Aggregation. *Biochemistry*. 56:149–159. https://doi.org/10.1021/acs.biochem.6b00660

Kanuru, M., J.J. Samuel, L.M. Balivada, and G.K. Aradhyam. 2009. Ion-binding properties of Calnuc, Ca2+ versus Mg2+--Calnuc adopts additional and unusual Ca2+-binding sites upon interaction with G-protein. *FEBS J*. 276:2529–2546. https://doi.org/10.1111/j.1742-4658.2009.06977.x

Kapoor, N., R. Gupta, S.T. Menon, E. Folta-Stogniew, D.P. Raleigh, and T.P. Sakmar. 2010. Nucleobindin 1 is a calcium-regulated guanine nucleotide dissociation inhibitor of Galphai1. *J. Biol. Chem*. 285:31647–31660. https://doi.org/10.1074/jbc.M110.148429

Kardash, E., J. Bandemer, and E. Raz. 2011. Imaging protein activity in live embryos using fluorescence resonance energy transfer biosensors. *Nat. Protoc*. 6:1835–1846. https://doi.org/10.1038/nprot.2011.395

Kean, M.J., K.C. Williams, M. Skalski, D. Myers, A. Burtnik, D. Foster, and M.G. Coppolino. 2009. VAMP3, syntaxin-13 and SNAP23 are involved in secretion of matrix metalloproteinases, degradation of the extracellular matrix and cell invasion. *J. Cell Sci*. 122:4089–4098. https://doi.org/10.1242/jcs.052761

Kessenbrock, K., V. Plaks, and Z. Werb. 2010. Matrix metalloproteinases: regulators of the tumor microenvironment. *Cell*. 141:52–67. https://doi.org/10.1016/j.cell.2010.03.015

Khokha, R., A. Murthy, and A. Weiss. 2013. Metalloproteinases and their natural inhibitors in inflammation and immunity. *Nat. Rev. Immunol*. 13:649–665. https://doi.org/10.1038/nri3499

Kienzle, C., and J. von Blume. 2014. Secretory cargo sorting at the trans-Golgi network. *Trends Cell Biol*. 24:584–593. https://doi.org/10.1016/j.tcb.2014.04.007

Kienzle, C., N. Basnet, A.H. Crevenna, G. Beck, B. Habermann, N. Mizuno, and J. von Blume. 2014. Cofilin recruits F-actin to SPCA1 and promotes Ca2+-mediated secretory cargo sorting. *J. Cell Biol*. 206:635–654. https://doi.org/10.1083/jcb.201311052

Könnecke, H., and I. Bechmann. 2013. The role of microglia and matrix metalloproteinases involvement in neuroinflammation and gliomas. *Clin. Dev. Immunol*. 2013. 914104. https://doi.org/10.1155/2013/914104

Kurokawa, K., H. Osakada, T. Kojidani, M. Waga, Y. Suda, H. Asakawa, T. Haraguchi, and A. Nakano. 2019. Visualization of secretory cargo transport within the Golgi apparatus. *J. Cell Biol*. 218:1602–1618. https://doi.org/10.1083/jcb.201807194

Larkin, H., S. Costantino, M.N.J. Seaman, and C. Lavoie. 2016. Calnuc Function in Endosomal Sorting of Lysosomal Receptors. *Traffic*. 17:416–432. https://doi.org/10.1111/tra.12374

Lavieu, G., H. Zheng, and J.E. Rothman. 2013. Stapled Golgi cisternae remain in place as cargo passes through the stack. *eLife*. 2. e00558. https://doi.org/10.7554/eLife.00558

Lavoie, C., T. Meerloo, P. Lin, and M.G. Farquhar. 2002. Calnuc, an EF-hand Ca(2+)-binding protein, is stored and processed in the Golgi and secreted by the constitutive-like pathway in AtT20 cells. *Mol. Endocrinol*. 16:2462–2474. https://doi.org/10.1210/me.2002-0079

Leung, A.K.-W., N. Ramesh, C. Vogel, and S. Unniappan. 2019. Nucleobindins and encoded peptides: From cell signaling to physiology. *Adv. Protein Chem. Struct. Biol*. 116:91–133. https://doi.org/10.1016/bs.apcsb.2019.02.001

Lin, P., H. Le-Niculescu, R. Hofmeister, J.M. McCaffery, M. Jin, H. Hennemann, T. McQuistan, L. De Vries, and M.G. Farquhar. 1998. The mammalian calcium-binding protein, nucleobindin (CALNUC), is a Golgi resident protein. *J. Cell Biol*. 141:1515–1527. https://doi.org/10.1083/jcb.141.7.1515

Lin, P., Y. Yao, R. Hofmeister, R.Y. Tsien, and M.G. Farquhar. 1999. Overexpression of CALNUC (nucleobindin) increases agonist and thapsigargin releasable Ca2+ storage in the Golgi. *J. Cell Biol*. 145:279–289. https://doi.org/10.1083/jcb.145.2.279

Linder, S., and G. Scita. 2015. RABGTPases in MT1-MMP trafficking and cell invasion: Physiology versus pathology. *Small GTPases*. 6:145–152. https://doi.org/10.4161/21541248.2014.985484

Linder, S., and C. Wiesner. 2015. Tools of the trade: podosomes as multipurpose organelles of monocytic cells. *Cell. Mol. Life Sci*. 72:121–135. https://doi.org/10.1007/s00018-014-1731-z

Linder, S., and C. Wiesner. 2016. Feel the force: Podosomes in mechanosensing. *Exp. Cell Res*. 343:67–72. https://doi.org/10.1016/j.yexcr.2015.11.026

Lissandron, V., P. Podini, P. Pizzo, and T. Pozzan. 2010. Unique characteristics of Ca2+ homeostasis of the trans-Golgi compartment. *Proc. Natl. Acad. Sci. USA*. 107:9198–9203. https://doi.org/10.1073/pnas.1004702107

Maeda, Y., and T. Kinoshita. 2010. The Acidic Environment of the Golgi Is Critical for Glycosylation and Transport. *Methods in Enzymology*. 480:495–510. . https://doi.org/10.1016/S0076-6879(10)80022-9

Malhotra, V., T. Serafini, L. Orci, J.C. Shepherd, and J.E. Rothman. 1989. Purification of a novel class of coated vesicles mediating biosynthetic protein transport through the Golgi stack. *Cell*. 58:329–336. https://doi.org/10.1016/0092-8674(89)90847-7

Margulis, N.G., J.D. Wilson, C.M. Bentivoglio, N. Dhungel, A.D. Gitler, and C. Barlowe. 2016. Analysis of COPII Vesicles Indicates a Role for the Emp47-Ssp120 Complex in Transport of Cell Surface Glycoproteins. *Traffic*. 17:191–210. https://doi.org/10.1111/tra.12356

McCaughey, J., and D.J. Stephens. 2018. COPII-dependent ER export in animal cells: adaptation and control for diverse cargo. *Histochem. Cell Biol*. 150:119–131. https://doi.org/10.1007/s00418-018-1689-2

Micaroni, M., G. Perinetti, D. Di Giandomenico, K. Bianchi, A. Spaar, and A.A. Mironov. 2010. Synchronous intra-Golgi transport induces the release of Ca2+ from the Golgi apparatus. *Exp. Cell Res*. 316:2071–2086. https://doi.org/10.1016/j.yexcr.2010.04.024

Mironov, A.A., and G.V. Beznoussenko. 2019. Models of Intracellular Transport: Pros and Cons. *Front. Cell Dev. Biol*. 7:146. https://doi.org/10.3389/fcell.2019.00146

Missiaen, L., L. Raeymaekers, L. Dode, J. Vanoevelen, K. Van Baelen, J.B. Parys, G. Callewaert, H. De Smedt, S. Segaert, and F. Wuytack. 2004. SPCA1 pumps and Hailey-Hailey disease. *Biochem. Biophys. Res. Commun*. 322:1204–1213. https://doi.org/10.1016/j.bbrc.2004.07.128

Miura, K., Y. Kurosawa, and Y. Kanai. 1994. Calcium-binding activity of nucleobindin mediated by an EF hand moiety. *Biochem. Biophys. Res. Commun*. 199:1388–1393. https://doi.org/10.1006/bbrc.1994.1384

Monteiro, P., C. Rossé, A. Castro-Castro, M. Irondelle, E. Lagoutte, P. Paul-Gilloteaux, C. Desnos, E. Formstecher, F. Darchen, D. Perrais, et al. 2013. Endosomal WASH and exocyst complexes control exocytosis of

Pacheco-Fernandez et al.
Nucleobindin-1 regulates MMP secretion

Journal of Cell Biology   22 of 23
https://doi.org/10.1083/jcb.201907058

MT1-MMP at invadopodia. *J. Cell Biol.* 203:1063–1079. https://doi.org/10.1083/jcb.201306162

Murphy, D.A., and S.A. Courtneidge. 2011. The 'ins' and 'outs' of podosomes and invadopodia: characteristics, formation and function. *Nat. Rev. Mol. Cell Biol.* 12:413–426. https://doi.org/10.1038/nrm3141

Orci, L., B.S. Glick, and J.E. Rothman. 1986. A new type of coated vesicular carrier that appears not to contain clathrin: its possible role in protein transport within the Golgi stack. *Cell.* 46:171–184. https://doi.org/10.1016/0092-8674(86)90734-8

Pettersen, E.F., T.D. Goddard, C.C. Huang, G.S. Couch, D.M. Greenblatt, E.C. Meng, and T.E. Ferrin. 2004. UCSF Chimera--a visualization system for exploratory research and analysis. *J. Comput. Chem.* 25:1605–1612. https://doi.org/10.1002/jcc.20084

Pizzo, P., V. Lissandron, and T. Pozzan. 2010. The trans-golgi compartment: A new distinct intracellular Ca store. *Commun. Integr. Biol.* 3:462–464. https://doi.org/10.4161/cib.3.5.12473

Poincloux, R., F. Lizárraga, and P. Chavrier. 2009. Matrix invasion by tumour cells: a focus on MT1-MMP trafficking to invadopodia. *J. Cell Sci.* 122:3015–3024. https://doi.org/10.1242/jcs.034561

Porat, A., and Z. Elazar. 2000. Regulation of intra-Golgi membrane transport by calcium. *J. Biol. Chem.* 275:29233–29237. https://doi.org/10.1074/jbc.M005316200

Rayl, M., M. Truitt, A. Held, J. Sargeant, K. Thorsen, and J.C. Hay. 2016. Penta-EF-hand protein peflin is a negative regulator of ER-to-Golgi transport. *PLoS One.* 11. e0157227. https://doi.org/10.1371/journal.pone.0157227

Reichel, C.A., M. Rehberg, P. Bihari, C.M. Moser, S. Linder, A. Khandoga, and F. Krombach. 2008. Gelatinases mediate neutrophil recruitment in vivo: evidence for stimulus specificity and a critical role in collagen IV remodeling. *J. Leukoc. Biol.* 83:864–874. https://doi.org/10.1189/jlb.1007666

Sakurai-Yageta, M., C. Recchi, G. Le Dez, J.B. Sibarita, L. Daviet, J. Camonis, C. D'Souza-Schorey, and P. Chavrier. 2008. The interaction of IQGAP1 with the exocyst complex is required for tumor cell invasion downstream of Cdc42 and RhoA. *J. Cell Biol.* 181:985–998. https://doi.org/10.1083/jcb.200709076

Sbai, O., L. Ferhat, A. Bernard, Y. Gueye, A. Ould-Yahoui, S. Thiolloy, E. Charrat, G. Charton, E. Tremblay, J.-J. Risso, et al. 2008. Vesicular trafficking and secretion of matrix metalloproteinases-2, -9 and tissue inhibitor of metalloproteinases-1 in neuronal cells. *Mol. Cell. Neurosci.* 39:549–568. https://doi.org/10.1016/j.mcn.2008.08.004

Sbai, O., A. Ould-Yahoui, L. Ferhat, Y. Gueye, A. Bernard, E. Charrat, A. Mehanna, J.-J. Risso, J.-P. Chauvin, E. Fenouillet, et al. 2010. Differential vesicular distribution and trafficking of MMP-2, MMP-9, and their inhibitors in astrocytes. *Glia.* 58:344–366. https://doi.org/10.1002/glia.20927

Scherer, P.E., G.Z. Lederkremer, S. Williams, M. Fogliano, G. Baldini, and H.F. Lodish. 1996. Cab45, a novel (Ca2+)-binding protein localized to the Golgi lumen. *J. Cell Biol.* 133:257–268. https://doi.org/10.1083/jcb.133.2.257

Schuck, P.. 2000. Size-distribution analysis of macromolecules by sedimentation velocity ultracentrifugation and lamm equation modeling. *Biophys. J.* 78:1606–1619. https://doi.org/10.1016/S0006-3495(00)76713-0

Shapovalov, M.V., and R.L. Dunbrack, Jr.. 2011. A smoothed backbone-dependent rotamer library for proteins derived from adaptive kernel density estimates and regressions. *Structure.* 19:844–858. https://doi.org/10.1016/j.str.2011.03.019

Shaverdashvili, K., P. Wong, J. Ma, K. Zhang, I. Osman, and B. Bedogni. 2014. MT1-MMP modulates melanoma cell dissemination and metastasis through activation of MMP2 and RAC1. *Pigment Cell Melanoma Res.* 27:287–296. https://doi.org/10.1111/pcmr.12201

Shimoda, M., and R. Khokha. 2017. Metalloproteinases in extracellular vesicles. *Biochim. Biophys. Acta Mol. Cell Res.* 1864(11 Pt A):1989–2000. https://doi.org/10.1016/j.bbamcr.2017.05.027

Tallant, C., A. Marrero, and F.X. Gomis-Rüth. 2010. Matrix metalloproteinases: fold and function of their catalytic domains. *Biochim. Biophys. Acta.* 1803:20–28. https://doi.org/10.1016/j.bbamcr.2009.04.003

Theocharis, A.D., D. Manou, and N.K. Karamanos. 2019. The extracellular matrix as a multitasking player in disease. *FEBS J.* 286:2830–2869. https://doi.org/10.1111/febs.14818

Thestrup, T., J. Litzlbauer, I. Bartholomäus, M. Mues, L. Russo, H. Dana, Y. Kovalchuk, Y. Liang, G. Kalamakis, Y. Laukat, et al. 2014. Optimized ratiometric calcium sensors for functional in vivo imaging of neurons and T lymphocytes. *Nat. Methods.* 11:175–182. https://doi.org/10.1038/nmeth.2773

Ton, V.K., and R. Rao. 2004. Functional expression of heterologous proteins in yeast: insights into Ca2+ signaling and Ca2+-transporting ATPases. *Am. J. Physiol. Cell Physiol.* 287:C580–C589. https://doi.org/10.1152/ajpcell.00135.2004

Toth, M., A. Sohail, and R. Fridman. 2012. Assessment of Gelatinases (MMP-2 and MMP-9) by Gelatin Zymography. *In* Metastasis Research Protocols. M. Dwek, S.A. Brooks, and U. Schumacher, editors. Humana Press, Totowa, NJ. pp. 121–135. https://doi.org/10.1007/978-1-61779-854-2_8

Tulke, S., P. Williams, A. Hellysaz, E. Ilegems, M. Wendel, and C. Broberger. 2016. Nucleobindin 1 (NUCB1) is a Golgi-resident marker of neurons. *Neuroscience.* 314:179–188. https://doi.org/10.1016/j.neuroscience.2015.11.062

Tyanova, S., T. Temu, P. Sinitcyn, A. Carlson, M.Y. Hein, T. Geiger, M. Mann, and J. Cox. 2016. The Perseus computational platform for comprehensive analysis of (prote)omics data. *Nat. Methods.* 13:731–740. https://doi.org/10.1038/nmeth.3901

Van Goethem, E., R. Poincloux, F. Gauffre, I. Maridonneau-Parini, and V. Le Cabec. 2010. Matrix architecture dictates three-dimensional migration modes of human macrophages: differential involvement of proteases and podosome-like structures. *J. Immunol.* 184:1049–1061. https://doi.org/10.4049/jimmunol.0902223

Vandooren, J., P.E. Van den Steen, and G. Opdenakker. 2013. Biochemistry and molecular biology of gelatinase B or matrix metalloproteinase-9 (MMP-9): the next decade. *Crit. Rev. Biochem. Mol. Biol.* 48:222–272. https://doi.org/10.3109/10409238.2013.770819

Vanoevelen, J., L. Raeymaekers, J.B. Parys, H. De Smedt, K. Van Baelen, G. Callewaert, F. Wuytack, and L. Missiaen. 2004. Inositol trisphosphate producing agonists do not mobilize the thapsigargin-insensitive part of the endoplasmic-reticulum and Golgi Ca2+ store. *Cell Calcium.* 35:115–121. https://doi.org/10.1016/j.ceca.2003.08.003

Vanoevelen, J., L. Raeymaekers, L. Dode, J.B. Parys, H. De Smedt, G. Callewaert, F. Wuytack, and L. Missiaen. 2005. Cytosolic Ca2+ signals depending on the functional state of the Golgi in HeLa cells. *Cell Calcium.* 38:489–495. https://doi.org/10.1016/j.ceca.2005.07.003

von Blume, J., A.-M. Alleaume, G. Cantero-Recasens, A. Curwin, A. Carreras-Sureda, T. Zimmermann, J. van Galen, Y. Wakana, M.A. Valverde, and V. Malhotra. 2011. ADF/cofilin regulates secretory cargo sorting at the TGN via the Ca2+ ATPase SPCA1. *Dev. Cell.* 20:652–662. https://doi.org/10.1016/j.devcel.2011.03.014

von Blume, J., A.-M. Alleaume, C. Kienzle, A. Carreras-Sureda, M. Valverde, and V. Malhotra. 2012. Cab45 is required for Ca(2+)-dependent secretory cargo sorting at the trans-Golgi network. *J. Cell Biol.* 199:1057–1066. https://doi.org/10.1083/jcb.201207180

Vorum, H., H. Hager, B.M. Christensen, S. Nielsen, and B. Honoré. 1999. Human calumenin localizes to the secretory pathway and is secreted to the medium. *Exp. Cell Res.* 248:473–481. https://doi.org/10.1006/excr.1999.4431

Wiech, H., B.M. Geier, T. Paschke, A. Spang, K. Grein, J. Steinkötter, M. Melkonian, and E. Schiebel. 1996. Characterization of green alga, yeast, and human centrins. Specific subdomain features determine functional diversity. *J. Biol. Chem.* 271:22453–22461. https://doi.org/10.1074/jbc.271.37.22453

Wiesner, C., K. El Azzouzi, and S. Linder. 2013. A specific subset of RabGTPases controls cell surface exposure of MT1-MMP, extracellular matrix degradation and three-dimensional invasion of macrophages. *J. Cell Sci.* 126:2820–2833. https://doi.org/10.1242/jcs.122358

Wiesner, C., J. Faix, M. Himmel, F. Bentzien, and S. Linder. 2010. KIF5B and KIF3A/KIF3B kinesins drive MT1-MMP surface exposure, CD44 shedding, and extracellular matrix degradation in primary macrophages. *Blood.* 116:1559–1569. https://doi.org/10.1182/blood-2009-12-257089
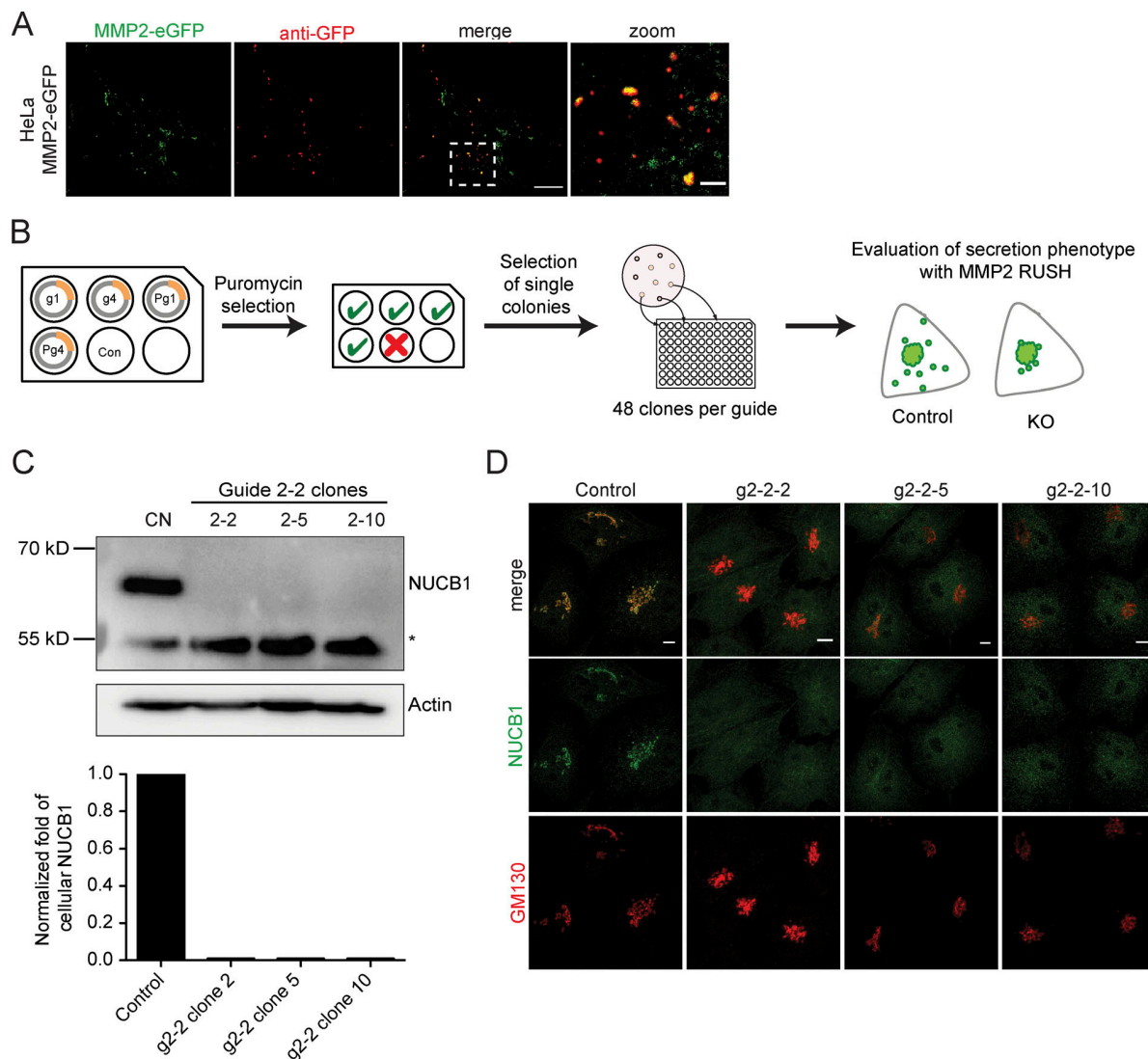
Figure S1.   **MMP2-eGFP secretion and evaluation of CRISPR NUCB1-KO clones. (A)** HeLa cells stably expressing SS-MMP2-eGFP were seeded on glass slides and incubated at 37°C for 3 d to evaluate MMP2-eGFP secretion. After fixation, cells were incubated with GFP antibody and Alexa Fluor 594. Confocal fluorescence images show colocalization of MMP2-eGFP and GFP antibody of nonpermeabilized cells, evidencing secretion of MMP2-eGFP to the extracellular space. Scale bars, 10 µm; zoom bar, 2 µm. **(B and C)** NUCB1-KO cells were generated using the CRISPR-Cas9 system with three different gRNAs and selection of single colonies. After puromycin selection, three NUCB1-KO clones were identified by WB (B) and later confirmed by immunofluorescence (C). *, unspecific band; KO, HeLa NUCB1-KO cells; CN, HeLa control. Semiquantitative analysis shows normalized NUCB1-to-β-actin signal.
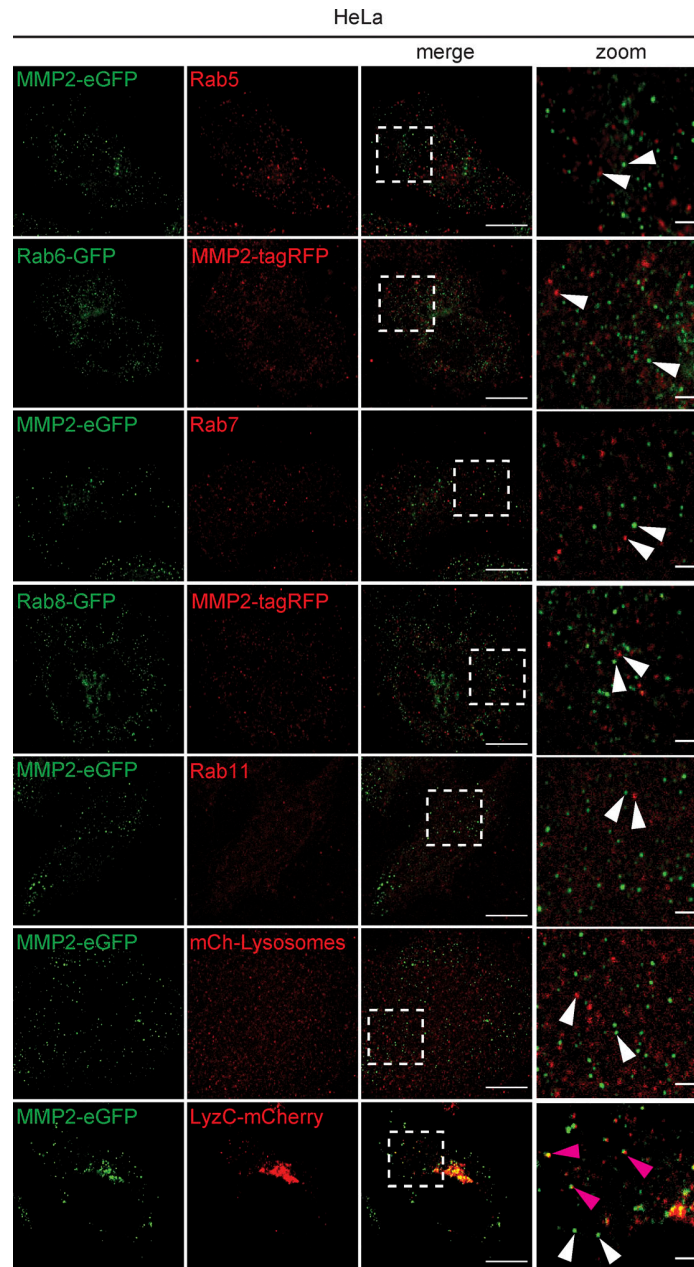
Figure S2.   **MMP2 is partially sorted in LyzC-positive secretory vesicles.** HeLa cells expressing MMP2-eGFP were immunolabeled with a-Rab5, a-Rab7, or Rab11 antibodies (red). MMP2-eGFP–expressing cells were cotransfected with mCherry (mCh)-lysosomes or LyzC-mCherry to label lysosomes or LyzC-positive secretory vesicles, respectively. Rab6-GFP or Rab8-GFP constructs were cotransfected with MMP2-tagRFP. Images were acquired by confocal microscopy. White arrowheads point to distinct vesicles; magenta arrowheads point to colocalizing vesicles. Bars, 10 μm; zoom, 2 μm.

Pacheco-Fernandez et al.
Nucleobindin-1 regulates MMP secretion

Journal of Cell Biology   S2
https://doi.org/10.1083/jcb.201907058

Figure S3. **Protein purification and evaluation of the direct interaction between MMP2 and NUCB1. (A)** Coomassie-stained SDS-PAGE for the evaluation of His-tag purified recombinant NUCB1-His (rNUCB1-His). **(B)** Anti-NUCB1 WB analysis of the elution fraction shown in line 4 from A. **(C)** WB analysis of purified His-SUMO-MMP2 using MMP2 antibody. **(D)** Recombinant His-SUMO-MMP2 (rHS-MMP2) was bioconjugated with Cy3 via maleimide labeling and subsequently analyzed by AUC. The lowest panel shows peak of sedimentation of rHS-MMP2 at 4.705 S. **(E)** AUC profile of rHis-SUMO-MMP2-Cy3 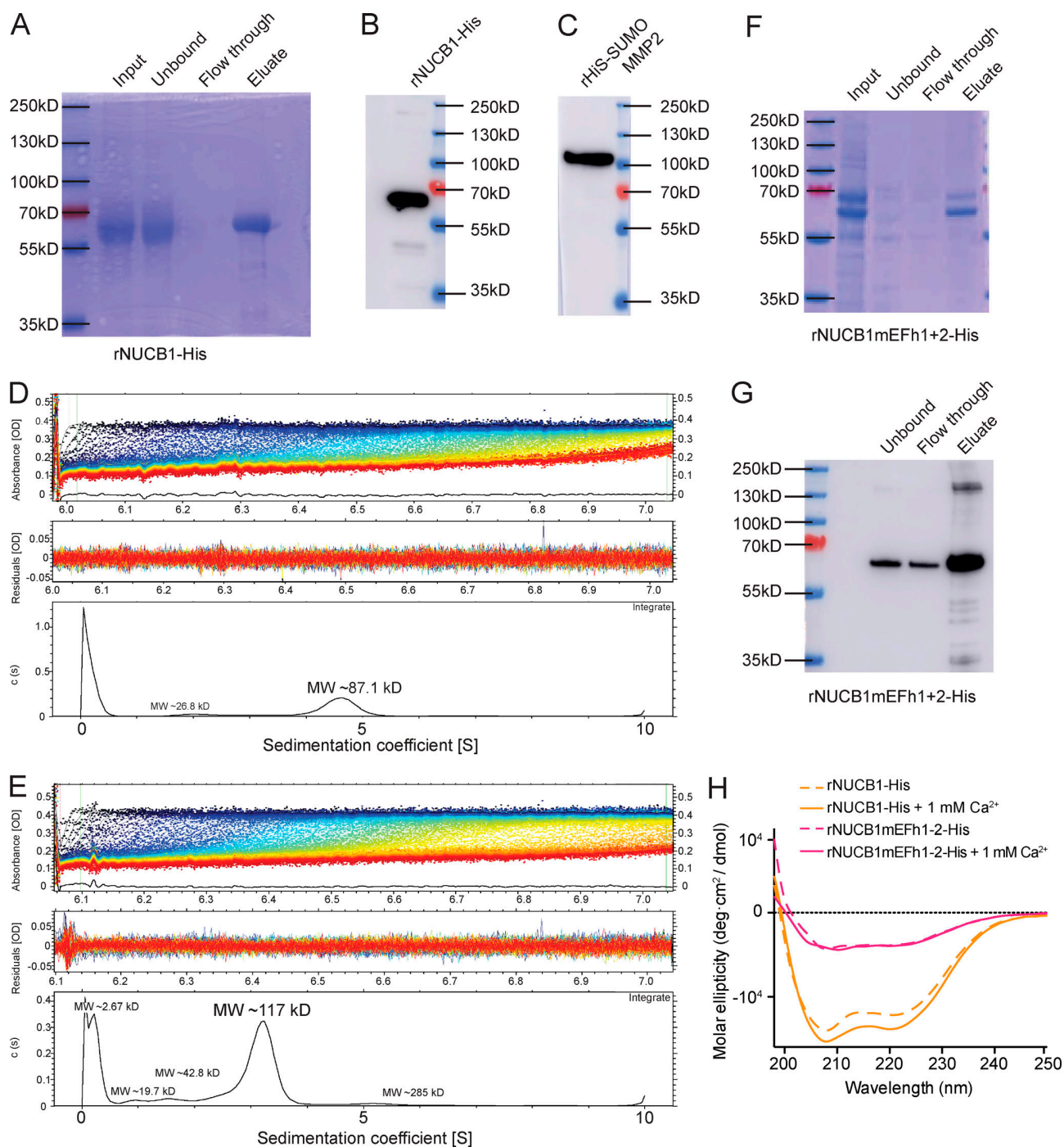and NUCB1-His. The lowest panel shows a peak at 3.189 S, indicating a change in the sedimentation velocity associated to a direct interaction of NUCB1 and MMP2. **(F)** Coomassie-stained SDS-PAGE of purified His-tagged NUCB1 Ca^{2+} binding mutant (rNUCB1mEFh1+2). **(G)** WB analysis of the elution fraction shown in line 4 of F using NUCB1 antibody. **(H)** CD measurement of rNUCB1-His and rNUCB1mEFh1+2-His under presence or absence of 1 mM Ca^{2+}. rNUCB1-mEF1+2 molar ellipticity is lower compared with rNUCB1-His. Evaluation of the CD spectra using CONTIN (Wiech et al., 1996) showed an increase in rNUCB1-His α-helicity upon Ca^{2+} addition (from 0.385 to 0.413) that was not observed in rNUCB1-mEFh1+2 (from 0.256 to 0.147). Instead, an increase in β-sheet content (from 0.151 to 0.322) was observed. These findings are in accordance with the results described by de Alba and Tjandra (2004).
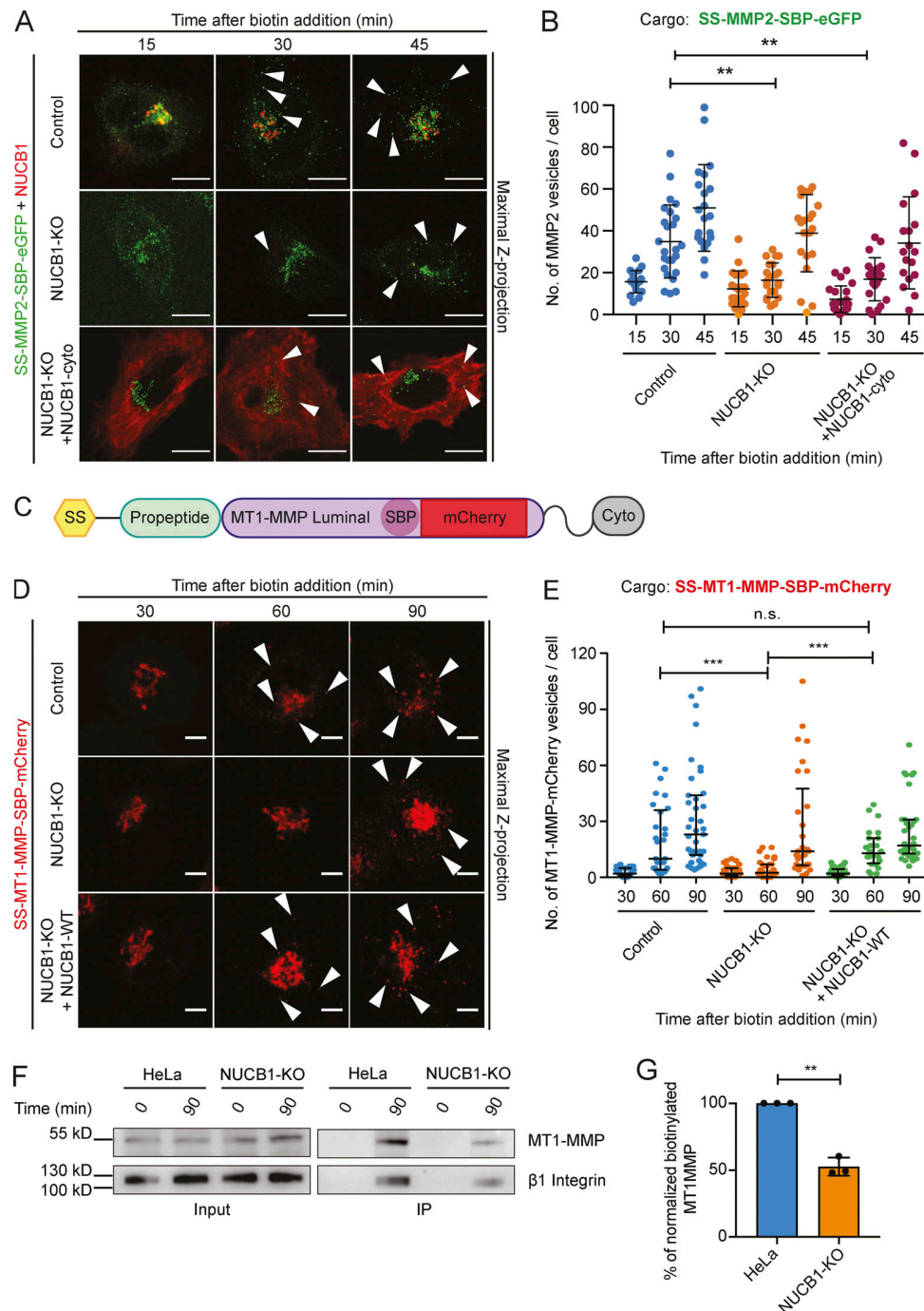
Figure S4. **MMP2 IG trafficking is exclusively dependent on Golgi-localized NUCB1, which also impairs IG trafficking of MT1-MMP. (A)** HeLa or NUCB1-KO cells expressing SS-SBP-MMP2-eGFP alone or with a cytosolic variant of NUCB1 lacking its SS (NUCB1-cyto) were fixed after 0, 15, 30, and 45 min of biotin incubation. Maximal Z-projection analysis of confocal microscopy images shows no differences in MMP2 trafficking of NUCB1-cyto transfected cells compared with NUCB1-KO cells (arrowheads). Scale bars, 10 μm. **(B)** Quantification of cytoplasmic MMP2 vesicles from cells in A. n > 18 cells; mean ± SD; two independent experiments. Significant differences with P < 0.05 were analyzed via nonparametric Kruskal–Wallis test with Dunn's multiple comparison, **, P < 0.01. **(C)** mCherry-tagged MT1-MMP RUSH construct (SS-MT1-MMP-SBP-mCh). Cyto, cytosolic domain. **(D)** Confocal fluorescence images of HeLa or NUCB1-KO cells transfected with or without NUCB1-WT and fixed after 30, 60, and 90 min of biotin incubation. Arrowheads, cytoplasmic vesicles. Scale bars, 5 μm. **(E)** Quantification of cytoplasmic vesicles observed in A. n = 24 cells; two independent experiments; median ± IQR; ***, P < 0.001; n.s., non-significant. **(F)** Cell surface biotinylation assay coupled with streptavidin pull-down. HeLa or NUCB1-KO cells were untreated (time 0) or incubated with sulfo-NHS-Biotin for 90 min to label cell surface proteins, and then pulled down with Neutravidin beads. WB analysis shows a reduction in the amount of endogenous active MT1-MMP at the surface of NUCB1-KO cells compared with HeLa control. β-1 integrin was used as loading control. **(G)** Semiquantitative analysis of surface labeled active MT1-MMP from F represented as % of normalized MT1-MMP intensity to β-1 integrin in comparison to control (100%). n = 3 independent experiments; one-sample t test, **, P < 0.01. Bars, mean ± SD.
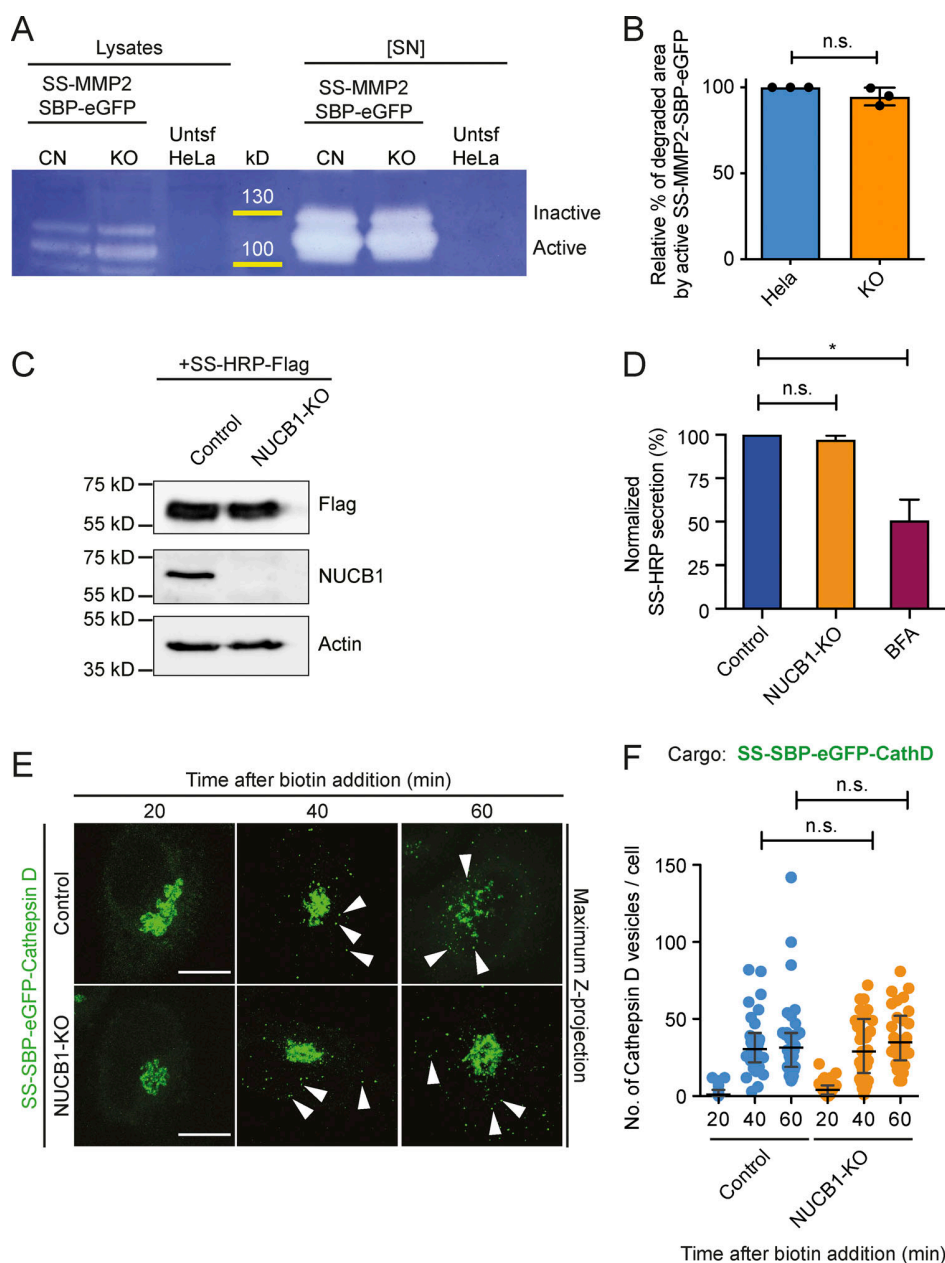
Figure S5. **NUCB1 does not affect MMP2 activation nor trafficking of other cargoes such as HRP and Cathepsin D. (A)** Zymography assay of HeLa cells expressing SS-MMP2-SBP-eGFP. Untsf HeLa, HeLa without transfection; [SN], 10×-concentrated supernatants; CN, HeLa control; KO, NUCB1-KO. **(B)** Semiquantitative analysis of experiment shown in A. n = 3 independent experiments; one-sample t test; n.s., nonsignificant. **(C)** Whole-cell lysates of HeLa and NUCB1-KO cells stably expressing SS-HRP-FLAG were analyzed by anti-FLAG, anti-NUCB1, and anti-β-actin WB. SS-HRP-FLAG is expressed in HeLa and NUCB1-KO cells to similar levels. **(D)** Cell culture supernatants of cells described in C were analyzed for HRP activity by chemiluminescence after 4-h secretion. BFA served as a positive control for perturbed secretion and was added for 1 h before HRP secretion analysis. No significant differences were observed between NUCB1-KO and HeLa control cells. *, P < 0.05. **(E)** HeLa or NUCB1-KO cells expressing SS-SBP-eGFP-Cathepsin D were fixed 20, 40, and 60 min after biotin addition. Representative maximum Z-projection images show Cathepsin D trafficking from Golgi to cytoplasmic vesicles (arrowheads). Scale bars, 10 µm. **(F)** Quantification of cytoplasmic Cathepsin D vesicles from cells shown in E. n > 30 HeLa and NUCB1-KO cells per time point; two independent experiments; mean ± SD. Statistical analysis was performed using a nonparametric Kruskal–Wallis test with Dunn's multiple comparison test. No significant differences with P < 0.05 were detected.

Provided online is one table. Table S1 lists protein candidates potentially involved in the trafficking of MMP2, found by MS.

3.2   Fam20C regulates protein secretion by Cab45-phosphorylation

Cargo molecules that follow the Secretory Pathway and traverse though the Golgi apparatus, reach the *trans*-Golgi network (TGN) – the main sorting hub of the cell. Here, cargo molecules are sorted into specific vesicles to be transported to their final destinations. Thereby, the sorting of most secreted molecules poses a conceptual challenge, as their sorting differs from the more classical, better-studied examples seen in transmembrane or endosomal/lysosomal proteins, where transmembrane domains or cargo recognition motifs are required for interaction with cytosolic, vesicle-forming components. Instead, some soluble secreted molecules are sorted via the Golgi-luminal protein Cab45 in a Ca^{2+}-dependent process. In this regard, our lab ascertained that Cab45 oligomerizes via binding of Ca^{2+} that has been locally pumped into the TGN by the Secretory Pathway Ca^{2+}- ATPase SPCA1. Upon oligomerization, Cab45 binds secretory proteins e.g. LyzC, is sorted together with its clients into sphingomyelin(SM)-rich vesicles and secreted from the cell. Nevertheless, details of the sorting and regulation of the Cab45-client-complex remain elusive.

Therefore, the recently discovered Golgi-kinase Fam20C garnered our interest, as it is the first - and as yet only - serine/threonine kinase found to act within the Secretory Pathway. To address if Fam20C actually plays a role in Cab45-dependent cargo sorting, we generated Fam20C-KO clones using the CRISPR/Cas9 technique and performed microscopy-based single cell cargo sorting assays (RUSH-assays) to monitor cargo sorting. Interestingly, these cells showed a reduced number of LyzC-positive vesicles budding from the TGN as well as a reduced LyzC secretion, which was corroborated by secretion assays (Hecht et al. 2020 - Figure 1).

Next, we sought to discover if Cab45 was itself a substrate of Fam20C. We isolated Golgi fractions of cells, expressing Fam20C-wt or a kinase-dead variant and analyzed them by mass spectrometry, whereas, together with annotated Fam20C substrates, phosphorylated Cab45 was identified only in the Fam20C-wt expressing cells. Further *in vitro* Fam20C kinase assays revealed that Fam20C specifically phosphorylates Cab45, but not the cargo protein LyzC (Hecht et al. 2020 - Figure 3).

As our mass spectrometry approach detected five specific Fam20C-dependent Cab45-phosphorylation sites, we further examined their specific role in Cab45-dependent cargo sorting at the TGN. Therefore, we mutated all of those residues to either alanine (Cab45-5pXA) or glutamic acid (Cab45-5pXE) to mimic the non-phosphorylated and the

phosphorylated status of Cab45, respectively, and compared them to Cab45-wt cells. Remarkably, only Cab45-5pXE localized in post-Golgi vesicles at steady state (Hecht et al. 2020 - Figure 4).

Strikingly, live-cell experiments of cells transfected with fluorophore-tagged Cab45 and Fam20C showed that both proteins are in close proximity with each other right before the budding event and furthermore leave the TGN together in SM-rich vesicles (Hecht et al. 2020 - Figure 2). Indeed, Fam20C-dependet phosphorylation of Cab45 results in increased export of Cab45 at the level of individual vesicle formation at the TGN. This goes in line with enhanced cargo sorting and secretion, which we specifically determined for Cab45 client LyzC, but not for non-Cab45 cargos like the lysosomal hydrolase CatD or secreted OPN[97] (Hecht et al. 2020 - Figures 5 and 6).

To further elucidate the role of phosphorylation of Cab45, we carried out a microscopy-based oligomerization assay. Using purified GFP-tagged wt and phosphomutant proteins, we observed that in contrast to the other tested proteins, Ca^{2+} addition to GFP-Cab45-5pXE resulted in the formation of smaller and less intense oligomeric structures, suggesting that phosphorylation influences the size of the oligomers (Hecht et al. 2020 - Figure 7).

---

[97] OPN = Osteopontin

ARTICLE

Fam20C regulates protein secretion by Cab45 phosphorylation

Tobias Karl-Heinz Hecht[1,2]*, Birgit Blank[1,2]*, Martin Steger[2], Victor Lopez[3], Gisela Beck[2], Bulat Ramazanov[1], Matthias Mann[2], Vincent Tagliabracci[3], and Julia von Blume[1,2]

The TGN is a key compartment for the sorting and secretion of newly synthesized proteins. At the TGN, soluble proteins are sorted based on the instructions carried in their oligosaccharide backbones or by a Ca^{2+}-mediated process that involves the cargo-sorting protein Cab45. Here, we show that Cab45 is phosphorylated by the Golgi-specific protein kinase Fam20C. Mimicking of phosphorylation translocates Cab45 into TGN-derived vesicles, which goes along with an increased export of LyzC, a Cab45 client. Our findings demonstrate that Fam20C plays a key role in the export of Cab45 clients by fine-tuning Cab45 oligomerization and thus impacts Cab45 retention in the TGN.

Introduction

The Golgi apparatus is the main sorting hub of the protein secretory pathway within cells. Much of this activity occurs in the most distal cisternae of the Golgi, known as the TGN (Chege and Pfeffer, 1990; Gleeson et al., 2004; Klumperman, 2011; De Matteis and Luini, 2008; Munro, 2005).

Over recent decades, studies have elucidated the mechanisms by which sorting takes place at the TGN to explain the trafficking of transmembrane proteins (Fölsch et al., 1999; 2001; Fölsch, 2005, 2008; Munro, 1995; Welch and Munro, 2019) and the transport of lysosomal hydrolases to endosomes and lysosomes (Mellman and Nelson, 2008). A process fundamental to all sorting events is the congregation of cargo molecules in the TGN, where they interact with cytosolic coat complexes that initiate the formation and budding of vesicles (Ang and Fölsch, 2012; Bonifacino, 2014; Guo et al., 2014; Traub and Bonifacino, 2013). However, many soluble secreted molecules contain neither a transmembrane domain nor a recognition motif for known cargo receptors, which poses a challenge as to how these molecules are sorted and trafficked (Kienzle and von Blume, 2014; Pakdel and von Blume, 2018).

We have previously described a novel sorting mechanism that explains the sorting of certain soluble secreted molecules. In this, secretory pathway Ca^{2+} ATPase 1 (SPCA1), a TGN-specific calcium ion (Ca^{2+}) ATPase, interacts with cofilin1 and F-actin at its cytosolic interface, promoting Ca^{2+} influx into the lumen of the TGN (von Blume et al., 2009, 2011, 2012; Kienzle et al., 2014; Pizzo et al., 2010). As a result of this local Ca^{2+} increase, the Ca^{2+}-binding protein calcium-binding protein 45 kD (Cab45) oligomerizes and binds secretory cargoes (clients), such as lysozyme C (LyzC),

thereby segregating them from the bulk milieu of the TGN lumen (Blank and von Blume, 2017; Crevenna et al., 2016). Cab45–client complexes are then sorted into specific sphingomyelin (SM)–rich vesicles and transported to the plasma membrane for secretion (Deng et al., 2018). Other factors that influence the sorting of the Cab45–client complexes into SM-rich vesicles remain unknown.

Family with sequence similarity 20 member C (Fam20C) is a recently discovered serine/threonine kinase found in the Golgi apparatus, which phosphorylates >100 secreted substrates within the secretory pathway (Tagliabracci et al., 2012, 2013, 2015). Interestingly, many of these are Ca^{2+}-binding and secreted proteins (Tagliabracci et al., 2015).

This study analyzes the influence of Fam20C on the SPCA1/Cab45 sorting machinery. We show that Fam20C phosphorylates Cab45 on distinct residues and thereby decreases Cab45 retention in the TGN. In this regard, our data present evidence that phosphorylation fine-tunes the oligomerization-dependent sorting process without modulating the general Ca^{2+}-binding ability of Cab45. Moreover, phosphorylation of Cab45 drives the sorting of Cab45-client LyzC into SM-rich vesicles, leading to enhanced secretion of the cargo. Overall we propose that Fam20C regulates Cab45-dependent client sorting by modulating its release into vesicles at the TGN.

Results

Depletion of Fam20C impairs secretion of LyzC

It has previously been shown that the majority of Fam20C substrates are secreted proteins (Tagliabracci et al., 2015);

....
[1]Department of Cell Biology, Yale University School of Medicine, New Haven, CT; [2]Max Planck Institute of Biochemistry, Department of Molecular Medicine, Martinsried, Germany; [3]Department of Molecular Biology, University of Texas Southwestern Medical Center, Dallas, TX.

*T.K.-H. Hecht and B. Blank contributed equally to this study; Correspondence to Julia von Blume: julia.vonblume@yale.edu.

however, whether the kinase has a directing role in cargo secretion has not yet been investigated. To address if Fam20C plays a role in Cab45-dependent cargo sorting, a Fam20C knockout (KO) cell line was generated using CRISPR/Cas9 technology (Cong et al., 2013). The sequencing of a clone (Fig. 1 A) detected the deletion of 22 bp at the predicted Cas9 cutting site and leads to the premature termination of the protein. Additionally, we confirmed the KO of Fam20C at the protein level by mass spectrometry (MS) analysis (Fig. S1, A and B).

We next examined the role of Fam20C in the secretion of the Cab45 client LyzC (von Blume et al., 2012; Crevenna et al., 2016; Deng et al., 2018). We transfected HeLa cells and Fam20C-KO cells with LyzC-Flag and analyzed the supernatants by SDS-PAGE and Western blotting. To investigate the role of Fam20C in the TGN export of LyzC, we incubated these cells at 20°C for 2 h to promote the accumulation of LyzC in the TGN followed by incubation at 37°C for 1 h to release the protein. Western blot analyses (Fig. 1 B) revealed a reduction of LyzC secretion after 37°C release in the Fam20C-KO cells of ∼50% compared with the WT cells (Fig. 1 C). This is in line with the reduced secretion in Cab45 KO-cells (Crevenna et al., 2016).

Next, we used the retention using selective hooks (RUSH) system to analyze the packaging of LyzC into secretory vesicles in Fam20C-KO cells. The RUSH system allowed us to track the cargo transport through the secretory pathway (Boncompain and Perez, 2012; Boncompain et al., 2012). Control and Fam20C-KO cells were transfected with the RUSH construct LyzC-streptavidin-binding peptide (SBP)-EGFP and fixed after various time points. We also analyzed rescued Fam20C-KO cells that stably reexpressed Fam20C-WT, as well as the kinase-dead variant Fam20C-D478A (Tagliabracci et al., 2012). The expression of Fam20C-WT and Fam20C-D478A was confirmed by staining cells with an α-HA antibody (Fig. 1 D). Without biotin, LyzC was trapped in the ER (0 min), whereas biotin addition induced LyzC transport through the secretory pathway. TGN-derived vesicles at different time points were quantified (Fig. 1 E). LyzC was observed to localize in the Golgi of the HeLa control cells 20 min after adding biotin; after 40 min, LyzC was sorted and packed into TGN-derived vesicles, with 32 ± 15 vesicles per cell (Fig. 1, D and E). To exclude that analyzed LyzC vesicles in the RUSH approach are following the endosomal/lysosomal pathway, we performed costainings in HeLa cells using specific endosomal/lysosomal markers (Fig. S1 C).

Consistent with the results of the secretion assay (Fig. 1, B and C), the Fam20C-KO cells showed a significant delay in the formation of LyzC vesicles after 40 min (with 19 ± 12 vesicles per cell). This effect was fully rescued by reexpressing Fam20C-WT in Fam20C-KO cells (resulting in 35 ± 22 vesicles per cell), but not with the kinase-dead variant (10 ± 7 vesicles per cell; Fig. 1, D and E). A comparison of the reexpression of Fam20C-WT versus Fam20C-D478A showed a significantly higher number of LyzC vesicles in the former, even at 60 min after biotin addition (with 53 ± 25 and 16 ± 12 vesicles per cell, respectively).

Together, these results indicate that Fam20C kinase activity drives the sorting and secretion of the Cab45-dependent client LyzC.

Fam20C buds with Cab45 in SM-rich vesicles

Given the finding that Fam20C depletion delayed the sorting of LyzC from the Golgi, we performed colocalization studies to investigate if there was an interconnection between the kinase and Cab45. First, we defined the localization of Fam20C and Cab45 relative to each other using immunofluorescence microscopy in fixed HeLa cells stained with antibodies against endogenous Cab45, Fam20C (HA antibody), and TGN46 (Fig. 2 A). Here, Fam20C colocalized with Cab45 (Pearson's correlation coefficient [r] = 0.754 ± 0.071) and TGN46 (r = 0.906 ± 0.026; Fig. 2 B). To investigate this co-occurrence in living cells, we monitored Cab45 and Fam20C budding by time-lapse imaging. HeLa cells were transfected with EGFP-Cab45 and mCherry-Fam20C, and vesicle formation was monitored over time. Interestingly, both proteins were budding from the TGN in the same vesicle (Fig. 2 C).

We reported recently that Cab45 is sorted into SM-rich vesicles and transported with its clients to the cell surface (Deng et al., 2018). To further verify the sorting of Fam20C, we investigated the colocalization of Fam20C with SM-rich vesicles in living cells. We used time-lapse microscopy to observe HeLa cells cotransfected with mCherry-Fam20C and EGFP-Cab45, EQ-SM-oxGFP (a nontoxic SM reporter protein derived from equinatoxin II [EQ]), or EQ-Sol-oxGFP (a nontoxic SM-binding–deficient reporter mutant). Fam20C vesicles were counted and analyzed for colocalization (Fig. 2 D). On average, out of 14 budded Fam20C vesicles, 9 were positive for Cab45 (65% ± 24%). Fam20C budded predominately in SM-positive vesicles (20 out of 26; 73% ± 17%), but not together with SM-binding–deficient EQ-Sol (13 out of 46; 30% ± 13%; Fig. 2 E).

These results suggested the close proximity of Fam20C and Cab45 at TGN exit sites before budding by going in the same transport carriers.

Fam20C phosphorylates Cab45 on distinct residues

The close proximity of Fam20C and Cab45 acts as a striking indicator that Fam20C could directly phosphorylate Cab45. This idea was also supported by the fact that many of the recently identified Fam20C substrates play roles in Ca²⁺ homeostasis or are actual Ca²⁺-binding proteins (Tagliabracci et al., 2015). So far, published screens indicated that Cab45 contains phosphorylated residues (e.g., Mertins et al., 2016; Zhou et al., 2013). However, to date, no kinase responsible for these modifications could be pinpointed.

To study the interdependence between the two proteins, recombinant Cab45 was purified from HEK293 cell culture supernatants (Li et al., 2013) and subsequently subjected to in vitro kinase assays with Fam20C-WT and the kinase-dead mutant Fam20C-D478A (Fig. 3 A). Osteopontin (OPN), a highly phosphorylated Fam20C substrate was used as a positive control (Tagliabracci et al., 2015). The results illustrated in Fig. 3 A clearly prove that Fam20C, but not the inactive mutant, is indeed able to phosphorylate Cab45 in vitro. Furthermore, the lack of phosphorylation of LyzC in the same Fam20C kinase assay (Fig. 3 B) additionally indicates that phosphorylation of Cab45, but not of LyzC itself, might be responsible for the sorting defect of LyzC (Fig. 1, B–E).
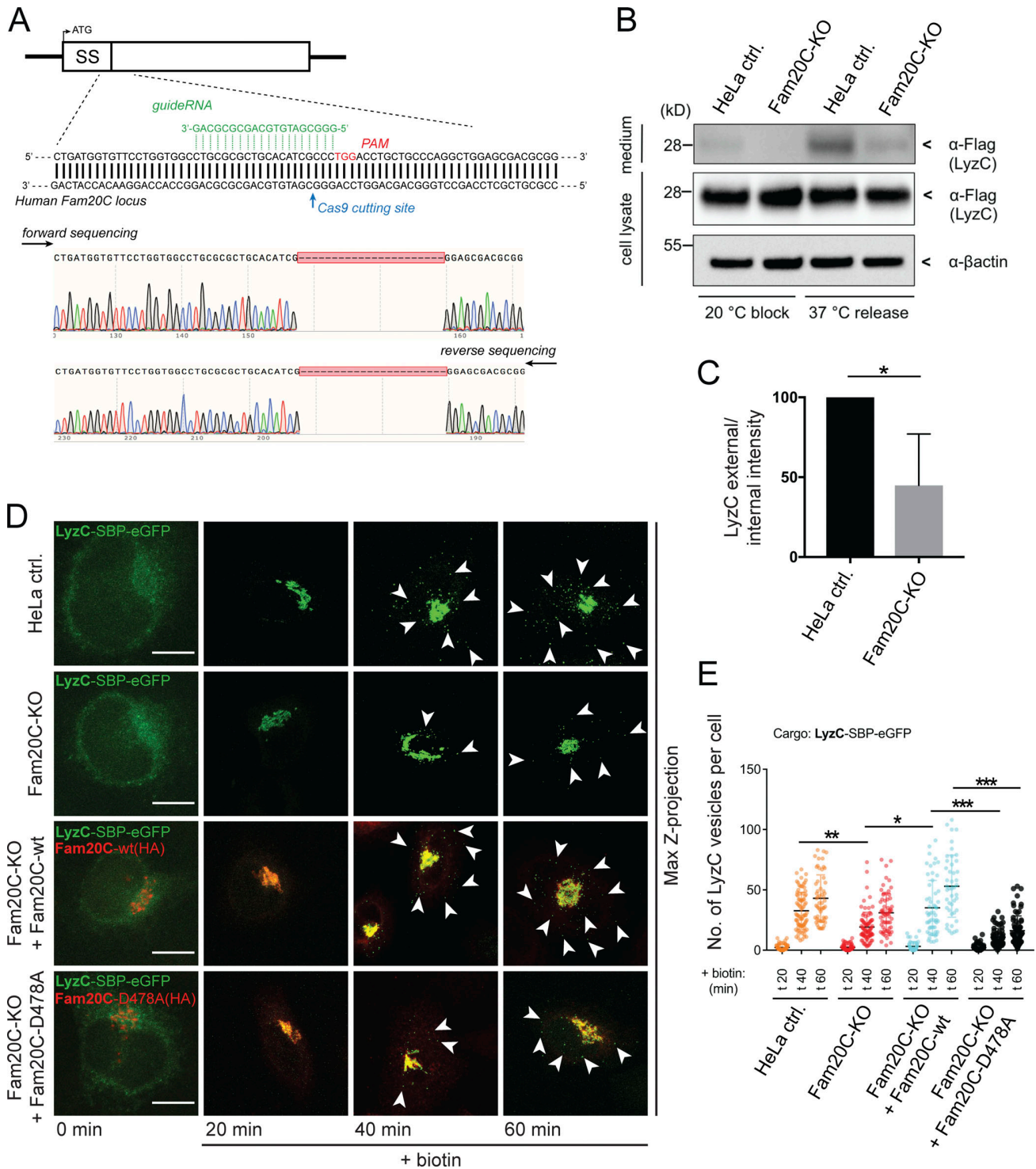
Figure 1. **Depletion of endogenous Fam20C impairs sorting and secretion of LyzC. (A)** HeLa Fam20C KO cells were generated using the CRISPR/Cas9 technique. Fam20C was targeted downstream of the signal sequence (SS) with gRNA next to Cas9 cutting site PAM. Sequencing of a Fam20C-KO clone highlight the deletion of 22 bp. **(B)** Western blot analysis of the secretion of LyzC-Flag in HeLa control (ctrl.) and Fam20C-KO cells after 20°C block and 37°C release. β-Actin was used as loading control. **(C)** Western blots of four independent experiments (B) were quantified by densitometry with ImageJ. The bar graph represents the means ± SD of densitometric values of external LyzC-Flag, normalized to internal levels in percentage. Statistical test, Kolmogorov–Smirnov. **(D)** Representative immunofluorescence images of the LyzC-RUSH experiments, showing LyzC transport in different cell lines. Cells were fixed at 0, 20, 40, and 60 min after biotin addition and costained with anti-HA antibody. Arrowheads indicate post-Golgi vesicles. Scale bars, 10 μm. **(E)** LyzC vesicle formation was quantified from RUSH experiments (D), analyzing z-stack images (d = 0.35 μm). A scatter dot plot represents the means (± SD) of at least three independent experiments ($n > 45$ cells per condition). Statistical test, Kruskal–Wallis. *, $P < 0.05$; **, $P < 0.01$.; ***, $P < 0.001$.
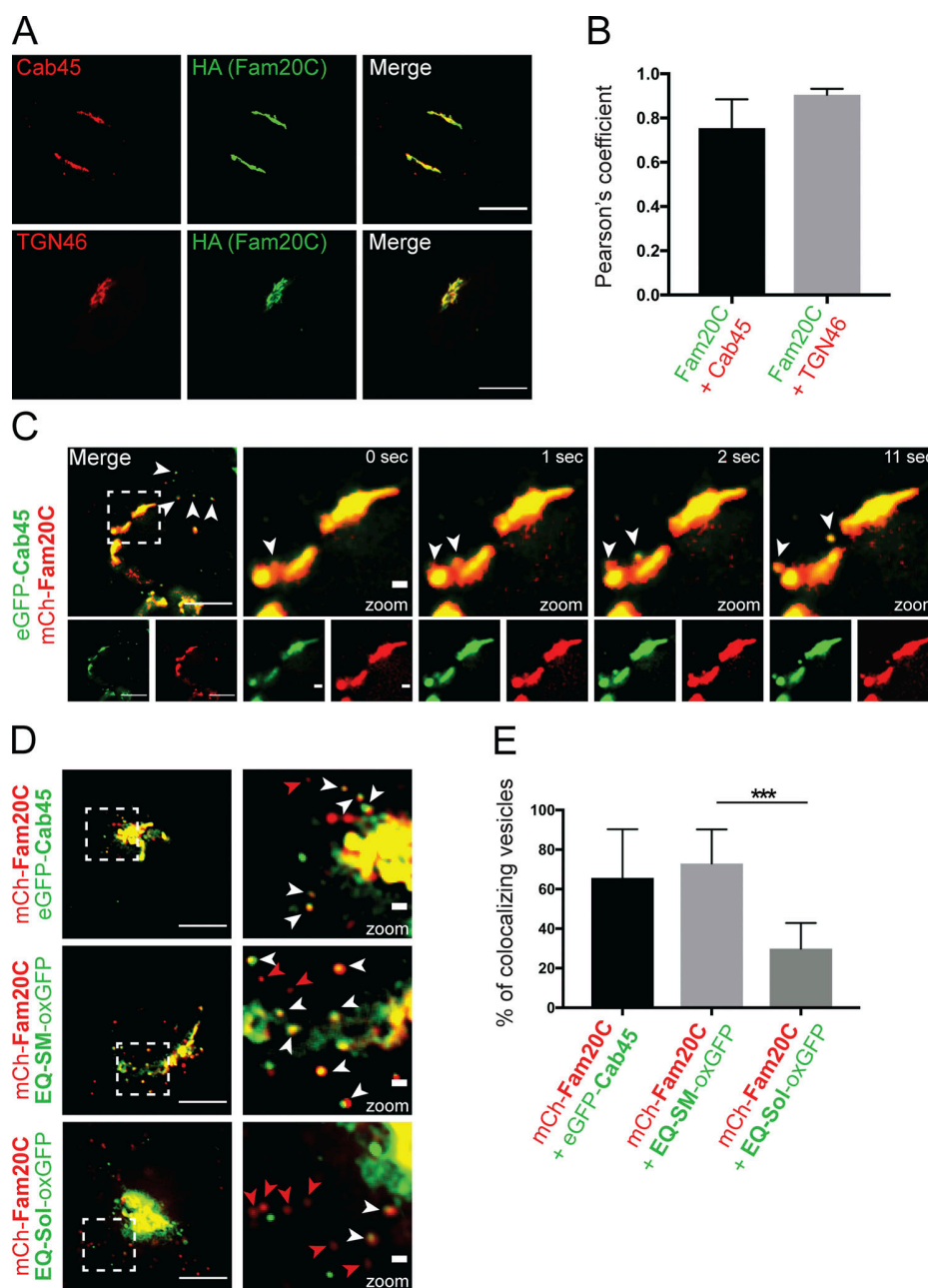
Figure 2. **Fam20C buds with Cab45 in TGN-derived vesicles.** **(A)** Colocalization of Fam20C-HA, Cab45, and TGN46 in stable Fam20C cell lines was demonstrated by using immunofluorescence microscopy. Scale bars, 10 μm. **(B)** Pearson's correlation coefficients were determined from A using ImageJ. The bar graph represents the means ± SD (*n* > 8 cells per condition). **(C)** The budding of Fam20C vesicles from the Golgi was observed in living cells expressing mCherry-Fam20C and EGFP-Cab45. Time-lapse movies were acquired. Scale bars, 10 μm. Arrowheads indicate colocalizing vesicles. Higher magnification shows Golgi (inset; scale bars, 1 μm). **(D)** Example micrographs are showing the Fam20C vesicle budding in living cells that expressed mCherry-Fam20C with EGFP-Cab45, EQ-SM-oxGFP, or EQ-Sol-oxGFP. Scale bars, 10 μm. Higher magnification shows Golgi (inset; scale bars, 1 μm). White arrowheads indicate colocalizing vesicles, and red arrowheads indicate Fam20C-only vesicles. **(E)** The numbers of colocalizing vesicles (D) were quantified. Data were collected from three independent experiments (*n* > 230 vesicles per condition). The bar graph illustrates the means (± SD) of colocalizing vesicles in percentage. Statistical test, Mann–Whitney. ***, P < 0.001.

To identify single Fam20C phosphorylation sites on Cab45 in living cells, we used sucrose gradient centrifugation to purify Golgi fractions from cells that stably express Fam20C-WT or Fam20C-D478A. These fractions were analyzed by MS and phosphoproteomics, verifying the phosphorylation status of Cab45 within the Golgi compartment (Fig. 3 C). In this regard, we predominantly found Fam20C-regulated phosphorylated sites in cells expressing Fam20C-WT, but not in D478A samples (Fig. S1 D), with a strong correlation between biological replicates (Fig. S1 E).

Cab45 phosphorylation sites:

Position	-Log10	Log2	Sequence window	Score	Detection
S99	3.62	-5.21	GKDLGGFDEDAEPRRSRRKLMVIFSKVDVNT	116.1	G, DB
T131*	2.18	-4.62	RKISAKEMQRWIMEKTAEHFQEAMEESKTHF	130.4	G
T131*	2.56	-3.51	RKISAKEMQRWIMEKTAEHFQEAMEESKTHF	130.4	G
S142*	3.11	-4.47	IMEKTAEHFQEAMEESKTHFRAVDPDGDGHV	178.6	G
S142*	3.38	-2.84	IMEKTAEHFQEAMEESKTHFRAVDPDGDGHV	178.6	G
T193	4.09	-5.33	ADAIRLNEELKVDEETQEVLENLKDRWYQAD	311.9	G, MS, DB
S349	5.25	-7.31	LEPEEVLKYSEFFTGSKLVDYARSVHEEF__	145.3	G, MS

* Multiplicity 2 (contains two detected phosphosites T131 & S142)
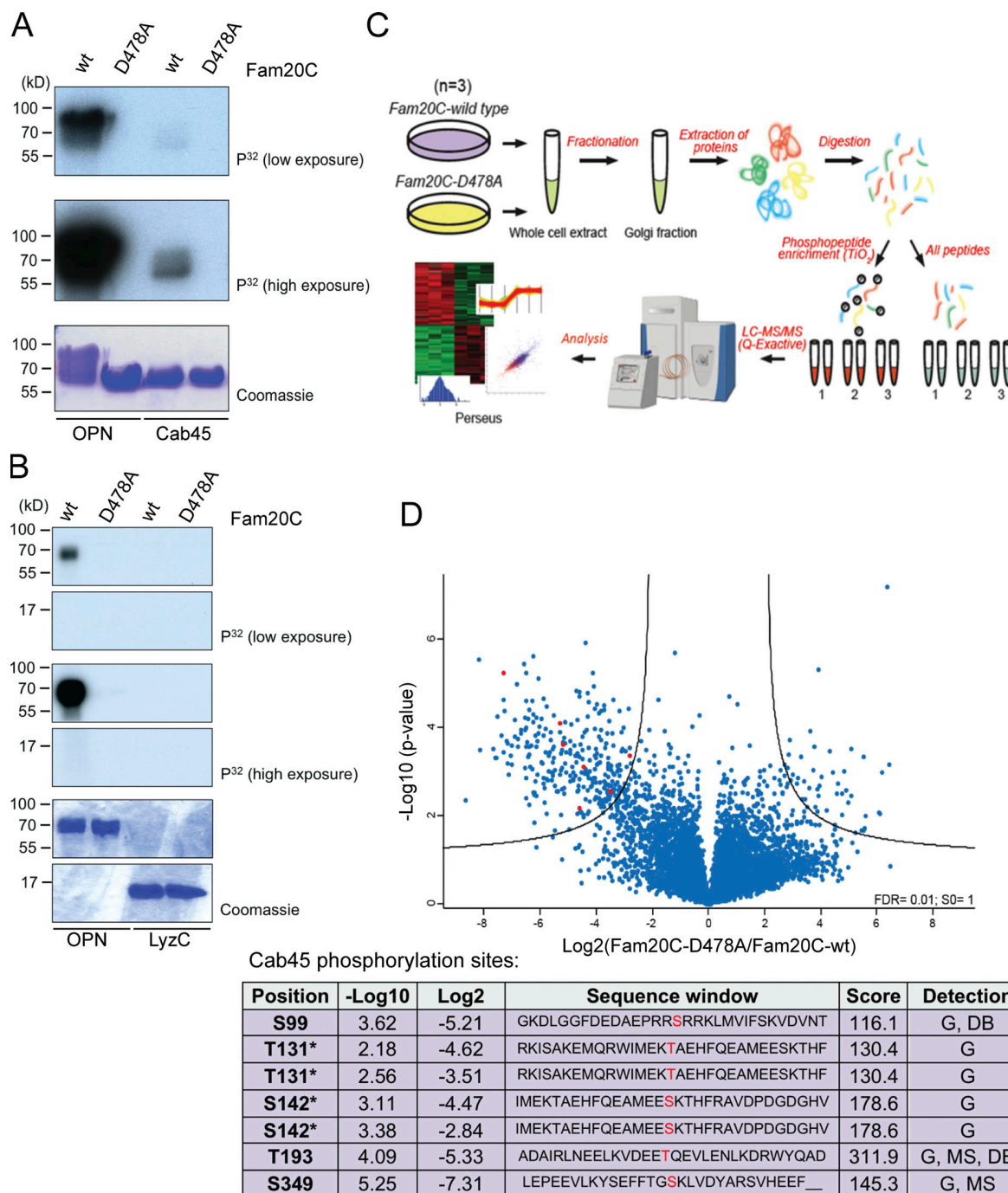
Figure 3. **Fam20C phosphorylates Cab45 on five distinct residues. (A and B)** In vitro Fam20C kinase assays. Recombinant Cab45-WT and LyzC were incubated with Fam20C-WT or Fam20C-D478A in the presence of [γ-^{32}P]ATP. ^{32}P incorporation was tested by SDS-PAGE and autoradiography. OPN was used as positive control. **(C)** Scheme of the MS approach used to identify Fam20C-dependent Cab45 phosphorylation in vivo. **(D)** Volcano plot is showing the phosphorylation change of phosphosites, detected in Golgi fractions of Fam20C-WT and D478A cells (C). Cab45 phosphorylation sites (red) are listed in Table 1. Abbreviations used: DB, database (www.phosphosites.org); G, sites detected in the Golgi fractions (C and D); MS, MS after kinase assay (A).

Among the hits, we detected phosphosites of typical Fam20C substrates (Tagliabracci et al., 2012, 2015), including nucleobindin, proprotein convertase subtilisin, and amyloid β A4 protein (data not shown), as well as phosphosites of Cab45. In total, five specific Cab45 residues were identified that were phosphorylated in Golgi fractions from Fam20C-WT, but not Fam20C-D478A, cells (labeled red and listed in Fig. 3 D). Strikingly, two of these sites (T193 and S349) were also identified in the in vitro kinase assay (Fig. 3 A), when the final product of the assay was analyzed by MS (data not shown). Sites S99 and T193

Table 1. **Primers and oligomers used for cloning of constructs**

Construct	Forward primer (5′ to 3′)	Reverse primer (5′ to 3′)
pLPCX-Cab45-5pXA	T131: GGATCATGGAGAAGGCGGCCGAGCACTTC	S99: AGCTTCCTCCGGGCCCGCCGCGGCTC
	T142: GAGGCCATGGAGGAGGCCAAGACACACTTCCG	
	S193: TCAAAGTGGATGAGGAAGCACAGGAAGTCCTGGA	
	S349: CGAGTTCTTCACGGGCGCCAAGCTGGTGGACTAC	
pLPCX-Cab45-5pXE	T131: GGATCATGGAGAAGGAAGCCGAGCACTTC	S99: AGCTTCCTCCGTTCCCGCCGCGGCTC
	T142: GAGGCCATGGAGGAGGAAAAGACACACTTCCG	
	S193: TCAAAGTGGATGAGGAAGAACAGGAAGTCCTGGA	
	S349: CGAGTTCTTCACGGGCGAAAAGCTGGTGGACTAC	
pB-T-PAF-Cab45-WT/5pXA/5pXE	Fragment1: GGCGGCCATCACAAGTTTGTACAGATGGCTACAGGCTCCCGG	Fragment1: GGTTGGCAGGCCGGCATTCACCTCC
	Fragment2: GGAGGTGAATGCCGGCCTGCCAACC	Fragment2: CCAGCACACTGGATCAGTTATCTATGCTTAAAACTCCTCGTGCACGCTGCG
pBT-PAF-GFP-Cab45-WT/5pXA/5pXE	Fragment1: GGCGGCCATCACAAGTTTGTACAGCTAGCATGGCTACAGGCTCCCG	Fragment1: CCGCTTCCACCTCCACCAGATCTGTGATGATGATGGTGATGAAGCTTTGTTC
	Fragment2: CTGGTGGAGGTGGAAGCGGTAGCAAAGGAGAAGAACTTTTCACTGG	Fragment2: CTTTGGAAGTACAGGTTCTCGGATCCGGCCGGCCGACCTCCACCTTTGTAGAGCTC
	Fragment3: GAGGTCGGCCGGCCGGATCCGAGAACCTGTACTTCCAAAGTGGCGCGCCACGGCCTGCCAACCAC	Fragment3: GGATCAGTTATCTATGCGGCCGCTCTAGATTAAAACTCCTCGTGCACGC
pLPCX-SS-EGFP-Cab45-5pXA/5pXE	Fragment1: CGTGACCGCCGCCCCGGAATTCCGGCCTGCCAACCACTCG	Fragment1: TTTATCGATGTTTGGCCGAGGCGACCGGTTTAAAACTCCTCGTGCACGCTGCG
pLPCX-Fam20C-HA	Fragment1: CGTAGATCTATGAAGATGATGCTGGTGCGCCG	Fragment1: GCACAATTGTTAAGCGTAGTCTGGGACGTCGTATGGGTACCTCGCCGAGGCGGCTCTGTG
pLPCX-Fam20C-D478A-HA	D478A: CATCATCCACTTAGCCAATGGAAGAGG	
pLPCX-mCherry-Fam20C	Fragment1: CCATAAAGCTTATACGAATTCATAGCCATGGCTACAGGCTCCCGGACGTCCCTGCTCCTGGCTTTTGGCCTGCTCTGCCTGCCCTGGCTTCAAGAGGGCAGTGCCTTCCCAACCATTCCCTTATCCTCGGGAA	Fragment1: TTCCCGAGGATAAGGGAATGGTTGGGAAGGCACTGCCCTCTTGAAGCCAGGGCAGGCAGAGCAGGCCAAAAGCCAGGAGCAGGGACGTCCGGGAGCCTGTAGCCATGG
	Fragment2: CCCTTATCCTCGGGAACAAAGCTTATGGTGAGCAAGGGCGAGG	Fragment2: CCTCCCCGGGGGAGAGGAATTCCTTAGCGTAGTCTGGGACGTCGTATGGGTA
	Fragment3: TACCCATACGACGTCCCAGACTACGCTAAGGAATTCCTCTCCCCCGGGGAGG	Fragment3: TATCGATGTTTGGCCGAGGCGGCCGCTTACCTCGCCGAGGCGGCTCTGTG
pIRESneo3-Str-KDEL_SS-SBP-tagRFP-Cab45	Fragment1: CTTGCCACAACCCGGGAGGCGCGCCATGGCTACAGGCTCCCGGACGTCCC	Fragment1: CTTAATCAGCTCTTCGCCCTTAGACACACCTGCAGGTGGTTCACGTTGACCTTG
	Fragment2: CAAGGTCAACGTGAACCACCTGCAGGTGTGTCTAAGGGCGAAGAGCTGATTAAG	Fragment2: AGTTAATTAATTGGCCCTCGAGGCCTTAAAACTCCTCGTGCACGCTGCGC

have previously been reported (Mertins et al., 2016; Zhou et al., 2013), confirming the results of the present phosphoproteomics. Interestingly, many of the identified protein hits could be clustered into four subgroups to Golgi-localizing, secreted, glycosylated, and Ca²⁺-binding proteins (Fig. S1 F), and Cab45 matches in all of these categories.

Phosphorylation-mimetic Cab45 accumulates in TGN-derived vesicles

To further analyze the role of the identified Cab45 phosphorylation sites, all five sites were mutated to either alanine (Cab45-5pXA), to generate a phosphorylation-deficient mutant of Cab45, or glutamic acid, to mimic the phosphorylated protein (Cab45-5pXE; Fig. 4 A). Stable cell lines expressing these constructs were generated by retroviral transduction of HeLa Cab45-KO cells (Crevenna et al., 2016). These cells were tested for equal Cab45 expression levels by Western blot analysis (Fig. 4 B). We fixed these cells and analyzed them by immunofluorescence microscopy. Surprisingly, we observed changes in the localization of the phospho-mimetic mutant Cab45-5pXE (Fig. 4 C); Cab45-WT and Cab45-5pXA almost completely co-localized with Golgi-marker peripheral trans-Golgi membrane protein (p230), whereas Cab45-5pXE showed strong accumulation of vesicular structures in close proximity to the TGN (Fig. 4 C). The number of Cab45 vesicles per cell in cells expressing Cab45-WT, Cab-5pXA, and Cab45-5pXE were quantified from z-stack images (d = 0.35 μm; Fig. 4 D). Overall, cells expressing Cab45-5pXE showed a significantly higher number
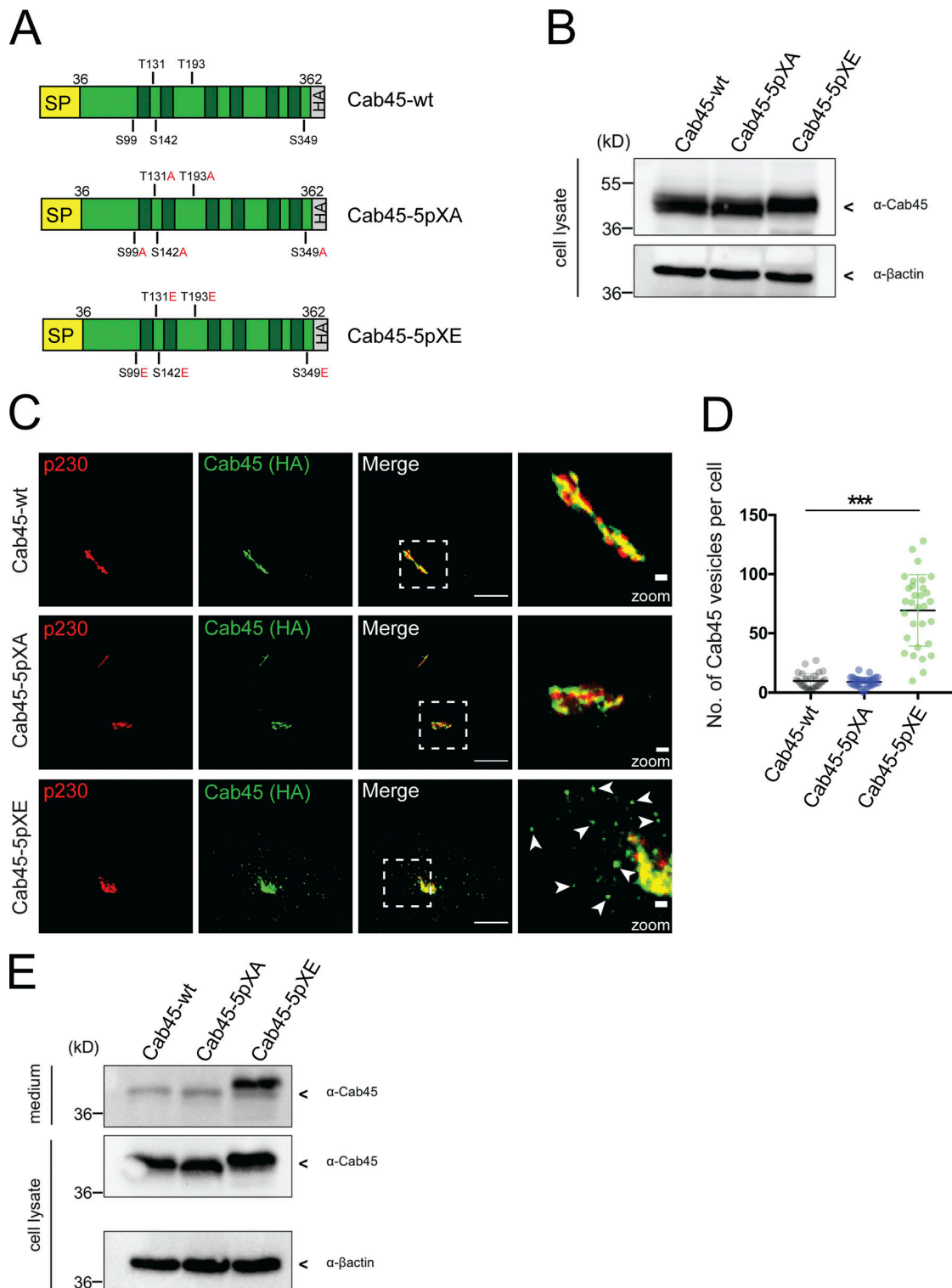
Figure 4. **Phospho-mimicking Cab45 localizes in post-Golgi vesicles. (A)** Schemes of WT and phosphomutant Cab45-HA constructs with signal peptide (SP). Identified phosphorylation sites (serine [S] and threonine [T]) were replaced by alanine (A) or glutamic acid (E). The constructs were stably transduced in Cab45-KO cells. **(B)** Western blot shows Cab45 expression levels of stable Cab45-WT and phosphomutant cell lines. β-Actin was used as a loading control. **(C)** Steady-state localization of Cab45-WT, Cab45-5pXA, and Cab45-5pXE was analyzed by immunofluorescence microscopy. Stable cell lines were stained with α-p230 and α-HA antibody (Cab45). Scale bars, 10 μm. Higher magnification (insets) show Golgi (scale bars, 1 μm). **(D)** The numbers of Cab45 vesicles (C) were quantified by analyzing z-stack images (d = 0.35 μm), n > 30 cells. A scatter dot plot represents mean ± SD of counted vesicles per cell. Statistical test, Kruskal–Wallis. **(E)** The post-Golgi origin of Cab45 vesicles was confirmed by Western blotting after performing a 20°C block in stable cell lines. β-Actin was used as loading control. ***, P < 0.001.

of Cab45 vesicles (69 ± 30 per cell) than cells expressing Cab45-WT (10 ± 6 vesicles per cell) and Cab45-5pXA (9 ± 4 vesicles per cell). We analyzed the origin of these vesicles by performing a block at 20°C for 2 h to inhibit protein export from the TGN. Analyses of the cell culture supernatants with SDS-PAGE and Western blotting detected Cab45-5pXE but almost no Cab45-WT or Cab45-5pXA (Fig. 4 E). In addition, we revealed no co-localization with a Sec16A marker (ER exit sites, Fig. S2 A). These results suggest that Cab45-5pXE vesicles are post-Golgi vesicles that have already left the TGN.

In a recent study, we used circular dichroism (CD) spectroscopy to examine Cab45, showing it to be rather unstructured but changing to a more α-helical secondary structure upon addition of Ca^{2+} (Deng et al., 2018). Adding EDTA reversed this effect completely. In the present study, we subjected recombinant Cab45-WT, Cab45-5pXA, and Cab45-5pXE to CD spectroscopy (Fig. S2 B). This showed no difference in secondary structure between Cab45-WT and the phosphomutants, either in the untreated protein sample or after adding Ca^{2+} and EDTA. Also, cargo binding was not changed in Cab45 phosphomutants, since we additionally performed coimmunoprecipitations to validate LyzC cargo binding of the Cab45 mutants (Fig. S2, C and D).

Together, these findings indicated that mimicking Cab45 phosphorylation accelerated export of Cab45 and promoted its occurrence in TGN-derived vesicles.

Mimicking Cab45 phosphorylation drives client secretion

Next, we investigated whether LyzC export was influenced by the phosphorylation status of Cab45 by using the RUSH system in cells expressing Cab45-WT, Cab45-5pXA, or Cab45-5pXE. Fig. S3 A shows representative images of cells at different time points after biotin addition. Quantification of the number of LyzC vesicles (Fig. 5 A) showed a significant reduction in the number of vesicles per cell, 40 min after biotin addition, in Cab45-5pXA cells (16 ± 11) compared with Cab45-WT (31 ± 14) and Cab45-5pXE cells (39 ± 19). The same phenotype was also observed 60 min after biotin addition (Cab45-WT: 39 ± 18 vesicles per cell; Cab45-5pXA: 28 ± 14 vesicles per cell; Cab45-5pXE: 55 ± 33 vesicles per cell). Overall, Cab45-5pXE showed significantly more LyzC vesicles than Cab45-5pXA at 40 and 60 min after biotin addition.

Furthermore, we correlated the number of vesicles with the actual secreted amount of protein. To this end, we examined protein secretion from these cells by Western blotting (Fig. 5 B). Consistent with the results of the RUSH assay, LyzC secretion quantified by densitometric analysis was lower in Cab45-5pXA cells (57%) than in cells expressing Cab45-5pXE (150%) and Cab45-WT (100%; Fig. 5 C).

We continued by performing rescue experiments in Fam20C-KO cells transfected with LyzC and cotransfected Cab45-WT, Cab45-5pXA, or Cab45-5pXE, respectively (Fig. 5, D and E). By doing so, we tested the impact of the phosphomutants on the secretion of LyzC in the absence of Fam20C and, accordingly, their ability to compensate for the loss of the kinase. Strikingly, only Fam20C-KO cells rescued with Cab45-5pXE showed significantly higher LyzC secretion, which indicates that the

phosphomimetic mutant is capable of compensating the loss of kinase activity in living cells.

In previous publications, we showed that Cab45-WT was packed together with LyzC in SM-rich vesicles (Deng et al., 2018). To address whether Cab45 phosphorylation changes sorting integrity into SM-rich vesicles, cell lines expressing the three Cab45 variants were cotransfected with LyzC-mCherry and EQ-SM-oxGFP and evaluated using time-lapse recordings. The LyzC vesicles per cell were counted, and colocalization with EQ-SM-oxGFP was examined (Fig. 5 F). Notably, the highest number of colocalizing vesicles per cell was monitored in cells expressing Cab45-5pXE (c, 16 ± 9) compared with Cab45-WT (a, 11 ± 6) and Cab45-5pXA (b, 8 ± 3). Of 104 LyzC vesicles observed in Cab45-WT cells, 91 were positive for EQ-SM-oxGFP (86% ± 10%). Similar ratios were determined for Cab45-5pXA cells (64 out of 71 vesicles; 91% ± 9%) and Cab45-5pXE cells (133 out of 158 vesicles; 84% ± 5%).

Using the same experimental setup, we also tested the co-localization of Cab45 and LyzC in transiently transfected HeLa cells. As expected, all three Cab45 proteins colocalized with LyzC-mCherry (Fig. S3 B). Based on these data, phosphorylation seems to promote secretion in general but does not influence sorting into correct vesicles.

To ensure that the phosphorylations particularly influence the sorting of Cab45 clients, two control proteins were tested, the bulk flow cargo OPN and the lysosomal hydrolase cathepsin D (CatD). OPN is a secreted protein and also phosphorylated by Fam20C (Tagliabracci et al., 2012). In contrast, CatD, a non-secretory (Fig. S4 A), lysosomal cargo (Fig. S4 B), is sorted via sortilin into clathrin-coated vesicles (Braulke and Bonifacino, 2009) and is therefore not dependent on the SPCA1/Cab45 sorting machinery (Crevenna et al., 2016; Deng et al., 2018). In summary, no differences in the formation of OPN-SBP-EGFP vesicles were observed by using the RUSH approach (Fig. 5 G and Fig. S4 C). Additionally, we verified the unaffected sorting of CatD in the Cab45 phosphomutant cell lines (Fig. S4, D and E) by the same method.

These data show that Cab45 phosphorylation modulates the rate of budding of secretory vesicles containing its specific clients.

Phosphorylation of Cab45 accelerates vesicle budding at the TGN

Given the finding that Cab45 sorting into SM-rich vesicles appeared not to be affected in the phosphomutant cells, we investigated the role of SM in this process. SM is synthesized by two isoforms of SM synthase (SMS) in the luminal leaflets of Golgi membranes (Barenholz and Thompson, 1980). We therefore depleted SMS1 and SMS2 in Cab45-5pXE cells with siRNA and analyzed z-stack images (d = 0.35 µm) to quantify the numbers of Cab45-5pXE vesicles stained with α-HA antibody (Fig. 6 A). We observed a significant decrease in the number of Cab45-5pXE vesicles in cells treated with siSMS1/2 siRNA (19 ± 13 vesicles per cell) compared with cells transfected with control siRNA (40 ± 20 vesicles per cell). From this, we concluded that SM is important for the TGN export of Cab45-5pXE.

To investigate if the phosphorylation status of Cab45 also influences the export and formation of SM-containing vesicles,
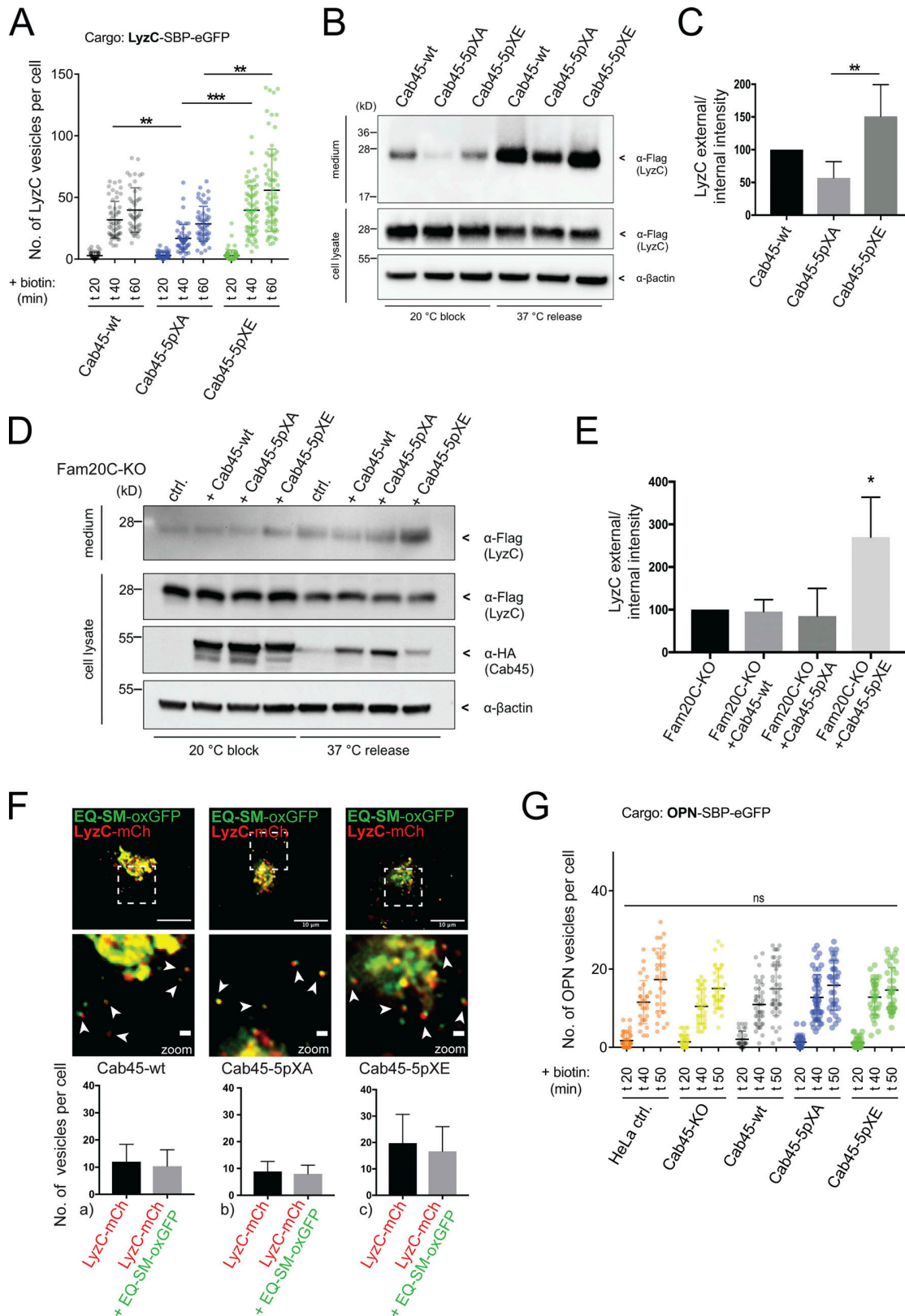
Figure 5. **Fam20C-dependent Cab45 phosphorylation drives client sorting and secretion. (A)** LyzC vesicle formation was quantified from LyzC-RUSH experiments by analyzing z-stack images (d = 0.35 μm). Cell lines were fixed at 0, 20, 40, and 60 min after biotin addition. A scatter dot plot represents the means ± SD of at least three independent experiments (*n* > 45 cells per condition). Statistical test, Kruskal–Wallis. **(B)** Western blot analysis of the secretion of LyzC-Flag in Cab45-WT and phosphomutant cells after 20°C block and 37°C release. β-Actin was used as loading control. **(C)** Western blots of four

independent experiments (B) were quantified by densitometry using ImageJ. The bar graph represents the means (± SD) of densitometric values of external LyzC-Flag, normalized to the internal levels in percentage. Statistical test, Kruskal–Wallis. **(D)** Western blot analysis of the secretion of LyzC-Flag in Fam20C-KO cells rescued with Cab45 and phosphomutants after 20°C block and 37°C release. β-Actin was used as loading control. **(E)** Western blots of three independent experiments (D) were quantified by densitometry using ImageJ. The bar graph represents the means ± SD of densitometric values of external LyzC-Flag, normalized to the internal levels in percentage. Statistical test, ordinary one-way ANOVA. **(F)** Sorting of LyzC in EQ-SM-vesicles was controlled by performing live-cell experiments acquiring time-lapse movies. Example micrographs depict the Golgi of Cab45-WT and phosphomutants that expressed LyzC-mCherry and EQ-SM-oxGFP. Scale bars, 10 μm; magnification scale bars, 1 μm. Arrowheads indicate secretory vesicles containing both fluorescence proteins. The means ± SD of post-Golgi LyzC vesicles per cell positive for EQ-SM were quantified (n = 8 cells per condition). **(G)** OPN vesicle formation was quantified from OPN-RUSH experiments by analyzing z-stack images (d = 0.35 μm). Cell lines were fixed at 0, 20, 40, and 50 min after biotin addition. A scatter dot plot represents the means ± SD of at least three independent experiments (n > 28 cells per condition). Statistical test, Kruskal–Wallis. *, $P < 0.05$; **, $P < 0.01$; ***, $P < 0.001$.

we transfected Cab45-WT and the phosphomutant cell lines with EQ-SM-oxGFP and performed a 20°C incubation block for 1 h followed by a release at 37°C for 1 h. An analysis of z-stack images detected significantly more EQ-SM-oxGFP vesicles in the cells expressing Cab45-5pXE (15 ± 5 vesicles per cell) than in those expressing Cab45-5pXA (10 ± 5 vesicles per cell; Fig. 6 B). We therefore conclude that mimicking the negative charges of Cab45 phosphorylation results in its increased TGN export. Next, we analyzed Cab45 vesicular budding using a semi-intact budding assay. Cab45-WT and phosphomutant cell lines were permeabilized with digitonin and incubated with an ATP regeneration system at 32°C to generate TGN-derived vesicles (Wakana et al., 2012; Deng et al., 2018). Vesicular fractions were collected by ultracentrifugation and analyzed by SDS-PAGE and Western blotting (Fig. 6 C). Beforehand, we validated budding of endogenous and overexpressed Cab45 in dependency of ATP and rat liver cytosol (Fig. S5 A). Similar to what was published in Deng et al. (2018), we could not promote budding of Cab45 with rat liver cytosol. Therefore, we performed our budding assays in the absence of rat liver cytosol.

Consistent with the results demonstrated in Fig. 4, C–E, we detected significantly more Cab45 in the vesicular fraction of cells expressing Cab45-5pXE than in cells expressing Cab45-5pXA (Fig. 6, C and D). Western blots against calnexin (CNX) were used as a control to show that samples were not contaminated with whole-cell lysate.

We followed the dependence of the Cab45 TGN export on the Fam20C activity (Fig. 6 E). Fam20C-KO cells that stably reexpressed Fam20C-WT or Fam20C-D478A were transfected with the RUSH construct SBP-tagRFP-Cab45 and fixed at specific time points. In the absence of biotin, Cab45 localized in the ER, whereas at 0–30 min after biotin addition, it was simultaneously transported to the Golgi in both cell lines (Fig. S5 B). When Cab45 was packaged into TGN-derived vesicles, at 40 min after biotin addition, there were significantly more Cab45 vesicles detectable in the cells reexpressing Fam20C-WT (26 ± 15 vesicles per cell) than in those expressing the kinase-dead variant (15 ± 9 vesicles per cell). In line with the LyzC-RUSH (Fig. S1 C), we performed costainings to exclude colocalization of Cab45 vesicles with endosomal/lysosomal compartments (Fig. S5 C).

Finally, we analyzed the vesicle budding of endogenous Cab45 (Fig. 6 F). Fam20C-KO cell lines were transfected with Fam20C-WT or Fam20C-D478A constructs, permeabilized, and incubated with an ATP regeneration system at 32°C. Consistent with the results of the Cab45-RUSH assay, this showed a significantly higher amount of endogenous Cab45 in the vesicular fraction of the cells transfected with Fam20C-WT compared with the cells transfected with Fam20C-D478A (Fig. 6 G). It was possible to detect both Fam20C variants (WT and D478) in the same vesicular fraction, but not CNX.

## Mutations of Cab45 phosphosites influence Cab45 oligomerization

Cab45 oligomerizes in a Ca^{2+}-dependent manner in vitro (Crevenna et al., 2016; Deng et al., 2018). To test the impact of phosphorylation on oligomerization, we investigated oligomerization behavior of the phosphomutant proteins using a confocal microscopy–based oligomerization assay (Fig. 7 A). For visualization, we purified GFP-Cab45-WT and GFP-phosphomutants. Whereas in the absence of Ca^{2+}, no Cab45 oligomers were observed (Fig. 7 A), we clearly could detect oligomer formation of all recombinant Cab45-variants after incubation with 2 mM Ca^{2+}. This effect was reversible by adding 2 mM EDTA.

Furthermore, we subdivided the observed particles into four groups: very small (3–5 pixel units), small (5–11 pixel units), medium (11–20 pixel units), and large oligomers (>20 pixel units; Fig. 7 B). Interestingly, very small oligomers were mainly formed by Cab45-WT and Cab45-5pXE (47% and 57% of all analyzed oligomers), whereas the major fraction of Cab45-5pXA had a pixel size of 5–11 units (37%). In general, among larger particles (>11 pixel units), Cab45-5pXA oligomers showed the highest proportion.

In addition, we determined the intensities of counted oligomers by measuring the pixel with the highest intensity within each particle. On average, we could detect significant higher intensity levels in oligomers formed by Cab45-5pXA, followed by Cab45-WT and Cab45-5pXE (Fig. 7 C). The same datasets were also used to display the distribution of oligomers according to their intensity values (Fig. 7 D). Strikingly, the highest number of oligomers of Cab45-WT (55%) and Cab45-5pXE (76%) showed low intensity (maximum <500 a.u.); in contrast, most Cab45-5pXA oligomers (38%) reached maximum intensity values between 500 and 1,000 a.u. Also among higher intensity levels (maximum >1,000 a.u.), oligomers formed by Cab45-5pXA made up the greatest fraction.

Overall, our data suggest that upon incubation with 2 mM of Ca^{2+}, the Cab45-5pXA mutant forms mainly larger oligomeric structures with higher intensities compared with oligomers formed by Cab45-WT and Cab45-5pXE. These findings indicate a
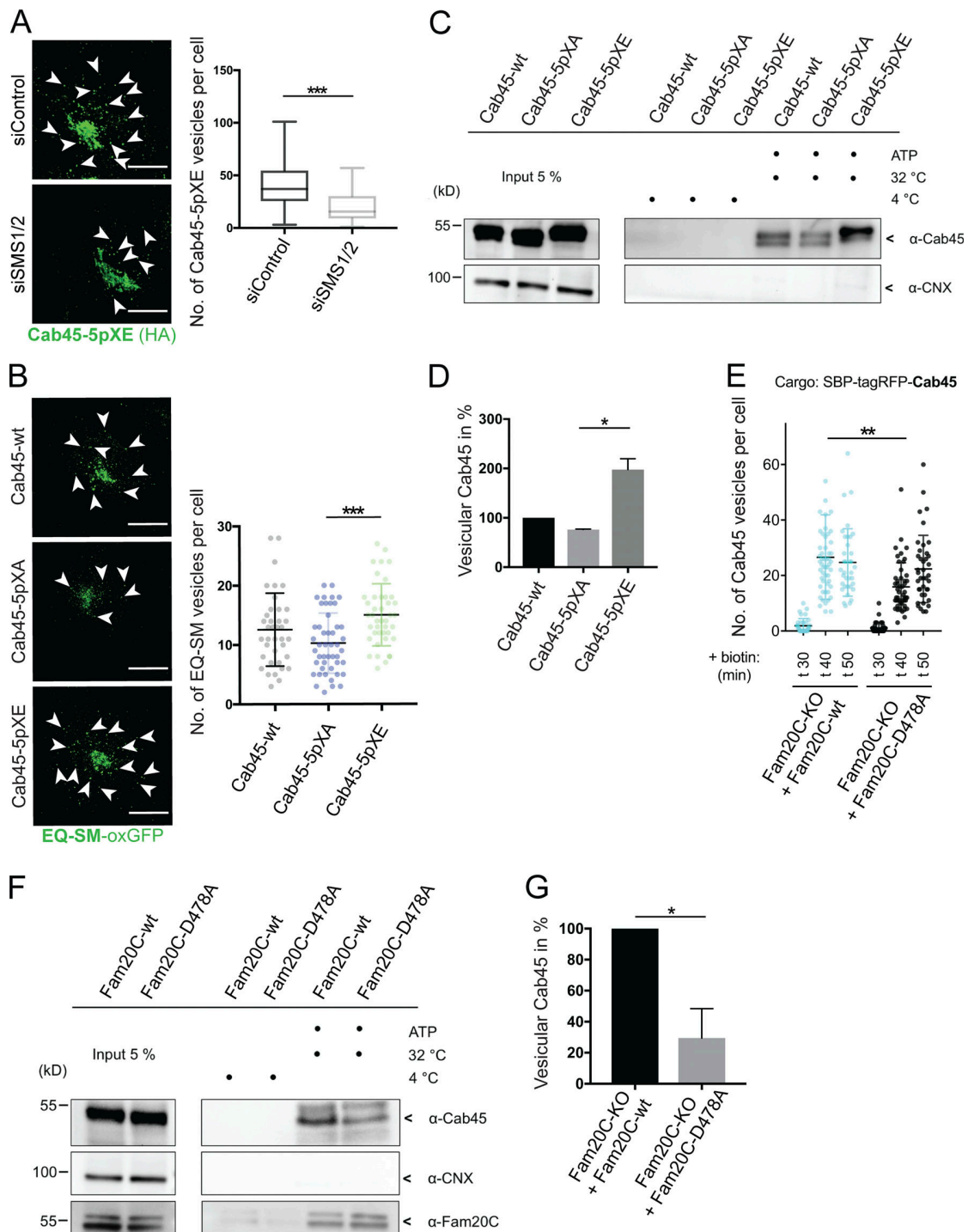
Figure 6. **Mimicking Cab45 phosphorylation results in accelerated TGN export. (A)** Representative immunofluorescence pictures of cells that stably expressed Cab45-5pXE, treated with control or SMS1/2 siRNA. Cells were stained against Cab45 (α-HA), and numbers of vesicles were quantified from z-stack images (d = 0.35 μm). Arrowheads indicate post-Golgi vesicles. Scale bars, 10 μm. Box and whiskers blot represents means with minimum to maximum values of at least three independent experiments (n > 57 cells per condition). Statistical test, Mann–Whitney. **(B)** Example micrographs of Cab45-WT and phosphomutant cell lines transfected with EQ-SM-oxGFP, after 20°C block and 37°C release. EQ-SM-oxGFP vesicles were quantified from z-stack images (d = 0.35 μm). Scale bars, 10 μm. A scatter dot plot represents means ± SD of at least three independent experiments (n > 37 cells per condition). Statistical test, Kruskal–Wallis. **(C)** Vesicular budding assay of Cab45 phosphomutants. TGN vesicle budding was initiated by an ATP regeneration system. Released vesicles were analyzed by Western blotting for Cab45 and CNX. **(D)** Western blots of three independent experiments (C) were quantified by densitometry with ImageJ. The bar graph represents the means ± SD of densitometric values of vesicular Cab45 in percentage. Statistical test, Kruskal–Wallis. **(E)** Cab45 vesicle formation was quantified from Cab45-RUSH experiments by analyzing z-stack images (d = 0.35 μm). Fam20C-KO cells expressing Fam20C-WT or Fam20C-D478A were fixed at 0, 30, 40, and 50 min after biotin addition. A scatter dot plot represents the means ± SD of at least three independent experiments (n > 35

cells per condition). Statistical test, Kruskal–Wallis. **(F)** Vesicular budding assay of endogenous Cab45. TGN vesicle budding was initiated by an ATP regeneration system in Fam20C-KO cells, which were transfected with Fam20C-WT and D478. Released vesicles were analyzed by Western blotting for Cab45, Fam20C (HA), and CNX. **(G)** Western blots of four independent experiments (F) were quantified by densitometry with ImageJ. The bar graph represents the means ± SD of densitometric values of vesicular Cab45 in percentage. Statistical test, Welch's unpaired t test. *, $P < 0.05$; **, $P < 0.01$; ***, $P < 0.001$.

potential oligomerization-prone behavior of the phosphorylation-deficient mutant.

Discussion

In this study, we demonstrate that Fam20C has a significant impact on protein sorting and secretion, specifically of Cab45 clients (Crevenna et al., 2016; Deng et al., 2018), by phosphorylating the sorting protein Cab45 on five distinct residues (S99, T131, S142, T193, and S349). Phosphorylation of Cab45 facilitates its exit from the TGN by reducing the size of the Cab45 oligomers, whereas Ca^{2+}-binding seems to be unaffected. Hence, phosphorylation of Cab45 enhances the sorting and secretion of its client LyzC, without impairing the cargo binding. For the first time, we propose a sorting event of soluble secreted proteins, mediated by a TGN luminal protein complex, which is regulated by phosphorylation.

Cab45 is a Ca^{2+}-binding protein with six EF-hand domains that localizes in the lumen of the Golgi apparatus (Blank and von Blume, 2017; von Blume and Hausser, 2019; von Blume et al., 2012; Crevenna et al., 2016; Pakdel and von Blume, 2018). In the presence of Ca^{2+} that has been locally pumped into the TGN by the Ca^{2+} ATPase SPCA1, Cab45 oligomerizes and sorts cargos (von Blume et al., 2012; Kienzle et al., 2014; Crevenna et al., 2016). This oligomerization process is required for packaging Cab45 clients into SM-rich transport vesicles at the TGN (Deng et al., 2018).

In search of other regulatory factors that contribute to the sorting of clients, we detected phosphorylation of Cab45 via Golgi kinase Fam20C. By mimicking the negative charges of the phosphorylation, Cab45-5pXE translocated in accumulated vesicles around the Golgi. A similar vesicular phenotype was observed before for Cab45-6EQ, a Ca^{2+}-binding-deficient mutant of Cab45, that is no longer able to form large oligomeric structures. Cab45-6EQ is highly secreted and was shown to mis-sort LyzC (von Blume et al., 2012; Crevenna et al., 2016, Deng et al., 2018). In contrast, we demonstrate the correct sorting of LyzC into SM-rich vesicles in cells expressing the phosphomutants Cab45-5pXA (phosphorylation-deficient) or Cab45-5pXE (Fig. 5 F). Strikingly, in vitro analyses of these phosphomutant proteins uncovered that preventing its phosphorylation results in an increased oligomerization potential of Cab45 (Fig. 7). Since none of the predicted phosphorylation sites target EF-hand domains, we presume that Ca^{2+} binding is not disturbed upon Cab45 phosphorylation. Additionally, CD data presented in Fig. S2 B support this hypothesis, as protein folding and therefore the overall ability to bind Ca^{2+} does not seem to be affected. Noteworthy, the recombinant WT protein behaves in a similar way as the phospho-mimicking mutant Cab45-5pXE in the oligomerization assay, which might indicate that the protein purified from HEK293 cells also has phosphorylated sites. This

behavior is also supported by experiments performed in cells (Fig. 5, A–C; and Fig. 6 B) where significant differences are more dominant between Cab45-5pXE and Cab45-5pXA, whereas the Cab45-WT phenotype is more similar to the Cab45-5pXE phenotype. In contrast, preventing phosphorylation of Cab45-WT by using transfected Fam20C-KO cells phenocopies the secretion phenotype of Cab45-5pXA (Fig. 5, D and E). This observation supports the idea that Cab45 is already phosphorylated under physiological conditions in the Golgi.

Is the localization of Cab45 also influenced by its oligomerization potential?

The oligomerization of Cab45 is a Ca^{2+}-dependent process and can be dissolved upon the incubation of recombinant protein with Ca^{2+} chelators like EGTA (Crevenna et al., 2016). Interestingly, endogenous Golgi-localized Cab45 was secreted in higher amounts when cells were treated with the Ca^{2+} ionophore A23187 (von Blume et al., 2012), indicating the requirement of Ca^{2+} for its retention in the TGN. Similar behavior was also suggested earlier for ER-located Ca^{2+}-binding proteins (e.g., reticuloplasmins) that are released from the ER when cells are treated with Ca^{2+} ionophores (Booth and Koch, 1989). The authors further suggest that perturbation of Ca^{2+} directly influences the retention of the proteins. So far, Cab45 was thought to reside in the Golgi (Scherer et al., 1996); however, not much is known about the retention mechanisms of Golgi-resident proteins, especially of soluble proteins. Nucleobindin 1, another soluble protein, has (similar to Cab45) two EF-hand domains and localizes mostly in the cis-Golgi before it is partly secreted (Miura et al., 1994; Lin et al., 1998, 1999). Interestingly, Nucleobindin 1 is a known Fam20C substrate (Tagliabracci et al., 2015), but how the protein regulates its localization and if it is able to oligomerize is not established. Since our data show that Cab45 localizes in the TGN but also goes together with its clients into SM-rich vesicles (Deng et al., 2018), we assume that the release of Cab45 into secretory vesicles is essential for the sorting. We therefore state that phosphorylation of Cab45 fine-tunes the size of the oligomers, which drives the export of the protein from the TGN in the following way (Fig. 8). Upon Ca^{2+} influx into the TGN by SPCA1, Cab45 oligomerizes, binds secretory clients, and segregates them away from the bulk of proteins (A). As a consequence, Cab45 forms large oligomeric structures, which are too big to be packaged into secretory vesicles and so are retained together with the clients in the TGN (B). This size according retention was hypothesized earlier for Golgi-resident transmembrane proteins that aggregate and so are excluded from transport vesicles (Nilsson et al., 1993). As a way to actively regulate the secretion of cargo molecules, we propose that Fam20C phosphorylates Cab45, which causes disassembly of the Cab45 multimers (C). This was also investigated for other proteins, such as Sae2, a protein involved in
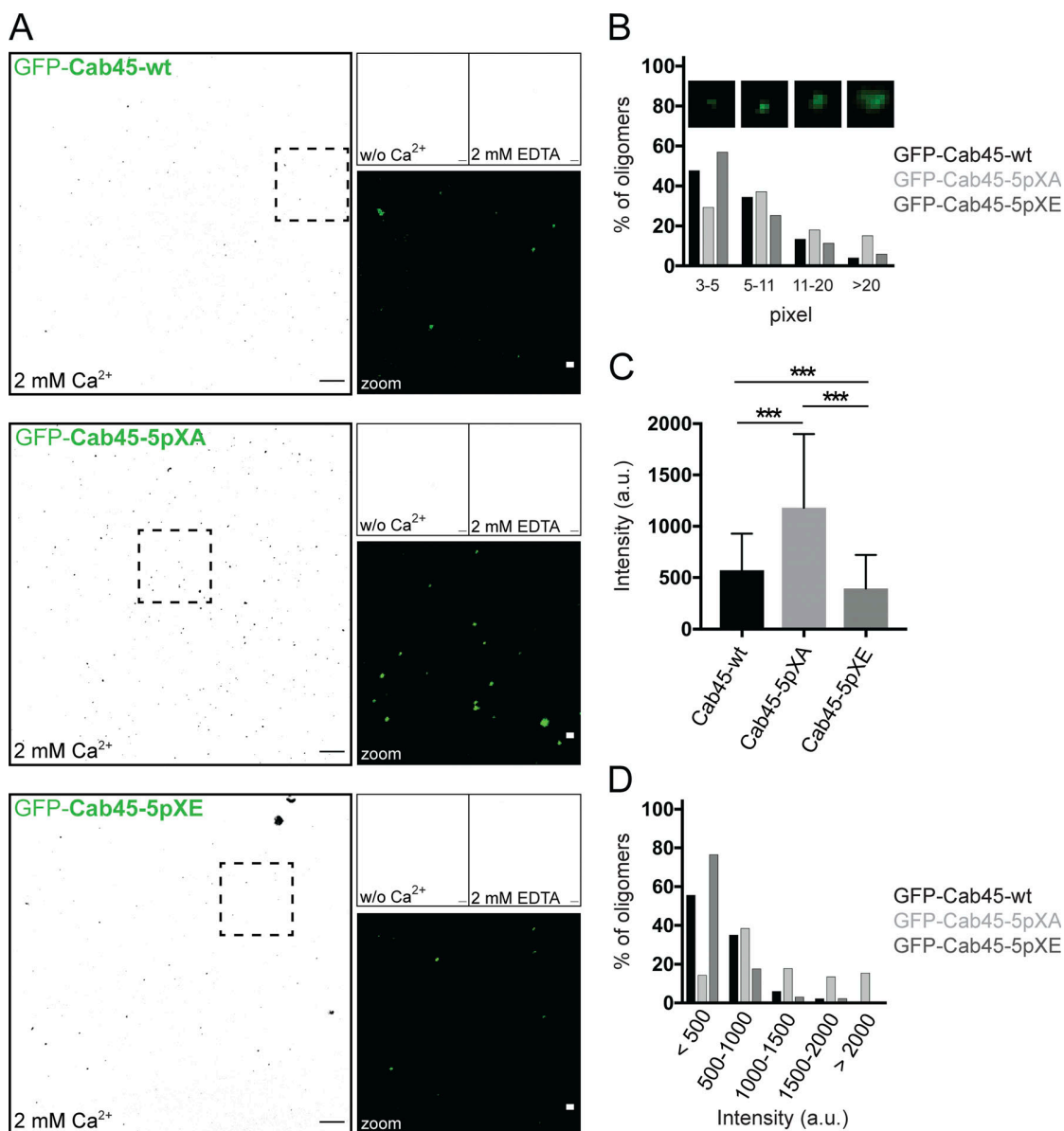
Figure 7. Mutations of Cab45 phosphosites influence Cab45 oligomerization. (A) In vitro oligomerization assay analyzed by confocal microscopy. Representative fluorescence pictures (black and white conversion) of recombinant GFP-Cab45WT and phosphomutants incubated without (w/o) Ca^{2+}, together with 2 mM Ca^{2+} or after additional treatment with 2 mM EDTA. Scale bars, 10 μm. Insets display higher magnification of recombinant proteins treated with 2 mM Ca^{2+} in original colors (scale bars, 1 μm). **(B)** Distribution of Cab45 oligomers (2 mM Ca^{2+}) according to their particle size in percentage. Insets show examples of oligomers with pixel units of 3–5, 5–11, 11-20, and >20. Data were collected from two independent experiments ($n > 268$ oligomers per condition) using ImageJ. **(C)** Average intensity values of oligomers formed by Cab45-WT and phosphomutants, incubated with 2 mM Ca^{2+}. For analysis, individual background intensities were subtracted, and the pixel with the highest intensity value within the oligomer was measured using ImageJ. Data were collected from two independent experiments ($n > 124$ oligomers per condition). Statistical test, Kruskal–Wallis. **(D)** Distribution of Cab45 oligomers according to their intensity values in percentage. Oligomers analyzed in C were grouped based on their intensities (<500 a.u., 500–1,000 a.u., 1,000–1,500 a.u., 1,500–2,000 a.u., and >2,000 a.u.). ***, $P < 0.001$.

double-strand break repair (Fu et al., 2014). Sae2 disassembles into active monomers in a stepwise manner upon phosphorylation, which in addition enhances Sae2's solubility. Similarly, phosphorylation of the heat shock protein αB-crystallin reduces the size of oligomers (Ito et al., 2001). We furthermore assume that oligomer dissociation decreases the retention of Cab45 within the TGN. In support of this idea, we found more

phosphorylation-mimicking Cab45 in vesicular fractions by performing semi-intact budding and RUSH assays (Fig. 6, C–G). Consequently, cargo that is bound to Cab45 is packed along with disassembled multimers into SM-rich vesicles for further transport. In this regard, secretion of LyzC was significantly reduced in Fam20C-KO cells (Fig. 1, B and C), even though LyzC itself is not phosphorylated by Fam20C (Fig. 3 B; and Fig. 5, D
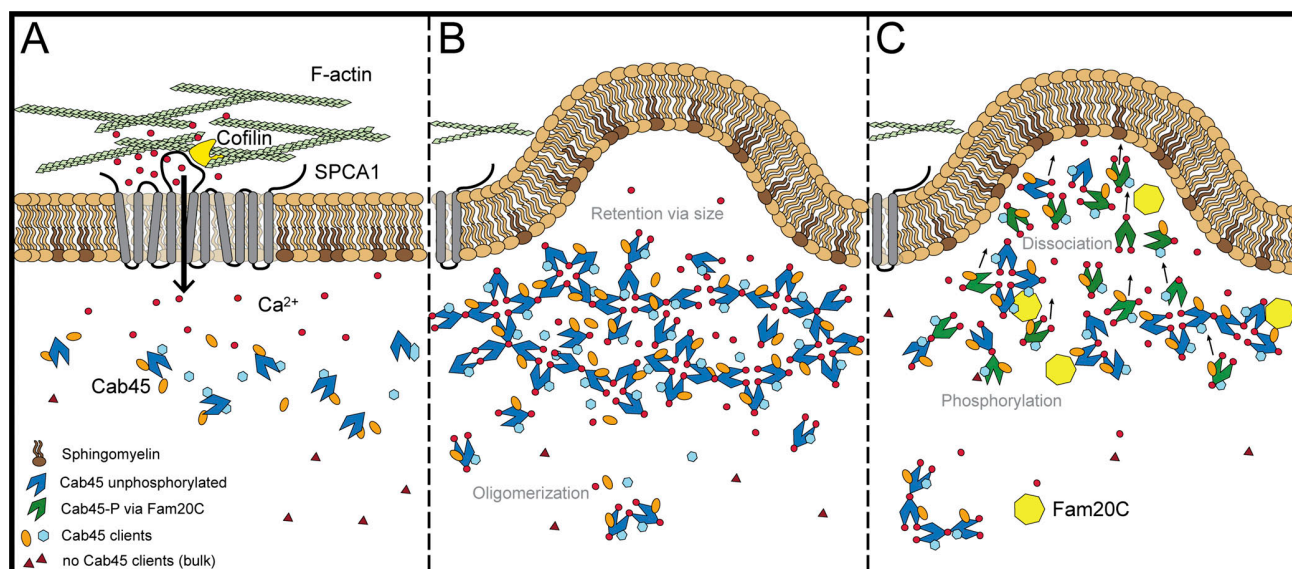
Figure 8. **Fam20C phosphorylates Cab45 and regulates client secretion by oligomer disassembly**. The model depicts the newly investigated role of Fam20C in Cab45 client sorting. A subset of soluble secretory proteins is sorted via the SPCA1/Cab45 sorting machinery. **(A)** SPCA1 interacts with cofilin1 on its cytosolic interface, recruits F-actin and promotes Ca^{2+} influx into the lumen of the TGN. **(B)** In the presence of Ca^{2+}, Cab45 binds secretory clients and forms large oligomeric structures, which are, because of their size, excluded from packaging into vesicles. **(C)** Fam20C phosphorylates Cab45 on specific residues, whereby Cab45 multimers disassemble and TGN retention is abolished. This allows clients together with Cab45 to be packed into SM-rich vesicles.

and E). Defects in LyzC secretion are phenocopied in Cab45-KO cells (Crevenna et al., 2016), further emphasizing the importance of Fam20C in Cab45-mediated cargo sorting. Since phosphorylation and dissociation of oligomers are occurring close to "TGN exit sites" (Fig. 2 C), this would in addition explain why Fam20C and Cab45 bud together in the same SM-rich vesicles. Overall, this process enables Fam20C to regulate the exact time point of cargo release by modifying Cab45, but it could also trigger its own secretion.

However, internal or external stimuli that are necessary to initiate Cab45 phosphorylation and control this process require further investigations. It is noteworthy that SPCA1 pumps Mn^{2+} along with Ca^{2+} into the Golgi, and Mn^{2+} was shown to be a crucial cofactor for Fam20C activity (Tagliabracci et al., 2012). This fact might explain how both processes, Ca^{2+}-binding and phosphorylation, are coordinated on time. Another question that has to be addressed is how the budding of SM-rich vesicles is regulated. Similar to Cab45, glycophosphatidylinositol-anchored proteins do not contain cytosolic tails to interact with coat components (Mayor and Riezman, 2004). In HeLa cells, these proteins are also sorted into SM-rich vesicles at the TGN (Deng et al., 2016). It is assumed that upon oligomerization of glycophosphatidylinositol-anchored proteins, tightly packed lipid platforms are combined that facilitate its sorting to the apical plasma membrane (Paladino et al., 2004). Potentially, Cab45 binds to transmembrane proteins or lipid components, whereas oligomerization creates similarly "SM-rich sorting domains." The Cab45–client complex might in addition have curvature-active properties analogous to the endocytosis of toxins such as Shiga toxin, which favors and stabilizes vesicle formation (Cummings et al., 1998; Johannes and Römer, 2010; Pezeshkian et al., 2017; Römer et al., 2007). Subsequently, the

dissociation of large oligomeric complexes upon Cab45 phosphorylation might promote its internalization into SM-rich vesicles. However, further investigations are necessary to elucidate this. So far, no interaction between Cab45 and transmembrane proteins or lipids has been described. From our semi-intact budding assays, we assume that budding may not require a cytosolic coat, such as clathrin.

In summary, we were able to demonstrate that phosphorylation of Cab45 by Fam20C regulates Cab45 retention within the TGN by changing its oligomerization potential and thus enhances secretion of Cab45 clients. As phosphorylation is a fast and controllable modification, the predicted mechanism not only contributes to the overall sorting capacity of the cell but also allows cells to dynamically adjust secretion to environmental changes. These results provide unique mechanistic insight into how secreted proteins are exported from the TGN, which is essential for the understanding of cellular homeostasis and communication.

Materials and methods
Cloning and constructs
All clonings were conducted using Phusion High-Fidelity Polymerase and T4 ligase (Thermo Fisher Scientific) according to the manufacturer's advice. Sequences of all plasmids were verified using the SmartSeq Kit from Eurofins Genomics or KECK sequencing (Yale University). All restriction enzymes were purchased from NEB and also used as recommended.

The cloning of the pLPCX-Cab45 constructs was previously described (Crevenna et al., 2016). Using site-directed mutagenesis, point mutations were introduced to generate missense mutations substituting five phosphorylation sites (S99, T131,

S142, T193, and S349) of Cab45 to alanine (A) or glutamic acid (E). The resulting constructs were named pLPCX-Cab45-5pXA (for alanine substitutions) and pLPCX-Cab45-5pXE (for glutamic acid substitutions). All three constructs contained a C-terminal HA tag.

For protein purification from mammalian HEK293 cells, Cab45-WT, Cab45-5pXA, and Cab45-5pXE were inserted into the piggyBac system as described previously (Li et al., 2013). The used piggyBac backbone vector (PB-T-PAF) and also PB-RN and PBase were a gift of James Rini, University of Toronto, Ontario, Canada (Li et al., 2013).

To generate a PB-T-PAF-His-SUMO-Cab45 construct, Gibson assembly with two fragments was used. The first fragment containing a SS-His-SUMO tag was amplified from the pI-sec-SUMOstar-Cab45 construct as described previously (Crevenna et al., 2016). The second fragment containing Cab45 or the phosphorylation mutants was amplified from the corresponding pLPCX constructs described above. The PB-T-PAF vector was linearized with NheI and NotI-HF restriction enzymes.

PB-T-PAF-GFP-Cab45 variants were cloned in a similar way. PB-T-PAF was linearized with NheI and NotI-HF restriction enzymes. Insert was integrated using three-fragment Gibson Assembly. Fragment 1 (SS-His-tag) and fragment 3 (Cab45-WT/variants) were amplified from PB-T-PAF-His-SUMO-Cab45 constructs above. Superfolder GFP (fragment 2) was amplified from sfGFP-N1 (Addgene; #54737). All fragments contained proper overlaps for Gibson Assembly approach.

For live-cell microscopy, pLPCX-Cab45 constructs were fused with EGFP. The cloning strategy of the EGFP-Cab45 construct was described before (Deng et al., 2018). For a one-fragment Gibson assembly, this vector was linearized with EcoRI-HF and NotI-HF. The Cab45 5pXA or 5pXE inserts were amplified with suitable overhangs from the corresponding pLPCX constructs described above.

Full-length Fam20C was amplified from a pCMV-Sports6 vector obtained from Vincent Tagliabracci's laboratory (UT Southwestern Medical Center, Dallas, TX) by PCR. This fragment was inserted with EcoRI/BglII restrictions sites into the pLPCX empty vector (Addgene). To generate an inactive kinase as a control, D478 was mutated to alanine by site-directed mutagenesis. For easy Western blot, an HA tag was attached at the C-terminus of Fam20C.

Cloning of pLPCX-LyzC-mCherry was previously described (Deng et al., 2018). For the mCherry-Fam20C fusion construct, three-fragment Gibson assembly was used. Fragment 1 (forward and reverse sequence) includes the signal peptide with overhangs to pLPCX vector and mCherry (fragment 2) and was directly ordered from IDT. mCherry was amplified from pLPCX-LyzC-mCherry (see above). Fam20C (fragment 3) was amplified from the full-length pLPCX plasmid described above. For this purpose, the backbone was linearized with the restriction enzymes BamHI-HF and NotI-HF.

The pIRESneo3-Str-SBP-EGFP vector was a gift from Franck Perez, Institut Curie Centre de Recherche, Paris, France (Addgene; plasmid #65264). The other RUSH constructs pIRESneo3-Str-KDEL-SBP-EGFP-CatD and pIRESneo3_Str-LyzC-KDEL-SBP-EGFP were published previously (Deng et al., 2018). Cab45 RUSH

construct pIRESneo3-Str-SBP-tagRFP-Cab45 was generated via two-fragment Gibson approach. Creating overlapping parts, Fragment 1 (SS-SBP) was amplified from CatD-RUSH construct (see Deng et al., 2018); tagRFP-Cab45 (fragment 2) was amplified from pLPCX-SP-tagRFP-Cab45 (not published). For this construct, tag-RFP was amplified from pCAG-tagRFP-NLS-HA-Bxb1 (Addgene; plasmid #65625). Fragments were reinserted into CatD-RUSH vector linearized with AscI and XhoI. The osteopontin (OPN) RUSH construct pIRESneo3-Str-OPN-SBP-EGFP was cloned via one-fragment Gibson assembly approach. OPN-V5 was amplified from cDNA4-OPN-V5 (a gift from Vincent Tagliabracci, UT Southwestern Medical Center, Dallas, TX) and inserted into pIRESneo3-Str-SBP-EGFP that was linearized with AscI and XhoI.

The pcDNA3.1_Flag-LyzC plasmid was a gift from V. Malhotra (Center of Genomic Regulation, Barcelona, Spain; von Blume et al., 2012).

The plasmids Eq-SM-oxGFP and Eq-sol-oxGFP are are gift from C. Burd (Yale University, New Haven, CT).

Cell culture and stable transfection

All cell lines were maintained in DMEM supplemented with 10% FCS (Gibco) and Penicillin/Streptomycin (P/S) at 37°C and 5% CO_2. To create stable expressing HeLa cell lines, plasmids of Cab45-WT, Cab45-5pXA, Cab45-5pXE, Fam20C-WT, and Fam20C-KD were introduced via VSV-G pseudotyped retroviral vectors as described previously (Crevenna et al., 2016).

Doxycycline-inducible stable HEK293 cell lines for protein expression were generated using the transposon-based piggyBac system (Li et al., 2013). Therefore, HEK293 cells were transfected with PB-T-PAF (gene of interest introduced), PB-RN, and PBase (total DNA 1.5 µg; ratio 8:1:1) using polyethylenimine (PEI; Alfa Aesar). Cell culture medium was removed the next day. 48 h after transfection, selection of cells was performed in supplemented DMEM containing 10 µg/ml puromycin dihydrochloride (Sigma-Aldrich) and 500 µg/ml G 418 disulfate salt (Sigma-Aldrich).

Transient transfection and siRNA knockdown

Cells were transiently transfected with 1.25 mg/ml PEI (Alfa Aesar) or Lipofectamine LTX PLUS (Thermo Fisher Scientific) following manufacturer protocols.

For siRNA knockdown, the following oligos were used, as well as scrambled negative control from Invitrogen: SMS1, 5′-GACGGCAGCUUCAGCAUCAAGAUUA-3′; SMS2: 5′-UCAAUA GUGGGACGCAGAUUCUGUU-3′.

20 nM siRNA was added to 100 µl Opti-MEM reduced serum medium (Gibco by Life Technologies) together with 12 µl Hi-PerFect Transfection Reagent (Qiagen). The siRNA transfection mix was incubated at room temperature for 15 min and added dropwise to the seeded cells. Transfection was performed 24–48 h before further analysis.

CRISPR/Cas9 KO cell lines

HeLa Fam20C KO cells were generated using the CRISPR/Cas9 technique. Fam20C was targeted downstream of the signal sequence with gRNA next to the Cas9 recognition site protospacer adjacent motif (PAM). 20 nt gRNA oligos targeting Fam20C

(DMP4) were designed using www.genome-engineering.org/crispr (Ran et al., 2013).

Fam20C-gRNA sequence: 5′-GGGCGATGTGCAGCGCGCAG-3′
gRNA sequences were synthesized by Metabion. Oligos (forward and reverse sequence) were cloned into mammalian expression vector pX459 (Addgene; plasmid #62988) using BbsI cutting sites. HeLa parental cells were transfected using PEI as described above. 24 h after transfection, cells were selected in 2 μg/ml puromycin for 48 h. Single clones were isolated, expanded, and checked for deletion by sequencing with following sequencing primers: forward, 5′-CACCGATGGACCTTGACCC-3′; reverse, 5′-AGTGGGACGAGAGGTTGGAG-3′.

In addition, KO was checked using MS analysis. Golgi fractions of HeLa WT and Fam20C-KO cells were isolated as described previously (Crevenna et al., 2016) and separated via SDS-PAGE. Samples from gel lanes were digested with trypsin by an in-gel digestion protocol, and peptides were extracted and purified via C18 StageTips. Peptides were analyzed in a Q Exactive HF machine using data dependent acquisition scheme using Higher Energy Collisional Dissocation (HCD) fragmentation. Raw data were processed using the Maxquant computational platform, and the peak lists were searched against human reference proteome database from UniProt. All identifications were filtered at 1% false discovery rate (FDR) and label-free quantification.

Protein expression and purification of His-Sumo-Cab45 variants
Doxycycline-inducible HEK293-Cab45 cells were grown in p15 culture dishes until they reached full confluence. Cells were carefully washed three times with DPBS (Gibco) before starting protein expression. Therefore, cells were incubated for 20 h with DMEM supplemented with 1 μg/ml doxycycline monohydrate (LKT Laboratories) and 1 μg/ml Aprotinin (Sigma-Aldrich). Cell culture supernatant was collected, centrifuged (5 min; 1,000 rpm, 4°C) to remove dead cells, and filtered via 0.2-μm syringe filters. His-SUMO/GFP-Cab45 variants were purified using nickel-based affinity chromatography as described previously (Crevenna et al., 2016). Protein was stored at −80°C with 10% vol/vol after snap freezing in liquid nitrogen. His-Cofilin-S3E was purified as described previously (Kienzle et al., 2014).

Antisera
The antisera used were rat monoclonal anti-HA (Roche; catalog #11867423001), rabbit monoclonal anti-KIAA0310 (Thermo Fisher Scientific; catalog #A300-648A-M), mouse monoclonal anti-cis-Golgi matrix protein 130 (BD Biosciences; catalog #610823), mouse monoclonal anti-CNX (Sigma-Aldrich; catalog #C7617), mouse monoclonal anti-p230 (BD Biosciences; catalog #611281), sheep polyclonal anti-TGN46 (AbD Serotec; catalog #AHP500G), mouse monoclonal anti-β-actin (Sigma-Aldrich; catalog #A5441), mouse monoclonal ANTI-FLAG M2-peroxidase (HRP; Sigma-Aldrich; catalog #A8592), mouse monoclonal anti-EEA1 antibody (BD Biosciences; catalog #610457), rabbit polyclonal anti-Rab11 antibody (gift from the De Camilli laboratory, Yale School of Medicine, New

Haven, CT, self-made), rabbit monoclonal anti-Lamp1 antibody (Cell Signaling; catalog #9091S), and mouse monoclonal anti-CatD antibody (BD Biosciences; catalog #610801).

Secondary antibodies were purchased from Thermo Fisher Scientific (catalog numbers A-11034, A-11029, A-21209, A-21208, A-21203, 32260, 31470, and 32230).

Anti-Cab45 antibody was generated by the animal facility (immunization service) of the Max Planck Institute of Biochemistry as described previously (Crevenna et al., 2016). Full-length recombinant Cab45 (His-Sumo tagged) was used for rabbit immunization.

Protein detection by immunoblotting, Coomassie staining, and immunofluorescence
For detection of intracellular proteins, cells were washed three times with PBS and lysed with 1% TritonX-100 in PBS. Secreted proteins in supernatants were concentrated using Centrifugal Filters (Amicon Ultra). Proteins were separated according to size via SDS-PAGE.

For Coomassie staining, SDS gel was rinsed with PBS and prefixed in 40% vol/vol MeOH, 10% vol/vol acetic acid (HOAc) for 10 min. Gel was incubated in 40% vol/vol MeOH, 10% vol/vol HOAc with 0.1% weight/vol Coomassie Brilliant Blue R overnight and destained using 40% vol/vol MeOH, 10% vol/vol HOAc until single bands were visible. For storage, gel was put in 7% HOAc at 4°C.

For immunoblotting, proteins were transferred to nitrocellulose membranes using a wet blot system (Bio-Rad). Membranes were incubated in 5% BSA in TBS for at least 1 h and incubated with specific primary and corresponding secondary HRP-coupled antibody with additional washing steps with TBS-Tween (0.1%) in between. Proteins were detected via chemiluminescence (Thermo Fisher Scientific), acquired with ChemiDoc Imaging System (Bio-Rad).

For immunostaining, cells were cultured in six wells on glass slides and fixed for 10 min with 4% paraformaldehyde. After washing with PBS, cells were permeabilized for 5 min in 0.2% Triton-X 100 and 0.5% SDS in 4% BSA or saponin for at least 30 min. After washing with PBS, cells permeabilized with Triton-X 100 were blocked with 4% BSA for 1 h. Cells were incubated with primary followed by corresponding secondary antibody for 1 h at room temperature in blocking buffer in the dark. Slides were washed three times with PBS after incubation with antibody. Glass slides were mounted with ProLong Gold (Thermo Fisher Scientific). Acquisition was done using confocal laser-scanning microscope (Carl Zeiss; 40×, LSM 780, software ZEN 2010). If contrast was changed for better visualization of e.g., vesicles, this was done equally for all conditions.

Pearson's correlation
Pearson's correlation was performed using ImageJ 1.52c.

Secretion assay after 20°C block
For the secretion assay, cells were washed three times with PBS and incubated for 2 h at 20°C in DMEM supplemented with 100 μg/ml cycloheximide. Supernatant of control cells was taken directly after 20°C incubation to check basal secretion during

block and concentrated for 5 min at 16,000 ×g at 4°C in Centrifugal Filters (Amicon Ultra; Ultracel 10K); cells were lysed with 1% TritonX-100 in PBS. Experimental cells were shifted to 37°C and incubated for 1 h to start protein release from the Golgi. Supernatants were taken and concentrated like before. Cells were lysed as well. Protein secretion was checked by Western blot analysis as described above. Protein levels (densitometry) were quantified from at least three independent experiments using Fiji 1.0 software. Supernatant signals were normalized to corresponding protein signals in cell lysates. Actin signals were used as loading controls. Values of controls (20°C block only) were subtracted from values of cells passed through 37°C release. Final values were normalized to WT cells (100%) and plotted as a bar graph.

RUSH cargo sorting assay using confocal microscopy

RUSH assay was performed as described previously (Deng et al., 2018). Different cells lines were cultured in six wells on glass slides and transfected with RUSH constructs. 16 h after transfection, cells were incubated with 40 µM d-Biotin (SUPELCO) in DMEM for different time points (20, 30, 40, 50, and 60 min or without d-Biotin (control). Cells were washed once with PBS, fixed in 4% PFA in PBS for 10 min, and mounted on coverslips using ProLong Gold (Thermo Fisher Scientific). If required, costaining was done (see above). Acquisition of either GFP or RFP was done at 20°C using a confocal laser-scanning microscope (Carl Zeiss; LSM 780 or LSM 880; 40×/1.4, 63×/1.4, 100×/1.46 NA Plan-Apochromat oil objectives, software ZEN 2010) by imaging z-stacks with a step size of 0.35 µm.

For quantification of vesicles, we empirically measured the sizes of objects between 4 and 20 pixels using the Analyze Particles function in ImageJ, which detects vesicular structures but omits larger structures such as the Golgi. While small-fragmented and isolated Golgi structures could be detected in error, such structures are rare. Furthermore, only vesicles of cells expressing the RUSH construct were counted. The Fiji macro count_fixed_vesicles_V1.3 (M. Pakdel) including the Particle Analyzer plug-in by Fiji was used to determine the number of vesicles.

Golgi vesicle budding assays

Microscopy budding assay

Live-cell experiments were done as described previously (Deng et al., 2018) at 37°C. HeLa cells were seeded in live cell µ-dishes and transfected with Fam20C-mCherry and EGFP-Cab45/Eq-SM-oxGFP/Eq-Sol-oxGFP. Stable HeLa Cab45 WT/mutant cells were transfected with LyzC-mCherry and Eq-SM-oxGFP. Medium was exchanged to live-cell imaging solution (Molecular Probes) supplemented with 10 mM glucose. Imaging was done by live-cell wide-field microscopy. Dual-channel acquisition for EGFP and mCherry was performed at 1-s intervals for 100 frames on a GE Healthcare DeltaVision Elite system based on an OLYMPUS IX-71 inverted microscope, an OLYMPUS 60×/1.42 PLAPON oil objective and a PCO sCMOS 5.5 camera. For deconvolution software softWoRx v.6.0 was used. Budding events and colocalizaton were scored manually from time-lapse series choosing one image out of frame (ImageJ).

The time-lapse movies were analyzed by identifying budding events from the Golgi. Fam20C budding events were scored whether they are EGFP-Cab45, Eq-SM-oxGFP, or Eq-Sol-oxGFP positive. For LyzC budding, presence of Eq-SM-oxGFP in Cab45-WT and mutant cells was checked.

The ratios of Cab45 budding with or without EQ-SM were calculated to total budding events. The mean and ±SD of the ratios were plotted as a bar graph.

Budding assay in semi-intact cells

Cells were incubated for 2 h at 20°C with DMEM, supplemented with FCS, Penicillin/Streptomycin, and 100 µg/ml cyclohexamide. Cells were washed 1x with PBS and trypsinized. Cells were counted, same amount of cells per condition was washed 2× with buffer A (20 mM Hepes, 250 mM D-sorbitol, 150 mM potassium acetate). Cells were permeabilized for 5 min with 40 µg/ml digitonin on ice and washed three times with buffer A. Cells were divided (control and experimental condition). Control cells were incubated for 45 min at 4°C in buffer A. Experimental cells were incubated for 45 min at 32°C with an ATP regenerating system (1 mM ATP, 40 mM creatine phosphate, 0.2 mg/ml creatine phosphokinase and 0.1 mM GTP). The reactions were centrifuged for 10 min at 10,000 g, supernatant was collected and centrifuged for 100,000 g for 1 h. Vesicular fraction (pellet) was dissolved in SDS-loading buffer and analyzed by Western blotting. Protein levels (densitometry) were quantified from at least three independent experiments using Fiji 1.0 software. Values of controls (4°C incubation) were subtracted from values of cells incubated with ATP regeneration system at 32°C. Final values were normalized to WT cells (100%) and plotted as a bar graph.

CD spectroscopy

CD spectroscopy measurements were performed in a 1-mm (path length) cuvette at 10°C on a JASCO J-715 spectrometer. Protein samples (0.2 mg/ml) were dissolved in CD buffer (20 mM Tris, pH 6.8, and 500 mM NaCl), and the indicated amounts of Ca^{2+} were added before spectra were recorded. An average of three (± Ca^{2+} analysis) independent spectra (from 195 to 250 nm with 0.1-nm spacing) were documented. Data were normalized to molecular ellipticity of protein, and a fast Fourier transform (FFT) filter was applied.

LyzC immunoprecipitation

Recombinant His-SUMO-Cab45 variants (purified as described above) and controls (His-Cofilin-S3E) were incubated with Ni^{2+}-agarose beads (Thermo Fisher Scientific; catalog #25214) for 2 h at 4°C on turning wheel, in immunoprecipitation buffer (50 mM Tris, 100 mM NaCl, and 0.1% TritonX-100 with protease inhibitors; Roche; catalog #11836170001) containing 100 µM Ca^{2+}. Beads were washed three times with immunoprecipitation buffer with Ca^{2+} and incubated for 2 h at 4°C with LyzC (Sigma-Aldrich) on a turning wheel. Beads were washed again three times and boiled in 1× Laemmli buffer. Coomassie staining was performed as described above.

MS for phosphoproteomic analysis

HeLa S3 suspensions cells stably expressing Fam20C or Fam20C-D478A (4 liter roller culture per condition) were

harvested and pelleted. Pellets were then washed once in Breaking Buffer (10 mM Tris, pH 7.4, and 250 mM sucrose), diluted 1:5 in Breaking Buffer supplemented with cOmplete Tablets Mini EDTA-free (Roche) and homogenized with an EMBL cell cracker (ball size, 8.002 mm; 9-μm gap). After addition of 1 mM EDTA, the sucrose concentration of the homogenate was adjusted to 37% (weight/vol) and overlayed with 35% and 29% sucrose in 10 mM Tris, pH 7.4. Cellular components were separated by ultracentrifugation for 3 h at 133,000 g. The Golgi membrane fraction was extracted, adjusted to Breaking Buffer conditions, and snap-frozen in liquid nitrogen for storage at –80°C.

For MS analysis, all samples were lysed in MS lysis buffer (10 mM Tris, pH 7.5, 4% SDS, and 10 mM DTT), boiled and sonicated, and precipitated overnight using ice-cold acetone (vol/vol 80%). After centrifugation (4,000 g), the pellet was washed at least twice with 80% ice-cold acetone before air drying and resuspension (sonication) in TFE buffer (10% 2-2-2-trifluorethanol and 100 mM ammonium bicarbonate). Proteins were digested using LyzC and trypsin (1:100) overnight at 37°C and phosphopeptides enriched as described previously (Humphrey et al., 2015). Samples were prepared in triplets.

For liquid chromatography–tandem mass spectrometry (LC-MS/MS) sample preparation peptides were purified using in-house prepared stage tips (Rappsilber et al., 2003) Empor SPE disks SDB-RPS (Sigma-Aldrich) before LC-MS/MS analysis as described previously (Kulak et al., 2014). Briefly, stage tips were prepared by inserting two layers of SDB-RPS matrix into a 200 μl pipette tip using an in-house–prepared syringe device. Stage tips were first activated with 100 μl MS buffer C (30% MeOH and 1% trifluoroacetic acid) and then washed with 100 μl MS buffer D (2% acetonitrile and 0.2% trifluoroacetic acid) before loading of the acidified peptides (1% trifluoroacetic acid). After centrifugation, the stage tips were washed three times (200 μl each) with MS buffer D. Elution was performed using 60 μl MS buffer E (60% acetonitrile and 1.25% ammonium hydroxide). Eluates were collected in 200-μl PCR tubes and dried using a Concentrator plus SpeedVac centrifuge (Eppendorf) at 60°C. Peptides were resuspended in MS buffer F (2% acetonitrile and 0.1% trifluoroacetic acid) and briefly sonicated (Branson Ultrasonics) before LC/MS-MS analysis.

For LC-MS/MS measurements, peptides were loaded on a 20- or 50-cm reversed phase column (75-μm inner diameter, packed in-house with ReproSil-Pur C18-AQ 1.9 μm resin [Dr. Maisch]). Column temperature was maintained at 55°C using a homemade column oven. An EASY-nLC 1200 system (Thermo Fisher Scientific) was directly coupled online with the mass spectrometer (Q Exactive) via a nanoelectrospray source, and peptides were separated with a binary buffer system of MS buffer A (0.1% formic acid) and MS buffer G (80% acetonitrile and 0.1% formic acid) at a flow rate of 250 or 350 nl/min. Peptides were eluted with a nonlinear 270-min gradient of 5–60% MS buffer G. After each gradient, the column was washed with 95% MS buffer G for 5 min. The mass spectrometer was programmed to acquire in a data-dependent mode (Top10) using a fixed ion injection time strategy. Full scans were acquired in the Orbitrap mass analyzer with resolution 60,000 at 200 m/z (3E6 ions were accumulated

with a maximum injection time of 25 ms). The top intense ions (N for TopN) with charge states ≥2 were sequentially isolated to a target value of 1E5 (maximum injection time of 120 ms, 20% underfill), fragmented by Higher Energy Collisional Dissocation (NCE 25, Q Exactive) and detected in the Orbitrap (Q Exactive, R = 15,000 at m/z 200).

Raw MS data were processed using MaxQuant version 1.5.3.15 (Cox and Mann, 2008) with an FDR <0.01 at the level of proteins, peptides, and modifications. Searches were performed against the Mouse or Human UniProt FASTA database (September 2015). Enzyme specificity was set to trypsin. The search included cysteine carbamidomethylation as a fixed modification and N-acetylation of protein; oxidation of methionine; and/or phosphorylation of serine, threonine, or tyrosine residue (PhosphoSTY) as variable modifications. Up to two missed cleavages were allowed for protease digestion. "Match between runs" was enabled, with a matching time window of 0.5–0.7 min. Bioinformatic analyses were performed with Perseus (www.perseus-framework.org) and Microsoft Excel and data visualized using Graph Prism (GraphPad Software) or Perseus (Tyanova et al., 2016). Significance was assessed using a one-sample t test, two-sample Student's t test, and ANOVA analysis, for which replicates were grouped, and statistical tests were performed with permutation-based FDR correction for multiple hypothesis testing. Were indicated, missing data points were replaced by data imputation after filtering for valid values (all valid values in at least one experimental group). Error bars represent mean ± SEM or mean ± SD.

In vitro kinase assays
In vitro kinase assays were performed by the Tagliabracci laboratory as described previously (Tagliabracci et al., 2012). Fam20C was purified from insect cells as described previously (Tagliabracci et al., 2012). Incorporation of ^{32}P into Cab45 or LyzC by Fam20C was tested by incubating 0.1 mg/ml recombinant Cab45 or OPN (control) with 0.5 mg/ml recombinant Fam20C-WT or Fam20C-KD for 2 h (reaction mixture: 50 mM Tris-HCl, pH 7.5, 10 mM MnCl2, and 1 mM [γ^{32}P]ATP [Specific Activity = 500 cpm/pmol]). Reaction was stopped by adding 15 mM EDTA and SDS loading buffer. Products were separated by SDS-PAGE followed by Coomassie blue staining and autoradiography. Recombinant Cab45-WT was purified as described above. LyzC was purchased from Sigma-Aldrich.

Cab45 oligomerization assay and analysis
For oligomerization assays, recombinant GFP-Cab45 proteins were purified as described above. Proteins were centrifuged for 10 min at 10,000 g at 4°C to remove aggregates. 0.2 mg/ml protein in 20 mM Tris, pH 7.4, was analyzed in a Lab-Tek 8 Chamber #1.0 borosilicate coverglass system (Nunc) with confocal microscopy (Carl Zeiss; 63×/1.4 NA Plan-Apochromat oil objective, LSM 880, software ZEN 2010) at 20°C. Proteins were incubated 10 min in buffer only, with 2 mM Ca²⁺ and 2 mM EDTA (after Ca²⁺ treatment), and z-stacks (0.35 μm) were taken at the bottom area of the well.

For analysis, image showing bottom of the well in focus was used. Individual background intensity for each picture was

subtracted (ImageJ macro: https://imagej.nih.gov/ij/macros/SubractMeasuredBackground.txt). Size distribution of oligomers was analyzed using ImageJ software (function: Analyze Particles; 0–1 Circularity). Oligomers were counted by the program according to their pixel size of (>3, >5, >11, and >20 pixel units). Intensity of vesicles was analyzed by measuring the intensity of the pixel with the highest intensity within a particle. According to the amount of oligomers formed by Cab45-5pXA, only a representative section of the image was analyzed.

Quantification and statistical analysis

For statistical evaluation, GraphPad Prism version 7.0b for Mac OS X (GraphPad Software) was used. Means ± SD are plotted in all analyzed graphs. Statistical details can be found in figure legends. Normality testing was performed using normality tests of D'Agositino–Pearson, Shapiro–Wilk, and Kolmogorov–Smirnov. A Kruskal–Wallis test followed by Dunn's multiple comparisons test was used for RUSH cargo sorting assays, Cab45 vesicle counting, LyzC secretion of Cab45 phosphomutants, Eq-SM vesicle counting, vesicle budding phosphomutants, LyzC immunoprecipitation, and intensity analysis of oligomers. An unpaired t test was used for vesicular budding assay of endogenous Cab45. A Mann–Whitney test was used for colocalization of Fam20C with Eq-SM and Eq-Sol vesicles as well as vesicle counting of Cab45-5pXE with SMS1/2 siRNA knockdown. A Kolmogorov–Smirnov test was used for LyzC secretion of Fam20C-KO. An ordinary one-way ANOVA test was used for LyzC secretion in Fam20C-KO cells rescued with Cab45 constructs. The following P value style was used: *, $P \leq 0.05$; **, $P \leq 0.01$; ***, $P \leq 0.001$.

Online supplemental material

Fig. S1 shows experiments related to Fig. 1 and Fig. 3 in which Fam20C-KO and Cab45 phosphorylation sites were identified using MS analysis. Fig. S2 shows additional results related to Fig. 4 in which Cab45 phosphomutants were analyzed for localization, secondary structure, and cargo binding. Fig. S3 shows experiments related to Fig. 5 in which LyzC sorting was further analyzed in Cab45 phosphomutants. Fig. S4 shows experiments related to Fig. 5 in which phosphomutants of Cab45 were additionally tested for specificity in cargo sorting. Fig. S5 shows experiments related to Fig. 6 in which TGN export of Cab45 was further characterized.

Acknowledgments

References

Ang, S.F., and H. Fölsch. 2012. The role of secretory and endocytic pathways in the maintenance of cell polarity. *Essays Biochem.* 53:29–39. https://doi.org/10.1042/bse0530029

Barenholz, Y., and Thompson, T.E. 1980. Sphingomyelins in bilayers and biological membranes. Biochimica Et Biophysica Acta Bba - Rev Biomembr. 604:129–158.

Blank, B., and J. von Blume. 2017. Cab45-Unraveling key features of a novel secretory cargo sorter at the trans-Golgi network. *Eur. J. Cell Biol.* 96: 383–390. https://doi.org/10.1016/j.ejcb.2017.03.001

Boncompain, G., and Perez, F. 2012. Synchronising protein transport in the secretory pathway. Curr Protoc Cell Biol. 15.19.1–15.19.16.

Boncompain, G., S. Divoux, N. Gareil, H. de Forges, A. Lescure, L. Latreche, V. Mercanti, F. Jollivet, G. Raposo, and F. Perez. 2012. Synchronization of secretory protein traffic in populations of cells. *Nat. Methods.* 9:493–498. https://doi.org/10.1038/nmeth.1928

Bonifacino, J.S.. 2014. Vesicular transport adds a Nobel. *Trends Cell Biol.* 24(1): 3–5. https://doi.org/10.1016/j.tcb.2013.11.001

Booth, C., and G.L. Koch. 1989. Perturbation of cellular calcium induces secretion of luminal ER proteins. *Cell.* 59:729–737. https://doi.org/10.1016/0092-8674(89)90019-6

Braulke, T., and J.S. Bonifacino. 2009. Sorting of lysosomal proteins. Biochimica Et Biophysica Acta Bba - Mol. Cell Res. 1793:605–614.

Chege, N.W., and S.R. Pfeffer. 1990. Compartmentation of the Golgi complex: brefeldin-A distinguishes trans-Golgi cisternae from the trans-Golgi network. *J. Cell Biol.* 111:893–899. https://doi.org/10.1083/jcb.111.3.893

Cong, L., F.A. Ran, D. Cox, S. Lin, R. Barretto, N. Habib, P.D. Hsu, X. Wu, W. Jiang, L.A. Marraffini, et al. 2013. Multiplex genome engineering using CRISPR/Cas systems. *Science.* 339:819–823. https://doi.org/10.1126/science.1231143

Cox, J., and M. Mann. (2008). MaxQuant enables high peptide identification rates, individualized p.p.b.-range mass accuracies and proteome-wide protein quantification. Nat. Biotechnol. 26:nbt.1511.

Crevenna, A.H., B. Blank, A. Maiser, D. Emin, J. Prescher, G. Beck, C. Kienzle, K. Bartnik, B. Habermann, M. Pakdel, et al. 2016. Secretory cargo sorting by Ca2+-dependent Cab45 oligomerization at the trans-Golgi network. *J. Cell Biol.* 213:305–314. https://doi.org/10.1083/jcb.201601089

Cummings, M.D., H. Ling, G.D. Armstrong, J.L. Brunton, and R.J. Read. 1998. Modeling the carbohydrate-binding specificity of pig edema toxin. *Biochemistry.* 37:1789–1799. https://doi.org/10.1021/bi971807f

De Matteis, M.A., and A. Luini. 2008. Exiting the Golgi complex. *Nat. Rev. Mol. Cell Biol.* 9:273–284. https://doi.org/10.1038/nrm2378

Deng, Y., F.E. Rivera-Molina, D.K. Toomre, and C.G. Burd. 2016. Sphingomyelin is sorted at the trans Golgi network into a distinct class of secretory vesicle. *Proc. Natl. Acad. Sci. USA.* 113:6677–6682. https://doi.org/10.1073/pnas.1602875113

Deng, Y., M. Pakdel, B. Blank, E.L. Sundberg, C.G. Burd, and J. von Blume. 2018. Activity of the SPCA1 Calcium Pump Couples Sphingomyelin Synthesis to Sorting of Secretory Proteins in the Trans-Golgi Network. *Dev. Cell.* 47:464–478.e8. https://doi.org/10.1016/j.devcel.2018.10.012

Fölsch, H.. 2005. The building blocks for basolateral vesicles in polarized epithelial cells. *Trends Cell Biol.* 15:222–228. https://doi.org/10.1016/j.tcb.2005.02.006

Fölsch, H.. 2008. Regulation of membrane trafficking in polarized epithelial cells. *Curr. Opin. Cell Biol.* 20:208–213. https://doi.org/10.1016/j.ceb.2008.01.003

Fölsch, H., H. Ohno, J.S. Bonifacino, and I. Mellman. 1999. A novel clathrin adaptor complex mediates basolateral targeting in polarized epithelial cells. *Cell.* 99:189–198. https://doi.org/10.1016/S0092-8674(00)81650-5

Fölsch, H., M. Pypaert, P. Schu, and I. Mellman. 2001. Distribution and function of AP-1 clathrin adaptor complexes in polarized epithelial cells. *J. Cell Biol.* 152:595–606. https://doi.org/10.1083/jcb.152.3.595

Fu, Q., J. Chow, K.A. Bernstein, N. Makharashvili, S. Arora, C.F. Lee, M.D. Person, R. Rothstein, and T.T. Paull. 2014. Phosphorylation-regulated transitions in an oligomeric state control the activity of the Sae2 DNA repair enzyme. *Mol. Cell. Biol.* 34:778–793.

Gleeson, P.A., J.G. Lock, M.R. Luke, and J.L. Stow. 2004. Domains of the TGN: coats, tethers and G proteins. *Traffic.* 5:315–326. https://doi.org/10.1111/j .1398-9219.2004.00182.x

Guo, Y., D.W. Sirkis, and R. Schekman. 2014. Protein sorting at the trans-Golgi network. *Annu. Rev. Cell Dev. Biol.* 30:169–206. https://doi.org/10 .1146/annurev-cellbio-100913-013012

Humphrey, S.J., Azimifar, B.S., and Mann, M. 2015. High-throughput phosphoproteomics reveals in vivo insulin signaling dynamics. Nat. Biotechnol. 33:nbt.3327.

Ito, H., K. Kamei, I. Iwamoto, Y. Inaguma, D. Nohara, and K. Kato. 2001. Phosphorylation-induced change of the oligomerization state of alpha B-crystallin. *J. Biol. Chem.* 276:5346–5352.

Johannes, L., and W. Römer. 2010. Shiga toxins--from cell biology to biomedical applications. *Nat. Rev. Microbiol.* 8:105–116. https://doi.org/10 .1038/nrmicro2279

Kienzle, C., and J. von Blume. 2014. Secretory cargo sorting at the trans-Golgi network. *Trends Cell Biol.* 24:584–593. https://doi.org/10.1016/j.tcb.2014.04.007

Kienzle, C., N. Basnet, A.H. Crevenna, G. Beck, B. Habermann, N. Mizuno, and J. von Blume. 2014. Cofilin recruits F-actin to SPCA1 and promotes Ca2+-mediated secretory cargo sorting. *J. Cell Biol.* 206:635–654. https:// doi.org/10.1083/jcb.201311052

Klumperman, J.. 2011. Architecture of the mammalian Golgi. *Cold Spring Harb. Perspect. Biol.* 3. a005181. https://doi.org/10.1101/cshperspect.a005181

Kulak, N.A., G. Pichler, I. Paron, N. Nagaraj, and M. Mann. 2014. Minimal, encapsulated proteomic-sample processing applied to copy-number estimation in eukaryotic cells. *Nat Methods.* 11:319–324. https://doi .org/10.1038/nmeth.2834

Li, Z., I.P. Michael, D. Zhou, A. Nagy, and J.M. Rini. 2013. Simple piggyBac transposon-based mammalian cell expression system for inducible protein production. *Proc. Natl. Acad. Sci. USA.* 110:5004–5009. https:// doi.org/10.1073/pnas.1218620110

Lin, P., H. Le-Niculescu, R. Hofmeister, J.M. McCaffery, M. Jin, H. Hennemann, T. McQuistan, L. De Vries, and M.G. Farquhar. 1998. The mammalian calcium-binding protein, nucleobindin (CALNUC), is a Golgi resident protein. *J. Cell Biol.* 141:1515–1527. https://doi.org/10.1083/jcb.141.7.1515

Lin, P., Y. Yao, R. Hofmeister, R.Y. Tsien, and M.G. Farquhar. 1999. Overexpression of CALNUC (nucleobindin) increases agonist and thapsigargin releasable Ca2+ storage in the Golgi. *J. Cell Biol.* 145:279–289. https://doi.org/10.1083/jcb.145.2.279

Mayor, S., and H. Riezman. 2004. Sorting GPI-anchored proteins. *Nat. Rev. Mol. Cell Biol.* 5:110–120. https://doi.org/10.1038/nrm1309

Mellman, I., and W.J. Nelson. 2008. Coordinated protein sorting, targeting and distribution in polarized cells. *Nat. Rev. Mol. Cell Biol.* 9:833–845. https://doi.org/10.1038/nrm2525

Mertins, P., D.R. Mani, K.V. Ruggles, M.A. Gillette, K.R. Clauser, P. Wang, X. Wang, J.W. Qiao, S. Cao, F. Petralia, et al; NCI CPTAC. 2016. Proteogenomics connects somatic mutations to signalling in breast cancer. *Nature.* 534:55–62. https://doi.org/10.1038/nature18003

Miura, K., Y. Kurosawa, and Y. Kanai. 1994. Calcium-binding activity of nucleobindin mediated by an EF hand moiety. *Biochem. Biophys. Res. Commun.* 199:1388–1393. https://doi.org/10.1006/bbrc.1994.1384

Munro, S.. 1995. An investigation of the role of transmembrane domains in Golgi protein retention. *EMBO J.* 14:4695–4704. https://doi.org/10.1002/ j.1460-2075.1995.tb00151.x

Munro, S.. 2005. The Golgi apparatus: defining the identity of Golgi membranes. *Curr. Opin. Cell Biol.* 17:395–401. https://doi.org/10.1016/j.ceb .2005.06.013

Nilsson, T., P. Slusarewicz, M.H. Hoe, and G. Warren. 1993. Kin recognition. A model for the retention of Golgi enzymes. *FEBS Lett.* 330:1–4. https://doi .org/10.1016/0014-5793(93)80906-B

Pakdel, M., and J. von Blume. 2018. Exploring new routes for secretory protein export from the *trans*-Golgi network. *Mol. Biol. Cell.* 29:235–240. https://doi.org/10.1091/mbc.E17-02-0117

Paladino, S., D. Sarnataro, R. Pillich, S. Tivodar, L. Nitsch, and C. Zurzolo. 2004. Protein oligomerization modulates raft partitioning and apical sorting of GPI-anchored proteins. *J. Cell Biol.* 167:699–709. https://doi .org/10.1083/jcb.200407094

Pezeshkian, W., H. Gao, S. Arumugam, U. Becken, P. Bassereau, J.-C. Florent, J.H. Ipsen, L. Johannes, and J.C. Shillcock. 2017. Mechanism of Shiga Toxin Clustering on Membranes. *ACS Nano.* 11:314–324. https://doi.org/ 10.1021/acsnano.6b05706

Pizzo, P., V. Lissandron, and T. Pozzan. 2010. The trans-golgi compartment: A new distinct intracellular Ca store. *Commun. Integr. Biol.* 3:462–464. https://doi.org/10.4161/cib.3.5.12473

Ran, F.A., P.D. Hsu, J. Wright, V. Agarwala, D.A. Scott, and F. Zhang. 2013. Genome engineering using the CRISPR-Cas9 system. *Nat Protoc.* 8(11): 2281–2308. https://doi.org/oi:10.1038/nprot.2013.143

Rappsilber, J., Y. Ishihama, and M. Mann. 2003. Stop and go extraction tips for matrix-assisted laser desorption/ionization, nanoelectrospray, and LC/MS sample pretreatment in proteomics. *Anal. Chem.* 75:663–670. https://doi.org/10.1021/ac026117i

Römer, W., L. Berland, V. Chambon, K. Gaus, B. Windschiegl, D. Tenza, M.R. Aly, V. Fraisier, J.-C. Florent, D. Perrais, et al. 2007. Shiga toxin induces tubular membrane invaginations for its uptake into cells. *Nature.* 450: 670–675. https://doi.org/10.1038/nature05996

Scherer, P.E., G.Z. Lederkremer, S. Williams, M. Fogliano, G. Baldini, and H.F. Lodish. 1996. Cab45, a novel (Ca2+)-binding protein localized to the Golgi lumen. *J Cell Biol.* 133(2):257–268. https://doi.org/10.1083/jcb.133.2 .257

Tagliabracci, V.S., J.L. Engel, J. Wen, S.E. Wiley, C.A. Worby, L.N. Kinch, J. Xiao, N.V. Grishin, and J.E. Dixon. 2012. Secreted kinase phosphorylates extracellular proteins that regulate biomineralization. *Science.* 336: 1150–1153. https://doi.org/10.1126/science.1217817

Tagliabracci, V.S., L.A. Pinna, and J.E. Dixon. 2013. Secreted protein kinases. *Trends Biochem. Sci.* 38:121–130. https://doi.org/10.1016/j.tibs.2012.11 .008

Tagliabracci, V.S., S.E. Wiley, X. Guo, L.N. Kinch, E. Durrant, J. Wen, J. Xiao, J. Cui, K.B. Nguyen, J.L. Engel, et al. 2015. A Single Kinase Generates the Majority of the Secreted Phosphoproteome. *Cell.* 161:1619–1632. https:// doi.org/10.1016/j.cell.2015.05.028

Traub, L.M., and J.S. Bonifacino. 2013. Cargo recognition in clathrin-mediated endocytosis. *Cold Spring Harb. Perspect. Biol.* 5. a016790. https://doi.org/ 10.1101/cshperspect.a016790

Tyanova, S., T. Temu, P. Sinitcyn, A. Carlson, M.Y. Hein, T. Geiger, M. Mann, and J. Cox. 2016. The Perseus computational platform for comprehensive analysis of (prote)omics data. *Nat. Methods.* 13:731–740. https://doi .org/10.1038/nmeth.3901

von Blume, J., and A. Hausser. 2019. Lipid-dependent coupling of secretory cargo sorting and trafficking at the trans-Golgi network. *FEBS Lett.* 593: 2412–2427. https://doi.org/10.1002/1873-3468.13553

von Blume, J., J.M. Duran, E. Forlanelli, A.-M. Alleaume, M. Egorov, R. Polishchuk, H. Molina, and V. Malhotra. 2009. Actin remodeling by ADF/ cofilin is required for cargo sorting at the trans-Golgi network. *J. Cell Biol.* 187:1055–1069. https://doi.org/10.1083/jcb.200908040

von Blume, J., A.-M. Alleaume, G. Cantero-Recasens, A. Curwin, A. Carreras-Sureda, T. Zimmermann, J. van Galen, Y. Wakana, M.A. Valverde, and V. Malhotra. 2011. ADF/cofilin regulates secretory cargo sorting at the TGN via the Ca2+ ATPase SPCA1. *Dev. Cell.* 20:652–662. https://doi.org/ 10.1016/j.devcel.2011.03.014

von Blume, J., A.-M. Alleaume, C. Kienzle, A. Carreras-Sureda, M. Valverde, and V. Malhotra. 2012. Cab45 is required for Ca(2+)-dependent secretory cargo sorting at the trans-Golgi network. *J. Cell Biol.* 199:1057–1066. https://doi.org/10.1083/jcb.201207180

Wakana, Y., J. van Galen, F. Meissner, M. Scarpa, R.S. Polishchuk, M. Mann, and V. Malhotra. 2012. A new class of carriers that transport selective cargo from the trans Golgi network to the cell surface. *EMBO J.* 31: 3976–3990. https://doi.org/10.1038/emboj.2012.235

Welch, L.G., and S. Munro. 2019. A tale of short tails, through thick and thin: investigating the sorting mechanisms of Golgi enzymes. *FEBS Lett.* 593: 2452–2465. https://doi.org/10.1002/1873-3468.13553

Zhou, H., S. Di Palma, C. Preisinger, M. Peng, A.N. Polat, A.J. Heck, and S. Mohammed. 2013. Toward a comprehensive characterization of a human cancer cell phosphoproteome. *J. Proteome Res.* 12:260–271. https:// doi.org/10.1021/pr300630k
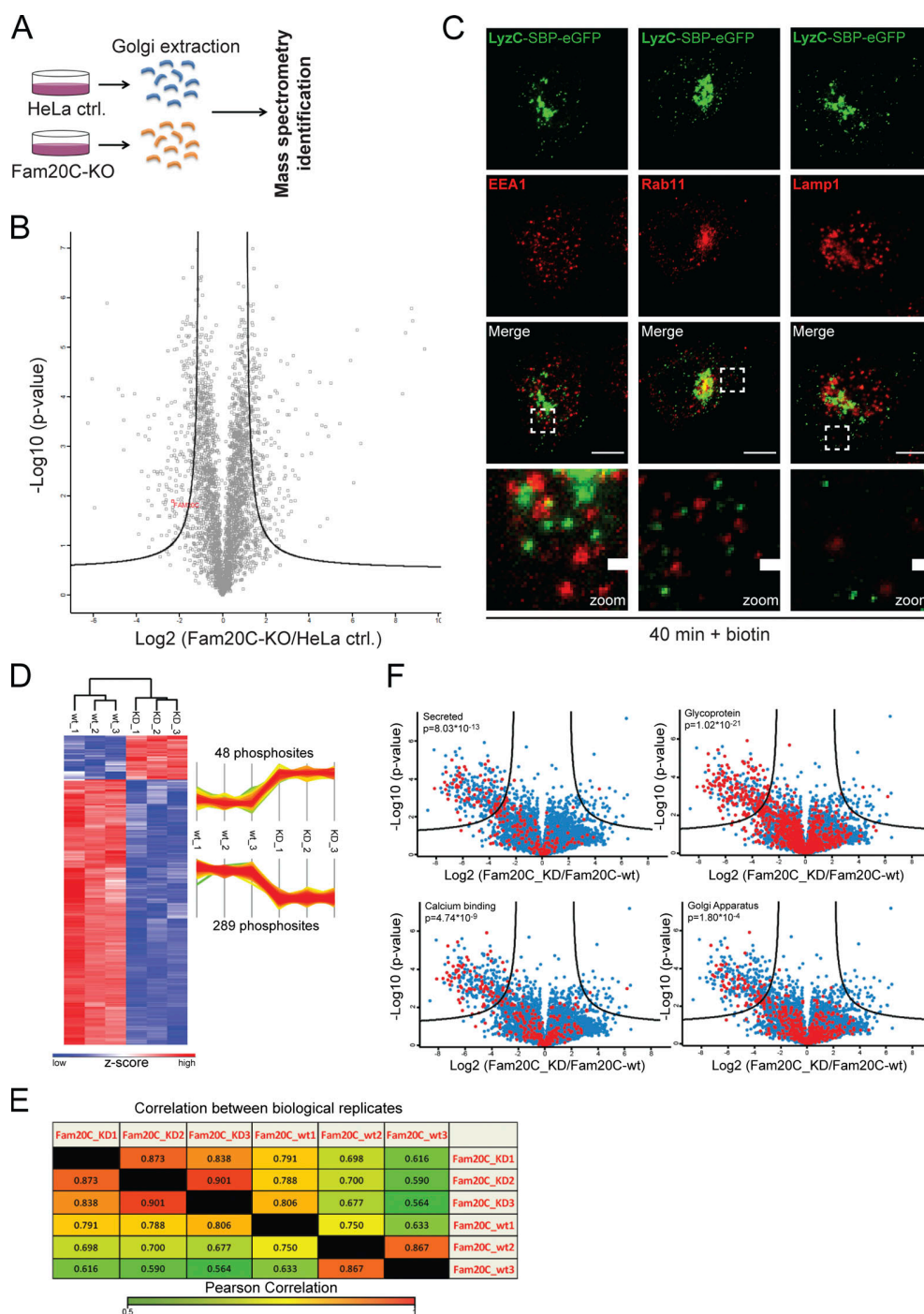
Figure S1. **MS analysis confirming Fam20C protein KO and Fam20C-dependent phosphorylation sites of Cab45 (related to Figs. 1 and 3). (A)** Scheme of the MS approach used to identify Fam20C protein KO. Golgi fractions of HeLa control and Fam20C-KO cells were isolated by sucrose gradient centrifugation. Equal protein amounts were separated by SDS PAGE and analyzed by MS (*n* = 3). **(B)** Volcano plot of the identified proteins of HeLa control cells versus Fam20C-KO cells. Fam20C was identified in HeLa-WT cells by MS/MS (indicated in red), but not in Fam20C-KO cells. **(C)** Colocalization of vesicular LyzC-SBP-EGFP against endosomal and lysosomal markers was analyzed using immunofluorescence microscopy. HeLa cells were transfected with RUSH construct LyzC-SBP-EGFP and incubated for 40 min with biotin. Cells were fixed and stained with α-EEA1 antibody (early endosomes), α-Rab11 antibody (recycling endosomes), and α-Lamp1 antibody (lysosomes). Scale bars, 10 μm. The magnification of the inset is shown in the lowest panel (scale bars, 1 μm). **(D)** Heatmap and profile plot illustrating hits that were significantly phosphorylated in the kinase-dead (KD) Fam20C samples (48 phosphosites) or Fam20C-WT samples (289 phosphosites). Red and blue represent the high and low z-scores, respectively. **(E)** Quantification of the analyzed Fam20C-WT and Fam20C-KD samples using Pearson correlation analysis. Hits from each sample were compared with hits from samples of the same group (biological replicates) as well as with hits from samples from the other group (Fam20C-WT vs. Fam20C-KD). High and low correlations between samples are indicated by red and green, respectively. **(F)** Categorization of the detected protein hits into subgroups (red dots). The phosphorylated proteins were analyzed for similarities (secreted, glycosylated, calcium-binding, and Golgi-localized proteins). P values describe the amount of enriched phosphorylated proteins in each subgroup.
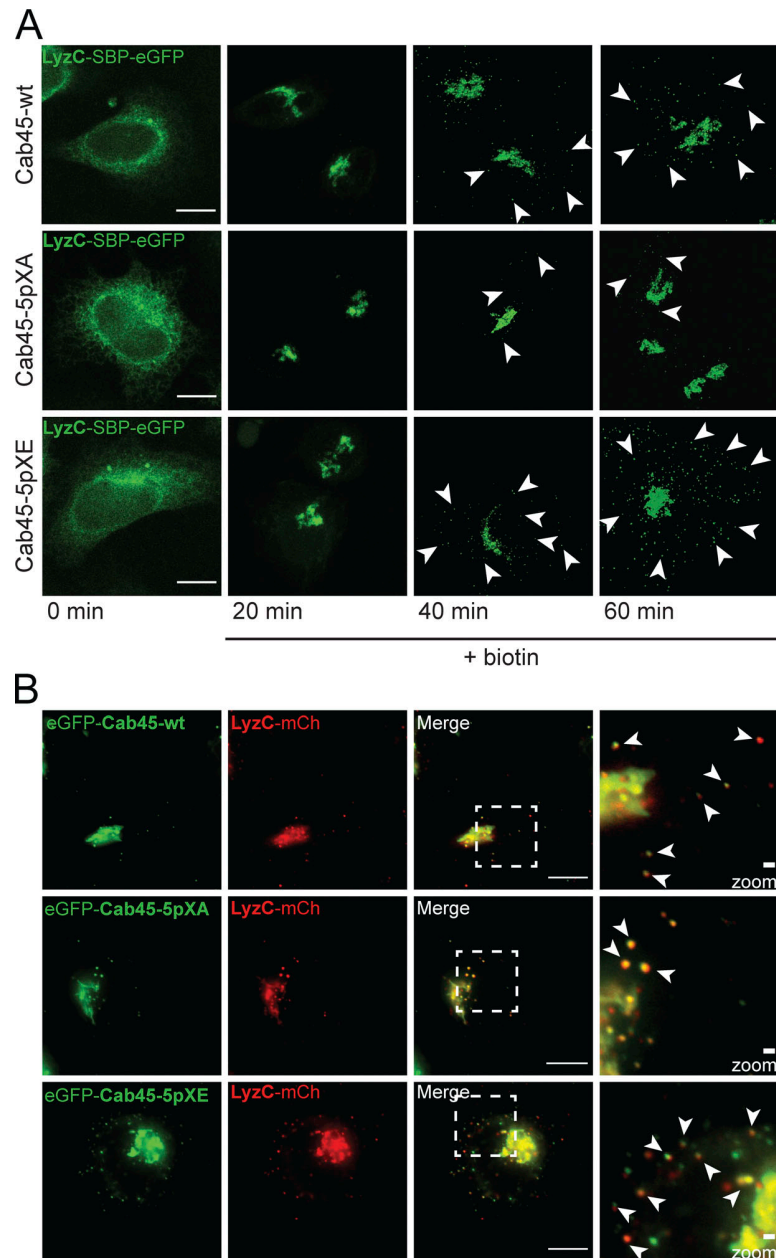
Figure S2. **Mutation of Cab45 phosphorylation sites alters the localization, but not the secondary structure or cargo-binding ability, of the protein (related to Fig. 4). (A)** Representative immunofluorescence images of cells that stably expressed Cab45-5pXE, stained against Cab45-5pXE (α-HA) and ER exit sites (α-Sec16A). Scale bar, 10 µm. The magnification of the inset is shown in the right panel (scale bar, 1 µm). The green arrowheads indicate Cab45-5pXE vesicles, and the red arrowheads indicate Sec16A-positive ER exit sites. **(B)** Far-ultraviolet CD spectroscopy measurements of recombinant Cab45-WT, Cab45-5pXA, and Cab45-5pXE. The secondary structures of the proteins were analyzed only in the buffer after adding 1 mM Ca^{2+} and followed by 2 mM EDTA. **(C)** Coimmunoprecipitation of recombinant LyzC with Cab45-WT and phosphomutants analyzed by Coomassie staining. Recombinant Cab45 proteins were enriched by Ni^{2+} beads, washed, and incubated with recombinant LyzC (upper blot). Cofilin-S3E was used as a negative control (lower blot). **(D)** Coomassie gels of three independent experiments described in C were quantified by densitometry with ImageJ software. The bar graph represents the means ± SD of densitometric values of LyzC signal normalized to Cab45 signal in percent. Statistical test, Kruskal–Wallis.

Figure S3. **Specific LyzC sorting of Cab45 phosphomutants (related to Fig. 5). (A)** Representative immunofluorescence images of RUSH experiments, showing LyzC transport in Cab45-WT and phosphomutant cell lines. The cells were transfected with LyzC-SBP-EGFP and fixed at 0, 20, 40, and 60 min after addition of biotin. Z-stack images (d = 0.35 µm) were analyzed. The arrowheads indicate cytoplasmic vesicles. Scale bars, 10 µm. **(B)** Cab45 phosphomutants and Cab45-WT were sorted together with LyzC into the same vesicles. HeLa WT cells were transfected with different EGFP-Cab45 constructs and LyzC-mCherry. Time-lapse movies were acquired to observe vesicle budding over time. Scale bars, 10 µm. The magnification of the inset is shown in the last panel. Bars, 1 µm. Arrowheads indicate secretory vesicles that contained both fluorescent proteins.
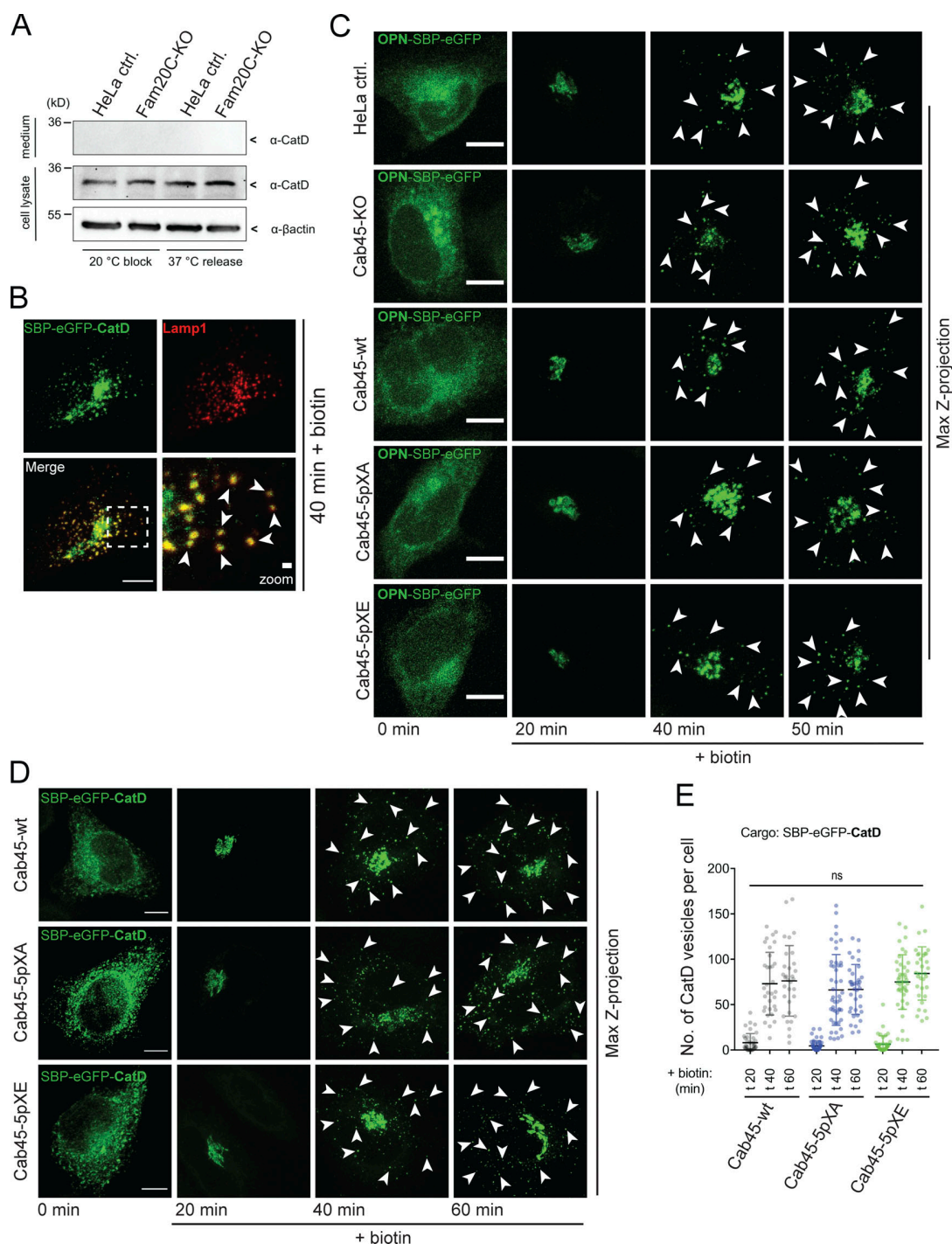
Figure S4. Sorting of non-Cab45 cargos is not affected in Cab45 phosphomutants (related to Fig. 5). (A) Western blot analysis of the secretion of CatD in HeLa control and Fam20C-KO cells. Endogenous CatD was trapped in the Golgi at 20°C and released for 1 h at 37°C. The supernatants (upper panel) and cell lysates (lower panels) were tested for CatD by Western blotting. β-Actin was used as loading control. **(B)** Representative immunofluorescence images of colocalization of vesicular SBP-EGFP-CatD with the lysosomal marker Lamp1. HeLa cells were transfected with RUSH construct and incubated for 40 min with biotin. Cells were fixed and stained with α-Lamp1 antibody. Scale bar, 10 µm. The magnification of the inset is shown in the lower right pane (scale bar, 1 µm). **(C)** Representative immunofluorescence images of RUSH experiments showing OPN transport in HeLa control, Cab45-KO, Cab45-WT, and Cab45 phosphomutant cell lines. Cells were transfected with OPN-SBP-EGFP and fixed at 0, 20, 40, and 50 min after the addition of biotin. Z-stack images (d = 0.35 µm) were analyzed. The arrowheads indicate cytoplasmic vesicles. Scale bars, 10 µm. **(D)** Representative immunofluorescence images of RUSH experiments showing cathepsin D (CatD) transport in Cab45-WT and phosphomutant cell lines. Cells were transfected with SBP-EGFP-CatD and fixed at 0, 20, 40, and 60 min after the addition of biotin. Z-stack images (d = 0.35 µm) were analyzed. The arrowheads indicate cytoplasmic vesicles. Scale bars, 10 µm. **(E)** The numbers of CatD budding vesicles (D) were quantified. The cytoplasmic vesicles were counted at each time point by analyzing z-stack images (d = 0.35 µm). Scatter dot plot represents the means ± SD of at least three independent experiments (n > 30 cells per condition). Statistical test, Kruskal–Wallis.
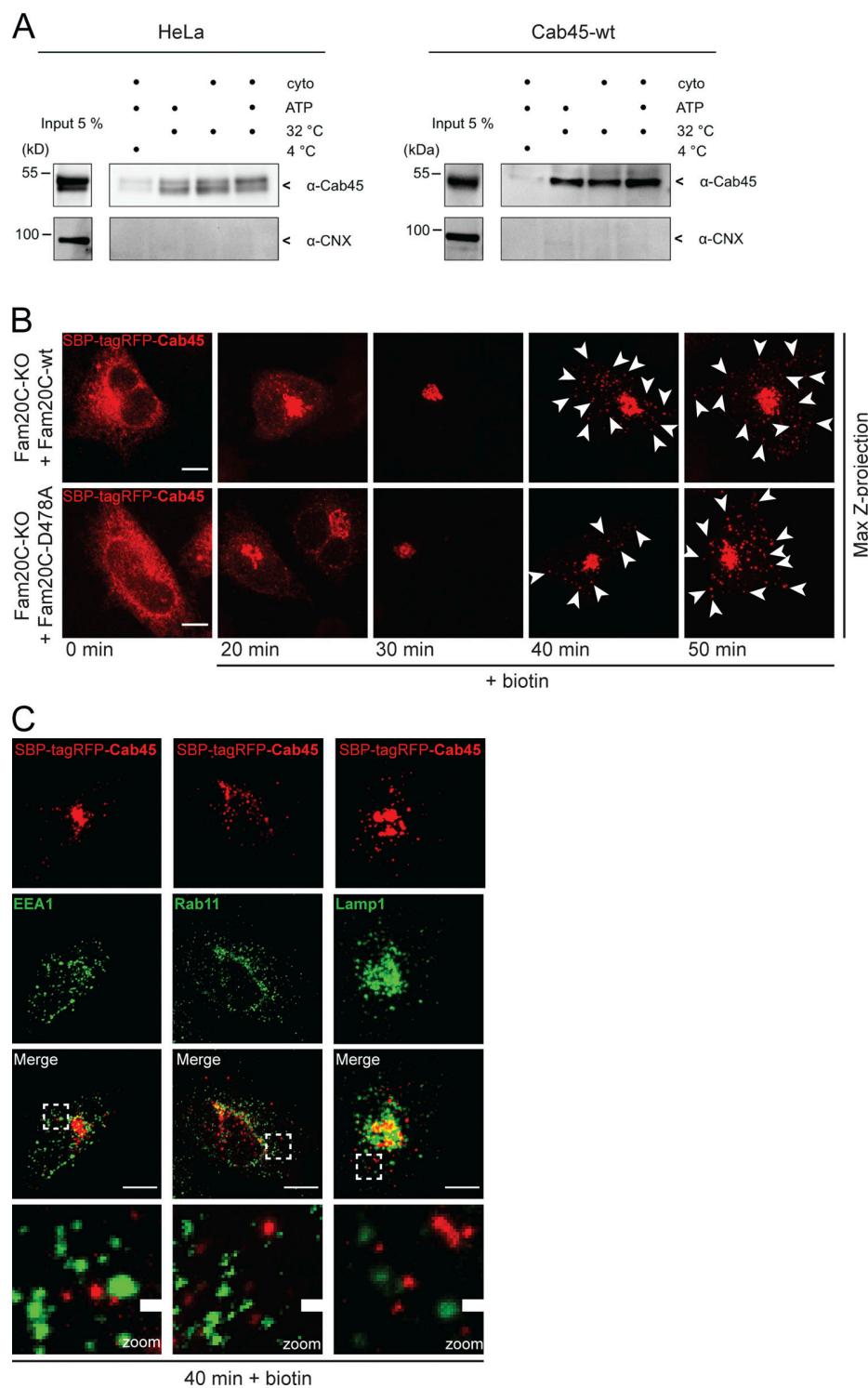
Figure S5. **TGN export of Cab45 (related to Fig. 6). (A)** Vesicular budding assays of Cab45. The budding of TGN-derived vesicles was tested in HeLa cells (left blot) and overexpressed Cab45-WT (right blot) in dependency of ATP and rat liver cytosol at 32°C. The released vesicles were collected and analyzed by Western blotting for Cab45 and CNX. Cells incubated at 4°C were used as the negative control. **(B)** Representative immunofluorescence images of RUSH experiments showing Cab45 transport in Fam20C KO cells that reexpress Fam20C-WT and the kinase-dead Fam20C-D478A. The cells were transfected with SBP-tagRFP-Cab45 and fixed at 0, 20, 30, 40, and 50 min after the addition of biotin. Z-stack images (d = 0.35 μm) were analyzed. The arrowheads indicate cytoplasmic vesicles. Scale bars, 10 μm. **(C)** Colocalization of vesicular SBP-tagRFP-Cab45 against endosomal and lysosomal markers was checked using immunofluorescence microscopy. HeLa cells were transfected with RUSH construct SBP-tagRFP-Cab45 and incubated for 40 min with biotin. Cells were fixed and stained with α-EEA1 antibody (early endosomes), α-Rab11 antibody (recycling endosomes) and α-Lamp1 antibody (lysosomes). Scale bars, 10 μm. The magnification of the inset is shown in the lowest panel. Scale bars, 1 μm.

4. Discussion

Vesicular transport is indispensable in eukaryotic cells as it mediates the exchange of proteins and lipids between membrane-bound organelles. Pioneered by the work of James Rothman, Randy Scheckman and Thomas Südhof, among others, three classes of transport vesicles have been functionally characterized to date, named according to their protein coats COPI, COPII and clathrin. As a basic step in all these vesicle-forming events is the interaction of cargo molecules with coat components that results in the incorporation of the cargo molecules into the nascent transport carrier and further is stabilizing the vesicle-budding complex. Whereas transmembrane proteins can directly interact with cytosolic coat components via sorting motifs in their cytoplasmic domains, soluble luminal proteins by definition have no such domains. Instead, special cargo receptors have been identified within different compartments in the Secretory Pathway. These proteins, including MPRs, p24 family proteins or ERGIC-53, with both intraluminal and cytoplasmic domains, have been shown to link soluble cargos to coat and adapter proteins in the cytosol (Bonifacino 2004, 2014; Ghosh and Kornfeld 2003). Nevertheless, the transport and sorting of especially soluble secreted molecules from the Golgi apparatus remain elusive as specific machineries for their recognition but also the types of vesicles in which these proteins are convoyed are mainly unknown (Pakdel and von Blume 2018). This is particularly astonishing, considering that highly active substances e.g. enzymes, whose secretion must be exquisitely regulated, are among those molecules (Malemud 2006; Rothman 2002).

The present thesis examines how Ca^{2+} and phosphorylation in the Golgi complex contribute to the intra-Golgi transport and secretion of soluble secreted proteins. This discussion will evaluate the current research in the context of existing literature, and consider possible mechanisms of how luminal Ca^{2+}-binding EF-hand proteins can drive protein transport processes.

4.1 NUCB1 and Cab45 bind soluble secretory proteins in a Ca^{2+}-dependent manner

Ca^{2+} is a major secondary messenger. Through influx from the extracellular space or release from intracellular Ca^{2+}-storage compartments like the ER, Ca^{2+} controls many cellular processes by activating enzymes, ion channels and other proteins that are working together in signaling cascades (Berridge et al. 2000). In this regard, increasing cytosolic Ca^{2+} levels were also shown to play multiple roles in membrane trafficking, e.g. in vesicle fusion via synaptotagmin - a Ca^{2+}-sensor located on vesicles that binds to the vesicle fusion machinery composed of SNAREs and other proteins (Himschoot et al. 2017; Pang and Südhof 2010). However, it is not only cytosolic Ca^{2+} that contributes to the cargo transport, luminal Ca^{2+} has also been shown to directly influences protein transport and polarized trafficking (Sepúlveda et al. 2009). Previously, it has been demonstrated that the TGN-localized Ca^{2+}-binding protein Cab45 oligomerizes in response to increasing luminal Ca^{2+} that has been locally pumped into the TGN by SPCA1. Consequently, cargo molecules like LyzC, COMP or MGP[98] - ready for secretion - can be bound by the oligomeric Cab45-complex and sorted into SM-rich vesicles (Deng et al. 2018).

In the scope of this thesis we could show that another EF-hand Ca^{2+}-binding protein NUCB1 that localizes in the *cis*-Golgi, might act in an analogous way. Similarly to Cab45, NUCB1 binds Ca^{2+} in a pairwise manner with its two EF-hand motifs (Blank and von Blume 2017; Kapoor et al. 2010). Likewise, Circular Dichroism revealed that binding of Ca^{2+} changes the secondary structure of NUCB1 from an open, rather unstructured conformation to a more alpha-helical state (Pacheco-Fernandez et al. 2020 - Figure S3H). Hereof, structural studies of several EF-hand Ca^{2+}-binding proteins like CaM[99], sorcin or proteins of the S100 family could confirm that Ca^{2+}-induced conformational change of these proteins exposes hydrophobic residues and favors protein-protein interactions (Donato et al. 2013; Ilari et al. 2002; Westerlund and Delemotte 2018). CaM for instance functions as a regulatory protein as it is able to bind more than 300 different peptides upon Ca^{2+}-binding. In line with this, NUCB1-wt but not the Ca^{2+}-binding-deficient mutant NUCB1mEFh1-2 that is also lacking structural change after Ca^{2+}-addition, was able to directly bind cargo molecules like the matrix

---

[98] MGP = Matrix glia protein
[99] CaM = Calmodulin

metalloproteinases MMP2 and MT1-MMP (Pacheco-Fernandez et al. 2020 - Figures 5 and S4).

Ca^{2+}- and consequently cargo binding of NUCB1 was important for intra-Golgi transport of MMPs and impairment of NUCB1 function resulted in their reduced conveyance and secretion (Pacheco-Fernandez et al. 2020 - Figures 2, 3, 4 and 5). MMP2 is known for its role in metastatic cancer by regulating ECM-degradation and cell invasion. In this regard, knockdown of NUCB1 was also associated with reduced invasion of MDA-MB-231 cells and defects in gelatin degradation of human macrophages (Pacheco-Fernandez et al. 2020 - Figures 7 and 8). As MT1-MMP activates MMP2 at the cell surface, zymography assays were performed to confirm that intra-Golgi transport of MMPs, but not activation of MMP2 was the reason for impaired ECM remodeling (Pacheco-Fernandez et al. 2020 - Figure S5A, B). Overall, Ca^{2+}-dependent cargo binding of both described EF-hand-proteins was essential for sorting and transport of soluble secreted proteins. But how are these processes facilitated?

4.2   Cab45 sorts cargo proteins by retention and release

Despite the multitude of evidences that have been made during the last decades, the sorting of soluble secreted molecules is comparatively poorly understood. This applies not only to soluble protein sorting at the TGN but also within sorting events in the early Secretory Pathway. According to their structural diversity and the absence of a consensus recognition motif, almost no cargo receptors are known for these soluble molecules that could facilitate sorting into vesicles. Recently, our lab has investigated a receptor-independent sorting mechanisms for soluble secreted proteins at the TGN, focusing on a role for the Ca^{2+}-dependent oligomerization of the EF-hand protein Cab45. However, how cargo proteins are actively sorted into post-Golgi vesicles is still an open question (Crevenna et al. 2016; Deng et al. 2018). To date, there are no cargo receptors or other membrane proteins known to bind Cab45 or to Cab45 client proteins, and also if the Cab45-client-complex interacts with lipids in the TGN membrane remains unclear. In scope of this thesis, we demonstrate that the Golgi kinase Fam20C phosphorylates Cab45 on five distinct residues (S99, T131, S142, T193, S349) (Hecht et al. 2020 - Figure 3), which significantly increases sorting and secretion of Cab45 clients and moreover reduces the size of the Cab45 oligomers (Hecht et al. 2020). But how does the size of the Cab45 oligomers affect the secretion of its client LyzC?

To comprehend sorting of soluble secreted molecules at the TGN, it might be worth considering how this process is accomplished at the ER, where packaging is limited to one defined class of transport carriers, the COPII vesicles. Here, some cargo receptors have been identified (e.g. ERGIC-53, or Erv proteins) responsible for the sorting of a subset of soluble proteins; nevertheless, for many cargo proteins no such receptors are known (Dancourt and Barlowe 2010). Accordingly, a certain amount of soluble secretory cargo sorting is thought to be an effect of bulk-flow - the packaging of proteins by default, whereas proteins are not actively concentrated or enriched in the vesicle (Barlowe and Helenius 2016). Multiple lines of evidence support the existence of a bulk-flow pathway: On the one hand, the lack of disruption to proteins' ER export despite the mutation or depletion of several key components e.g. potential recognition motifs or receptors (Castillon et al. 2011). On the other hand the efficient export and secretion of foreign proteins like GFP, HRP, bacterial proteins or single peptides, that most likely lack native sorting motifs or cargo receptors (Bard et al. 2006; Eiden-Plach et al. 2004; Thor et al. 2009; Wiedmann, Huth, and Rapoport 1984). As a consequence, it was hypothesized that proteins leave the ER and are secreted non-specifically in a bulk-flow manner, if they are not actively retained in the compartment or sorted via specific cargo receptors. In line with this, the overexpression of soluble secretory proteins often also increases its secretion rate, which was interpreted as oversaturation of the retention system and non-specific uptake into secretory vesicles. Moreover, secretion of ER-resident proteins was observed when recycling cargo receptors like p24 were depleted (Ma, Goldberg, and Goldberg 2017).

Besides the known recycling cargo receptors e.g. KDEL or ERGIC-53 that recognize soluble proteins at the ERGIC or *cis*-Golgi and mediate retrograde transport via COPI vesicles, the existence of an ER retention matrix was proposed. This "immobile matrix" consists of ER-resident proteins and unfolded or incorrectly folded proteins that are bound to chaperons. This matrix is distinguishable from the "mobile phase" that contains predominately proteins ready for ER-exit (Pfeffer and Rothman 1987). In support of this notion, ER-resident proteins such as the heat shock protein BiP are known to homo-oligomerize and can form multiple bindings with other ER-resident proteins and so have the potential to form a retention meshwork. Accordingly, secretion of misfolded proteins could be induced when chaperone interaction was abolished (Marcus and Perlmutter 2000).

Contradictory to the bulk-flow hypothesis, many soluble secreted proteins are active molecules e.g. ECM-degrading enzymes or hormones whereby secretion has to be tightly

regulated and triggered (Rothman 2002). According to the lack of sorting receptors and our recent discoveries, we propose a mechanism for the sorting of soluble secreted molecules at the TGN, which is sequentially based on the retention of those molecules via Cab45, followed by their regulated release (Hecht et al. 2020).

In the first step, Ca^{2+} that is imported into the TGN leads to the oligomerization of Cab45 and the binding of specific soluble secretory proteins (Cab45 clients). As a result, cargo proteins like LyzC or COMP are concentrated and segregated from bulk-flow cargo molecules e.g. OPN, which leave the TGN at irregular intervals (Crevenna et al. 2016; Deng et al. 2018; Hecht et al. 2020 - Figures 5G and S4C). To date, our *in vitro* analysis has been unable to determine a precise size for these Cab45-client-complexes, so one alternative possibility is that Cab45 may not form defined oligomers but adopt a mesh-like, "immobile matrix" conformation (data not shown). However, the transferability of these *in vitro* experiments has to be carefully considered, as existing studies have shown discrepancies between *in vivo* and *in vitro* observations. Indeed, protein concentration, pH, Ca^{2+}-availability as well as the presence of other cofactors or proteins in living cells may directly influence the assembly and disassembly of oligomers (Dunsing et al. 2018; Ruesink et al. 2019; Wang et al. 2018). Comparable to Cab45, many important chaperons and folding factors in the ER that form this potential "immobile matrix" are high-capacity Ca^{2+}-binding proteins e.g. PDI, BiP or CRT. Moreover, Ca^{2+}-depletion in the ER is associated with the aberrant secretion of misfolded as well as ER-resident proteins (Nigam et al. 1994; Sambrook 1990). Consistent with these observations, the ability of Cab45 to bind Ca^{2+} and to oligomerize directly influences its residence in the TGN. This is conclusive as we could detect Cab45 in cell culture supernatant in some experimental conditions, despite its annotation as a Golgi-resident protein (Scherer et al. 1996). In this regard, Cab45-6EQ, a Ca^{2+}-binding-deficient mutant that is no longer able to form higher molecular weight structures, accumulates in vesicles around the Golgi complex at steady state and was also observed to be hypersecreted into the extracellular space (Crevenna et al. 2016). A similar effect is seen in HeLa cells that have been treated with Ca^{2+} ionophore A23187, where the secretion of endogenous Cab45 is markedly increased (von Blume et al. 2012). These Ca^{2+}-dependent retention mechanisms may be a more general feature of ER-resident Ca^{2+}-binding proteins, as reticuloplasmins have been shown to be released from the ER when cells are treated with Ca^{2+} ionophores (Booth and Koch 1989). Moreover, in the aforementioned study, Booth and Koch claimed that these proteins form such an "immobile matrix" in their Ca^{2+}-bound state, which regulates their retention in the ER. In line with this,

also the "sorting by retention" model of SG proteins postulates the active retention of proteins via aggregation (Borgonovo, Ouwendijk, and Solimena 2006; Dannies 1999; Tooze 1998).

In the next step, we propose that phosphorylation of Cab45 by Fam20C disassembles the Cab45 "immobile matrix" and enables packaging into SM-rich vesicles. Our data has revealed that the phosphorylation-mimicking mutant Cab45-5pXE forms smaller and less intense oligomeric structures after Ca^{2+}-addition (Hecht et al. 2020 - Figures 7). The dissociation of multimer structures upon phosphorylation is not without precedence and has been shown for several other proteins including Sae2 or heat shock protein αB-crystallin (Fu et al. 2014; Ito et al. 2001). Furthermore, our data show that expression of Cab45-5pXE specifically enhances the sorting and secretion of Cab45 cargo LyzC (Hecht et al. 2020 - Figure 5). This is in opposition to the non-phosphorylated mutant Cab45-5pXA, which forms larger oligomeric structures *in vitro* and according to its expression, delays cargo secretion (Hecht et al. 2020 - Figures 5 and 7). Strikingly, the same phenotype is also observed in Fam20C-KO cells (Hecht et al. 2020 - Figure 1).

Cab45 phosphorylation sites are not located within the EF-hand domains, so it is not surprising that these different Cab45-phosphomutants are still able to bind Ca^{2+}, change their secondary structure and bind cargo molecules (LyzC) (Hecht et al. 2020 - Figure S2). Cab45 oligomerizes specifically at Ca^{2+}-rich microdomains, where SPCA1 is located and the SM-content is enriched. As a consequence, phosphorylated, disassembled Cab45 is no longer retained and is more efficiently sorted into SM-rich vesicles (Hecht et al. 2020 - Figure 6). This was reflected in the subcellular localization of the Cab45-5pXE mutant that was present in post-Golgi vesicles at steady state, similarly to Cab45-6EQ (Hecht et al. 2020 - Figure 4). As phosphorylation and dissociation of Cab45 multimers takes place in close proximity to "TGN exit sites", we could show that Fam20C buds together with Cab45 in SM-rich vesicles (Hecht et al. 2020 - Figure 2).

In contrast to the Cab45-phosphomutants, the vesicular located Ca^{2+}-binding-deficient mutant Cab45-6EQ shows a missorting phenotype. One assumption is that Cab45-6EQ, which is not able to bind Ca^{2+} and so form oligomers, is not concentrated together with the cargo proteins in those specific Ca^{2+}-rich/SPCA1/SM-rich microdomains but instead exits from the TGN at multiple sites. As a result, Cab45 clients like LyzC are not properly sorted but leave the ER in the form of bulk-flow vesicles, which are not specifically enriched in SM (Deng et al. 2018). The fact that cells expressing Cab45-6EQ or with reduced amounts of

endogenous Cab45 exhibit decreased LyzC secretion, might be because of these missorting effects or because of lower secretion rates via bulk-flow (Crevenna et al. 2016).
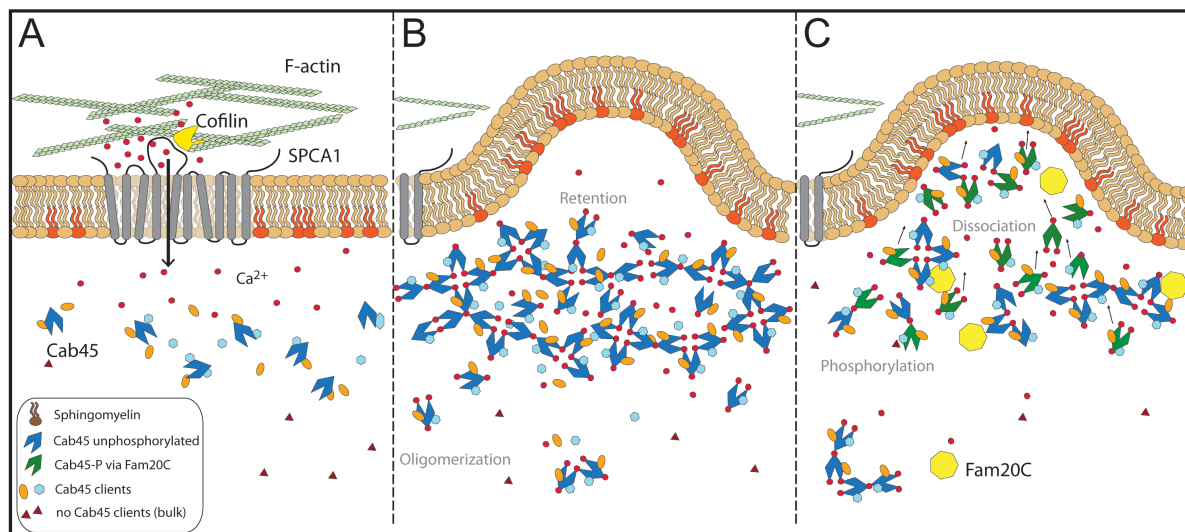
Figure 18: Fam20C phosphorylates Cab45 and regulates client secretion by oligomer disassembly. The model depicts the newly examined role of Fam20C in Cab45 client sorting. (A) SPCA1 interacts with cofilin via its second cytosolic loop, recruiting actin and promoting an influx of Ca^{2+} into the lumen of the TGN. (B) Cab45 oligomerizes in the presence of Ca^{2+}, binds secretory cargo molecules like LyzC and forms an immobile matrix that retains the Cab45-client-complex in the TGN. (C) After phosphorylation by Fam20C, Cab45 oligomers disassemble, which abolishes its TGN-retention and promotes the sorting into SM-rich vesicles (Hecht et al. 2020).

Overall, this leaves the question how dissociation of Cab45, or Cab45 in general can drive vesicle formation. One option would be the direct or indirect interaction of Cab45 with transmembrane proteins or lipids, e.g. as shown for the clustering of GPI-anchored proteins in form of lipid rafts (Paladino et al. 2004). By interaction with the TGN membrane, the Cab45-client-network could form a molecular scaffold that imposes internal forces on the luminal membrane to generate membrane bilayer asymmetry that ultimately promotes membrane deformation (Römer et al. 2007; Stachowiak et al. 2012). Therefore, the Cab45-complex would have curvature active properties analogous to the endocytosis of toxins such as STx[100]. Similar mechanisms have also been proposed for the cellular entry of CTx[101] and the VP1 capsid protein of simian vacuolating virus 40 (SV40), which generate membrane invaginations in the absence of a cytosolic machinery (Ewers et al. 2010; Johannes and Römer 2010; Ling et al. 1998; Pezeshkian et al. 2017). In this regard, higher molecular weight Cab45 complexes could actively initiate vesicle formation dependent on their sorting status. Subsequently, the disassembly of the "immobile matrix" due to phosphorylation by Fam20C would allow Cab45 as well as its clients to enter budding vesicles. Unfortunately, no such data

---

[100] STx = Shiga toxin
[101] CTx = Cholera toxin

exist for the interaction of Cab45 with the TGN membrane and warrants further investigation.

Altogether, Cab45 regulates the sorting of soluble secreted molecules due to the formation of high molecular weight structures, but how can NUCB1 drive intra-Golgi transport?

4.3 NUCB1 regulates MMP intra-Golgi transport via Ca^{2+}

Two major models of intra-Golgi transport models have been proposed over the last decades. Regarding the Golgi cisternal maturation model with tubules, *trans*-cisternae evolve from younger ones by the exchange of membrane components and Golgi enzymes. Thereby, cargo molecules are postulated to mainly remain within the "same" compartment, pending its maturation to *trans*-Golgi cisternae. Due to physical limitations in vesicular retrograde transport of Golgi resident proteins, and the observation that secreted cargo molecules exhibit different cargo transport rates, this initial cisternal maturation model was revised to reflect that tubules forming between the cisternae can also influence transport dynamics (Glick and Luini 2011). Interestingly, high resolution imaging techniques including correlative light-electron microscopy (CLEM) have shown that intercisternal tubules formed during active cargo transport and dissociate after cargo molecules leave the Golgi apparatus (Beznoussenko et al. 2014; Marsh et al. 2004; Trucco et al. 2004). According to the narrow distances between neighboring Golgi cisternae of 10-20 nm, studies also suggested that tube formation is a fact of lacking vesicle membrane fission (Linstedt 1999; Martínez-Alonso, Tomás, and Martínez-Menárguez 2013), wherefore it makes it difficult to clearly distinguish between tube and vesicle formation. However, specifically this vesicular transport is part and parcel of the vesicular transport model of Golgi traffic, which assumes static Golgi cisternae with resident enzymes, but the progression of cargo molecules through the stack in form of vesicles (Glick and Luini 2011). Comparison of different cargo molecules both in the data presented in this thesis and in existing literature have revealed that cargo molecules move through the Golgi with different velocity (Beznoussenko et al. 2014; Hecht et al. 2020; Mironov and Beznoussenko 2012; Pacheco-Fernandez et al. 2020). For example, MMP2 intra-Golgi transport was regulated by the expression of endogenous NUCB1 and additionally much faster than for example NUCB1-independent LyzC transport (Pacheco-Fernandez et al. 2020 - Figure 2). Overall, this indicates that NUCB1 clients are actively transported through the

Golgi apparatus via vesicles or tubules - accomplished by both aforementioned models, and do not traverse the Golgi in a bulk-flow process with other proteins.

Common to both intra-Golgi transport models is the requirement for membrane asymmetry to induce the membrane perturbations required during tubule and vesicle formation. Several cytosolic components are known to induce positive membrane curvatures and therefore contribute to the initiation of tube and vesicle formation. This includes membrane proteins with an intrinsic curvature (e.g. BAR proteins), coat-forming components (e.g. COPI) or proteins that upon membrane binding insert an amphipathic helix as a physical wedge within the lipid matrix (e.g. Sar1, Arf1) (Dunlop et al. 2017; Linstedt 1999; Martínez-Menárguez 2013; Zimmerberg and Kozlov 2006). Additionally, lipid modifying enzymes e.g. cytosolic lipid kinases or phospholipases, play a key role in membrane lipid regulation, which in turn can influence membrane dynamics and shape. One such enzyme, cPLA2α[102] has been previously implicated in intracisternal tube formation through the generation of the inverted-cone-shaped lysophosphatidic acid (LPA) (Martínez-Menárguez et al. 2001). It was revealed that silencing of cPLA2α and use of phosphoinhibitors could specifically block cisternal tube formation, whereas overexpression of cPLA2α resulted in hypertubulation. The ability to form intracisternal tubules was furthermore linked with proper cargo transport and intact Golgi morphology (De Figueiredo et al. 1998, 1999; San Pietro et al. 2009; Ward et al. 2012). Accordingly, vesicle or tube formation might be triggered from the cytosol; however, this raises the question why knockout or knockdown of NUCB1 only affects intra-Golgi transport of specific clients and not of other proteins like LyzC.

As discussed above, luminal proteins have the potential to induce membrane curvature upon molecular crowding and thereby control transport/sorting rates (Snead et al. 2017). Similarly to Cab45, NUCB1 directly binds its clients in a Ca^{2+}-dependent manner (Pacheco-Fernandez et al. 2020 - Figure 1 and S3D, E) and might also form high molecular weight structures that result in spontaneous membrane curvature. To date, there is no data available regarding NUCB1 oligomerization. However, preliminary data from the Miller laboratory suggest that also NUCB1 is indeed able to oligomerize upon Ca^{2+}-binding (not published; communication with Liz Miller, MRC Laboratory of Molecular Biology, UK). Along with Cab45, the ability to form higher molecular weight structures upon Ca^{2+}-binding is shared by several other EF-hand Ca^{2+}-binding proteins like CSQ[103], sorcin or members of the S100 protein family (Fritz

---

[102] cPLA2α = Cytosolic phospholipase A2 alpha
[103] CSQ = Calsequestrin

et al. 2010; Sanchez et al. 2012; Zamparelli et al. 1997). Interestingly, NUCB1 has been shown to associate with the Golgi membrane in an as yet unknown manner; further studies of the impact of NUCB1 oligomerization on membrane dynamics may help dissect these outstanding questions (Stachowiak et al., 2012; Pezehikian et al., 2016, Römer et al., 2007).

If the parallels between NUCB1 and Cab45 are correct, it may be that NUCB1 also forms an "immobile matrix" and the dissociation of this mesh-like structure would be essential for proper cargo transport. Intriguingly, analogous to Cab45, NUCB1 carries Fam20C phosphorylation sites (S86; T148; S369). These sites were confirmed by mass spectrometry and, comparable to Cab45 phosphorylation sites, do not localize within the EF-hand motifs of NUCB1, suggesting they may not influence Ca^{2+} binding but perform a similar regulatory role (Tagliabracci et al. 2015).
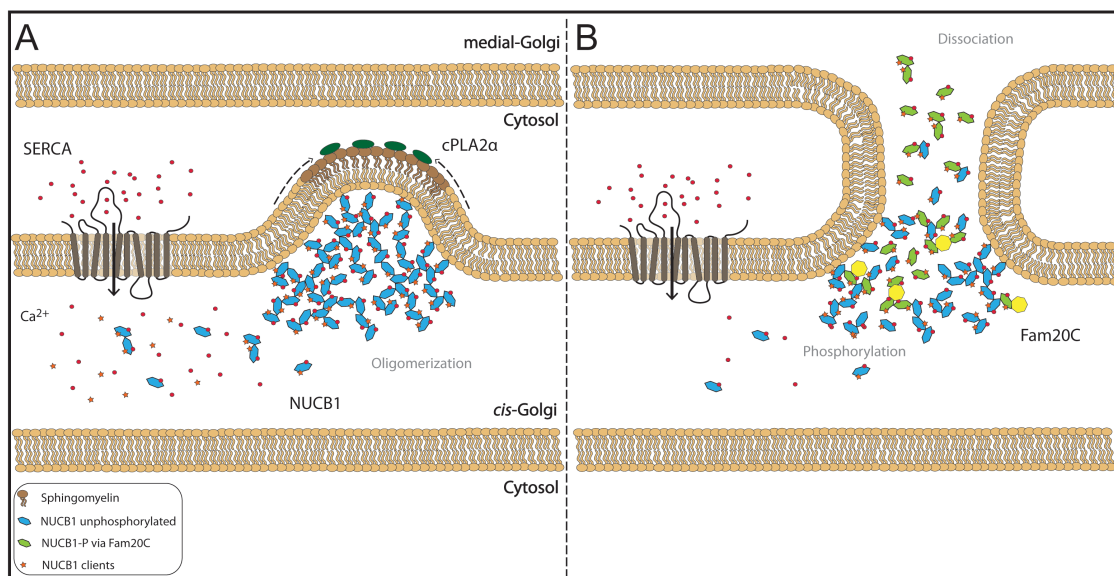
Figure 19: NUCB1 binds and transports clients in a Ca^{2+}-dependent manner. The model depicts the NUCB1-regulated intra-Golgi transport of clients. (A) The EF-hand Ca^{2+}-binding protein NUCB1 binds Ca^{2+} that is locally pumped into the lumen of the *cis*-Golgi by the Ca^{2+}-ATPase SERCA. As a result, NUCB1 interacts with cargo molecules like MMP2 and congregates them by forming higher molecular weight structures. This oligomerization process further induces membrane curvature and promotes vesicle or intracisternal tube formation, supported by cPLA2α. (B) The phosphorylation of NUCB1 by Golgi kinase Fam20C triggers the dissociation of the NUCB1-client-complexes and allows further transport into the medial-Golgi compartment (Pacheco et al. 2020).

As NUCB1 is travelling through the Golgi stack, this NUCB1 accumulation process might occur in every cisterna, whereas the effect is most dominant at the *cis*-Golgi were SERCA is highly expressed and Ca^{2+} concentrations are 3-fold higher compared to the TGN (Pacheco-Fernandez et al. 2020 - Figure 3 and 4; Pizzo et al. 2011). Evidently, it is of great relevance to investigate if NUCB1 actually forms higher molecular weight structures, and indeed, if like

Cab45 clients, this has any influence on MMP transport throughout the Golgi. Further studies are required to reveal the complexities of MMP sorting at the TGN and the role of NUCB1 and Cab45 in this process. In this regard, MMP2 was partially found together with LyzC in post-Golgi vesicles (Pacheco-Fernandez et al. 2020 - Figure S2) and also NUCB1 is secreted into the extracellular space (Miura et al. 1992; Petersson et al. 2004; Wendel et al. 1995).

Overall, Ca^{2+} seems to be a common factor for the described processes. Therefore, the last section will discuss how Ca^{2+}-signaling and Ca^{2+} homeostasis at the different Golgi compartments may influence trafficking and sorting events.

4.4 Regulation of Ca^{2+}-dependent transport and sorting processes at the Golgi apparatus

In case of Cab45-based cargo sorting, we could show that local Ca^{2+} levels are increased by the pumping activity of SPCA1 (Kienzle et al. 2014). As Ca^{2+} is involved in numerous signaling cascades with a high degree of cross-talk, I want to highlight how the ion not only contributes to the described Cab45- and NUCB1-dependent processes but potentially also initiates them. In line with this, several studies could demonstrate that Ca^{2+}-signaling triggers secretion of molecules in secretory cells e.g. goblet cells, a process called Ca^{2+}-triggered exocytosis and that Ca^{2+} homeostasis of the Golgi apparatus is crucial for membrane transport (Anantharam and Kreutzberger 2019; Lissandron et al. 2010; Micaroni et al. 2010).

Since many secretory proteins are active substances, their secretion should be tightly regulated and controlled by extracellular events (Rothman 2002). Therefore, we assume that if protein secretion is required, external stimuli are transmitted internally via signaling cascades e.g. via the secondary messenger Ca^{2+}. In this regard, Ca^{2+} itself might play a key role in the regulation of SPCA1. Kienzle et al. 2014 have shown that the ATPase is activated by un-phosphorylated cofilin1, which binds to SPCA1 in its second cytosolic loop. Meanwhile, de-phosphorylation of cofilin1 occurs by phosphatases of the SSH family (Bamburg 1999; Niwa et al. 2002), which are activated by the PI3K[104]/AKT signaling pathway and in turn is initiated by Ca^{2+}-influx into the cell (Danciu et al. 2003; Nishita et al. 2004; Wang, Shibasaki, and Mizuno 2005).

---

[104] PI3K = Phosphoinositide 3-kinase

Similarly, *in vitro* and *in vivo* studies could confirm that external stimulus e.g. by EGF[105] is activating PLC, which also controls membrane-associated cofilin1 (Van Rheenen et al. 2007). PLC additionally cleaves PIP_2 into DAG and IP_3, and IP_3 on the other hand opens the Ca^{2+}-release channel IP_3R of storage compartments like the ER (Bootman 2012; Thatcher 2010). As a consequence, these signaling cascades would not only activate SPCA1 but also provide a pool of cytosolic Ca^{2+} that could be pumped into the TGN by the Ca^{2+}-ATPase. Recent data on SPCA1a has furthermore shown that this isoform exhibit a N-terminal EF-hand-like domain, which binds Ca^{2+} and promotes ATPase activity (Chen et al. 2019).

Besides these cytosolic pathways, are there also luminal factors that might additionally control SPCA1 activity? Strikingly, analysis of mass spectrometry data revealed Fam20C as an interaction partner of SPCA1 (J. Zhang et al. 2018). This is interesting, as Fam20C might be regulated by SPCA1, which pumps also Mn^{2+} - the co-factor of the Fam20C kinase. Moreover, Fam20C activity is dependent on sphingolipids, whereas SM synthesis is coupled to SPCA1 activity (Cozza et al. 2015, 2017; Deng et al. 2018; Dode et al. 2006; Tagliabracci et al. 2012). As a result, activation of SPCA1 might not only leading to Ca^{2+}-influx into the TGN but also to Mn^{2+}-transport, which would spatiotemporally couple Ca^{2+}-dependent oligomerization, cargo binding and the phosphorylation-dependent dissociation of Cab45 by Fam20C.

Whereas Cab45 and SPCA1 act in Ca^{2+}-dependent transport events at the TGN, NUCB1 seems to play a key role in the transport of MMPs at early Golgi compartments. But how is Ca^{2+} homeostasis maintained at the *cis*-Golgi? Here, SERCA regulates the Ca^{2+}-influx and acts as an opponent to ion channels RyR and IP_3R (Pizzo et al. 2011). SERCA can be indirectly activated in a Ca^{2+}-dependent manner via cytosolic kinases PKA and CaMKII[106]. PKA is known to be activated by secondary messenger cyclic AMP (cAMP) in response to external stimuli; however, recent data have also revealed a cAMP-independent pathway operating via Ca^{2+} and the EF-hand Ca^{2+}-binding protein S100A (Dunn, Storm, and Feller 2009; Melville et al. 2017). Moreover, Ca^{2+} also controls CaMKII by Ca^{2+}-bound CaM that releases the autoinhibition of CaMKII and furthermore induces autophosphorylation and activation of the kinase (Scholz and Palfrey 1998; Shifman et al. 2006). In both cases, activation results in phosphorylation and dissociation of the cytosolic SERCA suppressors SLN[107] and PLN[108],

---

[105] EGF = Epidermal growth factor
[106] CaMKII = Calmodulin kinase II
[107] SLN = Sarcolipin
[108] PLN = Cardiac phospholamban

which regulate Ca^{2+}-influx into the organelle by increasing the Ca^{2+}-binding affinity of SERCA (Shaikh, Sahoo, and Periasamy 2016). Additionally, several luminal factors were shown to associate with the Ca^{2+}-pump and are involved in its activity. Paradoxically, this includes predominately SR/ER-resident proteins like ERp57, SAR and HRC or the Ca^{2+}-binding chaperons CRT and CNX; making it difficult to understand how the *cis*-localizing SERCA might be regulated from its luminal site (Vandecaetsbeek et al. 2011; Vanoevelen et al. 2005).

Within the cell, several EF-hand Ca^{2+}-binding proteins function as Ca^{2+}-sensors that according to structural changes in their Ca^{2+}-(un)bound state directly interfere with Ca^{2+}-pumps or ion release channels and therefore play a crucial role in Ca^{2+} homeostasis of the organelle. One example are STIM[109] proteins that oligomerize in the presence of low Ca^{2+} levels in the ER membrane and form a complex together with Orai1[110], which mediates Ca^{2+}-influx from the extracellular space directly into the lumen of the ER (Gudlur et al. 2018; Soboloff et al. 2012). CaM on the other hand monitors Ca^{2+} levels individually and can activate but also inactivate Ca^{2+}-release channels through different interaction sites and conformational states (Kovalevskaya et al. 2013; Shah et al. 2006).

Using a *cis*-Golgi-localizing FRET-based Ca^{2+}-sensor, we could demonstrate that functional NUCB1 is essential for Ca^{2+} homeostasis at the *cis*-Golgi. In contrast, the knockout of the protein did not affect Ca^{2+} levels in the TGN, where no SERCA is expressed (Pacheco-Fernandez et al. 2020 - Figure 6). Therefore, NUCB1 could have a similar function as STIM or another Ca^{2+}-binding protein calumenin and activate SERCA via binding to its luminal side when Ca^{2+} levels are low. In line with this, NUCB1 was also observed associated with the Golgi membrane (Lavoie et al. 2002; Leclerc et al. 2008) and interaction with SERCA could furthermore explain why NUCB1 is annotated as a *cis*-Golgi-localizing protein, even if it follows intra-Golgi transport and is partially secreted. After activation of SERCA and the increasing Ca^{2+} concentrations in the *cis*-Golgi, Ca^{2+} binds to NUCB1 with low affinity, which leads to a conformational change of the protein, its dissociation from SERCA and the binding of cargo molecules like MMP2 or MT1-MMP.

Although Ca^{2+}-signaling might play a key role in the activation of both described processes, this has to be carefully evaluated, as these are highly dynamic and very complex pathways. The activation of e.g. SERCA is often examined in the context of ER stress and Ca^{2+}-initiated apoptosis, where it interacts with cytosolic p53 to indirectly mediates Ca^{2+}-influx into the

---

[109] STIM = Stromal interaction molecule
[110] Orai1 = Ca^{2+}-release-activated Ca^{2+}-channel protein 1

mitochondria via mitochondria-associated membranes (MAM) (Giorgi et al. 2015; Kroemer, Bravo-San Pedro, and Galluzzi 2015). As a consequence, apoptotic factors like Cyt c[111], AIF[112] or pc-9[113] are released from the mitochondria into the cytosol (Giorgi et al. 2015). To counter this, the anti-apoptotic proteins Bcl-2[114] and Hax-I[115] also interact with SERCA on its cytosolic face and inactivate the Ca^{2+}-pump (Foyouzi-Youssefi et al. 2000; Schoneich, Dremina, and Hewarathna 2017). Therefore, the consequence of Ca^{2+} dysregulation can have disastrous consequences, yet more information is required regarding the regulation of SERCA activity under steady state conditions. Overall, organelle Ca^{2+} homeostasis is meticulously maintained by a combination of both cytosolic and luminal factors. This also explains why the behavior of compartments with similar subsets of Ca^{2+}-pumps and release channels e.g. the ER and the *cis*-Golgi is different upon a given stimulus (Canato et al. 2010; Pizzo et al. 2010; Yang et al. 2015).

Nevertheless, the activation of the Golgi ATPases SPCA1 and SERCA via cytosolic Ca^{2+}-signaling and their potential luminal interaction with Fam20C or NUCB1, respectively, would be an attractive way to regulate transport and sorting of soluble secreted molecules. Furthermore, Ca^{2+}-signaling might have multiple roles in the transport and sorting of NUCB1 and Cab45 clients, as it is also able to activate cytosolic kinases like cPLA2α that are involved in tube or vesicle formation through lipid modifications (San Pietro et al. 2009; Ward et al. 2012). Altogether, there are numerous ways in which Ca^{2+} can regulate sorting and transport processes of soluble secreted proteins both directly and indirectly. Consequently, there is much more to understand about the relevance of Ca^{2+} in membrane trafficking, which opens many possibilities for further in-depth investigations.

---

[111] Cyt c = Cytochrome c
[112] AIF = Apoptosis inducing factor
[113] pc-9 = Procaspase-9
[114] Bcl-2 = B-cell lymphoma 2
[115] Hax-I = HS-1 axxociated protien X-1

5.   Concluding remarks and outlook

Within the scope of this thesis we have investigated the two EF-hand Ca^{2+}-binding proteins NUCB1 and Cab45, and their role in the intra-Golgi transport and sorting of soluble secretory cargo molecules. In this regard, our results provide a unique insight into how luminal Ca^{2+} in the Golgi apparatus plays a key role in both of the aforementioned processes. As Cab45 and NUCB1 share similar features, we proposed a common mechanism that relies on the Ca^{2+}-dependent concentration and retention of cargo molecules followed by their regulated release upon phosphorylation by Golgi kinase Fam20C.

To prove our model it is imperative to understand the oligomerization behavior of NUCB1. Similarly to our Cab45 studies, we were able to purify NUCB1 from HEK293 cells, suggesting we can implement established assays like the microscopy-based oligomerization assay or native PAGE; but also other methods including dynamic light scattering, analytical ultracentrifugation or size exclusion chromatography can be used to determine the size of NUCB1 oligomers at different Ca^{2+} concentrations. Moreover, structural insights of both EF-hand proteins would support our understanding of how oligomers form and what functions they serve in transport and sorting of cargo molecules. Indeed, the effect of NUCB1 phosphorylation by Fam20C on its oligomerization potential will likely reveal further insight into this process and any similarities with Cab45.

So far, all described membrane transport events require an (in)direct interaction of cargo molecules with membrane or cytosolic components. Whereas NUCB1 associates with the Golgi membrane in an unknown manner, no such interaction was annotated for Cab45. Therefore, future experiments e.g. via BioID should investigate how and if both EF-hand proteins interact with (trans)membrane proteins to mediate transport. Additionally, the use of *in vitro* reconstitutions of liposomes or giant unilamellar vesicles (GUVs) can help to determine if any direct interaction with membrane lipids is taking place. As Cab45 client LyzC was found to be transported to the PM via CARTS, it might be interesting if the reported SM-rich vesicles actually are CARTS, positive for Rab6a and Rab8a, and if secretion is further dependent on PKD and Eg5.

As luminal Ca^{2+} plays an essential role in cargo transport and sorting, another significant question is how Ca^{2+}-influx into the Golgi is regulated. Particularly it would be interesting to test if NUCB1 and Fam20C can activate SERCA and SPCA1, respectively, from the luminal side. Immunoprecipitation experiments with luminal peptides can be used to analyze if there

is an interaction between the Ca^{2+}-ATPases and the luminal proteins. Additionally, existing Ca^{2+} and Mn^{2+}-sensors would enable analysis of whether these proteins can specifically trigger Ca^{2+}- or Mn^{2+}-influx.

Overall, answering these fundamental questions would help to understand how the Golgi apparatus manages to transport and sort soluble secreted proteins in the absence of cargo receptors, in a Ca^{2+}-dependent fashion.

6. References

Acharya, Chitrangada, Jasper H. N. Yik, Ashleen Kishore, Victoria Van Dinh, Paul E. Di Cesare, and Dominik R. Haudenschild. 2014. "Cartilage Oligomeric Matrix Protein and Its Binding Partners in the Cartilage Extracellular Matrix: Interaction, Regulation and Role in Chondrogenesis." *Matrix Biology* 37:102–11.

Agnew, Brian J., Laurie S. Minamide, and James R. Bamburg. 1995. "Reactivation of Phosphorylated Actin Depolymerizing Factor and Identifiction of the Regulatory Site." *The Journal of Biological Chemistry* 279(29):17582–87.

De Alba, Eva and Nico Tjandra. 2004. "Structural Studies on the Ca2+-Binding Domain of Human Nucleobindin (Calnuc)." *Biochemistry* 43(31):10039–49.

Alberts, Bruce, Alexander Johnson, Julian Lewis, Martin Raff, Keith Roberts, and Peter Walter. 2002. *Molecular Biology of the Cell.* 4th Editio. New York: Garland Science.

Alfalah, Marwan, Ralf Jacob, Ute Preuss, Klaus Peter Zimmer, Hussein Naim, and Hassan Y. Naim. 1999. "O-Linked Glycans Mediate Apical Sorting of Human Intestinal Sucrase-Isomaltase through Association with Lipid Rafts." *Current Biology* 9(11):593–96.

Almeida, Claudia G., Ayako Yamada, Daniele Tenza, Daniel Louvard, Graca Raposo, and Evelyne Coudrier. 2011. "Myosin 1b Promotes the Formation of Post-Golgi Carriers by Regulating Actin Assembly and Membrane Remodelling at the Trans-Golgi Network." *Nature Cell Biology* 13(7):779–89.

Alonso, María Teresa, Jonathan Rojo-Ruiz, Paloma Navas-Navarro, Macarena Rodríguez-Prados, and Javier García-Sancho. 2017a. "Measuring Ca2+ inside Intracellular Organelles with Luminescent and Fluorescent Aequorin-Based Sensors." *Biochimica et Biophysica Acta* 1864:894–99.

Alonso, María Teresa, Jonathan Rojo-Ruiz, Paloma Navas-Navarro, Macarena Rodríguez-Prados, and Javier García-Sancho. 2017b. "Measuring Ca2 + inside Intracellular Organelles with Luminescent and Fluorescent Aequorin-Based Sensors." *Biochimica et Biophysica Acta - Molecular Cell Research* 1864:894–99.

Alpy, Fabien and Catherine Tomasetto. 2005. "Give Lipids a START : The StAR-Related Lipid Transfer (START) Domain in Mammals." *Journal of Cell Science* 118:2791–2801.

Anantharam, Arun and Alex J. B. Kreutzberger. 2019. "Unraveling the Mechanisms of Calcium-Dependent Secretion." *Journal of General Physiology* 151(4):417–34.

Anelli, Tiziana, Leda Bergamelli, Eva Margittai, Alessandro Rimessi, Claudio Fagioli, Antonio Malgaroli, Paolo Pinton, Maddalena Ripamonti, Rosario Rizzuto, and Roberto Sitia. 2012. "Ero1 a Regulates Ca2+ Fluxes at the Endoplasmic-Mitochondira Interface (MAM)." *Antioxidants and Redox Signaling* 16(10):1077–87.

Ang, Agnes Lee, Heike Fölsch, Ulla Maija Koivisto, Marc Pypaert, and Ira Mellman. 2003. "The Rab8 GTPase Selectively Regulates AP-1B-Dependent Basolateral Transport in Polarized Madin-Darby Canine Kidney Cells." *Journal of Cell Biology* 163(2):339–50.

Ang, Agnes Lee, Tomohiko Taguchi, Stephen Francis, Heike Fölsch, Lindsay J. Murrells, Marc Pypaert, Graham Warren, and Ira Mellman. 2004. "Recycling Endosomes Can Serve as Intermediates during Transport from the Golgi to the Plasma Membrane of MDCK Cells." *Journal of Cell Biology* 167(3):531–43.

Anitei, Mihaela and Bernard Hoflack. 2011. "Exit from the Trans-Golgi Network: From Molecules to Mechanisms." *Current Opinion in Cell Biology* 23(4):443–51.

Apell, Hans-Jürgen. 2004. "How Do P-Type ATPases Transport Ions ?" *Bioelectrochemistry* 63:149–56.

Appenzeller-Herzog, Christian and Hans-Peter Hauri. 2006. "The ER-Golgi Intermediate Compartment (ERGIC): In Search of Its Identity and Function." *Journal of Cell Science* 119:2173–83.

Arakel, Eric C. and Blanche Schwappach. 2018. "Formation of COPI-Coated Vesicles at a Glance." *Journal of Cell Science* 131:1–9.

Araki, Kazutaka and Kazuhiro Nagata. 2012. "Protein Folding and Quality Control in the ER." *Cold Spring Harbor Perspectives in Biology* 4(8):1–25.

Arber, S., F. A. Barbayannis, H. Hanser, C. Schnelder, C. A. Stanyon, O. Bernards, and P. Caroni. 1998. "Regulation of Actin Dynamics through Phosphorylation of Cofilin by LIM- Kinase." *Nature* 393(6687):805–9.

Archibald, John M. 2015. "Endosymbiosis and Eukaryotic Cell Evolution." *Current Biology* 25:911–21.

Ardito, Fatima, Michele Giuliani, Donatella Perrone, Giuseppe Troiano, and Lorenzo Lo Muzio. 2017. "The Crucial Role of Protein Phosphorylation in Cell Signaling and Its Use as Targeted Therapy (Review)." *International Journal of Molecular Medicine* 40:271–80.

Arvan, Peter and David Castle. 1998. *Sorting and Storage during Secretory Granule Biogenesis : Looking Backward and Looking Forward.* Vol. 332.

Aviram, Naama and Maya Schuldiner. 2017. "Targeting and Translocation of Proteins to the Endoplasmic Reticulum at a Glance." *Journal of Cell Science* 130:4079–85.

References

Bagur, Rafaela and György Hajnoczky. 2017. "Intracellular Ca2+ Sensing: Role in Calcium Homeostasis Andsignaling." *Mol Cell.* 66(6):780–88.

Balla, Tamas, Nivedita Sengupta, and Yeun Ju Kim. 2019. "Lipid Synthesis and Transport Are Coupled to Regulate Membrane Lipid Dynamics in the Endoplasmic Reticulum." *Molecular and Cell Biology of Lipids* 1865(2020).

Bamburg, James R. 1999. "PROTEINS OF THE ADF/COFILIN FAMILY: Essential Regulators OfActin Dynamics." *Annu. Rev. Cell Dev. Biol* 15:185–230.

Bamburg, James R. and Barbara W. Bernstein. 2010. "Roles of ADF/Cofilin in Actin Polymerization and Beyond." *F1000 Biology Reports* 2(1):1–7.

Bankaitis, Vytas A., Rafael Garcia-Mata, and Carl J. Mously. 2012. "Golgi Membrane Dynamics Viewed Through a Lens of Lipids." *Curr Biol.* 22(10):1–7.

Bard, Frederic, Laetitia Casano, Arrate Mallabiabarrena, Erin Wallace, Kota Saito, Hitoshi Kitayama, Gianni Guizzunti, Yue Hu, Franz Wendler, Ramanuj DasGupta, Norbert Perrimon, and Vivek Malhotra. 2006. "Functional Genomics Reveals Genes Involved in Protein Secretion and Golgi Organization." *Nature* 439(7076):604–7.

Barinaga-Rementeria Ramirez, Irene and Martin Lowe. 2009. "Golgins and GRASPs: Holding the Golgi Together." *Seminars in Cell and Developmental Biology* 20(7):770–79.

Barlowe, Charles and Ari Helenius. 2016. "Cargo Capture and Bulk Flow in the Early Secretory Pathway." *Annu. Rev. Cell Dev. Biol* 32:1–26.

Barlowe, Charles K. and Elizabeth A. Miller. 2013. "Secretory Protein Biogenesis and Traffic in the Early Secretory Pathway." *Genetics* 193:383–410.

Benting, Jürgen H., Anton G. Rietveld, and Kai Simons. 1999. "N-Glycans Mediate the Apical Sorting of a GPI-Anchored, Raft-Associated Protein in Madin-Darby Canine Kidney Cells." *Journal of Cell Biology* 146(2):313–20.

Berridge, Michael J., Peter Lipp, and Martin D. Bootman. 2000. "THE VERSATILITY AND UNIVERSALITY OF CALCIUM SIGNALLING." *Nature Reviews Molecular Cell Biology* 1:11–21.

Beznoussenko, Galina V., Seetharaman Parashuraman, Riccardo Rizzo, Roman Polishchuk, Oliviano Martella, Daniele Di Giandomenico, Aurora Fusella, Alexander Spaar, Michele Sallese, Maria Grazia Capestrano, Margit Pavelka, Matthijn R. Vos, Yuri G. M. Rikers, Volkhard Helms, Alexandre A. Mironov, and Alberto Luini. 2014. "Transport of Soluble Proteins through the Golgi Occurs by Diffusion via Continuities across Cisternae." *ELife* 2014(3):1–27.

Bhattacharya, Shibani, Christopher G. Bunick, and Walter J. Chazin. 2004. "Target Selectivity in EF-Hand Calcium Binding Proteins." *Biochimica et Biophysica Acta - Molecular Cell Research* 1742(1–3):69–79.

Bieberich, Erhard. 2014. "Synthesis, Processing, and Function of N-Glycans in N- Glycoproteins." *Adv Neurobiol.* 9:47–70.

Blair, Adrienne, Andrew Tomlinson, Hung Pham, Kristin C. Gunsalus, Michael L. Goldberg, and Frank A. Laski. 2006. "Twinstar, the Drosophila Homolog of Cofilin/ADF, Is Required for Planar Cell Polarity Patterning." *Development* 133(9):1789–97.

Blair, Laura J., Jeremy D. Baker, Jonathan J. Sabbagh, and Chad A. Dickey. 2015. "The Emerging Role of Peptidyl-Prolyl Isomerase Chaperones in Tau Oligomerization, Amyloid Processing and Alzheimer's Disease." *J Neurochem.* 133(1):1–13.

Blank, Birgit and Julia von Blume. 2017. "Cab45—Unraveling Key Features of a Novel Secretory Cargo Sorter at the Trans-Golgi Network." *European Journal of Cell Biology* 96(5):383–90.

Blazquez, Mercedes, Christoph Thiele, Wieland B. Huttner, Kevin Docherty, and Kathleen I. J. Shennan. 2000. *Involvement of the Membrane Lipid Bilayer in Sorting Prohormone Convertase 2 into the Regulated Secretory Pathway*. Vol. 349.

Blom, Tomas, Pentti Somerharju, and Elina Ikonen. 2011. "Synthesis and Biosynthetic Trafficking of Membrane Lipids." *Cold Spring Harbor Perspectives in Biology* 3(8):1–16.

von Blume, Julia, Anne Marie Alleaume, Gerard Cantero-Recasens, Amy Curwin, Amado Carreras-Sureda, Timo Zimmermann, Josse van Galen, Yuichi Wakana, Miguel Angel Valverde, and Vivek Malhotra. 2011. "ADF/Cofilin Regulates Secretory Cargo Sorting at the TGN via the Ca2+ ATPase SPCA1." *Developmental Cell* 20(5):652–62.

von Blume, Julia, Anne Marie Alleaume, Christine Kienzle, Amado Carreras-Sureda, Miguel Valverde, and Vivek Malhotra. 2012. "Cab45 Is Required for Ca2+;-Dependent Secretory Cargo Sorting at the Trans-Golgi Network." *Journal of Cell Biology* 199(7):1057–66.

von Blume, Julia, Juan M. Duran, Elena Forlanelli, Anne Marie Alleaume, Mikhail Egorov, Roman Polishchuk, Henrik Molina, and Vivek Malhotra. 2009. "Actin Remodeling by ADF/Cofilin Is Required for Cargo Sorting at the Trans-Golgi Network." *Journal of Cell Biology* 187(7):1055–69.

von Blume, Julia and Angelika Hausser. 2019. "Lipid-Dependent Coupling of Secretory Cargo Sorting and

Trafficking at the Trans-Golgi Network." *FEBS Letters* 593(17):2412–27.

Boehm, M. and J. S. Bonifacino. 2001. "Adaptins: The Final Recount." *Molecular Biology of the Cell* 12(10):2907–20.

Bohnsack, Markus T. and Enrico Schleiff. 2010. "The Evolution of Protein Targeting and Translocation Systems." *Biochimica et Biophysica Acta - Molecular Cell Research* 1803:1115–30.

Boll, W., H. Ohno, Z. Songyang, I. Rapoport, L. C. Cantley, J. S. Bonifacino, and T. Kirchhausen. 1996. "Sequence Requirements for the Recognition of Tyrosine-Based Endocytic Signals by Clathrin AP-2 Complexes." *The EMBO Journal* 15(21):5789–95.

Boll, Werner, Iris Rapoport, Christian Brunner, Yorgo Modis, Siegfried Prehn, and Tomas Kirchhausen. 2002. "The M2 Subunit of the Clathrin Adaptor AP-2 Binds to FDNPVY and YppØ Sorting Signals at Distinct Sites." *Traffic* 3(8):590–600.

Bonfanti, Lidia, Alexander A. Jr. Mironov, Jose A. Martinez-Menarguez, Oliviano Martella, Aurora Fusella, Massimiliano Baldassarre, Roberto Buccione, Hans J. Geuze, Alexander A. Mironov, and Alberto Luini. 1998. "Procollagen Traverses the Golgi Stack without Leaving the Lumen of Cisternae : Evidence for Cisternal Maturation." *Cell* 95:993–1003.

Bonifacino, Juan S. 2004. "The GGA Proteins: Adaptors on the Move." *Nature Reviews Molecular Cell Biology* 5(1):23–32.

Bonifacino, Juan S. 2014. "Adaptor Proteins Involved in Polarized Sorting." *Journal of Cell Biology* 204(1):7–17.

Bonifacino, Juan S. and Benjamin S. Glick. 2004. "The Mechanisms of Vesicle Budding and Fusion." *Cell* 116:153–66.

Bonifacino, Juan S. and Linton M. Traub. 2003. "Signals for Sorting of Transmembrane Proteins to Endosomes and Lysosomes." *Annual Review of Biochemistry* 72(1):395–447.

Bonito-Oliva, Alessandra, Shahar Barbash, Thomas P. Sakmar, and W. Vallen Graham. 2017. "Nucleobindin 1 Binds to Multiple Types of Pre-Fibrillar Amyloid and Inhibits Fibrillization." *Scientific Reports* 7:1–12.

Booth, Catherine and Gordon L. E. Koch. 1989. "Perturbation of Cellular Calcium Induces Secretion of Luminal ER Proteins." *Cell* 59(4):729–37.

Bootman, Martin D. 2012. "Calcium Signaling." *Cold Spring Harbor Perspectives in Biology* 4:1–4.

Le Borgne, Roland and Bernard Hoflack. 1998. "Protein Transport from the Secretory to the Endocytic Pathway in Mammalian Cells." *Biochimica et Biophysica Acta - Molecular Cell Research* 1404(1–2):195–209.

Borgonovo, Barbara, Joke Ouwendijk, and Michele Solimena. 2006. "Biogenesis of Secretory Granules." *Current Opinion in Cell Biology* 18(4):365–70.

Braakman, Ineke and Neil J. Bulleid. 2011. "Protein Folding and Modification in the Mammalian Endoplasmic Reticulum." *Annual Review of Biochemistry* 80:71–99.

Braiterman, Lelita, Lydia Nyasae, Yan Guo, Rodrigo Bustos, Svetlana Lutsenko, and Ann Hubbard. 2009. "Apical Targeting and Golgi Retention Signals Reside within a 9-Amino Acid Sequence in the Copper-ATPase, ATP7B." *American Journal of Physiology - Gastrointestinal and Liver Physiology* 296(2).

Brandizzi, Federica and Charles Barlowe. 2013. "Organization of the ER–Golgi Interface for Membrane Traffic Control." *Nat Rev Mol Cell Biol.* 14(6):382–92.

Braulke, Thomas and Juan S. Bonifacino. 2009. "Sorting of Lysosomal Proteins." *Biochimica et Biophysica Acta - Molecular Cell Research* 1793(4):605–14.

Brewer, C. Fred, M. Carrie Miceli, and Linda G. Baum. 2002. "Clusters, Bundles, Arrays and Lattices: Novel Mechanisms for Lectin-Saccharide-Mediated Cellular Interactions." *Current Opinion in Structural Biology* 12(5):616–23.

Brini, Marisa and Ernesto Carafoli. 2009. "Calcium Pumps in Health and Disease." *Physiol Rev.* 89:1341–78.

Brown, Deborah A. and John K. Rose. 1992. "Sorting of GPI-Anchored Proteins to Glycolipid-Enriched Membrane Subdomains during Transport to the Apical Cell Surface." *Cell* 68(3):533–44.

Brown, J. R. and W. F. Doolittle. 1997. "Archaea and the Prokaryote-to-Eukaryote Transition." *Microbiology and Molecular Biology Reviews : MMBR* 61(4):456–502.

Brown, Paul S., Exing Wang, Benjamin Aroeti, Steven J. Chapin, Keith E. Mostov, and Kenneth W. Dunn. 2000. "Definition of Distinct Compartments in Polarized Madin-Darby Canine Kidney (MDCK) Cells for Membrane-Volume Sorting, Polarized Sorting and Apical Recycling." *Traffic* 1(2):124–40.

Bublitz, Maike, J. Preben Morth, and Poul Nissen. 2012. "P-Type ATPases at a Glance P-Type ATPases at a Glance." *Journal of Cell Science* 124(3917):2515–19.

Burgoyne, Thomas, Sandip Patel, and Emily R. Eden. 2015. "Calcium Signaling at ER Membrane Contact Sites." *Biochimica et Biophysica Acta* 1853:2012–17.

Cai, Huaqing, Karin Reinisch, and Susan Ferro-novick. 2007. "Coats , Tethers , Rabs , and SNAREs Work Together to Mediate the Intracellular Destination of a Transport Vesicle." *Developmental Cell* 12:671–82.

Callewaert, Lien and Chris W. Michiels. 2010. "Lysozymes in the Animal Kingdom." *Journal of Biosciences* 35(1):127–60.

Campbell, Iain D. 2008. "The Croonian Lecture 2006: Structure of the Living Cell." *Philosophical Transactions of the Royal Society B: Biological Sciences* 363:2379–91.

Canato, M., M. Scorzeto, M. Giacomello, F. Protasi, C. Reggiani, and G. J. M. Stienen. 2010. "Massive Alterations of Sarcoplasmic Reticulum Free Calcium in Skeletal Muscle Fi Bers Lacking Calsequestrin Revealed by a Genetically Encoded Probe." *PNAS* 107(51):22326–31.

Canuel, Maryssa, Ann Korkidakis, Kristin Konnyu, and Carlos R. Morales. 2008. "Sortilin Mediates the Lysosomal Targeting of Cathepsins D and H." *Biochemical and Biophysical Research Communications* 373(2):292–97.

Cao, Xinwang, Michal A. Surma, and Kai Simons. 2012. "Polarized Sorting and Trafficking in Epithelial Cells." *Cell Research* 22(5):793–805.

Caramelo, Julio J. and Armando J. Parodi. 2008. "Getting in and out from Calnexin/Calreticulin Cycles." *Journal of Biological Chemistry* 283(16):10221–25.

Casares, Doralicia, Pablo V. Escrib, and Catalina Ana Rossello. 2019. "Membrane Lipid Composition : Effect on Membrane and Organelle Structure, Function and Compartmentalization and Therapeutic Avenues." *International Journal of Molecular Sciences* 20(2167):1–30.

Casler, Jason C., Effrosyni Papanikou, Juan J. Barrero, and Benjamin S. Glick. 2019. "Maturation-Driven Transport and AP-1 – Dependent Recycling of a Secretory Cargo in the Golgi." *The Journal of Cell Biology* 218(5):1582–1601.

Castillon, Guillaume A., Auxiliadora Aguilera-Romero, Javier Manzano-Lopez, Sharon Epstein, Kentaro Kajiwara, Kouichi Funato, Reika Watanabe, Howard Riezman, and Manuel Muñiz. 2011. "The Yeast P24 Complex Regulates Gpi-Anchored Protein Transport and Quality Control by Monitoring Anchor Remodeling." *Molecular Biology of the Cell* 22(16):2924–36.

Cavalli, Giulio and Simone Cenci. 2020. "Autophagy and Protein Secretion." *Journal of Molecular Biology* 2525–45.

Di Cesare, P. E., C. S. Carlson, E. S. Stolerman, N. Hauser, H. Tulli, and M. Paulsson. 1996. "Increased Degradation and Altered Tissue Distribution of Cartilage Oligomeric Matrix Protein in Human Rheumatoid and Osteoarthritic Cartilage." *Journal of Orthopaedic Research* 14(6):946–55.

Di Cesare, Paul E., Frank S. Chen, Matthias Moergelin, Cathy S. Carlson, Michael P. Leslie, Roberto Perris, and Carrie Fang. 2002. "Matrix-Matrix Interaction of Cartilage Oligomeric Matrix Protein and Fibronectin." *Matrix Biology* 21(5):461–70.

Chanat, Eric and Wieland B. Huttner. 1991. *Milieu-Induced, Selective Aggregation of Regulated Secretory Proteins in the Trans-Golgi Network*. Vol. 115.

Chappie, Joshua S. and Fred Dyda. 2013. "Building a Fission Machine-Structural Insights into Dynamin Assembly and Activation." *J. Cell Sci.* 126(13):2773–84.

Chen, Faye H., Mary E. Herndon, Nichlesh Patel, Jacqueline T. Hecht, Rocky S. Tuan, and Jack Lawler. 2007. "Interaction of Cartilage Oligomeric Matrix Protein/Thrombospondin 5 with Aggrecan." *Journal of Biological Chemistry* 282(34):24591–98.

Chen, Faye H., Ashby O. Thomas, Jacqueline T. Hecht, Mary B. Goldring, and Jack Lawler. 2005. "Cartilage Oligomeric Matrix Protein/Thrombospondin 5 Supports Chondrocyte Attachment through Interaction with Integrins." *Journal of Biological Chemistry* 280(38):32655–61.

Chen, Ji-Long, Jatinder P. Ahluwalia, and Mark Stamnes. 2002. "Selective Effects of Calcium Chelators on Anterograde and Retrograde Protein Transport in the Cell." *The Journal of Biological Chemistry* 277(38):35682–87.

Chen, Jialin, Susanne Smaardijk, Charles Alexandre Mattelaer, Filip Pamula, Ilse Vandecaetsbeek, Jo Vanoevelen, Frank Wuytack, Eveline Lescrinier, Jan Eggermont, and Peter Vangheluwe. 2019. "An N-Terminal Ca2+-Binding Motif Regulates the Secretory Pathway Ca2+/Mn2+-Transport ATPase SPCA1." *Journal of Biological Chemistry* 294(19):7878–91.

Chen, Shuo, Lei Chen, Allen Jahangiri, Bo Chen, Yimin Wu, Hui-Hsiu Chuang, Chunlin Qin, and Mary Macdougall. 2008. "Expression and Processing of Small Integrin-Binding Ligand N-Linked Glycoproteins in Mouse Odontoblastic Cells." *Archives of Oral Biology* 53:879–89.

Chen, W. J., J. L. Goldstein, and M. S. Brown. 1990. "NPXY, a Sequence Often Found in Cytoplasmic Tails, Is Required for Coated Pit-Mediated Internalization of the Low Density Lipoprotein Receptor." *Journal of Biological Chemistry* 265(6):3116–23.

Chia, Pei Zhi Cheryl and Paul A. Gleeson. 2014. "Membrane Tethering." *F1000Prime Reports* 6(74):1–14.

Chmelar, Renée S. and Neil M. Nathanson. 2006. "Identification of a Novel Apical Sorting Motif and Mechanism of Targeting of the M2 Muscarinic Acetylcholine Receptor." *Journal of Biological Chemistry* 281(46):35381–96.

Chuang, Jen Zen and Ching Hwa Sung. 1998. "The Cytoplasmic Tail of Rhodopsin Acts as a Novel Apical Sorting Signal in Polarized MDCK Cells." *Journal of Cell Biology* 142(5):1245–56.

Clarke, David M., Tip W. Loo, Giuseppe Inesit, and David H. MacLennan. 1989. "Location of High Affinity Ca2+-Binding Sites within the Predicted Transmembrane Domain of the Sarco- Plasmic Reticulum Ca2+-ATPase." *Nature* 339:476–78.

Clerc, Simone, Christian Hirsch, Daniela Maria Oggier, Paola Deprez, Claude Jakob, Thomas Sommer, and Markus Aebi. 2009. "Htm1 Protein Generates the N-Glycan Signal for Glycoprotein Degradation in the Endoplasmic Reticulum." *Journal of Cell Biology* 184(1):159–72.

Clermont, Y., A. Rambourg, and L. Hermo. 1995. "Trans-Golgi Network (TGN) of Different Cell Types: Three-Dimension Al Structural Characteristics and Variability." *The Anatomical Record* 242:289–301.

Cocucci, Emanuele, Raphaël Gaudin, and Tom Kirchhausen. 2014. "Dynamin Recruitment and Membrane Scission at the Neck of a Clathrin-Coated Pit." *Molecular Biology of the Cell* 25(22):3595–3609.

Colomer, Veronica, Gregory A. Kicska, and Michael J. Rindler. 1996. "Secretory Granule Content Proteins and the Luminal Domains of Granule Membrane Proteins Aggregate in Vitro at Mildly Acidic PH*." *The Journal of Biological Chemistry* 271(1):48–55.

Conner, Sean D. and Sandra L. Schmid. 2003. "Regulated Portals of Entry into the Cell." *Nature* 422(6927):37–44.

Corthesy-Theulaz, Irene and Suzanne R. Pfeffer. 1992. "Microtubule-Mediated Golgi Capture by Semiintact Chinese Hamster Ovary Cells." *Methods in Enzymology* 219:159–65.

Coskun, Ünal and Kai Simons. 2011. "Cell Membranes : The Lipid Perspective." *Structure* 19:1543–48.

Coussen, Francoise, Annick Ayon, Anne Le Goff, Jacqueline Leroy, Jean Massoulie, and Suzanne Bon. 2001. "Addition of a Glycophosphatidylinositol to Acetylcholinesterase." *The Journal of Biological Chemistry* 276(30):27881–92.

Coutinho, Maria Francisca, Maria João Prata, and Sandra Alves. 2012. "Mannose-6-Phosphate Pathway: A Review on Its Role in Lysosomal Function and Dysfunction." *Molecular Genetics and Metabolism* 105(4):542–50.

Cowley, Darrin J., Yancy R. Mooret, Douglas S. Darling, Paul B. M. Joyce, and Sven Ulrik Gorr. 2000. "N- and C-Terminal Domains Direct Cell Type-Specific Sorting of Chromogranin A to Secretory Granules." *Journal of Biological Chemistry* 275(11):7743–48.

Cozza, Giorgio, Mauro Salvi, Sourav Banerjee, Elena Tibaldi, Vincent S. Tagliabracci, Jack E. Dixon, and Lorenzo A. Pinna. 2015. "A New Role for Sphingosine : Up-Regulation of Fam20C , the Genuine Casein Kinase That Phosphorylates Secreted Proteins." *Biochimica et Biophysica Acta* 1854:1718–26.

Cozza, Giorgio, Mauro Salvi, Vincent S. Tagliabracci, and Lorenzo A. Pinna. 2017. "Fam20C Is under the Control of Sphingolipid Signaling in Human Cell Lines." *FEBS Journal* 284:1246–57.

Craig, Elizabeth A. 2018. "Hsp70 at the Membrane: Driving Protein Translocation." *BMC Biology* 16:1–11.

Crevenna, Alvaro H., Birgit Blank, Andreas Maiser, Derya Emin, Jens Prescher, Gisela Beck, Christine Kienzle, Kira Bartnik, Bianca Habermann, Mehrshad Pakde, Heinrich Leonhardt, Don C. Lamb, and Julia von Blume. 2016. "Secretory Cargo Sorting by Ca2+-Dependent Cab45 Oligomerization at the Trans-Golgi Network." *Journal of Cell Biology* 213(3):305–14.

Cui, Jixin, Junyu Xiao, Vincent S. Tagliabracci, Jianzhong Wen, Meghdad Rahdar, and Jack E. Dixon. 2015. "A Secretory Kinase Complex Regulates Extracellular Protein Phosphorylation." *ELife* 4:1–18.

Cui, Jixin, Qinyu Zhu, Hui Zhang, Michael A. Cianfrocco, Andres E. Leschziner, Jack E. Dixon, and Junyu Xiao. 2017. "Structure of Fam20A Reveals a Pseudokinase Featuring a Unique Disulfide Pattern and Inverted ATP-Binding." *ELife* 6:1–16.

Cui, Ning, Min Hu, and Raouf A. Khalil. 2017. "Biochemical and Biological Attributes of Matrix Metalloproteinases." *Prog Mol Biol Tranl Sci* 147:1–73.

Curwin, Amy J., Julia von Blume, and Vivek Malhotra. 2012. "Cofilin-Mediated Sorting and Export of Specific Cargo from the Golgi Apparatus in Yeast." *Molecular Biology of the Cell* 23(12):2327–38.

Dacks, Joel B., Andrew A. Peden, and Mark C. Field. 2009. "Evolution of Specificity in the Eukaryotic Endomembrane System." *International Journal of Biochemistry and Cell Biology* 41:330–40.

Dahms, Nancy M., Linda J. Olson, and Jung Ja P. Kim. 2008. "Strategies for Carbohydrate Recognition by the Mannose 6-Phosphate Receptors." *Glycobiology* 18(9):664–78.

Danciu, Theodora E., Rosalyn M. Adam, Keiji Naruse, Michael R. Freeman, and Peter V. Hauschka. 2003. "Calcium Regulates the PI3K-Akt Pathway in Stretched Osteoblasts." *FEBS Letters* 536(1–3):193–97.

Dancourt, Julia and Charles Barlowe. 2010. "Protein Sorting Receptors in the Early Secretory Pathway." *Annual Review of Biochemistry* 79(1):777–802.

Daniels, Robert, Brad Kurowski, Arthur E. Johnson, and Daniel N. Hebert. 2003. "N-Linked Glycans Direct the Cotranslational Folding Pathway of Influenza Hemagglutinin." *Molecular Cell* 11(1):79–90.

Dannies, Priscilla S. 1999. "Protein Hormone Storage in Secretory Granules: Mechanisms for Concentration and Sorting*." *Endocrine Reviews* 20(1):3–21.

Dannies, Priscilla S. 2001. *Concentrating Hormones into Secretory Granules: Layers of Control.* Vol. 177.

Day, Kasey J., L. Andrew Staehelin, and Benjamin S. Glick. 2013. "A Three-Stage Model of Golgi Structure and Function." *Histochem Cell Biol* 140(3):239–49.

Deckers, Daphne, Dietrich Vanlint, Lien Callewaert, Abram Aertsen, and Chris W. Michiels. 2008. "Role of the Lysozyme Inhibitor Ivy in Growth or Survival of Escherichia Coli and Pseudomonas Aeruginosa Bacteria in Hen Egg White and in Human Saliva and Breast Milk." *Applied and Environmental Microbiology* 74(14):4434–39.

Delaye, Luis and Arturo Becerra. 2012. "Cenancestor, the Last Universal Common Ancestor." *Evolution: Education and Outreach* 5:382–88.

Deng, Yongqiang, Mehrshad Pakdel, Birgit Blank, Emma L. Sundberg, Christopfher G. Burd, and Julia von Blume. 2018. "Activity of the SPCA1 Calcium Pump Couples Sphingomyelin Synthesis to Sorting of Secretory Proteins in the Trans-Golgi Network." *Developmental Cell* 47(4):464–78.

Deng, Yongqiang, Felix E. Rivera-Molina, Derek K. Toomre, and Christopher G. Burd. 2016. "Sphingomyelin Is Sorted at the Trans Golgi Network into a Distinct Class of Secretory Vesicle." *Proceedings of the National Academy of Sciences of the United States of America* 113(24):6677–82.

Dickson, Eamonn J. and Bertil Hille. 2019. "Understanding Phosphoinositides: Rare, Dynamic, and Essential Membrane Phospholipids." *Biochem. J* 476(1):1–23.

Diekmann, Yoan and José B. Pereira-Leal. 2013. "Evolution of Intracellular Compartmentalization." *Biochemical Journal* 449:319–31.

Dikeakos, Jimmy D., Paola Di Lello, Marie-José E. Lacombe, Rodolfo Ghirlando, Pascale Legault, Timothy L. Reudelhuber, and James G. Omichinski. 2009. "Functional and Structural Characterization of a Dense Core Secretory Granule Sorting Domain from the PC1/3 Protease." *Proc. Natl. Acad. Sci.* 106(18):7408–13.

Dittié, Andrea S., Nasser Hajibagheri, and Sharon A. Tooze. 1996. "The AP-1 Adaptor Complex Binds to Immature Secretory Granules from PC12 Cells, and Is Regulated by ADP-Ribosylation Factor." *Journal of Cell Biology* 132(4):523–36.

Dittié, Andrea S., Judith Klumperman, and Sharon A. Tooze. 1999. "Differential Distribution of Mannose-6-Phosphate Receptors and Furin in Immature Secretory Granules." *Journal of Cell Science* 112(22):3955–66.

Dode, Leonard, Jens Peter Andersen, Luc Raeymaekers, Ludwig Missiaen, Bente Vilsen, and Frank Wuytack. 2005. "Functional Comparison between Secretory Pathway Ca2+ / Mn 2+ -ATPase (SPCA) 1 and Sarcoplasmic Reticulum Ca2+ -ATPase (SERCA) 1 Isoforms by Steady-State and Transient Kinetic Analyses." *The Journal of Biological Chemistry* 280(47):39124–34.

Dode, Leonard, Jens Peter Andersen, Jo Vanoevelen, Luc Raeymaekers, Ludwig Missiaen, Bente Vilsen, and Frank Wuytack. 2006. "Dissection of the Functional Differences between Human Isoenzymes by Steady-State and Transient Kinetic Analyses *." *The Journal of Biological Chemistry* 281(6):3182–89.

Dolman, Nick J. and Alexei V Tepikin. 2006. "Calcium Gradients and the Golgi." 40(August):505–12.

Donato, R., B. R. Cannon, G. Sorci, F. Riuzzi, K. Hsu, D. J. Weber, and C. L. Geczy. 2013. "Functions of S100 Proteins." *Curr Mol Med.* 13(1):1–59.

Dong, Ki Kim and Wook Joo Kwon. 2009. "Hyponatremia in Patients with Neurologic Disorders." *Electrolyte and Blood Pressure* 7(2):51–57.

Dröscher, Ariane. 1998. "Camillo Golgi and the Discovery of the Golgi Apparatus." *Histochem Cell Biol* 109:425–30.

Dunlop, Myun Hwa, Andreas M. Ernst, Lena K. Schroeder, Derek K. Toomre, Grégory Lavieu, and James E. Rothman. 2017. "Land-Locked Mammalian Golgi Reveals Cargo Transport between Stable Cisternae." *Nature Communications* 8(1).

Dunn, Timothy A., Daniel R. Storm, and Marla B. Feller. 2009. "Calcium-Dependent Increases in Protein Kinase-A Activity in Mouse Retinal Ganglion Cells Are Mediated by Multiple Adenylate Cyclases." *PLoS ONE* 4(11).

Dunsing, Valentin, Madlen Luckner, Boris Zühlke, Roberto A. Petazzi, Andreas Herrmann, and Salvatore Chiantia. 2018. "Optimal Fluorescent Protein Tags for Quantifying Protein Oligomerization in Living Cells." *Scientific Reports* 8(1):1–12.

van Echten, Gerhild and Konrad Sandhoff. 1989. "Modulation of Ganglioside Biosynthesis in Primary Cultured Neurons." *Journal of Neurochemistry* 52(1):207–14.

Egawa, Nagayasu, Naohiko Koshikawa, Taizo Tomari, Kazuki Nabeshima, Toshiaki Isobe, and Motoharu Seiki. 2006. "Membrane Type 1 Matrix Metalloproteinase (MT1-MMP/MMP-14) Cleaves and Releases a 22-KDa Extracellular Matrix Metalloproteinase Inducer (EMMPRIN) Fragment from Tumor Cells." *Journal of Biological Chemistry* 281(49):37576–85.

Eiden-Plach, Antje, Tatjana Zagorc, Tanja Heintel, Yvonne Carius, Frank Breinig, and Manfred J. Schmitt. 2004. "Viral Preprotoxin Signal Sequence Allows Efficient Secretion of Green Fluorescent Protein by Candida Glabrata, Pichia Pastoris, Saccharomyces Cerevisiae, and Schizosaccharomyces Pombe." *Applied and Environmental Microbiology* 70(2):961–66.

References

Von Einem, Bjoern, Anke Wahler, Tobias Schips, Alberto Serrano-Pozo, Christian Proepper, Tobias M. Boeckers, Angelika Rueck, Thomas Wirth, Bradley T. Hyman, Karin M. Danzer, Dietmar R. Thal, and Christine A. F. Von Arnim. 2015. "The Golgi-Localized γ-Ear-Containing ARF-Binding (GGA) Proteins Alter Amyloid-β Precursor Protein (APP) Processing through Interaction of Their GAE Domain with the Beta-Site APP Cleaving Enzyme 1 (BACE1)." *PLoS ONE* 10(6):1–22.

Elalaoui, Chafai Siham, Nada Al-Sheqaih, Ilham Ratbi, Jill E. Urquhart, James O'Sullivan, Sanjeev Bhaskar, Simon S. Williams, Mustapha Elalloussi, Jaber Lyahyai, Leila Sbihi, Cherkaoui Imane Jaouad, Abdelhafid Sbihi, William G. Newman, and Abdelaziz Sefiani. 2016. "European Journal of Medical Genetics Non Lethal Raine Syndrome and Differential Diagnosis." *European Journal of Medical Genetics* 59:577–83.

Elias, Salah, Charlene Delestre, Maite Courel, Youssef Anouar, and Maité Montero-Hadjadje. 2010. "Chromogranin A as a Crucial Factor in the Sorting of Peptide Hormones to Secretory Granules." *Cellular and Molecular Neurobiology* 30:1189–95.

Ellgaard, Lars, Nicholas McCaul, Anna Chatsisvili, and Ineke Braakman. 2016. "Co- and Post-Translational Protein Folding in the ER." *Traffic* 17(6):615–38.

Emr, Scott, Benjamin S. Glick, Adam D. Linstedt, Jennifer Lippincott-schwartz, Alberto Luini, Vivek Malhotra, Brad J. Marsh, Akihiko Nakano, Suzanne R. Pfeffer, Catherine Rabouille, James E. Rothman, Graham Warren, and Felix T. Wieland. 2009. "Journeys through the Golgi — Taking Stock in a New Era." *Journal of Cell Biology* 187(4):449–53.

Ewers, Helge, Winfried Römer, Alicia E. Smith, Kirsten Bacia, Serge Dmitrieff, Wengang Chai, Roberta Mancini, Jürgen Kartenbeck, Valérie Chambon, Ludwig Berland, Ariella Oppenheim, Günter Schwarzmann, Ten Feizi, Petra Schwille, Pierre Sens, Ari Helenius, and Ludger Johannes. 2010. "GM1 Structure Determines SV40-Induced Membrane Invagination and Infection." *Nature Cell Biology* 12(1):11–18.

Fagone, Paolo and Suzanne Jackowski. 2009. "Membrane Phospholipid Synthesis and Endoplasmic Reticulum Function." *Journal of Lipid Research* 50:311–16.

Faini, Marco, Rainer Beck, Felix T. Wieland, and John A. G. Briggs. 2013. "Vesicle Coats: Structure, Function, and General Principles of Assembly." *Trends in Cell Biology* 23(6):279–88.

Fang, Min, Marcos P. Rivas, and Vytas A. Bankaitis. 1998. "The Contribution of Lipids and Lipid Metabolism to Cellular Functions of the Golgi Complex." *Biochimica et Biophysica Acta* 1404:85–100.

Farhan, Hesso and Catherine Rabouille. 2011. "Signalling to and from the Secretory Pathway." *Journal of Cell Science* 124(4):669.

Fernandez-Catalan, Carlos, Wolfram Bode, Robert Huber, Dusan Turk, Juan J. Calvete, Andrea Lichte, Harald Tschesche, and Klaus Maskos. 1998. "Crystal Structure of the Complex Formed by the Membrane Type 1-Matrix Metalloproteinase with the Tissue Inhibitor of Metalloproteinases-2, the Soluble Progelatinase A Receptor." *EMBO Journal* 17(17):5238–48.

Fiedler, Klaus and Kai Simons. 1995. "The Role of N-Glycans in the Secretory Pathway." *Cell* 81(3):309–12.

Field, Mark C. and Joel B. Dacks. 2009. "First and Last Ancestors: Reconstructing Evolution of the Endomembrane System with ESCRTs, Vesicle Coat Proteins, and Nuclear Pore Complexes." *Current Opinion in Cell Biology* 21:4–13.

De Figueiredo, Paul, Daniel Drecktrah, John A. Katzenellenbogen, Marian Strang, and William J. Brown. 1998. "Evidence That Phospholipase A2 Activity Is Required for Golgi Complex and Trans Golgi Network Membrane Tubulation." *PNAS* 95(15):8642–47.

De Figueiredo, Paul, Renée S. Polizotto, Daniel Drecktrah, and William J. Brown. 1999. "Membrane Tubule-Mediated Reassembly and Maintenance of the Golgi Complex Is Disrupted by Phospholipase A2 Antagonists." *Molecular Biology of the Cell* 10(6):1763–82.

Fölsch, Heike, Hiroshi Ohno, Juan S. Bonifacino, and Ira Mellman. 1999. "A Novel Clathrin Adaptor Complex Mediates Basolateral Targeting in Polarized Epithelial Cells." *Cell* 99:189–98.

Ford, Marijn G. J., Ian G. Mills, Brian J. Peter, Yvonne Vallis, Gerrit J. K. Praefcke, Philip R. Evans, and Harvey T. Mcmahon. 2002. "Curvature of Clathrin-Coated Pits Driven by Epsin." *Nature* 419:361–66.

Foyouzi-Youssefi, Reyhaneh, Serge Arnaudeau, Christoph Borner, William L. Kelley, Jürg Tschopp, Daniel P. Lew, Nicolas Demaurex, and Karl Heinz Krause. 2000. "Bcl-2 Decreases the Free Ca2+ Concentration within the Endoplasmic Reticulum." *PNAS* 97(11):5723–28.

Fritz, Günter, Hugo M. Botelho, Ludmilla A. Morozova-Roche, and Cláudio M. Gomes. 2010. "Natural and Amyloid Self-Assembly of S100 Proteins: Structural Basis of Functional Diversity." *FEBS Journal* 277(22):4578–90.

Fu, Qiong, Julia Chow, Kara A. Bernstein, Nodar Makharashvili, Sucheta Arora, Chia-Fang Lee, Maria D. Person, Rodney Rothstein, and Tanya T. Paull. 2014. "Phosphorylation-Regulated Transitions in an Oligomeric State Control the Activity of the Sae2 DNA Repair Enzyme." *Molecular and Cellular Biology* 34(5):778–93.

Funato, Kouichi, Howard Riezman, and Manuel Muñiz. 2019. "Vesicular and Non-Vesicular Lipid Export from

the ER to the Secretory." *Molecular and Cell Biology of Lipids* 1865(2020).

Furtak, Vyacheslav, Frank Hatcher, and Josiah Ochieng. 2001. "Galectin-3 Mediates the Endocytosis of Beta-1 Integrins by Breast Carcinoma Cells." *Biochemical and Biophysical Research Communications* 289:845–50.

Futter, Clare E., Christopher N. Connolly, Daniel F. Cutler, and Colin R. Hopkins. 1995. "Newly Synthesized Transferrin Receptors Can Be Detected in the Endosome before They Appear on the Cell Surface." *The Journal of Biological Chemistry* 270(18):10999–3.

Gabaldón, Toni and Alexandros A. Pittis. 2015. "Origin and Evolution of Metabolic Sub-Cellular Compartmentalization in Eukaryotes." *Biochimie* 119:262–68.

Gaidarov, Ibragim, Jason G. Krupnick, John R. Falck, Jeffrey L. Benovic, and James H. Keen. 1999. "Arrestin Function in G Protein-Coupled Receptor Endocytosis Requires Phosphoinositide Binding." *EMBO Journal* 18(4):871–81.

Gallegos-Gomez, Martin-Leonardo, Elisa Greotti, Maria-Christina Lopez-Mendez, Victor-Hugo Sanchez-Vazquez, Juan-Manuel Arias, and Augustin Guerrero-Hernandez. 2018. "The Trans Golgi Region Is a Labile Intracellular Ca2+ Store Sensitive to Emetine." *Scientific Reports* 8:1–13.

Gao, Caiji, Yi Cai, Yejun Wang, Byung-ho Kang, Fernando Aniento, David G. Robinson, and Liwen Jiang. 2014. "Retention Mechanisms for ER and Golgi Membrane Proteins." *Trends in Plant Science* 19(8):1360–85.

Garcia-Moreno, Bertrand. 2009. "Adaptations of Proteins to Cellular and Subcellular PH." *Journal of Biology* 8(98):1–4.

Gayen, Jiaur R., Yusu Gu, Daniel T. O'Connor, and Sushil K. Mahata. 2009. "Global Disturbances in Autonomic Function Yield Cardiovascular Instability and Hypertension in the Chromogranin A Null Mouse." *Endocrinology* 150(11):5027–35.

Gayen, Jiaur R., Maziyar Saberi, Simon Schenk, Nilima Biswas, Sucheta M. Vaingankar, Wai W. Cheung, Sonia M. Najjar, Daniel T. O'Connor, Gautam Bandyopadhyay, and Sushil K. Mahata. 2009. "A Novel Pathway of Insulin Sensitivity in Chromogranin A Null Mice. A Crucial Role for Pancreastatin in Glucose Homeostasis." *Journal of Biological Chemistry* 284(42):28498–509.

Gayen, Jiaur R., Kuixing Zhang, Satish P. RamachandraRao, Manjula Mahata, Yunqing Chen, Hyung-Suk Kim, Robert K. Naviaux, Kumar Sharma, Sushil K. Mahata, and Daniel T. O'Connor. 2010. "Role of Reactive Oxygen Species in Hyper-Adrenergic Hypertension: Biochemical, Physiological, and Pharmacological Evidence from Targeted Ablation of the Chromogranin A (Chga) Gene." *Circ Cardiovasc Genet.* 3(5):414–25.

Geisler, Carsten, Jes Dietrich, Bodil L. Nielsen, Jesper Kastrup, Jens Peter H. Lauritsen, Niels Ødum, and Mette D. Christensen. 1998. "Leucine-Based Receptor Sorting Motifs Are Dependent on the Spacing Relative to the Plasma Membrane." *Journal of Biological Chemistry* 273(33):21316–23.

George, Anne and Arthur Veis. 2008. "Phosphorylated Proteins and Control Over Apatite Nulcleation, Crystal Growth and Inhibition." *Chem Rev* 108(11):4670–93.

Gerasimenko, Julia V., Mark Sherwood, Alexei V. Tepikin, Ole H. Petersen, and Oleg V. Gerasimenko. 2005. "NAADP , CADPR and IP 3 All Release Ca 2 + from the Endoplasmic Reticulum and an Acidic Store in the Secretory Granule Area." *Journal of Cell Science* 119:226–38.

Gerdes, Hans-Hermann, Patrizia Rosa, Elizabeth Phillips, Patrick A. Baeuerlesli, Rainer Frank, Patrick Argos, and Wieland B. Huttners. 1989. "THE JOURNAL OF BIOLOGICAL CHEMISTRY The Primary Structure of Human Secretogranin IT, a Widespread Tyrosine-Sulfated Secretory Granule Protein That Exhibits Low PH-and Calcium-Induced Aggregation*." *The Journal of Biological Chemistry* 264(20):12009–15.

Gericke, A., C. Qin, L. Spevak, Y. Fujimoto, W. T. Butler, E. S. Sorensen, and A. L. Boskey. 2005. "Importance of Phosphorylation for Osteopontin Regulation of Biomineralization." *Calcif Tissue Int* 77(1):45–54.

Ghartey-Kwansah, George, Zhongguang Li, Rui Feng, Liyang Wang, Xin Zhou, Frederic Z. Chen, Meng Meng Xu, Odell Jones, Yulian Mu, Shawn Chen, Joseph Bryant, Williams B. Isaacs, Jianjie Ma, and Xuehong Xu. 2018. "Comparative Analysis of FKBP Family Protein: Evaluation, Structure, and Function in Mammals and Drosophila Melanogaster." *BMC Developmental Biology* 18(1):1–12.

Ghosh, Pradipta, Nancy M. Dahms, and Stuart Kornfeld. 2003. "Mannose 6-Phosphate Receptors: New Twists in the Tale." *Nature Reviews Molecular Cell Biology* 4(3):202–12.

Ghosh, Pradipta and Stuart Kornfeld. 2003. "AP-1 Binding to Sorting Signals and Release from Clathrin-Coated Vesicles Is Regulated by Phosphorylation." *Journal of Cell Biology* 160(5):699–708.

Ghosh, Pradipta and Stuart Kornfeld. 2004. "The Cytoplasmic Tail of the Cation-Independent Mannose 6-Phosphate Receptor Contains Four Binding Sites for AP-1." *Archives of Biochemistry and Biophysics* 426(2):225–30.

Gillingham, Alison K. and Sean Munro. 2016. "Finding the Golgi : Golgin Coiled-Coil Proteins Show the Way." *Trends in Biotechnology* 26(6):399–408.

Gillon, Amanda D., Catherine F. Latham, and Elizabeth A. Miller. 2012. "Vesicle-Mediated ER Export of Proteins and Lipids." *Biochim Biophys Acta.* 1821(8):1040–49.

Gilmore, Reid, Peter Walter, and Günter Blobel. 1982. "Protein Translocation across the Endoplasmic Reticulum. II. Isolation and Characterization of the Signal Recognition Particle Receptor." *Journal of Cell Biology* 95:470–77.

Giorgi, Carlotta, Massimo Bonora, Giovanni Sorrentino, Sonia Missiroli, Federica Poletti, Jan M. Suski, Fabian Galindo Ramirez, Rosario Rizzuto, Francesco Di Virgilio, Ester Zito, Pier Paolo Pandolfi, Mariusz R. Wieckowski, Fabio Mammano, Giannino Del Sal, and Paolo Pinton. 2015. "P53 at the Endoplasmic Reticulum Regulates Apoptosis in a Ca2+-Dependent Manner." *PNAS* 112(6):1779–84.

Glick, Benjamin S. and Alberto Luini. 2011. "Models for Golgi Traffic : A Critical Assessment." *Cold Spring Harbor Perspectives in Biology* 3:1–15.

Golgi, Camillo. 1989. "On the Structure of Nerve Cells. 1898." *J Microsc.* 155(1):3–7.

Gong, Deshun, Ximin Chi, Kang Ren, Gaoxingyu Huang, Gewei Zhou, Nieng Yan, Jianlin Lei, and Quiang Zho. 2018. "Structure of the Human Plasma Membrane Ca2+-ATPase 1 in Complex with Its Obligatory Subunit Neuroplastin." *Nature Communications* 9(3623):1–9.

Gonzalez, Alfonso and Enrique Rodriguez-Boulan. 2009. "Clathrin and AP1B: Key Roles in Basolateral Trafficking through Trans-Endosomal Routes." *FEBS Letters* 583(23):3784–95.

Gonzalez, Veronica, Rituraj Pal, and Mahesh Narayan. 2010. "The Oxidoreductase Behavior of Protein Disulfide Isomerase Impedes Fold Maturation of Endoplasmic Reticulum-Processed Proteins in the Pivotal Structure-Coupled Step of Oxidative Folding: Implications for Subcellular Protein Trafficking." *Biochemistry* 49(29):6282–89.

Gravotta, Diego, Jose Maria Carvajal-Gonzalez, Rafael Mattera, Sylvie Deborde, Jason R. Banfelder, Juan S. Bonifacino, and Enrique Rodriguez-Boulan. 2012. "The Clathrin Adaptor AP-1A Mediates Basolateral Polarity." *Developmental Cell* 22(4):811–23.

Griffiths, Gareth, Stephen D. Fuller, Ruth Back, Michael Hollinshead, Steve Pfeiffer, and Kai Simons. 1989. *The Dynamic Nature of the Golgi Complex.* Vol. 108.

Griffiths, Gareth, Bernard Hoflack, Kai Simons, Ira Mellman, and Stuart Kornfeld. 1988. "The Mannose 6-Phosphate Receptor and the Biogenesis of Lysosomes." *Cell* 52(3):329–41.

Grigoriev, Ilya, Daniël Splinter, Nanda Keijzer, Phebe S. Wulf, Jeroen Demmers, Toshihisa Ohtsuka, Mauro Modesti, Ivan V. Maly, Frank Grosveld, Casper C. Hoogenraad, and Anna Akhmanova. 2007. "Rab6 Regulates Transport and Targeting of Exocytotic Carriers." *Developmental Cell* 13(2):305–14.

Grigoriev, Ilya, Ka Lou Yu, Emma Martinez-Sanchez, Andrea Serra-Marques, Ihor Smal, Erik Meijering, Jeroen Demmers, Johan Peränen, R. Jeroen Pasterkamp, Peter Van Der Sluijs, Casper C. Hoogenraad, and Anna Akhmanova. 2011. "Rab6, Rab8, and MICAL3 Cooperate in Controlling Docking and Fusion of Exocytotic Carriers." *Current Biology* 21(11):967–74.

Gudlur, Aparna, Ana Eliza Zeraik, Nupura Hirve, V. Rajanikanth, Andrey A. Bobkov, Guolin Ma, Sisi Zheng, Youjun Wang, Yubin Zhou, Elizabeth A. Komives, and Patrick G. Hogan. 2018. "Calcium Sensing by the STIM1 ER-Luminal Domain." *Nature Communications* 9(1):1–15.

Guo, Yusong, Daniel W. Sirkis, and Randy Schekman. 2014. " Protein Sorting at the Trans -Golgi Network ." *Annual Review of Cell and Developmental Biology* 30(1):169–206.

Gustafsen, Camilla, Mads Kjolby, Mette Nyegaard, Manuel Mattheisen, Jesper Lundhede, Henriette Buttenschøn, Ole Mors, Jacob F. Bentzon, Peder Madsen, Anders Nykjaer, and Simon Glerup. 2014. "The Hypercholesterolemia-Risk Gene SORT1 Facilitates PCSK9 Secretion." *Cell Metabolism* 19(2):310–18.

Gut, Anne, Felix Kappeler, Nevila Hyka, Maria S. Balda, Hans Peter Hauri, and Karl Matter. 1998. "Carbohydrate-Mediated Golgi to Cell Surface Transport and Apical Targeting of Membrane Proteins." *EMBO Journal* 17(7):1919–29.

Haglund, Kaisa, Pier Paolo Di Fiore, and Ivan Dikic. 2003. "Distinct Monoubiquitin Signals in Receptor Endocytosis." *Trends in Biochemical Sciences* 28(11):598–604.

Halic, Mario and Roland Beckmann. 2005. "The Signal Recognition Particle and Its Interactions during Protein Targeting." *Current Opinion in Structural Biology* 15:116–25.

Han, Kyu Yeon, Jennifer Dugas-Ford, Motoharu Seiki, Jin Hong Chang, and Dimitri T. Azar. 2015. "Evidence for the Involvement of MMP14 in MMP2 Processing and Recruitment in Exosomes of Corneal Fibroblasts." *Investigative Ophthalmology and Visual Science* 56(9):5323–29.

Hannun, Yusuf A. and Lina M. Obeid. 2008. "Principles of Bioactive Lipid Signalling : Lessons from Sphingolipids." *Nature Review* 9:139–50.

Hannun, Yusuf A. and Lina M. Obeid. 2018. "Sphingolipids and Their Metabolism in Physiology and Disease." *Nature Reviews* 19:175–91.

Hansen, Gert H., Lise-Lotte Niels-Christiansen, Evy Thorsen, Lissi Immerdal, and E. Michael Danielsen. 2000. "Cholesterol Depletion of Enterocytes." *Journal of Biological Chemistry* 275(7):5136–42.

Hanzal-Bayer, Michael F. and John F. Hancock. 2007. "Lipid Rafts and Membrane Traffic." *FEBS Letters* 581(11):2098–2104.

Hara-Kuge, Sayuri, Takashi Ohkura, Hiroko Ideo, Osamu Shimada, Saoko Atsumi, and Katsuko Yamashita. 2002. "Involvement of VIP36 in Intracellular Transport and Secretion of Glycoproteins in Polarized Madin-Darby Canine Kidney (MDCK) Cells." *Journal of Biological Chemistry* 277(18):16332–39.

Harayama, Takeshi and Howard Riezman. 2018. "Understanding the Diversity of Membrane Lipid Composition." *Molecular Cell Biology* 19:281–96.

Hardy, Eugenio, Anette Hardy-Sosa, and Carlos Fernandez-Patron. 2018. "MMP-2: Is Too Low as Bad as Too High in the Cardiovascular System?" *American Journal of Physiology - Heart and Circulatory Physiology* 315(5):H1332–40.

Hauri, Hans Peter, Christian Appenzeller, Franziska Kuhn, and Oliver Nufer. 2000. "Lectins and Traffic in the Secretory Pathway." *FEBS Letters* 476(1–2):32–37.

Hecht, Tobias Karl Heinz, Birgit Blank, Martin Steger, Victor Lopez, Gisela Beck, Bulat Ramazanov, Matthias Mann, Vincent Tagliabracci, and Julia von Blume. 2020. "Fam20C Regulates Protein Secretion by Cab45 Phosphorylation." *The Journal of Cell Biology* 219(6).

Helenius, Ari. 1994. "How N-Linked Oligosaccharides Affect Glycoprotein Folding in the Endoplasmic Reticulum." *Molecular Biology of the Cell* 5(3):253–65.

Helenius, Ari and Markus Aebi. 2004. "Roles of N-Linked Glycans in the Endoplasmic Reticulum." *Annual Review of Biochemistry* 73(1):1019–49.

Henley, John R., Hong Cao, and Mark A. Mcniven. 1999. "Participation of Dynamin in the Biogenesis of Cytoplasmic Vesicles." *FASEB J.* 13:243–47.

Hetz, Claudio. 2012. "The Unfolded Protein Response: Controlling Cell Fate Decisions under ER Stress and Beyond." *Nature Reviews Molecular Cell Biology* 13(2):89–102.

Hille-Rehfeld, Annette. 1995. "Mannose 6-Phosphate Receptors in Sorting and Transport of Lysosomal Enzymes." *Biochimica et Biophysica Acta* 1241:177–94.

Himschoot, Ellie, Roman Pleskot, Daniël Van Damme, and Steffen Vanneste. 2017. "The Ins and Outs of Ca2+ in Plant Endomembrane Trafficking." *Current Opinion in Plant Biology* 40:131–37.

Hinshaw, J. E. 2000. "DYNAMIN AND ITS ROLE IN MEMBRANE FISSION 1." *Annu. Rev. Cell Dev. Biol* 16:483–519.

Hirst, Jennifer, Nicholas A. Bright, Brian Rous, and Margaret S. Robinson. 1999. "Characterization of a Fourth Adaptor-Related Protein Complex." *Molecular Biology of the Cell* 10(8):2787–2802.

Hong, Wanjin. 2005. "SNAREs and Traffic." *Biochim Biophys Acta.* 1744:120–44.

Höning, Stefan, Miguel Sosa, Annette Hille-Rehfeld, and Kurt Von Figura. 1997. "The 46-KDa Mannose 6-Phosphate Receptor Contains Multiple Binding Sites for Clathrin Adaptors." *Journal of Biological Chemistry* 272(32):19884–90.

Honore, Bent. 2009. "The Rapidly Expanding CREC Protein Family: Members , Localization , Function , and Role in Disease." *BioEssays* 31:262–77.

Honore, Bent and Henrik Vorum. 2000. "The CREC Family, a Novel Family of Multiple EF-Hand , Low-Affinity Ca2+-Binding Proteins Localised to the Secretory Pathway of Mammalian Cells." *FEBS Letters* 466:11–18.

Hoogenraad, Casper C., Phebe Wulf, Natalia Schiefermeier, Tatiana Stepanova, Niels Galjart, J. Victor Small, Frank Grosveld, Chris I. de Zeeuw, and Anna Akhmanova. 2003. "Bicaudal D Induces Selective Dynein-Mediated Microtubule Minus End-Directed Transport." *The EMBO Journal* 22(22):6004–15.

Hosaka, Masahiro, Masayuki Suda, Yuko Sakai, Tetsuro Izumi, Tsuyoshi Watanabe, and Toshiyuki Takeuchi. 2004. "Secretogranin III Binds to Cholesterol in the Secretory Granule Membrane as an Adapter for Chromogranin A." *Journal of Biological Chemistry* 279(5):3627–34.

Huckaba, Thomas M., Anna Card Gay, Luiz Fernando Pantalena, Hyeong Cheol Yang, and Liza A. Pon. 2004. "Live Cell Imaging of the Assembly, Disassembly, and Actin Cable-Dependent Movement of Endosomes and Actin Patches in the Budding Yeast, Saccharomyces Cerevisiae." *Journal of Cell Biology* 167(3):519–30.

Hunziker, Walter, Cordula Harter, Karl Matter, and Ira Mellman. 1991. "Basolateral Sorting in MDCK Cells Requires a Distinct Cytoplasmic Domain Determinant." *Cell* 66(5):907–20.

Huttner, Wieland B. and Anne Schmidt. 2000. "Lipids, Lipid Modification and Lipid–Protein Interaction in Membrane Budding and Fission — Insights from the Roles of Endophilin A1 and Synaptophysin in Synaptic Vesicle Endocytosis." *Neuronal and Glia Cell Biology* 10:543–51.

Ilari, Andrea, Kenneth A. Johnson, Vassilios Nastopoulos, Daniela Verzili, Carlotta Zamparelli, Gianni Colotti, Demetrius Tsernoglou, and Emilia Chiancone. 2002. "The Crystal Structure of the Sorcin Calcium Binding Domain Provides a Model of Ca2+-Dependent Processes in the Full-Length Protein." *Journal of Molecular Biology* 317(3):447–58.

Imjeti, Naga Salaija, Stéphanie Lebreton, Simona Paladino, Erwin De La Fuente, Alfonso Gonzalez, and Chiara Zurzolo. 2011. "N-Glycosylation Instead of Cholesterol Mediates Oligomerization and Apical Sorting of GPI-APs in FRT Cells." *Molecular Biology of the Cell* 22(23):4621–34.

Ito, Hidenori, Keiko Kamei, Ikuko Iwamoto, Yutaka Inaguma, Daisuke Nohara, and Kanefusa Kato. 2001.

"Phosphorylation-Induced Change of the Oligomerization State of AB-Crystallin." *Journal of Biological Chemistry* 276(7):5346–52.

Jackson, Catherine L. 2009. "Mechanisms of Transport through the Golgi Complex." *Journal of Cell Science* 122:443–52.

Jackson, Catherine L., Laurence Walch, Jean-marc Verbavatz, and Institut Jacques Monod. 2016. "Lipids and Their Trafficking : An Integral Part of Cellular Organization." *Developmental Cell* 39:139–53.

Jackson, Lauren P. 2014. "Structure and Mechanism of COPI Vesicle Biogenesis." *Current Opinion in Cell Biology* 29:67–73.

Jacquemyn, Julie, Ana Cascalho, and Rose E. Goodchild. 2017. "The Ins and Outs of Endoplasmic Reticulum-Controlled Lipid Biosynthesis." *EMBO Reports* 18(11):1905–21.

Jamieson, James D. and E. Palade. 1968. "INTRACELLULAR TRANSPORT OF SECRETORY PROTEINS IN THE PANCREATIC EXOCRINE CELL." *Journal of Cell Biology* 39(3):589–603.

Jan, Calvin H., Christopher C. Williams, and Jonathan S. Weissman. 2014. "Principles of ER Cotranslational Translocation Revealed by Proximity-Specific Ribosome Profiling." *Science* 346(6210):748–51.

Janda, Claudia Y., Jade Li, Chris Oubridge, Helena Hernández, Carol V. Robinson, and Kiyoshi Nagai. 2010. "Recognition of a Signal Peptide by the Signal Recognition Particle." *Nature* 465:507–10.

Jensen, Anne-Marie Lund, Lykke-Møller Sørensen, Claus Olesen, Jesper Vuust Møller, and Poul Nissen. 2006. "Modulatory and Catalytic Modes of ATP Binding by the Calcium Pump." *The EMBO Journal* 25(11):2305–14.

Jensen, Devon and Randy Schekman. 2011. "COPII-Mediated Vesicle Formation at a Glance." *Journal of Cell Science* 123:1–4.

Jiménez, José L., Björn Hegemann, James RA. Hutchins, Jan-Michael Peters, and Richard Durbin. 2007. "A Systematic Comparative and Structural Analysis of Protein Phosphorylation Sites Based on the MtcPTM Database." *Genome Biology* 8(5):1–20.

Johannes, Ludger and Winfried Römer. 2010. "Shiga Toxins from Cell Biology to Biomedical Applications." *Nature Reviews Microbiology* 8(2):105–16.

Johnson, Nicholas, Katie Powis, and Stephen High. 2013. "Post-Translational Translocation into the Endoplasmic Reticulum." *Biochimica et Biophysica Acta - Molecular Cell Research* 1833:2403–9.

Kahl, Christina R. and Anthony R. Means. 2003. "Regulation of Cell Cycle Progression by Calcium/Calmodulin-Dependent Pathways." *Endocrine Reviews* 24(6):719–36.

Kakhlon, Or, Prabhat Sakya, Banafshe Larijani, Rose Watson, and Sharon A. Tooze. 2006. "GGA Function Is Required for Maturation of Neuroendocrine Secretory Granules." *EMBO Journal* 25(8):1590–1602.

Kanellos, Georgios and Margaret C. Frame. 2016. "Cellular Functions of the ADF/Cofilin Family at a Glance." *Journal of Cell Science* 129(17):3211–18.

Kapoor, Neeraj, Ruchi Gupta, Santosh T. Menon, Ewa Folta-Stogniew, Daniel P. Raleigh, and Thomas P. Sakmar. 2010. "Nucleobindin 1 Is a Calcium-Regulated Guanine Nucleotide Dissociation Inhibitor of Gαi1." *Journal of Biological Chemistry* 285(41):31647–60.

Kasai, Kazuo, Hye-Won Shin, Chisa Shinotsuka, Kazuo Murakami, and Kazuhisa Nakayama. 1999. *Dynamin II Is Involved in Endocytosis but Not in the Formation of Transport Vesicles from the Trans-Golgi Network1.* Vol. 125.

Keller, Patrick and Kai Simons. 1997. "Post-Golgi Biosynthetic Trafficking." *Journal of Cell Science* 110(24):3001–9.

Kellokumpu, Sakari. 2019. "Golgi PH , Ion and Redox Homeostasis : How Much Do They Really Matter ?" *Frontiers in Cell and Developmental Biology* 7(93):1–15.

Kelly, Regis B. 1985. "Pathways of Protein Secretion in Eukaryotes." *Science* 230(4721):25–32.

Kibbey, Richard G., Josep Rizo, Lila M. Gierasch, and Richard G. W. Anderson. 1998. "The LDL Receptor Clustering Motif Interacts with the Clathrin Terminal Domain in a Reverse Turn Conformation." *Journal of Cell Biology* 142(1):59–67.

Kienzle, Christine, Nirakar Basnet, Alvaro H. Crevenna, Gisela Beck, Bianca Habermann, Naoko Mizuno, and Julia von Blume. 2014. "Cofilin Recruits F-Actin to SPCA1 and Promotes Ca2+-Mediated Secretory Cargo Sorting." *Journal of Cell Biology* 206(5):635–54.

Kienzle, Christine and Julia von Blume. 2014. "Secretory Cargo Sorting at the Trans-Golgi Network." *Trends in Cell Biology* 24(10):584–93.

Kinoshita, Taroh. 2014. "Enzymatic Mechanism of GPI Anchor Attachment Clarified." *Cell Cycle* 13(12):1838–39.

Kirchhausen, Tomas. 2000a. "Three Ways to Make a Vesicle." *Nature Reviews Molecular Cell Biology* 1(3):187–98.

Kirchhausen, Tomas. 2000b. "THREE WAYS TO MAKE A VESICLE." *Nature Reviews* 1:187–98.

Klemm, Robin W., Christer S. Ejsing, Michal A. Surma, Hermann Josef Kaiser, Mathias J. Gerl, Julio L. Sampaio,

Quentin De Robillard, Charles Ferguson, Tomasz J. Proszynski, Andrej Shevchenko, and Kai Simons. 2009. "Segregation of Sphingolipids and Sterols during Formation of Secretory Vesicles at the Trans-Golgi Network." *Journal of Cell Biology* 185(4):601–12.

Klumperman, Judith. 2011. "Architecture of the Mammalian Golgi." *Cold Spring Harbor Perspectives in Biology* 3(7):1–19.

Klumperman, Judith, Regina Kuliawat, Janice M. Griffith, Hans J. Geuze, and Peter Arvan. 1998. "Mannose 6-Phosphate Receptors Are Sorted from Immature Secretory Granules via Adaptor Protein AP-1, Clathrin, and Syntaxin 6-Positive Vesicles." *Journal of Cell Biology* 141(2):359–71.

Koike, Toshiyasu, Tomomi Izumikawa, Jun-ichi Tamura, and Hiroshi Kitagawa. 2009. "FAM20B Is a Kinase That Phosphorylates Xylose in the Glycosaminoglycan – Protein Linkage Region." *Biochem. J* 421:157–62.

Koonin, Eugene V. 2010. "The Origin and Early Evolution of Eukaryotes in the Light of Phylogenomics." *Genome Biology* 11(209):1–12.

Kopitz, Jürgen. 2017. "Lipid Glycosylation : A Primer for Histochemists and Cell Biologists." *Histochemistry and Cell Biology* 147(2):175–98.

Kornfeld, Stuart. 1992. "Structure and Function of the Mannose 6-Phosphate/Insulin-like Growth Factor II Receptors." *Annu. Rev. Biochem.* 61:307–30.

Kosuri, Pallav, Jorge Alegre-Cebollada, Jason Feng, Anna Kaplan, Alvaro Inglés-Prieto, Carmen L. Badilla, Brent R. Stockwell, Jose M. Sanchez-Ruiz, Arne Holmgren, and Julio M. Fernández. 2012. "Protein Folding Drives Disulfide Formation." *Cell* 151(4):794–806.

Kovalevskaya, Nadezda V., Michiel Van De Waterbeemd, Fedir M. Bokhovchuk, Neil Bate, René J. M. Bindels, Joost G. J. Hoenderop, and Geerten W. Vuister. 2013. "Structural Analysis of Calmodulin Binding to Ion Channels Demonstrates the Role of Its Plasticity in Regulation." *European Journal of Physiology* 465(11):1507–19.

Kroemer, G., J. M. Bravo-San Pedro, and L. Galluzzi. 2015. "Novel Function of Cytoplasmic P53 at the Interface between Mitochondria and the Endoplasmic Reticulum." *Cell Death & Disease* 6:e1698.

Kroll, Katja A., Stefan Otte, Gregor Hirschfeld, Shitsu Barnikol-Watanabe, Hilde Götz, Hans Sternbach, Hartmut D. Kratzin, Heinz Ulrich Barnikol, and Norbert Hilschmann. 1999. "Heterologous Overexpression of Human NEFA and Studies on the Two EF-Hand Calcium-Binding Sites." *Biochemical and Biophysical Research Communications* 260(1):1–8.

Kühlbrandt, Werner. 2004. "Biology, Structure and Mechanism of P-Type ATPases." *Nature Reviews Molecular Cell Biology* 5(4):282–95.

Kuliawat, Regina and Peter Arvan. 1994. "Distinct Molecular Mechanisms for Protein Sorting within Immature Secretory Granules of Pancreatic β-Cells." *Journal of Cell Biology* 126(1):77–86.

Kuliawat, Regina, Judith Klumperman, Thomas Ludwig, and Peter Arvan. 1997. "Differential Sorting of Lysosomal Enzymes out of the Regulated Secretory Pathway in Pancreatic β-Cells." *Journal of Cell Biology* 137(3):595–608.

Kulkarni-Gosavi, Prajakta, Christian Makhoul, and Paul A. Gleeson. 2019. "Form and Function of the Golgi Apparatus : Scaffolds , Cytoskeleton and Signalling." *FEBS Letters* 593:2289–2305.

Kurokawa, Kazuo and Akihiko Nakano. 2019. "JB Special Review — Organelle Zone The ER Exit Sites Are Specialized ER Zones for the Transport of Cargo Proteins from the ER to the Golgi Apparatus." *The Journal of Biochemistryy* 165(2):109–14.

Kweon, Hee-Seok, Galina V. Beznoussenko, Massimo Micaroni, Roman S. Polishchuk, Alvar Trucco, Oliviano Martella, Daniele Di Giandomenico, Pierfrancesco Marra, Aurora Fusella, Alessio Di Pentima, Eric G. Berger, Willie J. C. Geerts, Abraham J. Koster, Koert N. J. Burger, Alberto Luini, and Alexander A. Mironov. 2004. "Golgi Enzymes Are Enriched in Perforated Zones of Golgi Cisternae but Are Depleted in COPI Vesicles." *Molecular Biology of the Cell* 15:4710–24.

Lakadamyali, Melike, Michael J. Rust, and Xiaowei Zhuang. 2006. "Ligands for Clathrin-Mediated Endocytosis Are Differentially Sorted into Distinct Populations of Early Endosomes." *Cell* 124(5):997–1009.

Lam, Patrick P. L., Kati Hyvärinen, Maria Kauppi, Laura Cosen-Binker, Saara Laitinen, Sirkka Keränen, Herbert Y. Gaisano, and Vesa M. Olkkonen. 2007. "A Cytosolic Splice Variant of Cab45 Interacts with Munc18b and Impacts on Amylase Secretion by Pancreatic Acini." *Molecular Biology of the Cell* 18(July):2473–80.

Lanner, Johanna T., Dimitra K. Georgiou, Aditya D. Joshi, and Susan L. Hamilton. 2010. "Ryanodine Receptors: Structure, Expression, Molecular Details, and Function in Calcium Release." *Cold Spring Harbor Perspectives in Biology* 2:1–21.

Lavoie, Christine, Timo Meerloo, Ping Lin, and Marilyn G. Farquhar. 2002. "Calnuc, an EF-Hand Ca2+-Binding Protein, Is Stored and Processed in the Golgi and Secreted by the Constitutive-like Pathway in AtT20 Cells." *Molecular Endocrinology* 16(11):2462–74.

Lazarovits, Janette and Michael Roth. 1988. "A Single Amino Acid Change in the Cytoplasmic Domain Allows the Influenza Virus Hemagglutinin to Be Endocytosed through Coated Pits." *Cell* 53(5):743–52.

Leclerc, Patrick, Jordane Biarc, Mireille St.-Onge, Caroline Gilbert, Andrée Anne Dussault, Cynthia Laflamme, and Marc Pouliot. 2008. "Nucleobindin Co-Localizes and Associates with Cyclooxygenase (COX)-2 in Human Neutrophils." *PLoS ONE* 3(5):1–10.

Leitch, Sharon, Mingye Feng, Sabine Muend, Lelita T. Braiterman, Ann L. Hubbard, and Rajini Rao. 2011. "Vesicular Distribution of Secretory Pathway Ca2+-ATPase Isoform 1 and a Role in Manganese Detoxification in Liver-Derived Polarized Cells." *Biometals* 24(1):159–70.

Lev, Sima. 2010. "Non-Vesicular Lipid Transport by Lipid-Transfer Proteins and Beyond." *Nature Reviews* 11:739–50.

Lev, Sima. 2012. "Nonvesicular Lipid Transfer from the Endoplasmic Reticulum." *Cold Spring Harbor Perspectives in Biology* 4(10):1–16.

Li, Gang, Marco Mongillo, King-Tung Chin, Heather Harding, David Ron, Andrew R. Marks, and Ira Tabas. 2009. "Role of ERO1a –Mediated Stimulation of Inositol 1,4,5-Triphosphate Receptor Activity in Endoplasmic Reticulum Stress–Induced Apoptosis." *Journal of Cell Biology* 186(6):783–92.

Li, Jie, Erpan Ahat, and Yanzhuang Wang. 2019. "Golgi Structure and Function in Health, Stress, and Diseases." Pp. 441–85 in *Results and Problems in Cell Differentiation*. Vol. 67. Springer Verlag.

Li, Li-Hua, Xiang-Rong Tian, Zheng Jiang, Liu-Wang Zeng, Wen-Fang He, and Zhi-Ping Hu. 2013. "The Golgi Apparatus : Panel Point of Cytosolic Ca2+ Regulation." *Neurosignals* 21:272–84.

Liljedahl, Monika, Yusuke Maeda, Antonino Colanzi, Inmaculada Ayala, Johan Van Lint, and Vivek Malhotra. 2001. "Protein Kinase D Regulates the Fission of Cell Surface Destined Transport Carriers from the Trans-Golgi Network." *Cell* 104(3):409–20.

Lin, Jonathan H., Peter Walter, and T. S. Benedict Yen. 2008. "Endoplasmic Reticulum Stress in Disease Pathogenesis." *Annu Rev Pathol* 3:399–425.

Lin, Ping, Helen Le-Niculescu, Robert Hofmeister, J. Michael McCaffery, Mingjie Jin, Hanjo Hennemann, Tammie McQuistan, Luc De Vries, and Marilyn Gist Farquhar. 1998. "The Mammalian Calcium-Binding Protein, Nucleobindin (CALNUC), Is a Golgi Resident Protein." *Journal of Cell Biology* 141(7):1515–27.

Lin, Ping, Yong Yao, Robert Hofmeister, Roger Y. Tsien, and Marilyn Gist Farquhar. 1999. "Overexpression of CALNUC (Nucleobindin) Increases Agonist and Thapsigargin Releasable Ca2+ Storage in the Golgi." *Journal of Cell Biology* 145(2):279–89.

Linders, Peter TA., Chiel van der Horst, Martin ter Beest, and Geert van den Bogaart. 2019. "Stx5-Mediated ER-Golgi Transport in Mammals and Yeast." *Cells* 8(780):1–16.

Ling, Hong, Amechand Boodhoo, Bart Hazes, Maxwell D. Cummings, Glen D. Armstrong, James L. Brunton, and Randy J. Read. 1998. "Structure of the Shiga-like Toxin I B-Pentamer Complexed with an Analogue of Its Receptor Gb3." *Biochemistry* 37(7):1777–88.

Lingwood, Daniel and Kai Simons. 2010. "Lipid Rafts as a Membrane-Organizing Principle." *Science* 327(5961):46–50.

Linstedt, Adam D. 1999. "Golgi Complex: Stacking the Cisternae." *Current Biology* 9(23):893–96.

Linxweiler, Maximilian, Bernhard Schick, and Richard Zimmermann. 2017. "Let's Talk about Secs: Sec61, Sec62 and Sec63 in Signal Transduction, Oncology and Personalized Medicine." *Signal Transduction and Targeted Therapy* 2:1–10.

Lipardi, Concetta, Lucio Nitsch, and Chiara Zurzolo. 2000. "Detergent-Insoluble GPI-Anchored Proteins Are Apically Sorted in Fischer Rat Thyroid Cells, but Interference with Cholesterol or Sphingolipids Differentially Affects Detergent Insolubility and Apical Sorting." *Molecular Biology of the Cell* 11(2):531–42.

Lippincott-Schwartz, Jennifer, Theresa H. Roberts, and Koret Hirschberg. 2000. "Secretory Protein Trafficking and Organelle Dynamics in Living Cells." *Annu. Rev. Cell Dev. Biol* 16:557–89.

Lissandron, Valentina, Paola Podini, Paola Pizzo, and Tullio Pozzan. 2010. "Unique Characteristics of Ca2+ Homeostasis of the Trans-Golgi Compartment." *PNAS* 107(20):9198–9203.

Liu, Chuan Yin and Randal J. Kaufman. 2003. "The Unfolded Protein Response." *Journal of Cell Science* 116(10):1861–62.

Liu, Peihong, Su Ma, Hua Zhang, Chao Liu, Yongbo Lu, Li Chen, and Chunlin Qin. 2017. "Specific Ablation of Mouse Fam20C in Cells Expressing Type I Collagen Leads to Skeletal Defects and Hypophosphatemia." *Scientific Reports* 7(3590):1–10.

Lupashin, Vladimir and Elizabeth Sztul. 2005. "Golgi Tethering Factors." *Biochimica et Biophysica Acta* 1744:325–39.

Ma, Tianji, Baiying Li, Ryan Wang, Pik Ki Lau, Yan Huang, Liwen Jiang, Randy Schekman, and Yusong Guo. 2018. "A Mechanism for Differential Sorting of the Planar Cell Polarity Proteins Frizzled6 and Vangl2 at the Trans-Golgi Network." *Journal of Biological Chemistry* 293(22):8410–27.

Ma, Wenfu, Elena Goldberg, and Jonathan Goldberg. 2017. "ER Retention Is Imposed by COPII Protein Sorting and Attenuated by 4-Phenylbutyrate." *ELife* 6:1–22.

Maccioni, Hugo J. F. 2007. "Glycosylation of Glycolipids in the Golgi Complex." *Journal of Neurochemistry* 103:81–90.

Malemud, Charles J. 2006. "Department of Medicine, Division of Rheumatic Diseases and Department of Anatomy, Case Western Reserve University School of Medicine, Cleveland, Ohio." *Frontiers in Bioscience* 11:1696–1701.

Malsam, Jörg, Ayano Satoh, Laurence Pelletier, and Graham Warren. 2005. "Golgin Tethers Define Subpopulations of COPI Vesicles." *Scientific* 307:1095–99.

Marcus, Nancy Y. and David H. Perlmutter. 2000. "Glucosidase and Mannosidase Inhibitors Mediate Increased Secretion of Mutant A1 Antitrypsin Z." *Journal of Biological Chemistry* 275(3):1987–92.

Marino, Marianna, Tatiana Stoilova, Carlotta Giorgi, Angela Bachi, Angela Cattaneo, Alberto Auricchio, Paolo Pinton, and Ester Zito. 2015. "SEPN1, an Endoplasmic Reticulum-Localized Selenoprotein Linked to Skeletal Muscle Pathology, Counteracts Hyperoxidation by Means of Redox-Regulating SERCA2 Pump Activity." *Human Molecular Genetics* 24(7):1843–55.

Marsh, Brad J. and Kathryn E. Howell. 2002. "The Mammalian Golgi - Complex Debates." *Nature Reviews Molecular Cell Biology* 3(October):789–95.

Marsh, Brad J., Niels Volkmann, J. Richard McIntosh, and Kathryn E. Howell. 2004. "Direct Continuities between Cisternae at Different Levels of the Golgi Complex in Glucose-Stimulated Mouse Islet Beta Cells." *PNAS* 101(15):5565–70.

Martínez-Alonso, Emma, Mónica Tomás, and José A. Martínez-Menárguez. 2013. "Golgi Tubules: Their Structure, Formation and Role in Intra-Golgi Transport." *Histochemistry and Cell Biology* 140(3):327–39.

Martínez-Menárguez, José A. 2013. "Intra-Golgi Transport: Roles for Vesicles, Tubules, and Cisternae." *ISRN Cell Biology* 2013:1–15.

Martínez-Menárguez, José A., Rytis Prekeris, Viola M. J. Oorschot, Richard Scheller, Jan W. Slot, Hans J. Geuze, and Judith Klumperman. 2001. "Peri-Golgi Vesicles Contain Retrograde but Not Anterograde Proteins Consistent with the Cisternal Progression Model of Intra-Golgi Transport." *The Journal of Cell BiologyCell Biology* 155(7):1213–24.

Matlin, Karl S. and Michael J. Caplan. 2017. "The Secretory Pathway at 50: A Golden Anniversary for Some Momentous Grains of Silver." *Molecular Biology of the Cell* 28:229–32.

De Matteis, Maria Antonietta and Alberto Luini. 2008. "Exiting the Golgi Complex." *Nature Reviews Molecular Cell Biology* 9(4):273–84.

Matter, Karl, Ellen M. Yamamoto, and Ira Mellman. 1994. "Structural Requirements and Sequence Motifs for Polarized Sorting and Endocytosis of LDL and Fc Receptors in MDCK Cells." *Journal of Cell Biology* 126(4):991–1004.

Mayor, Satyajit and Howard Riezman. 2004. "Sorting GPI-Anchored Proteins." *Nature Reviews Molecular Cell Biology* 5(2):110–20.

McMahon, Harvey T. and Emmanuel Boucrot. 2015. "Membrane Curvature at a Glance." *Journal of Cell Science* 128(6):1065–70.

McMahon, Harvey T. and Jennifer L. Gallop. 2005. "Membrane Curvature and Mechanisms of Dynamic Cell Membrane Remodelling." *Nature* 438:590–96.

McMahon, Harvey T. and Ian G. Mills. 2004. "COP and Clathrin-Coated Vesicle Budding: Different Pathways, Common Approaches." *Current Opinion in Cell Biology* 16(4):379–91.

Meas, Taly and Pierre Jean Guillausseau. 2011. "Abnormalities in Insulin Secretion in Type 2 Diabetes Mellitus." *Metabolic Syndrome: Underlying Mechanisms and Drug Therapies* 34:53–72.

van Meer, Gerrit and Anton I. P. M. de Kroon. 2011. "Lipid Map of the Mammalian Cell." *Journal of Cell Science* 124:5–8.

Van Meer, Gerrit, Dennis R. Voelker, and Gerald W. Feigenson. 2008. "Membrane Lipids: Where They Are and How They Behave." *Nature Reviews Molecular Cell Biology* 9(2):112–24.

Mellman, Ira and W. James Nelson. 2008. "Coordinated Protein Sorting, Targeting and Distribution in Polarized Cells." *Nature Reviews Molecular Cell Biology* 9(11):833–45.

Melville, Zephan, Erick O. Hernández-Ochoa, Stephen J. P. Pratt, Yewei Liu, Adam D. Pierce, Paul T. Wilder, Kaylin A. Adipietro, Daniel H. Breysse, Kristen M. Varney, Martin F. Schneider, and David J. Weber. 2017. "The Activation of Protein Kinase A by the Calcium-Binding Protein S100A1 Is Independent of Cyclic AMP." *Biochemistry* 56(17):2328–37.

Micaroni, Massimo, Giuseppe Perinetti, Daniele Di Giandomenico, Katiuscia Bianchi, Alexander Spaar, and Alexander A. Mironov. 2010. "Synchronous Intra-Golgi Transport Induces the Release of Ca2+ from the Golgi Apparatus." *Experimental Cell Research* 316:2071–86.

Mikhaylova, Marina, Pasham Parameshwar Reddy, Thomas Munsch, Peter Landgraf, Shashi Kumar Suman, Karl-Heinz Smalla, Eckart D. Gundelfinger, Yogendra Sharma, and Michael R. Kreutz. 2009. "Calneurons Provide a Calcium Threshold for Trans-Golgi Network to Plasma Membrane Trafficking." *PNAS*

106(22):9093–98.

Miller, Elizabeth A., Traude H. Beilharz, Per N. Malkus, Marcus C. S. Lee, Susan Hamamoto, Lelio Orci, and Randy Schekman. 2003. "Multiple Cargo Binding Sites on the COPII Subunit Sec24p Ensure Capture of Diverse Membrane Proteins into Transport Vesicles." *Cell* 114:497–509.

Miller, Paul M., Andrew W. Folkmann, Ana R. .. R. Maia, Nadia Efimova, Andrey Eifimov, and Irina Kaverina. 2009. "Golgi-Derived CLASP-Dependent Microtubules Control Golgi Organization and Polarized Trafficking in Motile Cells." *Nat Cell Biol* 11(9):1069–80.

Miller, Sharon E., Brett M. Collins, Airlie J. McCoy, Margaret S. Robinson, and David J. Owen. 2007. "A SNARE-Adaptor Interaction Is a New Mode of Cargo Recognition in Clathrin-Coated Vesicles." *Nature* 450(7169):570–74.

Miranda, Kevin C., Tatiana Khromykh, Perpetina Christy, Tam Luan Le, Cara J. Gottardi, Alpha S. Yap, Jennifer L. Stow, and Rohan D. Teasdale. 2001. "A Dileucine Motif Targets E-Cadherin to the Basolateral Cell Surface in Madin-Darby Canine Kidney and LLC-PK1 Epithelial Cells." *Journal of Biological Chemistry* 276(25):22565–72.

Mironov, Alexander A. and Galina V. Beznoussenko. 2012. "The Kiss-and-Run Model of Intra-Golgi Transport." *International Journal of Molecular Sciences* 13(6):6800–6819.

Mishra, Sanjay K., Peter A. Keyel, Matthew J. Hawryluk, Nicole R. Agostinelli, Simon C. Watkins, and Linton M. Traub. 2002. "Disabled-2 Exhibits the Properties of a Cargo-Selective Endocytic Clathrin Adaptor." *EMBO Journal* 21(18):4915–26.

Missiaen, Ludwig, Leonard Dode, Jo Vanoevelen, Luc Raeymaekers, and Frank Wuytack. 2007. "Calcium in the Golgi Apparatus." *Cell Calcium* 41(5):405–16.

Miura, Keiji, Yoshikazu Kurosawa, and Yoshiyuki Kanai. 1994. "Calcium-Biinding Activitiy of Nucleobindin Mediated by EF Hand Moiety." *Biochemical and Biophysical Research Communications* 199(3):1388–93.

Miura, Keiji, Koiti Titani, Yoshikazu Kurosawa, and Yoshiyuki Kanai. 1992. "MOLECULAR CLONING OF NUCLEOBINDIN, A NOVEL DNA-BINDING PROTEIN THAT CONTAINS BOTH A SIGNAL PEPTIDE AND A LEUCINE ZIPPER STRUCTURE." *Biochemical and Bio* 187(1):375–80.

Mogelsvang, Soren, Brad J. Marsh, Mark S. Ladinsky, and Kathryn E. Howell. 2004. "Predicting Function from Structure: 3D Structure Studies of the Mammalian Golgi Complex." *Traffic* 5(5):338–45.

Morel-Huaux, Valérie M., Marc Pypaert, Sandrine Wouters, Alan M. Tartakoff, Ulrich Jurgan, Kris Gevaert, and Pierre J. Courtoy. 2002. "The Calcium-Binding Protein P54/NEFA Is a Novel Luminal Resident of Medial Golgi Cisternae That Traffics Independently of Mannosidase II." *European Journal of Cell Biology* 81(2):87–100.

Moriyama, K. 1999. "Two Activities of Cofilin, Severing and Accelerating Directional Depolymerization of Actin Filaments, Are Affected Differentially by Mutations around the Actin-Binding Helix." *The EMBO Journal* 18(23):6752–61.

Morlot, Sandrine and Aurélien Roux. 2013. "Mechanics of Dynamin-Mediated Membrane Fission." *Annual Review of Biophysics* 42(1):629–49.

Morvan, Joëlle and Sharon A. Tooze. 2008. "Discovery and Progress in Our Understanding of the Regulated Secretory Pathway in Neuroendocrine Cells." *Histochemistry and Cell Biology* 129(3):243–52.

Mostov, Keith E. 1994. "Transepithelial Transport of Immunoglobulins." *Annu. Rev. Immunol.* 12:63–84.

Mostov, Keith, Tao Su, and Martin ter Beest. 2003. "Polarized Epithelial Membrane Traffic: Conservation and Plasticity." *Nature Cell Biology* 5(4):287–93.

Muñiz, Manuel and Chiara Zurzolo. 2014. "Sorting of GPI-Anchored Proteins from Yeast to Mammals - Common Pathways at Different Sites?" *Journal of Cell Science* 127(13):2793–2801.

Munro, Sean. 2011a. "The Golgin Coiled-Coil Proteins of the Golgi Apparatus." *Cold Spring Harbor Perspectives in Biology* 3(6):1–14.

Munro, Sean. 2011b. "What Is the Golgi Apparatus , and Why Are We Asking ?" *BMC Biology* 9(63):1–5.

Nakatsu, Fubito, Koji Hase, and Hiroshi Ohno. 2014. "The Role of the Clathrin Adaptor AP-1: Polarized Sorting and Beyond." *Membranes* 4(4):747–63.

Nalbant, Demet, Hyewon Youn, S. Isil Nalbant, Savitha Sharma, Everardo Cobos, Elmus G. Beale, Yang Du, and Simon C. Williams. 2005. "FAM20 : An Evolutionarily Conserved Family of Secreted Proteins Expressed in Hematopoietic Cells." *BMC Genomics* 6(11):1–21.

Narayanasamy, Sasirekha and Gopala Krishna Aradhyam. 2018. "The Differential Response to Ca2+ from Vertebrate and Invertebrate Calumenin Is Governed by a Single Amino Acid Residue." *Biochemistry* 57:722–31.

Nelson, W. James and Charles Yeaman. 2001. "Protein Trafficking in the Exocytic Pathway of Polarized Epithelial Cells." *Trends in Cell Biology* 11(12):483–86.

Nesterov, Alexandre, Royston E. Carter, Tatiana Sorkina, Gordon N. Gill, and Alexander Sorkin. 1999. "Inhibition of the Receptor-Binding Function of Clathrin Adaptor Protein AP-2 by Dominant-Negative

Mutant M2 Subunit and Its Effects on Endocytosis." *EMBO Journal* 18(9):2489–99.

Neumann, Ulla, Federica Brandizzi, and Chris Hawes. 2003. "Protein Transport in Plant Cells : In and Out of the Golgi." *Annals of Botany* 92:167–80.

Nigam, S. K., A. L. Goldberg, S. Ho, M. F. Rohde, K. T. Bush, and M. Y. Sherman. 1994. "A Set of Endoplasmic Reticulum Proteins Possessing Properties of Molecular Chaperones Includes Ca2+-Binding Proteins and Members of the Thioredoxin Superfamily." *Journal of Biological Chemistry* 269(3):1744–49.

Nishi, Hafumi, Alexey Shaytan, and Anna R. Panchenko. 2014. "Physicochemical Mechanisms of Protein Regulation by Phosphorylation." *Frontiers in Genetics* 5:1–10.

Nishita, Michiru, Yan Wang, Chinatsu Tomizawa, Akira Suzuki, Ryusuke Niwa, Tadashi Uemura, and Kensaku Mizuno. 2004. "Phosphoinositide 3-Kinase-Mediated Activation of Cofilin Phosphatase Slingshot and Its Role for Insulin-Induced Membrane Protrusion." *Journal of Biological Chemistry* 279(8):7193–98.

Niwa, Ryusuke, Kyoko Nagata-Ohashi, Masatoshi Takeichi, Kensaku Mizuno, and Tadashi Uemura. 2002. "Control of Actin Reorganization by Slingshot, a Family of Phosphatases That Dephosphorylate ADF/Cofilin." *Cell* 108(2):233–46.

Nyathi, Yvonne, Barrie M. Wilkinson, and Martin R. Pool. 2013. "Co-Translational Targeting and Translocation of Proteins to the Endoplasmic Reticulum." *Biochimica et Biophysica Acta - Molecular Cell Research* 1833:2392–2402.

Odorizzi, Greg and Ian S. Trowbridge. 1997. "Structural Requirements for Basolateral Sorting of the Human Transferrin Receptor in the Biosynthetic and Endocytic Pathways of Madin-Darby Canine Kidney Cells." *Journal of Cell Biology* 137(6):1255–64.

Ogunbayo, Oluseye A., Yingmin Zhu, Daniela Rossi, Vincenzo Sorrentino, Jianjie Ma, Michael X. Zhu, and A. Mark Evans. 2011. "Cyclic Adenosine Diphosphate Ribose Activates Ryanodine Receptors , Whereas NAADP Activates Two-Pore Domain Channels." *The Journal of Biological Chemistry* 286(11):9136–40.

Ohno, Hiroshi, Marie Christine Fournier, George Poy, and Juan S. Bonifacino. 1996. "Structural Determinants of Interaction of Tyrosine-Based Sorting Signals with the Adaptor Medium Chains." *Journal of Biological Chemistry* 271(46):29009–15.

Ohno, Hiroshi, Jay Stewart, Marie Christine Fournier, Herbert Bosshart, Ina Rhee, Shoichiro Miyatake, Takashi Saito, Andreas Gallusser, Tomas Kirchhausen, and Juan S. Bonifacino. 1995. "Interaction of Tyrosine-Based Sorting Signals with Clathrin-Associated Proteins." *Science* 269(5232):1872–75.

Ohyama, Yoshio, Ju-hsien Lin, Nattanan Govitvattana, I-ping Lin, Sundharamani Venkitapathi, Ahmed Alamoudi, Dina Husein, Chunying An, Hak Hotta, Masaru Kaku, and Yoshiyuki Mochida. 2016. "FAM20A Binds to and Regulates FAM20C Localization." *Scientific Reports* 6:1–11.

Orci, L., M. Ravazzola, M. Amherdt, D. Louvard, and A. Perrelet. 1985. "Clathrin-Immunoreactive Sites in the Golgi Apparatus Are Concentrated at the Trans Pole in Polypeptide Hormone-Secreting Cells." *Proceedings of the National Academy of Sciences of the United States of America* 82(16):5385–89.

Orci, Lelio, Mylène Amherdt, Mariella Ravazzola, Alain Perrelet, and James E. Rothman. 2000. "Exclusion of Golgi Residents from Transport Vesicles Budding from Golgi Cisternae in Intact Cells." *Journal of Cell Biology* 150(6):1263–69.

Orci, Lelio, Mark Stamnes, Mariella Ravazzola, Mylene Amherdt, Alain Perrelet, Thomas H. Söllner, and James E. Rothman. 1997. "Bidirectional Transport by Distinct Populations of COPI-Coated Vesicles." *Cell* 90:335–49.

Orzech, Ena, Shulamit Cohen, Aryeh Weiss, and Benjamin Aroeti. 2000. "Interactions between the Exocytic and Endocytic Pathways in Polarized Madin-Darby Canine Kidney Cells*." *The Journal of Biological Chemistry* 275(20):15207–19.

Ostermann, Joachim, Lelio Orcit, Katsuko Tani, Mylene Amherdtt, Mariella Ravauolat, Zvulun Elazar, and James E. Rothman. 1993. "Stepwise Assembly of Functionally Active Transport." *Cell* 75:1015–25.

Owen, David J., Brett M. Collins, and Philip R. Evans. 2004. "ADAPTORS FOR CLATHRIN COATS: Structure and Function." *Annual Review of Cell and Developmental Biology* 20(1):153–91.

Pacheco-Fernandez, Natalia, Mehrshad Pakdel, Birgit Blank, Ismael Sanchez-Gonzalez, Kathrin Weber, Mai Ly Tran, Tobias Karl Heinz Hecht, Renate Gautsch, Gisela Beck, Franck Perez, Angelika Hausser, Stefan Linder, and Julia von Blume. 2020. "Nucleobindin-1 Regulates ECM Degradation by Promoting Intra-Golgi Trafficking of MMPs." *Journal of Cell Biology* 219(8).

Paczkowski, Jon E., Brian C. Richardson, Amanda M. Strassner, and J. Christopher Fromme. 2012. "The Exomer Cargo Adaptor Structure Reveals a Novel GTPase-Binding Domain." *EMBO Journal* 31(21):4191–4203.

Pakdel, Mehrshad and Julia von Blume. 2018. "Exploring New Routes for Secretory Protein Export from the Trans-Golgi Network." *Molecular Biology of the Cell* 29(3):235–40.

Paladino, Simona, Stephanie Lebreton, Simona Tivodar, Vincenza Campana, Rosaria Tempre, and Chiara Zurzolo. 2008. "Different GPI-Attachment Signals Affect the Oligomerisation of GPI-Anchored Proteins and Their Apical Sorting." *Journal of Cell Science* 121(24):4001–7.

Paladino, Simona, Daniela Sarnataro, Rudolf Pillich, Simona Tivodar, Lucio Nitsch, and Chiara Zurzolo. 2004. "Protein Oligomerization Modulates Raft Partitioning and Apical Sorting of GPI-Anchored Proteins." *Journal of Cell Biology* 167(4):699–709.

Paladino, Simona, Daniela Sarnataro, Simona Tivodar, and Chiara Zurzolo. 2007. "Oligomerization Is a Specific Requirement for Apical Sorting of Glycosyl-Phosphatidylinositol-Anchored Proteins but Not for Non-Raft-Associated Apical Proteins." *Traffic* 8(3):251–58.

Pang, Zhiping P. and Thomas C. Südhof. 2010. "Cell Biology of Ca2+-Triggered Exocytosis Endocrine Exocytosis." *Cell* 22(4):496–505.

Partida-Sanchez, Santiago, Debra A. Cockayne, Simon Monard, Elaine L. Jacobson, Norman Oppenheimer, Beth Garvy, Kim Kusser, Stephen Goodrich, Maureen Howard, Allen Harmsen, Troy D. Randall, and Frances E. Lund. 2001. "Cyclic ADP-Ribose Production by CD38 Regulates Intracellular Calcium Release , Extracellular Calcium Influx and Chemotaxis in Neutrophils and Is Required for Bacterial Clearance in Vivo." *Nature Medicine* 7(11):1209–16.

Paulick, Margot G. and Carolyn R. Bertozzi. 2008. "The Glycosylphosphatidylinositol Anchor: A Complex Membrane-Anchoring Structure for Proteins." *Biochemistry* 47(27):6991–7000.

Pelham, Hugh R. B. and James E. Rothman. 2000. "The Debate about Transport in the Golgi — Two Sides of the Same Coin ?" *Cell* 102:713–19.

Peretti, Diego, Sohui Kim, Roberta Tufi, and Sima Lev. 2020. "Lipid Transfer Proteins and Membrane Contact Sites in Human Cancer." *Frontiers in Cell and Developmental Biology* 7:1–14.

Petersson, Ulrika, Eszter Somogyi, Finn P. Reinholt, Thore Karlsson, Rachael V. Sugars, and Mikael Wendel. 2004. "Nucleobindin Is Produced by Bone Cells and Secreted into the Osteoid, with a Potential Role as a Modulator of Matrix Maturation." *Bone* 34(6):949–60.

Pezeshkian, Weria, Haifei Gao, Senthil Arumugam, Ulrike Becken, Patricia Bassereau, Jean Claude Florent, John Hjort Ipsen, Ludger Johannes, and Julian C. Shillcock. 2017. "Mechanism of Shiga Toxin Clustering on Membranes." *ACS Nano* 11(1):314–24.

Pfeffer, Suzanne R. 2011. "Entry at the Trans-Face of the Golgi." *Cold Spring Harbor Perspectives in Biology* 3(3):1–11.

Pfeffer, Suzanne R. and James E. Rothman. 1987. "Biosynthethic Protein Transport and Sorting by the Endoplasmic Reticulum and Golgi." *Ann. Rev. Biochem* 56:829–52.

Pizzo, Paola, Valentina Lissandron, Paola Capitanio, and Tullio Pozzan. 2011. "Cell Calcium Ca2+ Signalling in the Golgi Apparatus." *Cell Calcium* 50:184–92.

Pizzo, Paola, Valentina Lissandron, and Tullio Pozzan. 2010. "The Trans-Golgi Compartment." *Communicative & Integrative Biology* 3(5):462–64.

Popova, N. V. Deyev, I. E. Petrenko, A. G. 2015. "Clathrin-Mediated Endocytosis and Adapter Proteins." *Acta Naturae* 5(3):62–73.

Porat, Amir and Zvulun Elazar. 2000. "Regulation of Intra-Golgi Membrane Transport by Calcium." *The Journal of Biochemistryy* 275(38):29233–37.

Potelle, Sven, André Klein, and François Foulquier. 2015. "Golgi Post-Translational Modifications and Associated Diseases." *J Inherit Metab Dis* 38:741–51.

Potter, Beth A., Gudrun Ihrke, Jennifer R. Bruns, Kelly M. Weixel, and Ora A. Weisz. 2004. "Specific N-Glycans Direct Apical Delivery of Transmembrane, but Not Soluble or Glycosylphosphatidylinositol-Anchored Forms of Endolyn in Madin-Darby Canine Kidney Cells." *Molecular Biology of the Cell* 15:1407–16.

Presley, John F., Carolyn Smith, Koty Hirschberg, Chad Miller, Nelson B. Cole, Kristien J. M. Zaal, and Jennifer Lippincott-schwartz. 1998. "Golgi Membrane Dynamics." *Molecular Biology of the Cell* 9(July):1617–26.

Prins, Daniel and Marek Michalak. 2011. "Organellar Calcium Buffers." *Cold Spring Harbor Perspectives in Biology* 3:1–17.

Prinz, William A. 2014. "Bridging the Gap : Membrane Contact Sites in Signaling , Metabolism , and Organelle Dynamics." *Journal of Cell Biology* 205(6):759–69.

Puertollano, R., R. C. Aguilar, I. Gorshkova, R. J. Crouch, and J. S. Bonifacino. 2001. "Sorting of Mannose 6-Phosphate Receptors Mediated by the GGAs." *Science* 292(5522):1712–16.

Quistgaard, Esben M., Peder Madsen, Morten K. Grøftehauge, Poul Nissen, Claus M. Petersen, and Søren S. Thirup. 2009. "Ligands Bind to Sortilin in the Tunnel of a Ten-Bladed β-Propeller Domain." *Nature Structural and Molecular Biology* 16(1):96–98.

Rabouille, Catherine and Adam D. Linstedt. 2016. "GRASP : A Multitasking Tether." *Frontiers in Cell and Developmental Biology* 4(1):1–8.

Ragland, Stephanie A. and Alison K. Criss. 2017. "From Bacterial Killing to Immune Modulation: Recent Insights into the Functions of Lysozyme." *PLoS Pathogens* 13(9):1–22.

Rajasekaran, Ayyappan K., Jeffrey S. Humphrey, Martina Wagner, Gero Miesenböck, André Le Bivic, Juan S. Bonifacino, and Enrique Rodriguez-Boulan. 1994. "TGN38 Recycles Basolaterally in Polarized Madin-

Darby Canine Kidney Cells." *Molecular Biology of the Cell* 5(10):1093–1103.

Reid, David W. and Christopher V. Nicchitta. 2015. "Diversity and Selectivity in MRNA Translation on the Endoplasmic Reticulum." *Nat Rev Mol Cell Biol.* 16(4):221–31.

Reily, Colin, Tyler J. Stewart, Matthew B. Renfrow, and Jan Novak. 2019. "Glycosylation in Health and Disease." *Nature Reviews* 15:347–66.

Remacle, Albert, Gillian Murphy, and Christian Roghi. 2003. "Membrane Type I-Matrix Metalloproteinase (MT1-MMP) Is Internalised by Two Different Pathways and Is Recycled to the Cell Surface." *Journal of Cell Science* 116(19):3905–16.

Reynders, Ellen, François Foulquier, Wim Annaert, and Gert Matthijs. 2011. "How Golgi Glycosylation Meets and Needs Trafficking: The Case of the COG Complex." *Glycobiology* 21(7):853–63.

Van Rheenen, Jacco, Xiaoyan Song, Wies Van Roosmalen, Michael Cammer, Xiaoming Chen, Vera DesMarais, Shu Chin Yip, Jonathan M. Backer, Robert J. Eddy, and John S. Condeelis. 2007. "EGF-Induced PIP2 Hydrolysis Releases and Activates Cofilin Locally in Carcinoma Cells." *Journal of Cell Biology* 179(6):1247–59.

Rodriguez-Boulan, Enrique, Geri Kreitzer, and Anne Müsch. 2005. "Organization of Vesicular Trafficking in Epithelia." *Nature Reviews Molecular Cell Biology* 6(3):233–47.

Rohde, Gundula, Dirk Wenzel, and Volker Haucke. 2002. "A Phosphatidylinositol (4,5)-Bisphosphate Binding Site within μ-Adaptin Regulates Clathrin-Mediated Endocytosis." *Journal of Cell Biology* 158(2):209–14.

Rohrer, Jack, Anja Schweizer, David Russell, and Stuart Kornfeld. 1996. "The Targeting of Lamp1 to Lysosomes Is Dependent on the Spacing of Its Cytoplasmic Tail Tyrosine Sorting Motif Relative to the Membrane." *Journal of Cell Biology* 132(4):565–76.

Römer, Winfried, Ludwig Berland, Valérie Chambon, Katharina Gaus, Barbara Windschiegl, Danièle Tenza, Mohamed R. E. Aly, Vincent Fraisier, Jean Claude Florent, David Perrais, Christophe Lamaze, Graça Raposo, Claudia Steinem, Pierre Sens, Patricia Bassereau, and Ludger Johannes. 2007. "Shiga Toxin Induces Tubular Membrane Invaginations for Its Uptake into Cells." *Nature* 450(7170):670–75.

Rothman, James E. 2002. "The Machinery and Principles of Vesicle Transport in the Cell." *Nature Medicine* 8(10):1059–62.

Rous, Brian A., Barbara J. Reaves, Gudrun Ihrke, John A. G. Briggs, Sally R. Gray, David J. Stephens, George Banting, and J. Paul Luzio. 2002. "Role of Adaptor Complex AP-3 in Targeting Wild- Type and Mutated CD63 to Lysosomes." *Molecular Biology of the Cell* 13:1071–82.

Rubio, Carlos A. 2015. "Increased Production of Lysozyme Associated with Bacterial Proliferation in Barrett's Esophagitis, Chronic Gastritis, Gluten-Induced Atrophic Duodenitis (Celiac Disease), Lymphocytic Colitis, Collagenous Colitis, Ulcerative Colitis and Crohn's Colitis." *Anticancer Research* 35(12):6365–72.

Ruesink, Harm, Lasse Reimer, Emil Gregersen, Arne Moeller, Cristine Betzer, and Poul Henning Jensen. 2019. "Stabilization of α-Synuclein Oligomers Using Formaldehyde." *PLoS ONE* 14(10):1–11.

Sacher, Michael, Jemima Barrowman, Wei Wang, Joe Horecka, Yueyi Zhang, Marc Pypaert, and Susan Ferro-novick. 2001. "TRAPP I Implicated in the Specificity of Tethering in ER-to-Golgi Transport." *Molecular Cell* 7:433–42.

Sambrook, Joseph F. 1990. "The Involvement of Calcium in Transport of Secretory Proteins from the Endoplasmic Reticulum." *Cell* 61(2):197–99.

San Pietro, Enrica, Mariagrazia Capestrano, Elena V. Polishchuk, Alessio DiPentima, Alvar Trucco, Pasquale Zizza, Stefania Mariggiò, Teodoro Pulvirenti, Michele Sallese, Stefano Tete, Alexander A. Mironov, Christina C. Leslie, Daniela Corda, Alberto Luini, and Roman S. Polishchuk. 2009. "Group IV Phospholipase A2α Controls the Formation of Inter-Cisternal Continuities Involved in Intra-Golgi Transport." *PLoS Biology* 7(9).

Sanchez, Emiliano J., Kevin M. Lewis, Benjamin R. Danna, and Chul Hee Kang. 2012. "High-Capacity Ca 2+ Binding of Human Skeletal Calsequestrin." *Journal of Biological Chemistry* 287(14):11592–601.

Sandoval, Ignacio V., Juan S. Bonifacino, Richard D. Klausner, Maryanna Henkart, and Jürgen Wehland. 1984. "Role of Microtubules in the Organization and Localization of the Golgi Apparatus." *The Journal of Cell Biology* 99(1):113–18.

Sanger, Anneri, Jennifer Hirst, Alexandra K. Davies, and Margaret S. Robinson. 2019. "Adaptor Protein Complexes and Disease at a Glance." *Journal of Cell Science* 132(20).

Saraste, J. and M. Marie. 2016. "Intermediate Compartment: A Sorting Station between the Endoplasmic Reticulum and the Golgi Apparatus." *Encyclopedia of Cell Biology* 2:168–82.

Saraste, Jaakko and Kristian Prydz. 2019. "A New Look at the Functional Organization of the Golgi Ribbon." *Frontiers in Cell and Developmental Biology* 7(171):1–21.

Sato, Ken and Akihiko Nakano. 2007. "Mechanisms of COPII Vesicle Formation and Protein Sorting." *FEBS Letters* 581:2076–82.

Scheiffele, Peter, Johan Peränen, and Kai Simons. 1995. "N-Glycans as Apical Sorting Signals in Epithelial Cells."

Nature 378(November):96–98.

Scherer, Philipp E., Gerardo Z. Lederkremer, Suzanne Williams, Michael Fogliano, Giulia Baldini, and Harvey F. Lodish. 1996. "Cab45, a Novel Ca2+-Binding Protein Localized to the Golgi Lumen." *Journal of Cell Biology* 133(2):257–68.

Scholz, Wendy K. and H. Clive Palfrey. 1998. "Activation of Ca2+/Calmodulin-Dependent Protein Kinase II by Extracellular Calcium in Cultured Hippocampal Pyramidal Neurons." *Journal of Neurochemistry* 71(2):580–91.

Schoneich, Christian, Elena Dremina, and Asha Hewarathna. 2017. "Bcl-2 Modulates ER / SR Calcium Uptake by Interaction with SERCA and Heat Shock Proteins Impact of the Age-Related Protein Aggregate Lipofuscin on β -Cell Functionality Circulating MtDNA Levels as an Early Marker for Metabolic Syndrome." *Free Dadical Biology and Medicine* 108:S73.

Schwarz, Dianne S. and Michael D. Blower. 2016. "The Endoplasmic Reticulum: Structure, Function and Response to Cellular Signaling." *Cellular and Molecular Life Sciences* 73:79–94.

Sepúlveda, M. Rosario, Jo Vanoevelen, Luc Raeymaekers, Ana M. Mata, and Frank Wuytack. 2009. "Silencing the SPCA1 (Secretory Pathway Ca2+-ATPase Isoform 1) Impairs Ca2+ Homeostasis in the Golgi and Disturbs Neural Polarity." *Journal of Neuroscience* 29(39):12174–82.

Shah, Vikas N., Benjamin Chagot, and Walter J. Chazin. 2006. "Calcium-Dependent Regulation of Ion Channels." *Calcium Bind Proteins* 1(4):203–12.

Shaikh, Sana A., Sanjaya K. Sahoo, and Muthu Periasamy. 2016. "Phospholamban and Sarcolipin: Are They Functionally Redundant or Distinct Regulators of the Sarco(Endo)Plasmic Reticulum Calcium ATPase?" *J Mol Cell Cardiol* 91:81–91.

Shao, Sichen and Ramanujan S. Hegde. 2011. "Membrane Protein Insertion at the Endoplasmic Reticulum." *Annu. Rev. Cell Dev. Biol* 27:25–56.

Sheth, Jayesh, Riddhi Bhavsar, Ajit Gandhi, Frenny Sheth, and Dhairya Pancholi. 2018. "A Case of Raine Syndrome Presenting with Facial Dysmorphy and Review of Literature." *BMC Medical Genetics* 19(76):1–13.

Shiba, Yoko, Yohei Katoh, Tomoo Shiba, Kaori Yoshino, Hiroyuki Takatsu, Hiromi Kobayashi, Hye Won Shin, Soichi Wakatsuki, and Kazuhisa Nakayama. 2004. "GAT (GGA and Tom1) Domain Responsible for Ubiquitin Binding and Ubiquitination." *Journal of Biological Chemistry* 279(8):7105–11.

Shifman, Julia M., Mee H. Choi, Stefan Mihalas, Stephen L. Mayo, and Mary B. Kennedy. 2006. "Ca2+/Calmodulin-Dependent Protein Kinase II (CaMKII) Is Activated by Calmodulin with Two Bound Calciums." *PNAS* 103(38):13968–73.

Shih, Susan C., David J. Katzmann, Joshua D. Schnell, Myra Sutanto, Scott D. Emr, and Linda Hicke. 2002. "Epsins and Vps27p/Hrs Contain Ubiquitin-Binding Domains That Function in Receptor Endocytosis." *Nature Cell Biology* 4(5):389–93.

Short, Benjamin, Alexander Haas, and Francis A. Barr. 2005. "Golgins and GTPases, Giving Identity and Structure to the Golgi Apparatus." *Biochimica et Biophysica Acta* 1744:383–95.

Simmen, Thomas, Stefan Höning, Ann Icking, Ritva Tikkanen, and Walter Hunziker. 2002. "AP-4 Binds Basolateral Signals and Participates in Basolateral Sorting in Epithelial MDCK Cells." *Nature Cell Biology* 4(2):154–59.

Simmen, Thomas, Emily M. Lynes, Kevin Gesson, and Gary Thomas. 2010. "Oxidative Protein Folding in the Endoplasmic Reticulum: Tight Links to the Mitochondria-Associated Membrane (MAM)." *Biochim Biophys Acta.* 1798(8):1465–73.

Simons, Kai and Mathias J. Gerl. 2010. "Revitalizing Membrane Rafts: New Tools and Insights." *Nature Reviews Molecular Cell Biology* 11(10):688–99.

Simons, Kai and Elina Ikonen. 1997. "Functional Rafts in Cell Membranes." *Nature* 387(6633):569–72.

Simons, Kai and Gerrit Van Meer. 1988. "Lipid Sorting in Epithelial Cells." *Biochemistry* 27(17):6197–6202.

Snead, Wilton T., Carl C. Hayden, Avinash K. Gadok, Chi Zhao, Eileen M. Lafer, Padmini Rangamani, and Jeanne C. Stachowiak. 2017. "Membrane Fission by Protein Crowding." *PNAS* 114(16):E3258–67.

Soboloff, Jonathan, Brad S. Rothberg, Muniswamy Madesh, and Donald L. Gill. 2012. "STIM Proteins: Dynamic Calcium Signal Transducers." *Nat Rev Mol Cell Biol.* 13(9):549–65.

Sreelatha, Anju, Lisa N. Kinch, and Vincent S. Tagliabracci. 2015. "Biochimica et Biophysica Acta The Secretory Pathway Kinases ☆." *Biochimica et Biophysica Acta* 1854:1687–93.

Stachowiak, Jeanne C., Eva M. Schmid, Christopher J. Ryan, Hyoung Sook Ann, Darryl Y. Sasaki, Michael B. Sherman, Phillip L. Geissler, Daniel A. Fletcher, and Carl C. Hayden. 2012. "Membrane Bending by Protein-Protein Crowding." *Nature Cell Biology* 14(9):944–49.

Stalder, Danièle and David C. Gershlick. 2020. "Direct Trafficking Pathways from the Golgi Apparatus to the Plasma Membrane." *Seminars in Cell and Developmental Biology* (April).

Stanley, Pamela. 2011. "Golgi Glycosylation." *Cold Spring Harbor Perspectives in Biology* 3:1–13.

Stechly, Laurence, Willy Morelle, Anne Frédérique Dessein, Sabine André, Georges Grard, Dave Trinel, Marie José Dejonghe, Emmanuelle Leteurtre, Hervé Drobecq, Germain Trugnan, Hans Joachim Gabius, and Guillemette Huet. 2009. "Galectin-4-Regulated Delivery of Glycoproteins to the Brush Border Membrane of Enterocyte-like Cells." *Traffic* 10(4):438–50.

Stefanovic, Sandra and Ramanujan S. Hegde. 2007. "Identification of a Targeting Factor for Posttranslational Membrane Protein Insertion into the ER." *Cell* 128(6):1147–59.

Stephens, David J. and Rainer Pepperkok. 2002. "Imaging of Procollagen Transport Reveals COPI- Dependent Cargo Sorting during ER-to-Golgi Transport in Mammalian Cells." *Journal of Cell Science* 115:1149–60.

Straube, Tamara, Tobias Von Mach, Ellena Hönig, Christoph Greb, Dominik Schneider, and Ralf Jacob. 2013. "PH-Dependent Recycling of Galectin-3 at the Apical Membrane of Epithelial Cells." *Traffic* 14(9):1014–27.

Strynadka, Natalie C. J. and Michael N. G. James. 1989. "Crystal Structures of the Helix-Loop-Helix Calcium-Binding Proteins." *Annu. Rev. Biochem.* 58:951–98.

Surma, Michal A., Christian Klose, and Kai Simons. 2012. "Lipid-Dependent Protein Sorting at the Trans-Golgi Network." *Biochimica et Biophysica Acta - Molecular and Cell Biology of Lipids* 1821(8):1059–67.

Svensson, Liz, Attila Aszódi, Dick Heinegård, Ernst B. Hunziker, Finn P. Reinholt, Reinhard Fässler, and Åke Oldberg. 2002. "Cartilage Oligomeric Matrix Protein-Deficient Mice Have Normal Skeletal Development." *Molecular and Cellular Biology* 22(12):4366–71.

Tagliabracci, Vincent S., James L. Engel, Jianzhong Wen, Sandra E. Wiley, Carolyn A. Worby, Lisa N. Kinch, Junyu Xiao, Nick V. Grishin, and Jack E. Dixon. 2012. "Secreted Kinase Phosphorylates Extracellular Proteins That Regulate Biomineralization." *Science* 336(6085):1150–53.

Tagliabracci, Vincent S., Lorenzo A. Pinna, and Jack E. Dixon. 2013. "Secreted Protein Kinases." *Trends in Biochemical Sciences* 38(3):121–30.

Tagliabracci, Vincent S., Sandra E. Wiley, Xiao Guo, Lisa N. Kinch, Eric Durrant, Jianzhong Wen, Junyu Xiao, Jixin Cui, Kim B. Nguyen, James L. Engel, Joshua J. Coon, Nick Grishin, Lorenzo A. Pinna, David J. Pagliarini, and Jack E. Dixon. 2015. "A Single Kinase Generates the Majority of the Secreted Phosphoproteome." *Cell* 161(7):1619–32.

Tallant, Cynthia, Aniebrys Marrero, and F. Xavier Gomis-Rüth. 2010. "Matrix Metalloproteinases: Fold and Function of Their Catalytic Domains." *Biochimica et Biophysica Acta - Molecular Cell Research* 1803(1):20–28.

Taylor, Colin W. and Stephen C. Tovey. 2010. "IP3 Receptors: Toward Understanding Their Activation." *Cold Spring Harbor Perspectives in Biology* 2:1–22.

Thatcher, Jack D. 2010. "The Inositol Trisphosphate (IP3) Signal Transduction Pathway." *Sci. Signal* 3(119):1.

Thor, Friederike, Matthias Gautschi, Roger Geiger, and Ari Helenius. 2009. "Bulk Flow Revisited: Transport of a Soluble Protein in the Secretory Pathway." *Traffic* 10(12):1819–30.

Thur, Jochen, Krisztina Rosenberg, D. Patric Nitsche, Tero Pihlajamaa, Leena Ala-Kokko, Dick Heinegård, Mats Paulsson, and Patrik Maurer. 2001. "Mutations in Cartilage Oligomeric Matrix Protein Causing Pseudoachondroplasia and Multiple Epiphyseal Dysplasia Affect Binding of Calcium and Collagen I, II, and IX." *Journal of Biological Chemistry* 276(9):6083–92.

Tooze, John and Sharon A. Tooze. 1986. "Clathrin-Coated Vesicular Transport of Secretory Proteins during the Formation of ACTH-Containing Secretory Granules in ART20 Cells." *The Journal of Cell Biology* 103:839–50.

Tooze, Sharon A. 1998. "Biogenesis of Secretory Granules in the Trans-Golgi Network of Neuroendocrine and Endocrine Cells." *Biochimica et Biophysica Acta* 1404:231–44.

Toyoshima, Chikashi, Masayoshi Nakasako, Hiromi Nomura, and Haruo Ogawa. 2000. "Crystal Structure of the Calcium Pump of Sarcoplasmic Reticulum 2.4A Resolution." *Nature* 405:647–55.

Traub, Linton M. 2005. "Common Principles in Clathrin-Mediated Sorting at the Golgi and the Plasma Membrane." *Biochimica et Biophysica Acta - Molecular Cell Research* 1744(3 SPEC. ISS.):415–37.

Traub, Linton M. and Stuart Kornfeld. 1997. "The Trans-Golgi Network: A Late Secretory Sorting Station." *Current Opinion in Cell Biology* 9(4):527–33.

Trucco, Alvar, Roman S. Polischuck, Oliviano Martella, Alessio Di Pentima, Aurora Fusella, Daniele Di Giandomenico, Enrica San Pietro, Galina V. Beznoussenko, Elena V. Polischuk, Massimiliano Baldassarre, Roberto Buccione, Willie J. C. Geerts, Abraham J. Koster, Koert N. J. Burger, Alexander A. Mironov, and Alberto Luini. 2004. "Secretory Traffic Triggers the Formation of Tubular Continuities across Golgi Sub-Compartments." *Nature Cell Biology* 6(11):1071–81.

Tucker, Ward C. and Edwin R. Chapman. 2002. "Role of Synaptotagmin in Ca 2 +-Triggered Exocytosis." *Biochem. J* 366:1–13.

Ubersax, Jeffrey A. and James E. Jr. Ferrell. 2007. "Mechanisms of Specificity in Protein Phosphorylation." *Nature Reviews* 8:530–42.

Urbé, Sylvie, Lesley J. Page, and Sharon A. Tooze. 1998. *Homotypic Fusion of Immature Secretory Granules during Maturation in a Cell-Free Assay*. Vol. 143.

Valastyan, Julie S. and Susan Lindquist. 2014. "Mechanisms of Protein-Folding Diseases at a Glance." *DMM Disease Models and Mechanisms* 7(1):9–14.

Valencia, C. Alexander, Steve W. Cotten, Jinzhu Duan, and Rihe Liu. 2008. "Modulation of Nucleobindin-1 and Nucleobindin-2 by Caspases." *FEBS Letters* 582(2):286–90.

Vandecaetsbeek, Ilse, Peter Vangheluwe, Luc Raeymaekers, Frank Wuytack, and Jo Vanoevelen. 2011. "The Ca2+ Pumps of the Endoplasmic Reticulum and Golgi Apparatus." *Cold Spring Harbor Perspectives in Biology* 3(5):1–24.

Vanoevelen, Jo, L. Raeymaekers, L. Dode, J. B. Parys, H. De Smedt, G. Callewaert, F. Wuytack, and L. Missiaen. 2005. "Cytosolic Ca2+ Signals Depending on the Functional State of the Golgi in HeLa Cells." *Cell Calcium* 38(5):489–95.

Varki, Ajit, Pascal Gagnuex, Richard D. Cummings, Jeffrey D. Esko, Pamela Stanley, Gerald W. Hart, Markus Aebi, Alan G. Darvill, Taroh Kinoshita, Nicolle H. Pracker, James H. Prestegard, Roland L. Schnaar, and Peter H. Seeberg. 2015. "Biological Functions of Glycans." Pp. 77–88 in *Essentials of Glycobiology*, edited by 3rd Edition. New York: Cold Spring Harbor Laboratory Press.

Varki, Ajit, John B. Lowe, Richard D. Cummings, Jeffrey D. Esko, Hudson H. Freeze, Pamela Stanley, Carolyn R. Bertozzi, Gerald W. Hart, and Marilynn E. Etzler. 2009. "Biological Roles of Glycans." in *Essentials of Glycobiology*. New York.

Venditti, Rossella, Cathal Wilson, and Maria Antonietta De Matteis. 2014. "Exiting the ER : What We Know and What We Don ' t." *Trends in Cell Biolognds in Cell Biology* 24(1):9–18.

Villarreal, Laura, Olga Méndez, Cándida Salvans, Josep Gregori, José Baselga, and Josep Villanueva. 2013. "Unconventional Secretion Is a Major Contributor of Cancer Cell Line Secretomes." *Molecular and Cellular Proteomics* 12(5):1046–60.

Vishwanath, B., K. Srinivasa, and M. Veera Shankar. 2014. "Raine Syndrome." *Indian J Hum Genet.* 20(1):72–74.

Wakana, Yuichi, Josse Van Galen, Felix Meissner, Margherita Scarpa, Roman S. Polishchuk, Matthias Mann, and Vivek Malhotra. 2012. "A New Class of Carriers That Transport Selective Cargo from the Trans Golgi Network to the Cell Surface." *EMBO Journal* 31(20):3976–90.

Wakana, Yuichi, Richika Kotake, Nanako Oyama, Motohide Murate, Toshihide Kobayashi, Kohei Arasaki, Hiroki Inoue, and Mitsuo Tagaya. 2015. "CARTS Biogenesis Requires VAP-Lipid Transfer Protein Complexes Functioning at the Endoplasmic Reticulum-Golgi Interface." *Molecular Biology of the Cell* 26(25):4686–99.

Wakana, Yuichi, Julien Villeneuve, Josse van Galen, David Cruz-Garcia, Mitsuo Tagaya, and Vivek Malhotra. 2013. "Kinesin-5/Eg5 Is Important for Transport of CARTS from the Trans-Golgi Network to the Cell Surface." *Journal of Cell Biology* 202(2):241–50.

Wang, Chao Wen, Susan Hamamoto, Lelio Orci, and Randy Schekman. 2006. "Exomer: A Coat Complex for Transport of Select Membrane Proteins from the Trans-Golgi Network to the Plasma Membrane in Yeast." *Journal of Cell Biology* 174(7):973–83.

Wang, Miao and Randal J. Kaufman. 2016. "Protein Misfolding in the Endoplasmic Reticulum as a Conduit to Human Disease." *Nature* 529(7586):326–35.

Wang, Xiaofang, Suzhen Wang, Yongbo Lu, Monica P. Gibson, Ying Liu, Baozhi Yuan, Jian Q. Feng, and Chunlin Qin. 2012. "FAM20C Plays an Essential Role in the Formation of Murine." *The Journal of Biological Chemistry* 287(43):35934–42.

Wang, Yan, Futoshi Shibasaki, and Kensaku Mizuno. 2005. "Calcium Signal-Induced Cofilin Dephosphorylation Is Mediated by Slingshot via Calcineurin." *Journal of Biological Chemistry* 280(13):12683–89.

Wang, Yu-Chieh, Suzanne E. Peterson, and Jeanne F. Loring. 2014. "Protein Post-Translational Modifications and Regulation of Pluripotency in Human Stem Cells." *Cell Research* 24:143–60.

Wang, Zhaoshuai, Wei Lu, Prasangi Rajapaksha, Thomas Wilkop, Yuguang Cai, and Yinan Wei. 2018. "Comparison of in Vitro and in Vivo Oligomeric States of a Wild Type and Mutant Trimeric Inner Membrane Multidrug Transporter." *Biochemistry and Biophysics Reports* 16:122–29.

Ward, Katherine E., James P. Ropa, Emmanuel Adu-Gyamfi, and Robert V. Stahelin. 2012. "C2 Domain Membrane Penetration by Group IVA Cytosolic Phospholipase A 2 Induces Membrane Curvature Changes." *Journal of Lipid Research* 53(12):2656–66.

Watson, Peter, Anna K. Townley, Pratyusha Koka, Krysten J. Palmer, and David J. Stephens. 2006. "Sec16 Defines Endoplasmic Reticulum Exit Sites and Is Required for Secretory Cargo Export in Mammalian Cells." *Traffic* 7:1678–87.

Wendel, Mikael, Yngve Sommarin, Tomas Bergman, and Dick Heinegard. 1995. "Isolation, Characterization, and Primary Structure of a Calcium-Binding 63-KDa Bone Protein." *The Journal of Biological Chemistry* 270(11):6125–33.

Westerlund, Annie M. and Lucie Delemotte. 2018. "Effect of Ca2+on the Promiscuous Target-Protein Binding of Calmodulin." *PLoS Computational Biology* 14(4):1–27.

Wiedmann, M., A. Huth, and Tom A. Rapoport. 1984. "Xenopus Oocytes Can Secrete Bacterial Beta-Lactamase." *Nature* 309(5969):637–39.

Wu, Xudong, Tom A. Rapoport, and Longwood Avenue. 2018. "Mechanistic Insights into ER-Associated Protein Degradation." *Curr Opin Cell Biol.* 53:22–28.

Xiang, Yi and Yanzhuang Wang. 2011. "New Components of the Golgi Matrix." *Cell Tissue Res.* 344(3):365–79.

Xiao, Junyu, Vincent S. Tagliabracci, Jianzhong Wen, Soo-a Kim, and Jack E. Dixon. 2013. "Crystal Structure of the Golgi Casein Kinase." *PNAS* 110(26):10574–79.

Xie, Xiaohua, Su Ma, Changcheng Li, Peihong Liu, Xaixia Wang, Li Chen, and Chunlin Qin. 2014. "Expression of Small Integrin-Binding LIgand N-Linked Glycoproteins (SIBLINGs) in the Reparative Dentin of Rat Molars." *Dental Traumatology* 30:285–95.

Xu, Chengchao and Davis T. W. Ng. 2015. "Glycosylation-Directed Quality Control of Protein Folding." *Nature Reviews Molecular Cell Biology* 16(12):742–52.

Xu, Haoxing, Enrico Martinoia, and Ildiko Szabo. 2016. "Organellar Channels and Transporters Haoxing." *Physiology & Behavior* 176(1):139–48.

Yadav, Smita and Adam D. Linstedt. 2011. "Golgi Positioning." *Cold Spring Harbor Perspectives in Biology* 3(5):1–17.

Yamamoto, Yasunori and Toshiaki Sakisaka. 2012. "Molecular Machinery for Insertion of Tail-Anchored Membrane Proteins into the Endoplasmic Reticulum Membrane in Mammalian Cells." *Molecular Cell* 48(3):387–97.

Yamashita, Katsuko, Sayuri Hara-Kuge, and Takashi Ohkura. 1999. "Intracellular Lectins Associated with N-Linked Glycoprotein Traffic." *Biochimica et Biophysica Acta - General Subjects* 1473(1):147–60.

Yang, Zhaokang, Hannah M. Kirton, David A. Macdougall, John P. Boyle, James Deuchars, Brenda Frater, Sreenivasan Ponnambalam, Matthew E. Hardy, Edward White, Sarah C. Calaghan, Chris Peers, and Derek S. Steele. 2015. "The Golgi Apparatus Is a Functionally Distinct Ca2+ Store Regulated by the PKA and Epac Branches of the B1-Adrenergic Signaling Pathway." *Cell Biology* 8(398):1–12.

Yeaman, Charles, M. Ayala, Jessica Wright, Frederic Bard, Carine Bossard, A. Ang, Y. Maeda, Thomas Seufferlein, I. Mellman, W. Nelson, and V. Malhotra. 2004. "Protein Kinase D Regulates Basolateral Membrane Protein Exit from Trans-Golgi Network." *Nat Cell Biol* 6(2):106–12.

Yeaman, Charles, Annick H. Le Gall, Anne N. Baldwin, Laure Monlauzeur, Andre Le Bivic, and Enrique Rodriguez-Boulan. 1997. "The O-Glycosylated Stalk Domain Is Required for Apical Sorting of Neurotrophin Receptors in Polarized MDCK Cells." *Journal of Cell Biology* 139(4):929–40.

Yu, Sidney, Ayano Satoh, Marc Pypaert, Karl Mullen, Jesse C. Hay, and Susan Ferro-novick. 2006. "MBet3p Is Required for Homotypic COPII Vesicle Tethering in Mammalian Cells." *The Journal of Cell Biology* 174(3):359–68.

Zamparelli, Carlotta, Andrea Ilari, Daniela Verzili, Paola Vecchini, and Emilia Chiancone. 1997. "Calcium- and PH-Linked Oligomerization of Sorcin Causing Translocation from Cytosol to Membranes." *FEBS Letters* 409(1):1–6.

Zappa, Francesca, Mario Failli, and Maria Antonietta De Matteis. 2018. "The Golgi Complex in Disease and Therapy." *Current Opinion in Cell Biology* 50:102–16.

Zhang, Hui, Qinyu Zhu, Jixin Cui, Yuxin Wang, Mark J. Chen, Xing Guo, Vincent S. Tagliabracci, Jack E. Dixon, and Junyu Xiao. 2018. "Structure and Evolution of the Fam20 Kinases." *Nature Communications* 9(1218):1–12.

Zhang, Jianchao, Qinyu Zhu, Xi Wang, Jiaojiao Yu, Xinxin Chen, Jifeng Wang, Xi Wang, Junyu Xiao, Chih-chen Wang, and Lei Wang. 2018. "Secretory Kinase Fam20C Tunes Endoplasmic Reticulum Redox State via Phosphorylation of Ero1a." *The EMBO Journal* 37:1–16.

Zhang, Xiaoyan and Yanzhuang Wang. 2016. "Glycosylation Quality Control by the Golgi Structure." *J Mol Biol* 428(16):3183–93.

Zhang, Zhenlu, Guijuan He, Natalie A. Filipowicz, Glenn Randall, George A. Belov, Benjamin G. Kopek, and Xiaofeng Wang. 2019. "Host Lipids in Positive-Strand RNA Virus Genome Replication." *Frontiers in Microbiology* 10:1–18.

Zhou, Yubin, Shenghui Xue, and Jenny J. Yang. 2013. "Calciomics: Integrative Studies of Ca2+-Binding Proteins and Their Interactomes in Biological Systems." *Metallomics* 5(1):29–42.

Zhu, Y., B. Doray, A. Poussu, V. P. Lehto, and S. Kornfeld. 2001. "Binding of GGA2 to the Lysosomal Enzyme Sorting Motif of the Mannose 6-Phosphate Receptor." *Science* 292(5522):1716–18.

Zimmerberg, Joshua and Michael M. Kozlov. 2006. "How Proteins Produce Cellular Membrane Curvature." *Nature Reviews Molecular Cell Biology* 7(1):9–19.

Zurzolo, Chiara and Kai Simons. 2016. "Glycosylphosphatidylinositol-Anchored Proteins : Membrane

Organization and Transport." *Biochim Biophys Acta.* 1858:632–39.

Danksagung

CURRICULUM VITAE

Tobias Karl-Heinz Hecht

PERSONAL DATA

Date of birth:	03.02.1991
Place of birth:	Marktredwitz
Nationality:	German

EDUCATION

Since 05/2019
Yale University, New Haven
Visiting Assistant in Research at Yale Graduate School of Arts and Sciences
PhD student at Yale School of Medicine (Dep. Cell Biology)

01/2017 - 12/2019
Max Planck Institute of Biochemistry, Martinsried
PhD student, Department of Molecular Medicine
Research group: Molecular Basis of Protein Trafficking
Enrolled at the University of Munich (Dep. Biology)

04/2014 - 11/2016
Technical University of Munich
Master of Science, Molecular Biotechnology

10/2010 - 03/2014
University of Applied Sciences Ansbach
Bachelor of Science, Industrial Biotechnology

09/2008 - 07/2010
Gustav-von-Schlör-Schule Weiden, College of further education

WORK EXPERIENCE

Since 05/2019
Yale School of Medicine, New Haven
Methods: Lipid-binding assays, Generation of unilamellar liposomes, Budding Assays

01/2017 - 04/2019
Max Planck Institute of Biochemistry, Martinsried
Methods: Confocal microscopy, Protein purification, Trafficking Assays

04/2016 - 10/2016
Chair of Microbiology (TUM), Freising
Methods: Cloning, Secretion Assays, Enzyme Assays, IF-microscopy, Zymography, Metagenomic Screenings

10/2015 - 03/2016
Max Planck Institute of Biochemistry, Martinsried
Methods: CRISPR/Cas, Protein crystallization, Protein purification

08/2015 - 09/2015	**Helmholtz-Zentrum, Munich**
	Methods: Cryosectioning of brains, Immunohistological stainings, Stereo-microscopy
10/2013 - 01/2014	**Max Planck Institute of Biochemistry, Martinsried**
	Methods: Cell cultivation, qRT-PCR, Western Blotting, siRNA-knockdown, IR-microscopy, Secretion assays, Immunoprecipitation
03/2013 - 08/2013	**Biontex Laboratories GmbH, Martinsried**
	Methods: Cell cultivation, Lipofection, Electroporation (DNA, mRNA, siRNA)

PUBLICATIONS

06/2020	Natalia Pacheco-Fernandez, Mehrshad Pakdel, Birgit Blank, Ismael Sanchez-Gonzalez, Kathrin Weber, May Li Tran, **Tobias Karl-Heinz Hecht**, Renate Gautsch, Gisela Beck, Frank Perez, Angelika Hauser, Stefan Lindner, Julia von Blume; Nucleobindin-1 regulates ECM degradation by promoting intra-Golgi trafficking of MMP2. J Cell Biol 8 March 2020; 219 (8): e201907058. doi: https//doi.org/10.1083/jcb. 201907058.
05/2020	**Tobias Karl-Heinz Hecht** *, Birgit Blank *, Martin Steger, Victor Lopez, Gisela Beck, Bulat Ramazanov, Matthias Mann, Vincent Tagliabracci, Julia von Blume; Fam20C regulates protein secretion by Cab45 phosphorylation. J Cell Biol 1 June 2020; 219 (6): e201910089. doi: https://doi.org/10.1083/jcb.201910089. * These authors contributed equally to this work.

ATTENDET CONFERENCES

07/2018	**Gordon Research Conference**, New England, NH, USA
	Protein Processing, Trafficking and Secretion
07/2018	**Gordon Research Seminar**, New England, NH, USA
	Protein Processing, Trafficking and Secretion
05/2017	**EMBO Workshop**, Pulla, Sardinia, Italy
	Trafficking and Signalling

New Haven, 8th of September 2020

TOBIAS KARL-HEINZ HECHT